

식물의 생장조절과 신호전달 네트워크 연구를 통한 신기능성 식물체 개발

Development of Functional Plants by Controlling Plant
Development and the Related Signal Transduction Networks

신호전달 조절유전자군의 발굴 및 기능 네트워크 연구

Signal Transduction Genes and their
Function Networks in Plants

한국생명공학연구원

과 학 기 술 부

제 출 문

과학기술부 장관 귀하

본 보고서를 “신호전달 조절유전자군의 발굴 및 기능네트워크 연구” 과제의 최종보고서로 제출합니다.

2003 년 8 월 14 일

주관연구기관명 : 한국생명공학연구원

총괄연구책임자 : 배 현 숙

연 구 원 : 조 혜 선

연 구 원 : 이 상 숙

연 구 원 : 이 정 희

연 구 원 : 김 문 일

연 구 원 : 안 준 우

연 구 원 : 김 도 명

연 구 원 : 김 유 경

연 구 원 : 임 정 화

연 구 원 : 양 경 실

연 구 원 : 박 중 아

보고서 초록

과제관리번호		해당단계 연구기간	2000.09.16 - 2003.06.30	단계 구분	(1단계) / (총3단계)
연구사업명	중 사업명	21C 프론티어연구개발사업			
	세부사업명	자생식물이용기술개발사업			
연구과제명	중 과제명	식물의 성장조절과 신호전달 네트워크 연구를 통한 신기능성 식물체 개발			
	세부(단위)과제명	신호전달 조절유전자군의 발굴 및 기능네트워크 연구			
연구책임자	배현숙	해당단계 참여연구원수	총 : 13 명 내부 : 2 명 외부 : 11 명	해당단계 연구비	정부: 250,000 천원 기업: 천원 계: 천원
연구기관명 및 소속부서명	한국생명공학연구원 식물유전체연구실		참여기업명		
국제공동연구	상대국명 :		상대국연구기관명 :		
위탁연구	연구기관명 :		연구책임자 :		
요약(연구결과를 중심으로 개조식 500자이내)				보고서 면수	
<p>이 연구의 목적은 식물발달을 조절하는 신호전달체계의 분자적 기작을 이해하는 것이다. 이 연구를 통하여 식물발달 과정을 컨트롤하는 새로운 신호전달 유전자들을 발굴하며 각각의 신호전달 유전자 간의 상호작용을 탐구함으로써 식물발달 신호전달의 전체 네트워크를 이해하고자 하였다. 먼저 여러 식물조직 및 발생학적 시기의 신호전달 유전자를 동정하였고 northern blot analysis를 통하여 유전자발현을 탐구하였으며 여러 분자생물학적, 생화학적, 세포생물학적인 테크닉을 이용하여 신호전달 유전자와 단백질의 특성을 탐구하였다. 유전자의 식물발생관련 기능을 동정하기 위하여 RNAi, VIGS, 과대발현 등의 방법을 이용하였고 식물발생의 형태학적, 해부학적 연구를 위하여 tissue sections, scanning electron microscopy, transmission electron microscopy, confocal laser microscopy 을 이용하였다. Yeast two hybrid 방법을 이용하여 신호전달단백질 상호작용에 관하여 연구하였고 식물 기능유전체적인 방법을 이용하여 세포 내 신호전달 네트워크를 조사하였다. 이러한 연구를 통하여 FHA transcription factor의 구조와 기능 (JBC 2002), proteasome과 NtCDPK1의 상호작용 (Plant J, 2003), proteasome의 suppression이 일으키는 programmed cell death (JBC, 2003) 등에 관한 논문들을 발표하였다.</p>					
색인어 (각 5개 이상)	한글	신호전달체계, 인산화효소, 탈인산화효소, 유전자기능, 단백질 간 상호작용			
	영어	signal transduction, protein kinase, protein phosphatase, gene function, protein-protein interaction			

여 백

요 약 문

I. 제 목

신호전달 조절유전자군의 발굴 및 기능네트워크 연구

II. 연구개발의 목적 및 필요성

세계인구의 폭발적인 증가와 생활수준의 향상으로 인한 식량수요의 급증으로 생산효율이 높고 자연환경에 내성이 강한 품종을 개발하여 단위경작지 당 작물생산성을 증가시키는 것은 현대 농업의 긴급한 문제이다. 이 목적을 위해서 유용 유전자의 발굴과 그 유전자들을 도입한 유전자조작 작물의 개발은 필수적인 전략이다. 이를 위하여 현재 이미 완료된 *Arabidopsis*와 벼의 전체유전체의 염기서열을 이용하여 유전자의 기능을 대량으로 밝히는 식물 기능유전체 연구에 전세계적인 경쟁이 치열할 전망이다. 즉 신기능성 유전자를 이용한 새로운 품종의 형질전환체 개발은 농업상업적으로 매우 중요하다. 이러한 상황 하에 국제적으로 경쟁력을 가지기 위해서는 식물의 특별한 기능에 초점을 맞춘 제한된 기능 유전체 연구가 전략적으로 효과적이라고 사료된다.

가역적인 단백질 인화작용은 거의 모든 생물학적 과정을 조절하는 핵심작용이다. 고등식물의 약 5%의 유전자가 단백질 인화작용에 의한 신호전달에 직접적으로 관련되어 있다. 그러나 현재 기능이 밝혀진 식물 신호전달 유전자는 매우 제한되어 있다. 현재까지 기능이 알려져 있지 않은 대다수의 신호전달 유전자들의 발현양상 분석과 기능탐구를 통하여 작물품질개량에 직접적으로 사용될 기능성 유전자원을 발굴하여 이용하는 것이 본 연구의 목표이다. 특히 본 연구팀은 식물발생 및 분화에서 조절기능을 가지는 신호전달 유전자에 특히 관심을 갖고 연구를 수행하였다. 담배와 야생담배(*Nicotiana benthamiana*)는 주요작물이자 model 식물체로서 분자생물학적 연구가 많이 되어있고 *Arabidopsis*보다 크기 때문에 생식기관이나 발생종자 등의 미세 조직을 얻기 쉬우며 최근에 개발된 virus-induced gene silencing 기술을 통해 유전자 기능을 어느 방법보다도 간단하게 분석할 수 있다는 장점을 가지고 있어 쌍자엽식물 중 *Arabidopsis*를 보완하는 시스템이라고 사료된다.

이 연구의 목적은 식물발달을 조절하는 신호전달체계의 분자적 기작을 이해하는 것이다. 이 연구를 통하여 식물발달 과정을 콘트롤하는 새로운 신호전달 유전자들을 발굴하며 각각의 신호전달 유전자 간의 상호작용을 탐구함으로써 식물발달 신호전달의 전체 네트워크

를 이해하고자 하였다. 먼저 여러 식물조직 및 발생학적 시기의 신호전달 유전자를 동정하였고 northern blot analysis를 통하여 유전자발현을 탐구하였으며 여러 분자생물학적, 생화학적, 세포생물학적인 테크닉을 이용하여 신호전달 유전자와 단백질의 특성을 탐구하였다. 유전자의 식물발생관련 기능을 동정하기 위하여 RNAi, VIGS, 과대발현 등의 방법을 이용하였고 식물발생의 형태학적, 해부학적 연구를 위하여 tissue sections, scanning electron microscopy, transmission electron microscopy, confocal laser microscopy을 이용하였다. Yeast two hybrid 방법을 이용하여 신호전달단백질 상호작용에 관하여 연구하였고 식물 기능유전체적인 방법을 이용하여 세포 내 신호전달 네트워크를 조사하였다. 이러한 연구를 통하여 FHA transcription factor의 구조와 기능 (JBC 2002), proteasome과 NtCDPK1의 상호작용 (Plant J, 2003), proteasome의 suppression이 일으키는 programmed cell death (JBC, 2003) 등에 관한 논문들을 발표하였다.

III. 연구개발의 내용 및 범위

- 식물신호전달 유전자와 단백질의 특성 연구
 - NtDSK1 dual-specificity kinase
 - CHRK1 receptor-like kinase
 - FHT1 transcription factor / NtARC
 - NtCDPK1 kinase
 - 신호전달 유전자와 단백질의 발현 연구
 - 유전자의 특징 및 Genomic 구조 연구
 - 단백질의 생화학적, 세포생물학적 특성 연구
 - 모델식물의 형질전환을 통한 기능 연구
- RT-PCR을 이용한 고추의 다양한 조직의 kinase 및 phosphatase 유전자의 cloning
- 식물신호전달 유전자와 단백질의 특성 연구 및 생물학적 기능 분석
 - 신호전달 유전자와 단백질의 발현 연구
 - 단백질의 생화학적, 세포생물학적 특성 연구
 - 모델식물의 형질전환을 통한 기능 연구
 - Yeast two hybrid system을 이용한 상호작용하는 단백질의 탐색
- 식물 신호전달 단백질의 신호전달체계 내 위치 및 다른 신호전달 단백질과의 상

호조절 작용 조사

- o yeast two hybrid system
- o 단백질 상호조절 작용의 생화학적 기작 탐구
- o Arabidopsis T-DNA tagging mutant screening
- o 모델식물의 형질전환을 통한 기능 연구

● 신호전달 유전자 조절에 의한 신기능성 형질전환체의 개발

IV. 연구개발결과

1) CHRK1 receptor-like kinase의 식물발생과 cytokinin 합성에의 기능

-transgenic line의 세포내 축적 ethylene 양을 조사: ethylene 양은 거의 detect 되지 않았다.

-transgenic line의 세포내 축적 cytokinin 양 조사: #209 line은 zeatin, zeatinriboside, zeatinriboside-5-monophosphate, isopentenyladenine, isopentenyl-adenosine, isopentenyl-adenosine-5-monophosphate 등의 cytokinin 을 3-5배 함유하고 있었다. #210 line은 zeatinriboside-5-monophosphate 만을 3배 이상 함유하고 있었다.

-subtractive PCR cloning된 300개 유전자를 sequencing하여 분석하였다. 그 결과 #210 line에는 PR 유전자들이 다량으로 발현되고 그외 embryo에서 많이 발현되는 유전자들, nutrient transporter들이 높게 발현되었다.

-10개 이상의 subtractive PCR cloning된 유전자를 probe로 사용하여 #210 line의 northern hybridization을 수행하였다. subtraction의 결과대로 조사한 모든 유전자의 mRNA level이 크게 증가하였다.

-callus phenotype을 보이는 #203 line의 RNA를 추출하여 위의 probe를 사용하여 northern hybridization한 결과 #210 line과 같이 mRNA level이 크게 증가하여 #210 line과 동일한 양상을 보였다.

-CHRK1 유전자의 genomic organization을 조사한 결과 3개의 intron이 있는데 1개는 chitinase domain에 2개는 kinase domain에 위치하며 크기는 42-105 bp로 작다.

-CHRK1 callus line과 tobacco genetic tumor line의 유사점 조사

CHRK1 캘러스는 1) shooty callus, 2) hormone-autonomous organogenesis, 3) gene expression profile 면에서 tobacco genetic tumor와 유사하다. tumour에 높이 발현되는 유전자는 주로 defense에 관련된 PR gene 이고 tumor-related gene 들의 발현도 높다.

-CHRK1 캘러스의 gene expression 양상을 PCR subtractive cloning과 northern

blot analysis로 조사하니 osmotin, beta-glucosidase, glycine-rich protein, proteinase inhibitor 등 PR 유전자들이 높이 발현되며 그외 transcription factor 들, tumor-related gene과 embryo에서 많이 발현되는 유전자들이 발현된다. 이러한 양상은 tobacco genetic tumour의 gene expression과 매우 유사한 양상이다.

-tobacco genetic tumor의 parent species내의 CHRK1 유전자의 structure 조사
chitinase domain과 kinase domain에 대응하는 primer를 사용하여 RT-PCR한 결과 *Nicotiana glauca*는 chitinase와 kinase domain을 모두 가지고 있으나 *N. langsdorffii*는 kinase domain만을 가지는 것으로 나타났다.

-CHRK1 transgenic line의 cell death phenotype 조사

CHRK1 callus는 PR gene이 높이 발현되고 있으며 죽는 세포를 염색할 수 있는 Evans Blue로 staining하였을 때 짙게 염색되므로서 cell death가 진행 된다는 것을 증명하였다

-CHRK1 callus의 homeobox 유전자들과 CycD3 cyclin 유전자의 발현양상 조사:
CHRK1 callus에서는 NTH15, 20, 23 homeobox 유전자와 cyclinD3 유전자의 발현이 control에 비해 증가되어 있었다. 또한 genetic tumor line에서도 그들 유전자가 높이 발현되고 있었다.

-PCR을 이용한 tobacco genetic tumor의 parent species내의 CHRK1의 구조조사:
PCR을 이용하여 *Nicotiana glauca*와 *Nicotiana langsdorffii*의 chitinase domain과 kinase domain의 구조를 조사하였는데 *N. langsdorffii*는 chitinase domain과 kinase domain을 모두 가지고 있으나 *N. glauca*의 경우는 kinase domain만 있고 chitinase domain은 없었다.

-Progeny analysis (#209 line): genomic southern을 이용하여 transgene segregation을 조사하였는데 209 line은 두개의 transgene을 가지고 있는데 phenotype은 특정 transgene과 cosegregation되지 않고 dosage-dependent하게 나타나게 된다.

-CHRK1 promoter-GUS 형질전환체 분석을 통한 CHRK1 gene expression 조사.

1.2. kb, 2 kb CHRK1 promoter를 GenomeWalker를 이용하여 tobacco genome에서 cloning 하였으며 이를 GUS에 융합시켜 *Arabidopsis* 형질전환체를 만들었다. 그 결과 CHRK1 유전자는 shoot primordia stipule, flower buds, root meristem 등에서 발현되는 것을 보였다.

-CHRK1-GUS 분석을 통한 CHRK1 유전자의 호르몬을 비롯한 여러 외부자극에 의한 inducibility 조사: cytokinin, auxin 등의 호르몬 처리에 약하게 반응하였다.

-flower 조직을 이용한 endogenous CHRK1의 northern analysis를 수행하여 CHRK1

transgene이 높이 발현되고 endogenous gene이 suppression되는 것을 보였다.

-CHRK1 interacting protein의 yeast two hybrid screening: CHRK1 kinase domain을 bait로 100,000개의 colony를 yeast two hybrid로 분석하였다.

-CHRK1 interactor 유전자 분석: CHRK1 kinase domain을 bait로 분석한 결과 NtARCI이라고 명명된 amadillo motif와 U-box motif를 가지는 단백질이 CHRK1과 interact하는 것이 발견되었다. 이 단백질은 SRK receptor kinase들과 interact하며 self-incompatibility 작용의 downstream signaling element이다. 그러므로 NtARCI은 CHRK1의 signal transduction의 component라고 생각된다.

-CHRK1과 interactor 간의 in vitro protein binding assay

CHRK1 kinase domain을 GST에 fusion 시켜 recombinat protein을 제조 및 분리하였고 NtARCI은 in vitro translation시켜 GST resin을 이용하여 pull down assay를 수행하였을 때 Brassica ARCI,은 나오지 않고 NtARCI이 선택적으로 pull down 되었다.

2) FHT1 transcription factor (NtFHA1)의 식물세포 내 기능

-NtFHA1와 GFP의 융합단백질의 protoplast transfection을 통한 subcellular localization 연구를 수행하였는데 핵으로 targeting됨을 발견하였다.

-NtFHA1 유전자의 식물 조직 및 발생시기에 따른 발현을 조사하였을 때 대부분의 조직에서 발현되었고 종자발아시, 수정 후 여러 시기에도 발현되었다.

-NtFHA1 유전자의 genomic organization: genomic Southern analysis를 통하여 NtFHA1 유전자가 2 copy로 존재함을 밝혔다.

-NtFHA1 유전자와 cell cycle marker(histone H4와 cyclin B1 유전자)의 BY2 cell의 cell cycle 중 발현양상을 조사한 결과 NtFHA1은 S, G2, M phase에서 발현되며 G1에서는 발현 양이 매우 적었다. histone H4와 cyclin B1은 S와 M phase에 특이적으로 발현하였다.

-NtFHA1의 FHA domain을 yeast 내에서 과대발현하기 위하여 galactose-inducible system을 이용한 과대발현 vector를 제작하였고 yeast에서 발현하여 과대발현 형질을 조사한 결과 yeast의 성장이 크게 저하됨을 보였다.

-또한 FHA domain이 과대발현 됨을 northern analysis와 western blot을 통하여 확인.

-mutant FHA domain의 yeast 내 과대발현 phenotype 조사: NtFHA1-FHA domain을 yeast에서 과대발현 하였을 때 yeast growth가 크게 방해받았으나 FHA domain

mutant (Arg34 or Ser55)의 과대발현은 yeast growth에 영향을 주지않았다.

-yeast FHL1의 FHA domain과의 유사점 조사: NtFHA1과 yeast FHL1의 FHA domain은 유사하여 NtFHA1-FHA domain을 가지는 chimeric FHL1 및 FHL1 FHA domain의 과대발현 역시 yeast growth를 크게 방해한다.

-NtFHA1-FHA domain을 가지는 chimeric FHL1의 yeast *fh11* mutant의 complementation: yeast *Fhl1*의 FHA domain을 식물 NtFHA1의 FHA domain으로 치환하여 chimera를 만들어 *fh11* mutant로 넣었을 때 완전히 complementation을 할 수 있어 두 domain이 매우 유사함을 알 수 있다.

-FHA domain-overexpressing yeast cell들의 cell cycle analysis: overexpressing yeast cell은 *fh11* mutant 같이 성장이 매우 지연되는 phenotype을 보이는데 FACS를 이용하여 cell cycle 중 G1/S phase가 지연된다는 것을 보였다.

-FHA domain-overexpressing yeast cell들의 rRNA content 조사: northern blot을 이용하여FHA domain overexpressing yeast cell의 ribosomal RNA의 양이 훨씬 적다는 것을 밝혔다.

-FHA overexpressing yeast cell의 pre-rRNA processing을 *fh11* mutant와 비교분석: pre-rRNA들에 존재하는 ITS-1-1, ITS-1-2, ITS-2 sequence에 대응하는 primer를 이용하여 이들 overexpressor의 rRNA processing이 delay됨을 보였다. 또한 rRNA processing의 특별한 pathway가 아니라 전반적인 pathway전체가 delay되거나 abnormal 하였다.

-cFHL1의 deletion mutant의 *fh11* mutant의 complementation을 수행하였는데 FHL1 promoter에서는 완전히 complementation이 가능하나 GAL1 promoter를 이용했을 때는 전혀 complementation되지 않았다. 이 사실은 cFHL1이 FHL1의 기능을 정확하게 수행하고overexpression 시의 결과는 mutant phenotype과 일치한다는 것을 보인다.

-*fh11* deletion mutant와 cFHL1으로 complementation된 yeast의 pre-rRNA processing을 ITS primer들을 이용하여 분석하였을 때 *fh11*의 rRNA processing defect를 cFHL1이 완전히 복구시키는 것을 보였다. 또한 rRNA processing의 3 pathway 모두 *fh11* mutation에 의해 영향을 받는다.

-cFHL1 Δ 33의 제작 및 yeast *fh11* deletion mutant로의 complementation 가능성 조사: enzyme digestion을 통하여 33 아미노산을 deletion한 cFHL1 Δ 33을 제조하여 yeast로 transformation하였고 이 construct가 *fh11* deletion mutation을 complementation할 수 없었다

3) NtCDPK1 Ca⁺⁺-dependent kinase와 proteasome과의 상호작용기작

-정제된 NtCDPK1 deletion mutant protein들과 Nt21D7 deletion mutant protein의 in vitro interaction 탐구: in vitro binding assay를 통하여 두 단백질이 interaction 함을 보였다.

-NtCDPK1-GFP 융합단백질의 protoplast transfection을 통한 subcellular localization: 핵과 plasma membrane에 위치 함을 보였다.

-Arabidopsis protoplast를 이용하여 NtCDPK1와 Nt21D7를 green fluorescent protein (GFP)와 red fluorescent protein (RFP)를 융합시켜 subcellular targeting을 조사하였다. 그 종류는 다음과 같다.

a) NtCDPK1-GFP, b) Nt21D7-RFP, c) RFP-21D7, d) NLS-GFP

-NtCDPK1과 Nt21D7의 BY2 cell의 cell cycle 중의 발현 조사: 두 유전자는 S, G1 phase를 걸쳐 mid-M phase까지 같은 양상으로 발현된다.

-NtCDPK1과 Nt21D7의 protoplast transfection을 이용한 subcellular localization: GFP와 RFP tagging을 통하여 NtCDPK1과 Nt21D7이 핵과 plasma membrane으로 targeting되는 것을 확인하였고 세포 내에서 colocalization함을 보였다.

-NtCDPK1과 Nt21D7의 VIGS에 의한 gene silencing phenotype 조사: PVX genome을 가지는 VIGS용 PGR106 vector에 두 유전자의 cDNA를 cloning 하여 Agrobacterium infiltration을 이용하여 N. benthamiana식물체에 도입하였다. Nt21D7과 NtCDPK1 모두 잎의 세포 (특히 공변세포) 가 abnormal morphology를 가지고 cell death가 일어난다.

-NtCDPK1과 Nt21D7의 protoplast transfection을 이용한 subcellular localization을 수행.

-NLS-RFP와의 colocalization: NtRpn3-GFP 혹은 GFP-NtRpn3는 NLS(nuclear localization signal)-RFP와 핵에서 overlapping signal을 보인다. 그러나 핵외에도 NtRpn3는 NtCDPK1과 마찬가지로 plasma membrane에서 detect된다.

-NtCDPK1 kinase domain-GFP는 NtCDPK1 full length와 다르게 plasma membrane에만 detect 되는데 이 사실은 C-terminus의 calcium-binding domain이 NtCDPK1의 nuclear localization을 조절한다는 것을 의미한다.

-GFP와 RFP의 위치를 앞 혹은 뒤에 융합시켰을 때 targeting되는 양상은 변하지 않았다.

-onion cell로 particle bombard했을 때의 결과는 protoplast transfection과 일치하였다.

-NtCDPK1과 Nt21D7의 VIGS에 의한 gene silencing phenotype의 자세한 조사.

1) Cell morphology 및 programmed cell death

둘다 irregular cell division/expansion 및 irregular cell morphology pattern을 보였고 tissue에 HR-like lesion (NtCDPK1) 혹은 massive cell death (NtRpn3)가 일어남.

2) Gene expression analysis는 두 VIGS line 모두에서 HR cell death중에 발현되는 많은 PR 유전자들이 높이 발현되는 것을 보였다.

-NtCDPK1 promoter-GUS와 NtRpn3 promoter-GUS를 도입한 Arabidopsis 형질전환체 분석: Agrobacterium에 의한 transformation 후 T2 식물체에서 GUS assay를 수행한 결과 NtCDPK1와 NtRpn3 유전자 모두 shoot apex, root meristem 및 elongation zone, young flower bud등 cell division이 왕성한 곳에서 선택적으로 발현되었으며 이미 분화된 조직에서는 그 발현이 거의 없었다. 또한 auxin과 cytokinin 처리에 의해 GUS 발현이 shoot apex와 root meristem, elongation zone에서 크게 증가되었다. 이 사실은 두 유전자가 모두 cell division과 관련되어 있다는 사실과 auxin과 cytokinin의 phytohormone과의 관계도 시사하고 있다.

-NtCDPK1 expression의 RT-PCR analysis-특히 cell division과 관련하여 조사.

GUS assay를 뒷받침하기 위하여 담배에서도 RT-PCR을 이용하여 NtCDPK1과 NtRpn3 유전자의 발현을 여러 조직에서 조사하였다. 그 결과는 GUS assay와 정확히 일치하여 shoot apex, root meristem 및 elongation zone, young flower bud등 cell division이 왕성한 곳에서 선택적으로 발현되었으며 이미 분화된 조직에서는 그 발현이 거의 없었다.

V. 연구개발결과의 활용계획

- 신호전달 유전자 기능연구 방법의 세계적 수준 확보
- 국내의 고유성이 있으며 세계와 경쟁할 수 있는 식물계능 연구의 원천기술 확보
- 다수의 지적재산권을 확보하여 신 종자산업의 기반이 되는 원천기술을 개발
- 타작물로부터의 기능성 유전자의 발굴에 기여
- 타작물의 신품종을 유전공학적으로 개발하는데 기여
- 기능성유전자를 통한 기술료 수익
- 발굴된 유용 유전자의 경제작물로의 형질전환을 통하여 품종개량을 위한 육종소재로 개발
- 새로운 유용 유전자의 특허 획득 및 지적재산권의 산업화

주요 농작물에의 확대적용을 통한 고부가가치 신종자 개발 및 산업화
RNAi와 overexpression등으로 도출된 유용 유전자는 다양한 작물육종에 쓰일 것이
며 우수 품종 개발은 농업생산성의 증가로 연결될 것이다.
기능성 유전자들의 licensing과 기업으로의 기술이전을 추진하여 기술료 수익이 예상
되고 개발된 기술을 이용하여 벤처기업을 육성하는 등 산업적인 효과가 기대된다.
기술적인 측면으로는 식물 기능유전체 연구 관련기술을 개발하여 세계적 수준을 확보
하며 기능성유전자 분리 분석기술을 향상시킬 수 있다. 또한 다수의 식물 신호전달 유
전자의 기능을 대량으로 분석하므로써 우수논문을 발표하여 기초학문으로서의 가치가
크다.
개발된 기술을 활용 희망 연구자에게 이전. 또한 활용 희망자에게 발굴된 유전자들에
관한 정보 및 유전자 제공
분리된 기능성 유전자를 고추, 배추등 국내 종묘산업의 관심작물에 도입시켜 품종육
성

여 백

S U M M A R Y

The purpose of this study is to understand molecular mechanism of signal transduction pathways that regulate plant development. We planned to identify novel signaling components that modulate plant developmental processes, and to probe the protein-protein interaction in order to understand the global picture of developmental signal transduction network. In this research, we identified plant signal transduction genes, analyzed various signal transduction genes and proteins using molecular and biochemical tools, analyzed expression of signal transduction genes, analyzed functions of plant signal transduction genes, and carried out protein-protein interaction mapping to understand the cellular signaling network in plants. The results obtained in this projects were summarized below.

Using yeast two hybrid system, we identified NtRpn3, a regulatory subunit of 26S proteasome, as an interacting protein of NtCDPK1 calcium-dependent protein kinase in *Nicotiana tabacum*. Rpn3 in yeast is an essential protein involved in proteolysis of cell cycle regulatory proteins, and the carrot homologue of Rpn3 was previously isolated as a nuclear antigen that is mainly expressed in the meristem. NtCDPK1 physically interacts with NtRpn3 *in vitro* in a Ca²⁺-independent manner, and phosphorylates NtRpn3 in a Ca²⁺-dependent manner with Mg²⁺ as a cofactor. NtCDPK1 and NtRpn3 are colocalized in the nucleus, nuclear periphery and around plasma membrane *in vivo*. Both *NtCDPK1* and *AtRpn3*, an *NtRpn3* homolog of *Arabidopsis*, are mainly expressed in the rapidly proliferating tissues including shoot and root meristems, and developing floral buds. Virus-induced gene silencing of either *NtRpn3* or *NtCDPK1* resulted in the phenotypes of abnormal cell morphology and premature cell death in newly emerged leaves. Finally, NtCDPK1 interacts with NtRpn3 *in vivo* as shown by co-immunoprecipitation. Based on these results, we propose that NtCDPK1 and NtRpn3 are interacting in a common signal transduction pathway possibly for regulation of cell division, differentiation, and cell death in tobacco.

Proteasomes constitute the major machinery to degrade or process

proteins by ATP/ubiquitin-mediated proteolysis. Recent findings suggest a pivotal role of the ubiquitin/proteasome pathway in the regulation of apoptosis in animal cells. Here we show that virus-induced gene silencing of two different subunits of the 26S proteasome, the $\alpha 6$ subunit of the 20S proteasome and RPN9 subunit of 19S regulatory complex, both activated the programmed cell death (PCD) program, accompanied by reduced proteasome activity and accumulation of polyubiquitinated proteins. These results demonstrate that disruption of proteasome function leads to PCD in plant cells. The affected cells showed morphological markers of PCD including nuclear condensation and DNA fragmentation, accompanied by the 10-fold higher production of reactive oxygen species and increased ion leakage for three-fold. Similar to apoptosis in animal system, mitochondrial membrane potential was decreased, cytochrome *c* released from mitochondria to cytosol, and caspase 9- and caspase 3-like proteolytic activities detected in the cells. Interestingly, this proteasome-mediated PCD stimulated the expression of only a subset of transcripts that are highly induced during pathogen-mediated HR cell death, indicating that the two PCD pathways are differentially regulated. Taken together, these results provide the first direct evidence that proteasomes play a role in the regulatory program of PCD in plants. Controlled inhibition of proteasome activities may be involved in developmentally- or environmentally-activated plant cell death programs.

The 26S proteasome involved in degradation of proteins covalently modified with polyubiquitin consists of the 20S proteasome and 19S regulatory complex. The *NbPAF* gene encoding the $\alpha 6$ subunit of the 20S proteasome was identified from *Nicotiana benthamiana*. *NbPAF* exhibits high sequence homology with the corresponding genes from *Arabidopsis*, human and yeast. The deduced amino acid sequence of *NbPAF* reveals that this protein contains the proteasome α -type subunits signature and nuclear localization signal at the N-terminus. The genomic Southern blot analysis suggests that the *N. benthamiana* genome contains one copy of *NbPAF*. The *NbPAF* mRNA was detected abundantly in flowers and weakly in roots and stems, but it was almost undetectable in mature leaves. In response to stresses, accumulation of the *NbPAF* mRNA was stimulated by methyl jasmonate, NaCl and salicylic acid, but

not by abscisic acid and cold treatment in leaves. The NbPAF-GFP fusion protein was localized in the cytoplasm and nucleus.

NtFHA1 encodes a novel protein containing the FHA (Forkhead-associated) domain and the acidic domain in *Nicotiana tabacum*. NtFHA1 functions as a transactivator and targeted to the nucleus. The FHA domain of NtFHA1 is significantly homologous in sequences to that of Fhl1 forkhead transcription factor of yeast. *FHL1* was previously identified as a suppressor of RNA polymerase III mutations, and the *fh11* deletion mutant exhibited severe growth defects and impaired rRNA processing. Ectopic expression of the FHA domain of NtFHA1, but not its mutant form, resulted in severe growth retardation in yeast. Similarly, expression of Fhl1, its FHA domain, or the chimeric Fhl1 containing the NtFHA1-FHA domain also inhibited yeast growth. Yeast cells overexpressing the FHA domains of NtFHA1 and Fhl1 contained lower levels of mature rRNAs and exhibited rRNA processing defects similarly to the *fh11* null mutant. The chimeric Fhl1, but not the mutant form with a small deletion in its FHA domain, fully complemented the growth and rRNA processing defects of the *fh11* null mutant, demonstrating that the FHA domain of NtFHA1 can functionally substitute for the FHA domain of Fhl1. These results demonstrate that the FHA domains of NtFHA1 and Fhl1 are conserved in their structure and function, and that the FHA domain of Fhl1 is critically involved in regulation of rRNA processing in yeast. NtFHA1 function in plants may be analogous with that of Fhl1 in yeast.

여 백

CONTENTS

Chapter 1 Background and Significance.....	23
Chapter 2 State of Art.....	27
Chapter 3 Contents and Results of Research.....	31
Section 1: Molecular characteristics and differential expression of two nuclear factors containing the FHA domain in <i>Arabidopsis</i> .	
Section 2: CHRK1, a chitinase-related receptor-like kinase, interacts with NtARCL1, an armadillo repeat protein, in tobacco.	
Section 3: Activation of the programmed cell death pathway by inhibition of proteasome function in plants.	
Section 4: Interaction of NtCDPK1 calcium-dependent protein kinase with NtRpn3 regulatory subunit of the 26S proteasome in <i>Nicotiana tabacum</i> .	
Section 5: Molecular characterization of <i>NbPAF</i> encoding the $\alpha 6$ subunit of the 20S proteasome in <i>Nicotiana benthamiana</i> .	
Section 6: FHA domain of tobacco NtFHA1 and yeast FHL1 forkhead transcription factor is functionally conserved.	
Section 7: A novel dual-specificity protein kinase targeted to the chloroplast in tobacco.	
Chapter 4 Objectives of R & D and Contribution to the Research Field.....	103
Chapter 5 Application Plans.....	105
Chapter 6 Collected Information.....	105
Chapter 6 References.....	107

여 백

목 차

제 1 장 연구개발과제의 개요.....	23
제 2 장 국내외 기술개발 현황.....	27
제 3 장 연구개발수행 내용 및 결과.....	31
제 1절: Molecular characteristics and differential expression of two nuclear factors containing the FHA domain in <i>Arabidopsis</i> .	
제 2 절: CHRK1, a chitinase-related receptor-like kinase, interacts with NtARC1, an armadillo repeat protein, in tobacco.	
제 3 절: Activation of the programmed cell death pathway by inhibition of proteasome function in plants.	
제 4 절: Interaction of NtCDPK1 calcium-dependent protein kinase with NtRpn3 regulatory subunit of the 26S proteasome in <i>Nicotiana tabacum</i> .	
제 5 절: Molecular characterization of <i>NbPAF</i> encoding the $\alpha 6$ subunit of the 20S proteasome in <i>Nicotiana benthamiana</i> .	
제 6 절: FHA domain of tobacco NtFHA1 and yeast FHL1 forkhead transcription factor is functionally conserved.	
제 7 절: A novel dual-specificity protein kinase targeted to the chloroplast in tobacco.	
제 4 장 목표달성도 및 관련분야에의 기여도.....	103
제 5 장 연구개발결과의 활용계획.....	105
제 6 장 연구개발과정에서 수집한 해외과학기술정보.....	105
제 7 장 참고문헌.....	107

여 백

제 1 장 연구개발과제의 개요

세계인구의 폭발적인 증가와 생활수준의 향상으로 인한 식량수요의 급증으로 생산효율이 높고 자연환경에 내성이 강한 품종을 개발하여 단위경작지 당 작물생산성을 증가시키는 것은 현대 농업의 긴급한 문제이다. 이 목적을 위해서 유용 유전자의 발굴과 그 유전자들을 도입한 유전자조작 작물의 개발은 필수적인 전략이다. 이를 위하여 현재 이미 완료된 *Arabidopsis*와 벼의 전체유전체의 염기서열을 이용하여 유전자의 기능을 대량으로 밝히는 식물 기능유전체 연구에 전세계적인 경쟁이 치열할 전망이다. 즉 신기능성 유전자를 이용한 새로운 품종의 형질전환체 개발은 농업상업적으로 매우 중요하다. 이러한 상황 하에 국제적으로 경쟁력을 가지기 위해서는 식물의 특별한 기능에 초점을 맞춘 제한된 기능 유전체 연구가 전략적으로 효과적이라고 사료된다.

가역적인 단백질 인화작용은 거의 모든 생물학적 과정을 조절하는 핵심작용이다. 고등식물의 약 5%의 유전자가 단백질 인화작용에 의한 신호전달에 직접적으로 관련되어 있다. 그러나 현재 기능이 밝혀진 식물 신호전달 유전자는 매우 제한되어 있다. 현재까지 기능이 알려져 있지 않은 대다수의 신호전달 유전자들의 발현양상 분석과 기능탐구를 통하여 작물품질개량에 직접적으로 사용될 기능성 유전자원을 발굴하여 이용하는 것이 본 연구의 목표이다. 특히 본 연구팀은 식물발생 및 분화에서 조절기능을 가지는 신호전달 유전자에 특히 관심을 갖고 연구를 수행하였다. 담배와 야생담배(*Nicotiana benthamiana*)는 주요작물이자 model 식물체로서 분자생물학적 연구가 많이 되어있고 *Arabidopsis*보다 크기 때문에 생식기관이나 발생종자 등의 미세 조직을 얻기 쉬우며 최근에 개발된 virus-induced gene silencing 기술을 통해 유전자 기능을 어느 방법보다도 간단하게 분석할 수 있다는 장점을 가지고 있어 쌍자엽식물 중 *Arabidopsis*를 보완하는 시스템이라고 사료된다.

우리 나라 육종은 세계적 수준이며 많은 유전재료를 보유하고 있으나 농업적으로 중요한 유전특성 (내병성, 환경저항성 등)의 유전자 분리 개발 및 품종육성은 미흡한 상태이다. 따라서 쌀을 주식으로 하는 우리나라의 경제 및 대외 경쟁력을 고려하였을 때 기존의 우량품종에 내병성(특히 곰팡이 병 저항성)과 관련된 유전자들을 도입한 벼 품종개발로 환경친화적 농업개발이 요구된다 하겠다. 현재 전세계적으로 병충해에 의한 농업 생산성 감소는 총생산량의 36%에(James, 1996) 달하고 있으며 이중 곰팡이 병에 의한 피해는 12%를 차지하고 있다. 또한 병방제에 사용되는 농약은 전세계적으로 연간 \$27.8 billion (약 28조원)이 소요되어 막대한 비용 뿐 아니라 환경오염 및 인명에 대한 피해는 돈으로 계산하기 어려운 상황이다. 벼에 발생하는 곰팡이 병은 도열병(*Magnaporthe grisea*), 입고병(*Rhizoctonia*

solani)으로 대표될 수 있는 데 이 두가지 병에 의한 피해정도는 1975-1990년 사이에 조사된 바에 의하면 전세계적으로 매년 약 30%의 생산량 감소를 가져왔다 (Science, 1997).

식물에 있어서는 획기적인 형질전환 기법의 확립과 함께 현재 유전공학 기술로 1997년까지 전 세계적으로 3800여종의 신형질 작물이 포장시험 실시 중이며 50여종이 이미 상품화 되었고 대부분은 4-5년 내에 실용화 될 것으로 전망된다 (James, 1997). 이러한 신형질 작물의 출현은 유전자의 확보 및 새로운 유전자의 개발에 크게 의존하고 있어 이의 관련 유용 유전자의 개발 또한 매우 시급한 당면 과제이다. 총 1000억원의 예산으로 1991년부터 시작된 일본의 10개년 벼 게놈 연구는 지난 6년간의 연구결과 약 30,000개 유전자의 정보를 밝혀내었고, 2,000 여개의 표지유전자를 개발하여 벼 유용 유전자의 이용개발에 선도적 역할을 수행하고 있어서 벼의 분자생물학적인 정보가 다른 주곡작물에 비해 훨씬 많이 축적되어 있다. 국내연구로는 과기처 선도기술개발과제로 수행된 벼 게놈연구에서(1994 - 1997년) 6,000개의 미숙종자 발현 유전자를 개발 확보하였고 이중 400여종의 유전자의 기능이 확인되었다.

식물 형질전환에 사용되는 기술은 현재 유전자 총 (Particle Gun) 이용법이 널리 사용되고 있으며 (Kim et al, 1994) 최근에 *Agrobacterium*을 이용하는 방법이 개발되어 있고(Hiel et al, 1994) 국내에서도 이미 형질전환기술이 정착되어 있다 (Lee et al, 1998; Kim et al., 1998; Jang et al., 1998). 벼 형질전환 기술이 보급되면서, Bt toxin유전자 (Fujimoto et al, 1993) 혹은 Protenase inhibitor 유전자 (Ray Wu et al, 1994)를 이용한 내충성 벼, chitinase 유전자 도입에 의한 내병성 벼(Lin et al, 1995), RIP유전자 도입 및 제초제 저항성 벼 (Kim et al, 1998) 등이 개발되어 포장시험 중에 있다. 이와 같이 작물에 외래유전자를 도입함으로써 병 저항성, 환경친화형 품종을 개발하여 이용하는 방법은 기존의 방법보다 비용이 적게 들고, 농업생산성을 극대화 할 뿐 아니라 농약의 과다 사용에서 오는 환경과 괴를 막는 데 크게 기여 하게 될 전망이다. 또한 유전공학 기법에 의한 벼의 신품종 개발 기술을 확보하는 것은 다른 단자엽식물체의 형질전환에 파급 효과가 매우 크다고 사료된다. 형질전환 벼가 개발되면 재래 육종법과 상호보완적인 연구가 가능하여 전통적인 육종연구의 시간과 노력의 절감에 상당히 기여 할 것으로 기대된다.

특수기능을 가지는 고부가가치 생물공학이용 농업 신상품의 개발에 따른 수출증대가 가능하며 2000년도 수출전략 품목화으로서 고부가가치 신품종개발로 인한 농업생산성 향상 및 농가소득 증대에 일익을 담당하며 농업의 차세대 산업화 가능

성을 제시할수 있다. 또한 유용유전자의 확보로 미래에 분자생물학적 방법을 이용한 유용유전자 발현 작물을 손쉽게 확보할 수 있다. 세계시장의 추세에 미루어 볼 때 유전공학적 기법을 통해 재래적 육종방법으로는 불가능 했던 새로운 품종의 육종은 불가피함하므로 신품종 개발의 주도권을 확보하며 고유 브랜드를 육성하고 특성화된 작물의 우수품질 생산으로 타작물 수출에 기여할 것이다.

우리의 식문화는 쌀을 중심으로 발전해온 쌀의 문화이며, 논농사와 쌀은 우리의 문화와 전통풍습에 중요한 역할을 해 왔다. 벼농사는 홍수를 방지하며, 수자원을 함양하고 자연환경과 국토를 관리하는 엄청난 크기의 공익적 기능도 수행하고 있다. 따라서 벼농사는 자연환경의 보존기능과 전통문화의 존속이라는 다양한 공익적 기능을 가지고 있다. 그러나 현재 우리나라는 UR로 대표되는 농수산물 수출입 시장의 전면 개방, 농촌인구의 고령화, 타산업 대비 저부가가치, 농촌생활환경의 상대적 낙후 등으로 인하여 매우 어려운 상황에 직면해 있다. 이와같이 국제화 개방화시대의 한국농업의 위기를 효과적으로 대처하고 다가오는 21세기 선진국 시대의 농업의 위상을 정립하기 위한 방법으로 전통적인 농업생산 기술에 유전공학적인 기법을 접목 시키므로써 새로운 형태의 고 생산성 농업을 창출해낼 수 있을 것이다. 형질전환 식물체를 이용한 외래 유전자의 발현 및 이를 이용하여 새로운 형질을 가진 식물체를 개발하는 것은 차세대 농업의 성공여부를 좌우할 중요한 기술로 부각되고 있다. 최근의 외국농산물 수입등에 의한 안정적 소득작물의 개발이 시급한 실정에서 신품종의 농업작물이 개발된다면 그 경제성이 클 것이고 이를 통해서 UR등에 대비한 농업경쟁력 향상에 의한 농가소득 향상 및 국가경쟁력 향상이 이루어질 것이다. 우리나라의 고르지 못한 기후환경속에서 도열병 등 곰팡이 병에 의한 수도생산력 피해의 심각성을 생각할 때 병 저항성 벼 개발에 의한 경제 산업적인 효과는 짐작하기 어려울 정도로 클 것이며 환경친화적 형질전환작물의 개발은 안전한 식량공급과 생산성 제고에 크게 기여함으로써 보다 쾌적하고 안락한 생활을 가져다 줄 것으로 생각된다. 또한 막대한 양의 농약 사용에 따른 환경오염의 피해를 줄일 수 있고 농약사용에 따른 인명피해에 의한 농정 불안요인을 완화시킬 수 있다.

이 연구의 목적은 식물발달을 조절하는 신호전달체계의 분자적 기작을 이해하는 것이다. 이 연구를 통하여 식물발달 과정을 컨트롤하는 새로운 신호전달 유전자들을 발굴하며 각각의 신호전달 유전자 간의 상호작용을 탐구하므로서 식물발달 신호전달의 전체 네트워크를 이해하고자 하였다. 먼저 여러 식물조직 및 발생학적 시기의 신호전달 유전자를 동정하였고 northern blot analysis를 통하여 유전자발현을 탐구하였으며 여러 분자생물학적, 생화학적, 세포생물학적인 테크닉을 이용하여 신호전달 유전자와 단백질의 특성을 탐구하였다.

유전자의 식물발생관련 기능을 동정하기 위하여 RNAi, VIGS, 과대발현 등의 방법을 이용하였고 식물발생의 형태학적, 해부학적 연구를 위하여 tissue sections, scanning electron microscopy, transmission electron microscopy, confocal laser microscopy을 이용하였다. Yeast two hybrid 방법을 이용하여 신호전달단백질 상호작용에 관하여 연구하였고 식물 기능유전체적인 방법을 이용하여 세포 내 신호전달 네트워크를 조사하였다. 이러한 연구를 통하여 FHA transcription factor의 구조와 기능 (JBC 2002), proteasome과 NtCDPK1의 상호작용 (Plant J, 2003), proteasome의 suppression이 일으키는 programmed cell death (JBC, 2003) 등에 관한 논문들을 발표하였다.

제 2 장 국내외 기술개발 현황

세계인구의 폭발적인 증가와 생활수준의 향상으로 인해 필요한 식량의 양이 급속히 증가하고 있다. 100억 인구를 예상하는 2050년에는 현재 식량의 약 3배가 필요할 것으로 예상되고 있다. 비록 작물생산성은 아직 증가하고 있으나 그 증가율은 감소하고 있으며 이러한 현상은 주로 경작 감소와 지구환경의 악화로 인한 것인데 이미 전통 육종을 이용한 방법으로는 21세기의 100억 인구를 먹일 수 없다는 것이 널리 받아들여지는 견해이다. 그러므로 유일한 해결책은 생산효율이 높고 자연환경에 내성이 강한 Super 품종의 개발을 통하여 단위경작지 당 작물생산성을 증가하는 것이다. 이 목적을 위해서 유용 유전자의 발굴과 그 유전자들을 도입한 유전자조작 작물의 개발은 필수적인 전략이다. 이를 위하여 현재 이미 완료된 Arabidopsis와 벼의 전체유전체의 염기서열을 이용하여 유전자의 기능을 대량으로 밝히는 식물 기능유전체 연구에 전세계적인 경쟁이 치열할 전망이다. 즉 신기능성 유전자를 이용한 새로운 품종의 형질 전환체 개발은 농업상업적으로 매우 중요하다. 야생종을 비롯한 다양한 식물로부터 유용 유전자를 발굴하고 그 유전자들을 경제작물에 도입하여 개량형질의 우수품종을 개발하는 것이 새로운 전략이다. 따라서 현재 전세계적으로 기능성 유전자 발굴을 위한 경쟁이 치열하다.

농업생명공학의 전세계적인 매출규모는 의약생명공학에 비해 적을 것으로 예상된다. 미국의 1996년 농업생명공학 관련 매출은 3억불이었으며 의약생명공학은 860억불이었다. 그러나 농업생명공학 상품 수익은 현재 제 1세대 형질전환체의 목적형질인 input 농업형질에서 작물의 특별한 영양을 강화시킨 output 품질형질로 전환하면서 곧 크게 증가하리라고 예상되며 최근 Du Pont사와 Pioneer사와의 합병은 그 시장을 목표한 것이라고 예측된다. 이미 종자, 농약 산업계는 이미 지난 2년간 80억불을 기업인수에 투자하였으며 생명공학기술 관련 인수 합병은 당분간 계속될 것으로 전망된다. 형질전환작물의 재배 면적은 북아메리카, 호주, 중국에서 크게 증가하리라고 생각되며 형질전환작물의 전세계 시장 규모는 1996년의 5억불 미만에서 2000년의 20-30억불, 2005년의 60억불, 2010년의 200억불로 신장할 것으로 예측된다. 그러므로 신품종 형질전환식물제조에 필수불가결한 유전자원 확보는 경제적으로 매우 중요하다 하겠다.

표8. 형질전환 식물의 세계시장 규모

연 도	시장규모 (억불)
1995	0.75
1996	2.35
1997	6.20
1998	15
2000	30
2005	60 (추정)
2010	200 (추정)

유용유전자 자원을 먼저 확보하여 활용하는 것은 고부가가치를 창출할 수 있을 뿐 아니라 선진국의 식량시장, 생물산업과 기술의 독점을 견제하여 국가경제적으로 중요한 일이다. 현재 유용유전자는 특허에 의하여 보호받고 있으며 이를 선점하는 것은 미래 생명공학 경쟁력의 핵심이라 하겠다.

현재 지구상에는 8억에 해당하는 인구가 심각한 기아와 영양 부족으로 고통 받고 있으며 이런 상황에서도 세계 곡물 재고는 13% 수준으로 떨어져 해마다 곡물 가격이 상승하고 있어 식량의 자원화가 어느 때 보다도 필요한 실정이다. 식량 자유무역이 더욱 확대되는 현재실정 하에서 우리나라와 같은 식량 수입국들은 앞으로 더 큰 폭으로 시장을 개방하지 않을 수 없어 국내 농가뿐 아니라 전체 경제에 큰 타격이 예상된다. 우리나라 곡물 생산은 비교적 소규모로 국가의 경제 상태만 고려한 추곡 수매가에 의하여 농민들의 소득이 크게 좌우되는 실정이므로 새로운 유전자의 확보를 통한 분자 육종으로 전체 생산량을 높이게 되어 농민 경제의 안정을 가져오게 된다

계놈연구는 계놈구조연구 (Structural Genomics)와 계놈기능연구 (Functional Genomics)로 구분하는데 계놈구조연구의 목표가 염기서열완성 그 자체인데 비해 계놈기능연구는 혁신적인 기술을 개발하여 계놈구조로부터 광범위하게 도출된 유전정보를 이용하여 전체유전자의 생체 내 기능을 유추하는 것이다. 따라서 계놈기능 연구의 전략은 기존의 단일 유전자의 기능 연구가 아닌 통합적 방법을 통해 한번에 모든 유전자를 대상으로 하는 기능분석을 지향한다. 유전자의 기능을 밝히는 방법은 insertional mutagenesis, antisense suppression, activation tagging 등 다양한 유전적 방법이 있으며 단백질 수준에서 기능을 유추하는 proteomics 분야도 최근 급성장하고 있다. 최근 애기장대와 벼의 전체유전자 sequencing이 종료되었으며 physical map 작성 및 EST 분석 등 유전체구조 연구가 병행되었다. 범국가적인 협동과 기술혁신으로 위의 목표는 조기 달성되고 있으며 유전체 구조로부터 광범위하게 도출된 유전정보를 이용하여 전체

유전자의 생체내 기능을 유추하는 기능유전체 연구에 관심이 집중되고 있다. 또한 전체 유전자 sequencing이 어려운 다양한 농작물에서 EST analysis와 특정한 분야에 초점을 둔 기능유전체연구가 활발히 진행되고 있다.

국내에서는 농업과학기술원, 포항공대, 경상대에서 벼 구조 및 기능유전체 연구를 적극적으로 수행하고 있고 그외 식물의 기능유전체 연구는 포항공대와 금호연구소등에서 수행되고 있다.

여 백

제 3 장 연구개발수행 내용 및 결과

가. 논문 (8건)

1. J.-W. Ahn, M. Kim, J. W. Bang, and H.S. Pai* (2003) Molecular characteristics and differential expression of two nuclear factors containing the FHA domain in *Arabidopsis*. **Plant Science**, In Press.
2. M. Kim, H.S. Cho, J.H. Lee, and H.S. Pai* (2003) CHRK1, a chitinase-related receptor-like kinase, interacts with NtARCl, an armadillo repeat protein, in tobacco. **BBA-Proteins and Proteomics**, In Press.
3. M.C. Suh, S.-K. Oh, Y.-C. Kim, H.-S. Pai, and D. Choi* (2003) Expression of a novel tobacco gene, NgCDM1, is preferentially associated with pathogen-induced cell death. **Physiol. Mol. Plant Pathology**, In Press.
4. M. Kim, J.-W. Ahn, O. Jin, K.-H. Paek, H.S. Pai*. (2003) Activation of the programmed cell death pathway by inhibition of proteasome function in plants. **Journal of Biological Chemistry**, 278, 19406-19415.
5. S.S. Lee, H.S. Cho, G.M. Yoon, J.-W. Ahn, H.H. Kim, H.S. Pai*. (2003) Interaction of NtCDPK1 calcium-dependent protein kinase with NtRpn3 regulatory subunit of the 26S proteasome in *Nicotiana tabacum*. **The Plant Journal**, 33: 825-840
6. M. Kim, K.-S. Yang, Y.-K. Kim, K.-H. Paek, H.S. Pai* (2003) Molecular characterization of *NbPAF* encoding the $\alpha 6$ subunit of the 20S proteasome in *Nicotiana benthamiana*. **Molecules and Cells**, 15; 127-132
7. M. Kim, J.-W. Ahn, K. Song, K.-H. Paek, H.S. Pai*. (2002) FHA domain of tobacco NtFHA1 and yeast FHL1 forkhead transcription factor is functionally conserved. **Journal of Biological Chemistry** 277; 38781-38790.
8. H.S. Cho, G.M. Yoon, I. Hwang, Y.A. Kim, D. Choi, H.S. Pai* (2001) A novel dual-specificity protein kinase targeted to the chloroplast in tobacco. **FEBS Letters** 497: 124-130 (Cover Story)

나. 특허등록 (3건)

1. 식물호르몬 지베렐린의 신호전달과정에 관여하는 새로운 키나제 및 그 유전자, 2001년 7월 27일, 등록번호: 305281, 한국, 한국생명공학연구원
2. 키틴결합능이 있는 새로운 수용체 키나제, 그 유전자 및 그의 용도, 2001년 11월 5일, 등록번호 314907, 한국, 한국생명공학연구원
3. 키틴결합능이 있는 새로운 수용체 키나제 및 그 유전자, 2002년 6월 25일, 등록번호 6,410,706, 미국, 한국생명공학연구원

여 백



ELSEVIER

Available online at www.sciencedirect.com

SCIENCE @ DIRECT®

PLANT
SCIENCE

Plant Science xxx (2003) xxx–xxx

www.elsevier.com/locate/plantsci

Molecular characteristics and differential expression of two nuclear factors containing the FHA domain in *Arabidopsis*

Joon-Woo Ahn^{a,b}, Moonil Kim^a, Jae Wook Bang^b, Hyun-Sook Pai^{a,*}

^a *Laboratory of Plant Genomics, Korea Research Institute of Bioscience and Biotechnology, Oun-dong 52, Yusong-gu, Taejeon 305-333, South Korea*

^b *Department of Biology, Chungnam National University, Taejeon 305-764, South Korea*

Received 9 May 2003; received in revised form 23 June 2003; accepted 1 July 2003

Abstract

The forkhead-associated (FHA) domain identified in a wide variety of proteins is a small module that recognizes phosphothreonine epitopes on proteins. *AtFHA1* and *AtFHA2* of *Arabidopsis* are homologs of tobacco *NtFHA1* encoding a FHA domain-containing transcription activator. Previously, we showed that the FHA domain of *NtFHA1* functionally substitutes for that of the Fhl1 forkhead transcription factor involved in rRNA processing in yeast, despite significant differences in their protein structures. In this study, we characterized *AtFHA1* and *AtFHA2* of *Arabidopsis* and analyzed their expression patterns. *AtFHA1* and *AtFHA2* contain an N-terminal FHA domain and a C-terminal acidic region, but lack any known DNA-binding motifs. Both proteins were targeted to the nucleus. GUS staining of transgenic *Arabidopsis* plants containing the promoter-GUS fusion gene demonstrated high expression of *AtFHA2* in whole tissues throughout plant development. In contrast, *AtFHA1* was temporally expressed at low levels in roots and vascular tissues of stems. Interestingly, *AtFHA1* expression was significantly induced in whole plants in response to external stimuli. The observed differential expression of *AtFHA1* and *AtFHA2* implies that these two genes have distinct regulatory roles in *Arabidopsis*.

© 2003 Published by Elsevier Ireland Ltd.

Keywords: Forkhead-associated domain; Nuclear localization; Promoter-GUS fusion; rRNA processing

1. Introduction

Forkhead-associated (FHA) domains are highly diverse protein-protein interaction modules characterized by a 55–75 residue motif [1]. Recent studies have shown that FHA is a modular phosphopeptide recognition domain, with specificity for phosphothreonine-containing epitopes [2]. FHA domains were initially identified in a group of forkhead transcription factors [1] and have since been found in more than 200 different proteins, ranging from prokaryotes to higher eukaryotes. The domain is associated with proteins involved in numerous processes, including signal transduction, transcription, protein transport and DNA repair [2].

Rad53, a protein kinase involved in DNA damage response and cell cycle arrest in yeast, contains two FHA domains separated by a central Ser/Thr kinase domain [3]. Other FHA-containing kinases, include DUN1 and MEK1 of yeast, function in DNA replication and repair within the nucleus [4]. The kinesin family is the largest group of FHA-containing proteins in eukaryotes. More than 20 different kinesin-like proteins contain FHA domains [2]. The FHA domain is located close to the active site of kinesin KIF1A. It is, therefore, proposed that the transport process mediated by KIF1A is regulated by FHA-mediated phosphorylation-dependent interactions [5]. Some ring finger proteins, such as yeast dma1 and human Chfr, also contain the FHA domain [6,7]. These two proteins possibly function in the cell cycle checkpoint pathway [6,7]. The presence of the ring finger (a catalytic motif in a variety of E3 ubiquitin ligases) in FHA-containing proteins is highly suggestive of a role in protein ubiquitination and degradation [8].

* Corresponding author. Tel.: +82-42-860-4195; fax: +82-42-860-4608.

E-mail address: hyunsook@kribb.re.kr (H.-S. Pai).

59 In plants, the FHA domain was identified in *Arabidopsis*
60 kinase-associated protein phosphatase (KAPP) through
61 interaction cloning using an *Arabidopsis* receptor-like
62 kinase as bait [9]. The FHA domain in KAPP is involved
63 in phosphorylation-dependent protein-protein interac-
64 tions with various receptor-like kinases [10]. Unlike
65 many FHA-containing proteins localized in the nucleus,
66 KAPP is involved in plant receptor kinase signaling
67 pathways on the inner face of the plasma membrane.

68 In *Saccharomyces cerevisiae*, several forkhead trans-
69 cription factors, including Fhl1, Fkh1 and Fkh2,
70 contain the FHA domain in addition to the forkhead
71 DNA-binding domain [11–14]. Fkh1 and Fkh2 are
72 master regulators of G2-specific transcription in yeast
73 [14,15]. These proteins are components of the Swi5
74 factor and regulate transcription of the *CLB2* and *SIC1*
75 cluster [14]. Fhl1 is a multicopy suppressor of mutations
76 in RNA polymerase III and its transcription factor,
77 TFIIC. Mutation of *FHL1* leads to aberrant rRNA
78 processing [12]. Thus Fhl1 plays a role in the control of
79 RNA polymerase III transcription and rRNA matura-
80 tion, presumably by acting as a transcriptional regulator
81 of genes specifically involved in those processes.

82 Previously, we showed that the FHA domains of
83 NtFHA1, a novel transcriptional activator in tobacco,
84 and of yeast Fhl1 forkhead transcription factor have
85 conserved functions in the regulation of cell growth and
86 rRNA processing in yeast [16]. NtFHA1 is a small
87 protein of 209 amino acids which contains the FHA
88 domain and an acidic region, while yeast Fhl1 consists
89 of 936 amino acids, including two large acidic domains
90 at the N and C termini, FHA domain, and a DNA-
91 binding forkhead domain in the center. Despite the
92 significantly different overall structures of the two
93 proteins, the FHA domains of NtFHA1 and Fhl1 are
94 functionally interchangeable. Ectopic expression of the
95 FHA domains of these two proteins induced rRNA
96 processing defects in yeast, leading to severe growth
97 retardation, similar to that observed with the *fhl1* null
98 mutation. Chimeric Fhl1 containing the FHA domain of
99 NtFHA1 was fully functional in regulating rRNA
100 processing as well as yeast growth. Our data further
101 demonstrated that the FHA domain of Fhl1 is critically
102 involved in the regulation of rRNA processing in yeast
103 [16]. The results indicated that the function of NtFHA1
104 in plant cells is analogous to that of yeast Fhl1 in rRNA
105 processing and RNA polymerase III transcription,
106 probably by associating with other transcription factors.

107 In this study, we identified and characterized two
108 homologs of NtFHA1 in *Arabidopsis*, designated
109 *AtFHA1* and *AtFHA2*. Expression patterns of the two
110 genes were investigated by analyzing *Arabidopsis* trans-
111 genic plants expressing the promoter-GUS fusion gene.
112 *AtFHA1* and *AtFHA2* displayed significantly different
113 patterns of expression. *AtFHA2* expression was strong,
114 constitutive, and tissue-general, while *AtFHA1* expres-

sion was temporal and induced in response to external
stimuli, indicating that these two genes may have
different regulatory roles. The *AtFHA2* promoter may
be employed to drive transgene expression to high levels
in the plant system.

2. Materials and methods

2.1. Cloning of *AtFHA1* and *AtFHA2* cDNA

AtFHA1 and *AtFHA2* cDNA were cloned by PCR
using an *Arabidopsis* cDNA library as template. PCR
amplification was performed with 1 U of Taq DNA
polymerase (Promega), 100 μ M of each dNTP, and
100 pmol forward and reverse primers (for *AtFHA1*,
5'-ATGGCTACAGCCGTTGGA-3' and 5'-TCAGG-
GATAGCCCAGTCT-3'; for *AtFHA2*, 5'-ATGGC-
TACGGCTGTTGGT-3' and 5'-TCATGAGAGTA-
GGGTAAC-3'). PCR products were cloned into pBlue-
script vector, and confirmed by sequencing.

2.2. Nuclear localization of *AtFHA1*- and *AtFHA2*-GFP proteins

AtFHA1 and *AtFHA2* cDNA fragments containing
the entire protein coding regions were amplified by PCR
and cloned into the 326-GFP vector [17], using *Bam*HI
to generate a GFP in-frame fusion under control of the
cauliflower mosaic virus 35S promoter. *AtFHA1*-GFP
and *AtFHA2*-GFP plasmids were introduced into onion
epidermal cells by particle bombardment. Expression of
fusion constructs was monitored at 12 h after transfor-
mation using a Zeiss Axioplan fluorescence microscope
(Jena, Germany). XF116 filters (exciter, 474AF20;
dichroic, 500DRLP; emitter, 510AF23) were employed
to visualize the green fluorescent protein (GFP). To
mark nuclei, the same onion epidermal layers were
stained with DAPI (100 μ g/ml) for 30 min, prior to
microscopic observation.

2.3. GUS histochemical assay

The *AtFHA1* (1.1 kb) and *AtFHA2* (2.0 kb) promo-
ters were isolated by PCR using the *Arabidopsis*
genomic DNA as a template. Primers used for PCR
amplification include: 5'-ATCAAGCTTACGAAAAG-
TACCGAGACG-3' and 5'-ATCGGATCCGCCGT-
GAAATTTCTCCGA-3' for *AtFHA1*, and 5'-
ATCGTCGACATTGGAGCATTAAAGTTA-3' and
5' ATCGGATCCGCCGTGAAATTCTCCGAT-3' for
AtFHA2. Promoters were cloned into the pBI101 vector
using *Sal*I/*Bam*HI sites to generate in-frame *AtFHA1*
promoter- or *AtFHA2* promoter-GUS fusion genes.
Fixation, staining and clearing of transgenic *Arabidopsis*
plants (ecotype Columbia) with X-Gluc were performed,

163 as described previously [18]. To determine the inducible
164 expression of *AtFHA2*, *AtFHA2::GUS* seedlings were
165 treated with 1 μ M auxin (2,4-D and IAA), 1 μ M
166 cytokinin (zeatin), 5 μ M brassinosteroid, 10 μ M ABA,
167 and 10 μ M gibberellin (GA_3) for 24 h before the GUS
168 assay was performed. For hypoxia, the *AtFHA2::GUS*
169 seedlings were submerged under water for 24 h prior to
170 the GUS assay.

171 2.4. RNA gel blot analysis

172 For RNA gel blot analysis, total RNA was prepared
173 by using TRIzol™ Reagent (GIBCO-BRL) following
174 manufacturer's instructions. Approximately 20 μ g of
175 total RNA was electrophoresed on an agarose gel
176 containing 5.1% (v/v) formaldehyde and blotted onto
177 Hybond-N Nylon membrane. The membrane was
178 hybridized with a 96 bp probe containing the C-terminal
179 end of the *AtFHA2* coding region, which is absent in
180 *AtFHA1*. The probe was synthesized by PCR using two
181 primers (5'-CTGGAGGAAAAAGATGTT-3' and 5'-
182 ACCGAATGAAGTTTTTCC-3'), and *AtFHA2* cDNA
183 as a template. Prehybridization and hybridization was
184 carried out in 5 \times SSC, 5 \times Denhardt's solution, and
185 0.5% SDS at 60 °C overnight. The membranes were
186 washed twice in 2 \times SSC and 1% SDS at room
187 temperature, then washed in 0.1 \times SSC and 0.1% SDS
188 at 60 °C for 30 min.

189 3. Results

190 3.1. *Arabidopsis AtFHA1 and AtFHA2 are putative* 191 *homologs of tobacco NtFHA1*

192 *AtFHA1* (GenBank AAF20220.1) and *AtFHA2*
193 (GenBank AAF20224.1) encode proteins of 251 and
194 320 amino acids with estimated molecular weights of
195 27980 and 35994 Da, respectively. These proteins are
196 putative functional homologs of the NtFHA1 transcrip-
197 tion activator of tobacco, whose FHA domain is
198 functionally conserved with that of the yeast forkhead
199 transcription factor Fhl1 [16]. *AtFHA1*, *AtFHA2* and
200 NtFHA1 contain the FHA domain in the N-terminus
201 and an acidic region as a putative transactivation
202 domain at the C-terminus, but lack any known DNA-
203 binding motifs (Fig. 1A). Yeast Fhl1, comprised of 936
204 amino acids, contains two large acidic domains at the N
205 and C termini, the FHA domain and a DNA binding
206 forkhead (FH) domain in the center (Fig. 1A). The
207 sequence homology between NtFHA1, *AtFHA1* and
208 *AtFHA2* is very high within the FHA domain (94–95%
209 identity), but lower in the other regions (Fig. 1B).
210 *AtFHA1* and *AtFHA2* exhibit extremely high sequence
211 identity, except at the C-terminal end of the protein-
212 coding region (Fig. 1B). All the residues conserved in the

213 FHA domains of animal and yeast proteins are present
214 in these three proteins, except that the Asn residue is
215 replaced by Glu (marked in Fig. 1B). FHA domains of
216 NtFHA1, *AtFHA1* and *AtFHA2* display significant
217 sequence similarity to that of yeast Fhl1. An alignment
218 of the FHA domains of *AtFHA1*, *AtFHA2* and Fhl1 is
219 shown in Fig. 1C. The FHA domain of NtFHA1
220 displays 46% amino acid sequence identity to that of
221 Fhl1 [16], while *AtFHA1* and *AtFHA2* exhibit 43%
222 identity to Fhl1 in the FHA domain. Full-length
223 *AtFHA1* and *AtFHA2* cDNA were isolated from an
224 *Arabidopsis* cDNA library using PCR.

225 *AtFHA1* and *AtFHA2* are among 15 FHA domain-
226 containing ORFs in the *Arabidopsis* genome database.
227 Among these, only the biological functions of KAPP
228 [9,10] and zeaxanthin epoxidase [19,20] have been
229 characterized. Alignment of the FHA domains of the
230 15 *Arabidopsis* ORFs reveals a number of conserved
231 amino acid residues (Fig. 2A). Seven conserved residues
232 (marked in Fig. 2A) within the FHA domain have been
233 identified in animal and yeast systems. Based on the
234 structures of the FHA domains of yeast Rad53 and
235 human Chk2, the FHA homology region encompasses
236 multiple β strands interspersed between the three loops
237 that bind to the phosphothreonine peptide [21,22]. Six of
238 the seven conserved residues (except the most C-
239 terminal Asn residue) are located close to the peptide-
240 binding site [21,22]. Thus the conserved residues of the
241 FHA domain are either associated with direct ligand
242 interactions or form the structural framework upon
243 which peptide binding loops are displayed. The three
244 residues (two Asn and one Gly) near β -sheets 7 and 8
245 conserved in the FHA domains of animal and yeast
246 proteins, were not strictly conserved in *Arabidopsis*
247 FHA domains, while other four residues were highly
248 conserved (Fig. 2A). Although the roles of the conserved
249 residues in the *Arabidopsis* FHA domains remain to be
250 determined, their positions in the vicinity of the
251 predicted β -sheets suggest that at least some are required
252 for the formation of the β -sheet structure of the FHA
253 domain (Fig. 2A). Phylogenetic analysis of the FHA
254 domains of 15 *Arabidopsis* proteins and NtFHA1
255 clearly reveals that NtFHA1 is grouped with *AtFHA1*
256 and *AtFHA2* (Fig. 2B).

257 3.2. Nuclear localization of *AtFHA1* and *AtFHA2*

258 Cellular localization of *AtFHA1* and *AtFHA2* was
259 examined by constructing fusion proteins with GFP
260 expressed under the control of the CaMV 35S promoter
261 (Fig. 3). The fusion constructs, *AtFHA1-GFP* and
262 *AtFHA2-GFP*, were introduced into onion epidermal
263 cells by particle bombardment. After incubation for 12 h
264 at 25 °C, expression of the introduced genes was
265 examined under a fluorescent microscope. As a positive
266 control for nuclear localization, the same epidermal

267 layer was stained with DAPI, prior to microscopic
268 observation. The green fluorescent signal completely
269 overlapped with DAPI staining in the nucleus, indicat-

ing that both AtFHA1 and AtFHA2 were targeted to
the nucleus (Fig. 3). In contrast, the GFP control was
mainly localized in the cytosol.

270
271
272

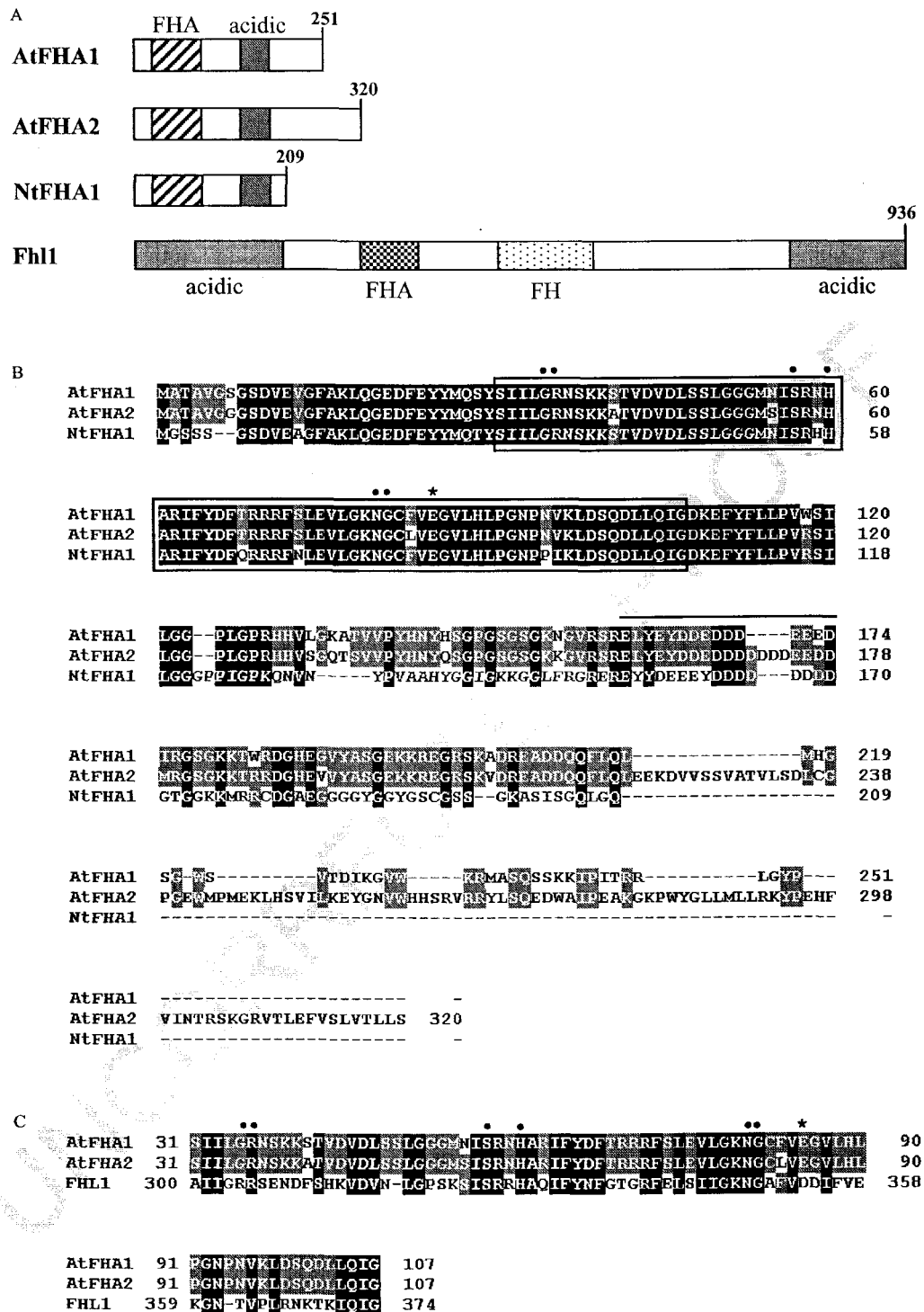


Fig. 1

273 3.3. *AtFHA2* is constitutively expressed in whole plant
274 tissues at a high level

275 The expression patterns of the two genes were
276 investigated by generating transgenic *Arabidopsis* plants
277 containing *AtFHA1* promoter-*GUS* and *AtFHA2* pro-
278 moter-*GUS* fusion constructs. *AtFHA1::GUS* and *AtF-*
279 *HA2::GUS* fusion constructs were comprised of the 1.1
280 kb *AtFHA1* and 2.0 kb *AtFHA2* promoters fused in-
281 frame to the *GUS* gene, respectively. Histochemical
282 *GUS* staining disclosed strong *AtFHA2* expression in
283 whole tissues from the earliest stages of seedling devel-
284 opment to mature plants (Fig. 4A–K). In particular, the
285 shoot apex and vascular tissue were strongly stained
286 (Fig. 4B, F). *GUS* staining in the roots was also strong,
287 particularly in the root meristem and elongation zone
288 (Fig. 4C, E). In flowers, *AtFHA2* was strongly expressed
289 throughout the reproductive meristem and all four
290 whorls of flower buds (Fig. 4J). In general, high levels
291 of *AtFHA2* were observed in all the plant tissues
292 examined throughout the entire developmental stage.

293 We also examined the expression of *AtFHA2* mRNA
294 in different *Arabidopsis* tissues, using RNA gel blot
295 analysis. The probe employed was a 96 bp amplified
296 DNA fragment corresponding to the C-terminal end of
297 the *AtFHA2* coding region, which is absent in *AtFHA1*.
298 The 1.5 kb *AtFHA2* transcript was strongly detected in
299 all the tissues examined, with the lowest levels in mature
300 leaves (Fig. 5). This expression pattern is consistent with
301 *GUS* staining observed in *AtFHA2::GUS* transgenic
302 plants (Fig. 4).

303 3.4. *AtFHA1* expression is low, but stimulated by
304 external stimuli

305 Histochemical *GUS* staining of *Arabidopsis* plants
306 containing the *AtFHA1::GUS* fusion gene revealed low
307 expression of *GUS* activity in roots and vascular tissues
308 near the shoot apex in young seedlings (Fig. 6A–C).
309 However, as plants developed, *AtFHA1* expression was
310 no longer detected in any of the tissues, including roots,
311 flowers and leaves (Fig. 6D–F). Thus, *AtFHA1* expres-
312 sion appears to be developmentally regulated. This low
313 expression of *AtFHA1* prompted us to examine whether
314 the levels were elevated by external stimuli. Phytohor-
315 mones, including auxin, cytokinin, gibberellin, abscisic
316 acid and brassinosteroid, and abiotic stress factors, such

as hypoxia, significantly enhanced *GUS* staining in the
shoot apex, roots and vascular tissues in leaves (Fig.
6G–K). In flowers, *GUS* staining was detected in the
anther, stamen, petal and receptacle, in response to the
stimuli. These results clearly demonstrate that *AtFHA1*
expression is induced by external stimuli, including
hormones and stress factors.

324 3.5. Discussion

325 Two *Arabidopsis* homologs of NtFHA1 in tobacco,
326 *AtFHA1* and *AtFHA2*, have been identified and
327 characterized. These are small proteins comprised of
328 the FHA domain and an acidic region. The proteins
329 constitute the only group of FHA-containing nuclear
330 factors in plants. Recent findings have suggested that
331 FHA domain is significantly larger than the previously
332 described FHA homology region [2,23]. The domain
333 spans approximately 80–100 amino acid residues folded
334 into an 11-stranded β sandwich, which sometimes
335 includes small helical insertions between the loops
336 connecting the strands. The FHA homology region
337 spans only eight β -strands (β 3– β 10) on one face of the
338 sandwich [21]. The homology between NtFHA1 and
339 *AtFHA* proteins is mostly limited to the N-terminal
340 region (including the FHA homology region; marked in
341 Fig. 1B). Between positions 8 and 123, only six residues
342 of *AtFHA1* and seven residues of *AtFHA2* are distinct
343 from the corresponding sequence of NtFHA1 [16]. The
344 entire region spanning residues three to 123 in *AtFHA1*
345 and *AtFHA2* possibly constitutes the functional FHA
346 domain. Other parts of the amino acid sequences of
347 *AtFHA1* and *AtFHA2* are significantly different from
348 NtFHA1, except for a small area enriched with acidic
349 amino acid residues. The data indicate that the FHA
350 domain is functionally important in this group of
351 proteins. Indeed, the FHA domain of NtFHA1 plays a
352 critical role in the regulation of growth and rRNA
353 processing in yeast by mimicking the function of the
354 FHA domain of the yeast Fhl1 forkhead transcription
355 factor [16]. The structural and functional conservation
356 of the FHA domains of Fhl1 and NtFHA1 strongly
357 suggests that the plant factors play similar roles as yeast
358 Fhl1. However, the mechanisms of action of the two
359 proteins are possibly different, since the plant factors
360 lack the forkhead DNA-binding domain identified in
361 Fhl1. NtFHA1, *AtFHA1*, and *AtFHA2* proteins may

Fig. 1. Structure and amino acid sequence comparison of *AtFHA1* and *AtFHA2*. (A) Schematic representation of *AtFHA1* and *AtFHA2* proteins of *Arabidopsis* in comparison with tobacco NtFHA1 and yeast Fhl1. The FHA homology region (FHA) [23], forkhead domain (FH), acidic domain, and residue numbers are indicated. (B) Deduced amino acid sequences and alignment of *AtFHA1*, *AtFHA2* and NtFHA1. The numbers on the right indicate amino acid residues. Gaps, which were introduced to maximize alignment, are indicated by dashes. Residues conserved in all three sequences are boxed in black, and those conserved in two of the compared sequences are boxed in light gray. FHA homology and acidic regions are indicated by brackets and overlining, respectively. Conserved residues in the FHA domain are marked with filled circles above the sequences. The conserved Asn residue of the FHA domain replaced by Glu in the aligned sequences is indicated by asterisks. (C) Sequence alignment of the FHA homology region of *AtFHA1*, *AtFHA2* and yeast Fhl1.

362 interact with other transcription factors to produce a functional transcription complex. Fkh2, a yeast fork- 363

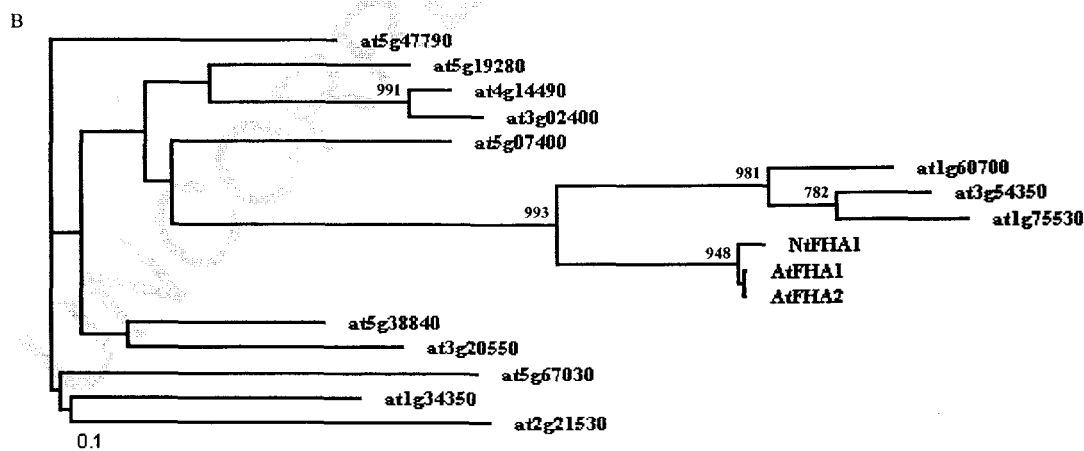
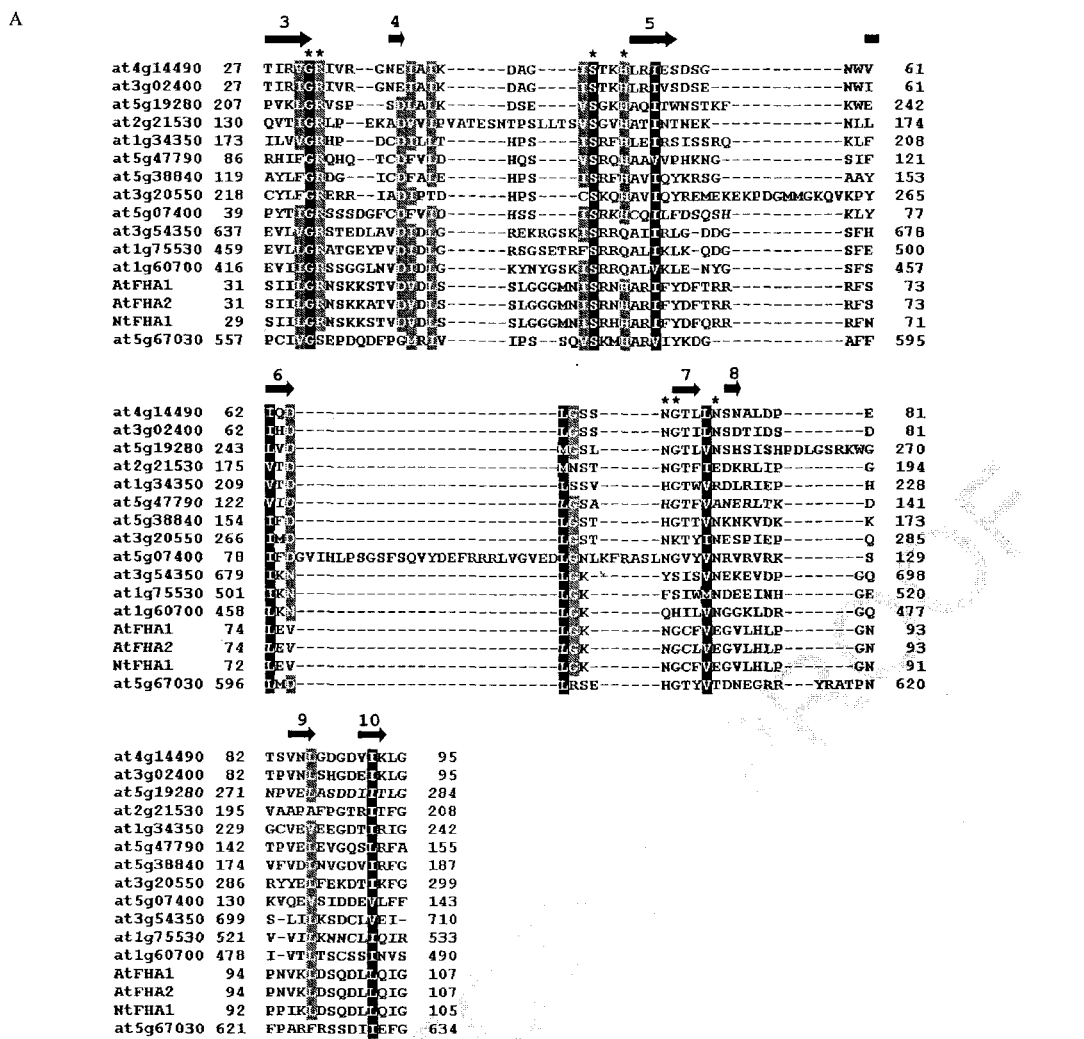


Fig. 2

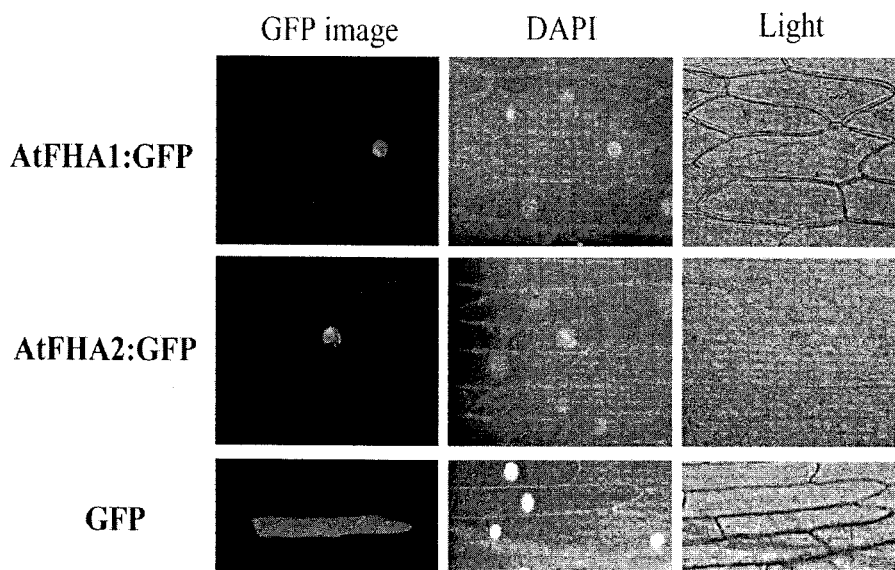


Fig. 3. Nuclear localization of AtFHA1 and AtFHA2. Fusion constructs of *AtFHA1:GFP* (green fluorescent protein) and *AtFHA2:GFP* were introduced into onion epidermal cells, using particle bombardment. Localization of GFP fluorescent signals was examined at 12 h after transformation under a fluorescence microscope, and compared with DAPI staining of the nucleus. As a control, expression of GFP alone was analyzed.

364 head transcription factor, forms a transcription complex
365 with the MADS-box protein, Mcm1, to control cell
366 cycle periodicity of *SWI5* and *CLB2* gene expression
367 [14,24]. Proteins containing the forkhead DNA binding
368 domain are potential candidates for interacting partners
369 of the FHA-containing plant factors. However, no
370 proteins identified in the plant database to date contain
371 the forkhead domain. The identification of interacting
372 proteins is an important step in elucidating the function
373 of this group of plant transcription regulators.

374 The presence of the FHA domain in a wide variety of
375 proteins suggests involvement of this domain in different
376 processes, although the specific cellular targets of the
377 FHA-containing proteins are largely unknown. *Arabi-*
378 *dopsis* contains 15 FHA domain-containing ORFs, of
379 which only the biological functions of KAPP [9,10] and
380 zeaxanthin epoxidase [19,20] have been characterized.
381 The roles of the FHA domains in these ORFs are yet to
382 be defined, except that of *Arabidopsis* KAPP being
383 involved in phosphorylation-dependent binding to mul-
384 tiple plant receptor-like kinases [10]. Sequence analysis
385 of the FHA-containing ORFs of *Arabidopsis* indicates

386 that these proteins have diverse functions and subcel-
387 lular localizations. Some of the encoded proteins display
388 homology with prokaryotic diacylglycerol kinase
389 (at1g34350), kanadapin-like protein (at5g38840), serine
390 protease (at3g20550), and A+T-hook DNA binding
391 domain protein (at3g02400). It is predicted that these
392 proteins are targeted to various subcellular locations,
393 including the nucleus, plasma membrane, mitochondria,
394 and chloroplast. In view of these diverse characteristics
395 of these proteins, it is likely that the targets of their FHA
396 domains are also distinct. Functions of these plant FHA
397 domains remain to be determined.

398 Analysis of *Arabidopsis* transgenic plants expressing
399 the promoter-GUS fusion gene reveals strikingly differ-
400 ent expression patterns of *AtFHA1* and *AtFHA2*.
401 *AtFHA2* is expressed ubiquitously at very high levels.
402 In contrast, *AtFHA1* is only temporally expressed, but
403 elevated levels are observed in response to external
404 stimuli. These differential expression patterns imply that
405 *AtFHA1* and *AtFHA2* have different regulatory roles.
406 Constitutive expression of *AtFHA2* in whole plant
407 tissues suggests that this protein is the main regulator

Fig. 2. Sequence alignment and phylogenetic tree of the FHA homology regions from 15 FHA domain-containing proteins of *Arabidopsis* (A) Sequence alignment. Conserved residues are boxed in black or light gray, based on the degree of conservation. The seven conserved residues identified in the FHA domains of animal and yeast proteins [2] are marked with asterisks above the alignment. Black arrows above the alignment indicate the predicted β -sheet, based on the Rad53 FHA domain structure [2]. At5g19280 and At5g67030 encode KAPP and zeaxanthin epoxidase precursor, respectively. The numbers on the left and right indicate the amino acid positions. (B) Phylogenetic tree based on the analysis of amino acid sequences of the FHA homology regions. Sequence alignment was performed by use of the CLUSTALW program. The neighbor-joining method was applied to generate the phylogenetic tree by using the TREEVIEW program. Numbers next to the nodes present bootstrap values from 1000 replicates (only those with more than 70% bootstrap support are indicated).

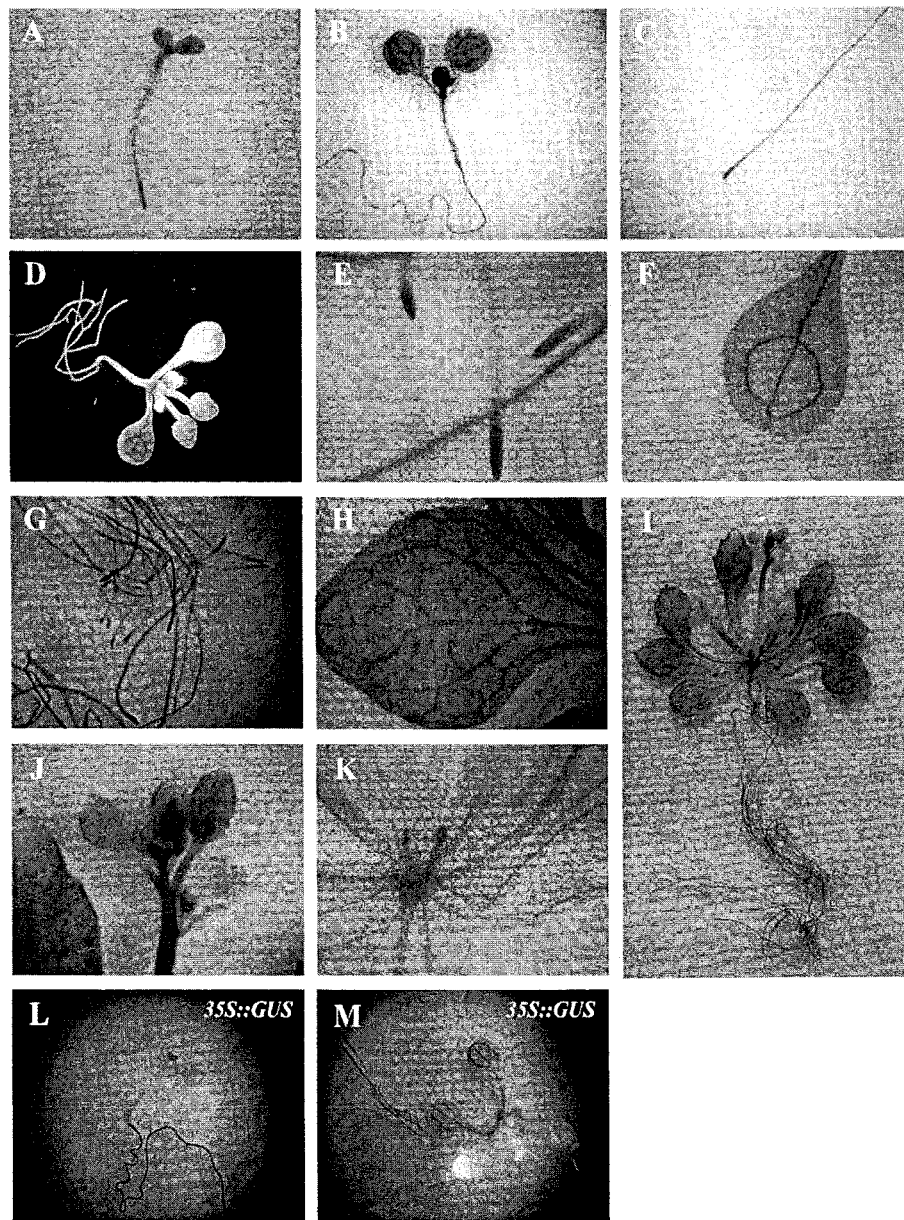


Fig. 4. Histochemical staining of transgenic *Arabidopsis* plants containing the *AtFHA2* promoter-*GUS* fusion gene. (A–B) *GUS* staining in whole seedlings at 2 days (A) and 7 days after sowing (B). (C) *GUS* staining in roots at 7 days after sowing (DAS). (D–F) *GUS* staining in whole seedlings (D), roots (E), and leaves (F) at 14 DAS. The root meristem, elongation zone, and vascular tissues in the leaves are strongly stained. (G–I) *GUS* staining in roots (G), leaves (H), whole plants (I), flower buds (J), and shoot apex (K) at 28 DAS. (L–M) *GUS* staining in whole seedlings containing the pBI121 (*35S* promoter:*GUS*) vector at 7 DAS (L) and 14 DAS (M) as controls.

408 of transcription activation. The expression pattern is
 409 consistent with its proposed role as a transactivating
 410 factor for rRNA processing and RNA polymerase III
 411 transcription. *AtFHA1* may be responsible for modulat-
 412 ing the rate of rRNA processing and RNA polymerase
 413 III transcription in response to environmental changes.
 414 Synthesis and processing of ribosomal RNA are closely
 415 monitored in cells responding to internal and external

information. When signals are perceived, newly synthe- 416
 sized *AtFHA1* may integrate into the transcription 417
 complex replacing *AtFHA2*, resulting in the assembly 418
 of a different transcription complex, and consequent 419
 modification of target gene expression. However, 420
 despite this intriguing possibility, the functions of 421
AtFHA1 and *AtFHA2* in plant cells remain to be 422
 clarified. Finally, from an applied perspective, the 423

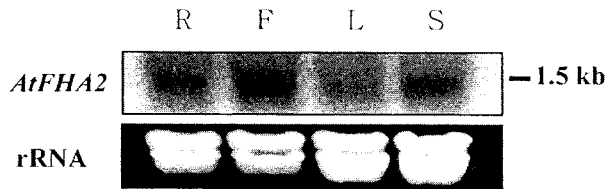


Fig. 5. RNA gel blot analysis of *AtFHA2* expression in *Arabidopsis*. Each lane represents 20 μ g total RNA from roots (R), flowers (F), leaves (L), and stems (S). EtBr-stained rRNA was visualized to verify the amount of RNA in each lane. The size of the mRNA is indicated.

424 strong constitutive *AtFHA2* promoter might be utilized
425 to drive expression of transgenes to a high level in the
426 plant system.

427 Acknowledgements

428 The authors thank Yu-Kyung Kim (KRIBB) for
429 technical help. This research was supported by grants
430 from Plant Diversity Research Center of the 21st
431 Century Frontier Research Program and National
432 Research Laboratory Program funded by Ministry of
433 Science and Technology of Korean government.

434 References

- 435 [1] K. Hofmann, P. Bucher, The FHA domain: a putative nuclear
436 signalling domain found in protein kinases and transcription
437 factors, *Trends Biochem. Sci.* 20 (1995) 347–349.
438 [2] D. Durocher, S.P. Jackson, The FHA domain, *FEBS Lett.* 513
439 (2002) 58–66.
440 [3] P. Zheng, D.S. Fay, J. Burton, H. Xiao, J.L. Pinkham, D.F.
441 Stern, SPK1 is an essential S-phase-specific gene of *Saccharo-*
442 *myces cerevisiae* that encodes a nuclear serine/threonine/tyrosine
443 kinase, *Mol. Cell. Biol.* 13 (1993) 5829–5842.
444 [4] D. Moras, Polymerases. Two sisters and their cousin, *Nature* 364
445 (1993) 572–573.
446 [5] M. Kikkawa, E.P. Sablin, Y. Okada, H. Yajima, R.J. Fletterick,
447 N. Hirokawa, Switch-based mechanism of kinesin motors, *Nature*
448 411 (2001) 439–445.
449 [6] M. Murone, V. Simanis, The fission yeast *dmal* gene is a
450 component of the spindle assembly checkpoint, required to
451 prevent septum formation and premature exit from mitosis if
452 spindle function is compromised, *EMBO J.* 15 (1996) 6605–6616.
453 [7] D.M. Scolnick, T.D. Halazonetis, Chfr defines a mitotic stress
454 checkpoint that delays entry into metaphase, *Nature* 406 (2000)
455 430–435.
456 [8] M. Tyers, P. Jorgensen, Proteolysis and the cell cycle: with this
457 RING I do thee destroy, *Curr. Opin. Genet. Dev.* 10 (2000) 54–
458 64.
459 [9] J.M. Stone, M.A. Collinge, R.D. Smith, M.A. Horn, J.C. Walker,
460 Interaction of a protein phosphatase with an Arabidopsis serine-
461 threonine receptor kinase, *Science* 266 (1994) 793–796.

- [10] J. Li, G.P. Smith, J.C. Walker, Kinase interaction domain of
462 kinase-associated protein phosphatase, a phosphoprotein-binding
463 domain, *Proc. Natl. Acad. Sci. USA* 96 (1999) 7821–7826. 464
[11] G. Zhu, E.G. Muller, S.L. Amacher, J.L. Northrop, T.N. Davis,
465 A dosage-dependent suppressor of a temperature-sensitive calmo-
466 dulin mutant encodes a protein related to the forkhead family of
467 DNA-binding proteins, *Mol. Cell. Biol.* 13 (1993) 1779–1787. 468
[12] S. Hermann-Le Denmat, M. Werner, A. Sentenac, P. Thuriaux,
469 Suppression of yeast RNA polymerase III mutations by *FHL1*, a
470 gene coding for a fork head protein involved in rRNA processing,
471 *Mol. Cell. Biol.* 14 (1994) 2905–2913. 472
[13] P.C. Hollenhorst, M.E. Bose, M.R. Mielke, U. Muller, C.A. Fox,
473 Forkhead genes in transcriptional silencing, cell morphology and
474 cell cycle. Overlapping and distinct functions for FKH1 and
475 FKH2 in *Saccharomyces cerevisiae*, *Genetics* 154 (2000) 1533–
476 1548. 477
[14] G. Zhu, P.T. Spellman, T. Volpe, P.O. Brown, D. Botstein, T.N.
478 Davis, B. Futcher, Two yeast forkhead genes regulate the cell
479 cycle and pseudohyphal growth, *Nature* 406 (2000) 90–94. 480
[15] M. Koranda, A. Schleiffer, L. Endler, G. Ammerer, Forkhead-
481 like transcription factors recruit Ndd1 to the chromatin of G2/M-
482 specific promoters, *Nature* 406 (2000) 94–98. 483
[16] M. Kim, J.-W. Ahn, K. Song, K.-H. Paek, H.-S. Pai, Forkhead-
484 associated domains of the tobacco N(FHA1) transcription acti-
485 vator and the yeast Fhl1 forkhead transcription factor are
486 functionally conserved, *J. Biol. Chem.* 277 (2002) 38781–38790. 487
[17] Y.J. Lee, D.H. Kim, Y.-W. Kim, I. Hwang, Identification of a
488 signal that distinguishes between the chloroplast outer envelope
489 membrane and the endomembrane system in vivo, *Plant Cell* 13
490 (2001) 2175–2190. 491
[18] R.A. Jefferson, T.A. Kavanagh, M.W. Bevan, GUS fusions: beta-
492 glucuronidase as a sensitive and versatile gene fusion marker in
493 higher plants, *EMBO J.* 6 (1987) 3901–3907. 494
[19] C. Sun, J.L. Woolford, Jr, The yeast NOP4 gene product is an
495 essential nucleolar protein required for pre-rRNA processing and
496 accumulation of 60S ribosomal subunits, *EMBO J.* 13 (1994)
497 3127–3135. 498
[20] J. Venema, D. Tollervey, Processing of pre-ribosomal RNA in
499 *Saccharomyces cerevisiae*, *Yeast* 11 (1995) 1629–1650. 500
[21] D. Durocher, I.A. Taylor, D. Sarbassova, L.F. Haire, S.L.
501 Westcott, S.P. Jackson, S.J. Smerdon, M.B. Yaffe, The molecular
502 basis of FHA domain: phosphopeptide binding specificity and
503 implications for phospho-dependent signaling mechanisms, *Mol.*
504 *Cell* 6 (2000) 1169–1182. 505
[22] L. Li, B.L. Williams, L.F. Haire, M. Goldberg, E. Wilker, D.
506 Durocher, M.B. Yaffe, S.P. Jackson, S.J. Smerdon, Structural
507 and functional versatility of the FHA domain in DNA-damage
508 signaling by the tumor suppressor kinase Chk2, *Mol. Cell* 9 (2002)
509 1045–1054. 510
[23] B.L. Pike, A. Hammet, J. Heierhorst, Role of the N-terminal
511 forkhead-associated domain in the cell cycle checkpoint function
512 of the Rad53 kinase, *J. Biol. Chem.* 276 (2001) 14019–14026. 513
[24] A. Pic, F.-L. Lim, S.J. Ross, E.A. Veal, A.L. Johnson, M.R.A.
514 Sultan, A.G. West, L.H. Johnston, A.D. Sharrocks, B.A.
515 Morgan, The forkhead protein Fkh2 is a component of the yeast
516 cell cycle transcription factor SFF, *EMBO J.* 19 (2000) 3750–
517 3761. 518

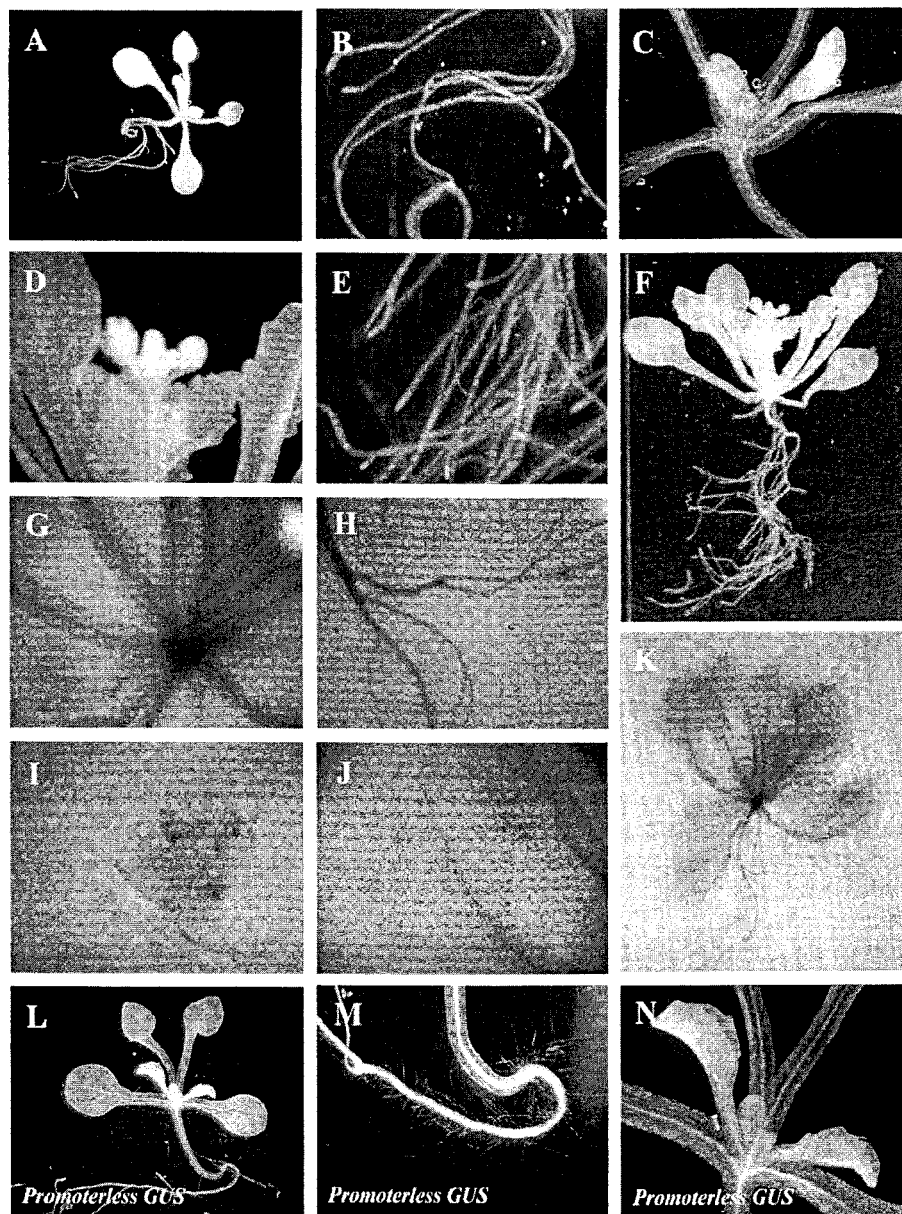


Fig. 6. Histochemical staining of transgenic *Arabidopsis* plants containing the *AtFHA1* promoter-*GUS* fusion gene. (A–C) *GUS* staining in seedlings at 14 days after sowing (DAS). Roots and vascular tissues near the shoot apex are weakly stained. (D–F) *GUS* staining in flowers (D), roots (E), and whole plants (F) at 28 DAS. No *GUS* staining was detected at this stage. (G–K) *GUS* staining in the shoot apex (G), roots (H), flower buds (I), leaves (J), and whole plants (K) at 28 DAS in response to brassinosteroid (5 μ M). Plants were treated with the hormone for 24 h before the *GUS* assay was performed. (L–N) *GUS* staining in whole seedlings (L), roots (M), and shoot apex (N) containing the pBI101 (promoterless *GUS*) vector at 14 DAS as a control. No *GUS* staining was observed.



CHRK1, a chitinase-related receptor-like kinase, interacts with NtPUB4, an armadillo repeat protein, in tobacco[☆]

Moonil Kim, Hye Sun Cho, Do-Myung Kim, Jeong Hee Lee, Hyun-Sook Pai^{*}

Laboratory of Plant Genomics, Korea Research Institute of Bioscience and Biotechnology, 52 Oun-dong, Yusong-gu, Taejeon 305-333, South Korea

Received 4 March 2003; received in revised form 23 June 2003; accepted 14 July 2003

Abstract

CHRK1 is a receptor-like kinase containing a chitinase-related sequence in the extracellular domain in *Nicotiana tabacum*. The previous study indicated that CHRK1 plays a role in a signaling pathway regulating plant development and the endogenous cytokinin levels. In this study, we identified NtPUB4 as a CHRK1-interacting protein using yeast two-hybrid screening. NtPUB4 contains the U-box and five arm repeats, and is homologous to *Arabidopsis* AtPUB4 with unknown function and to *Brassica* arm repeat containing 1 (ARC1) that interacts with SRK receptor-like kinases during self-incompatibility response. The arm repeats of NtPUB4 are important for the interaction with CHRK1. CHRK1–NtPUB4 interaction was confirmed by in vitro binding assay using the recombinant proteins. NtPUB4 exhibited spatial and temporal expression patterns that are very similar to those of CHRK1. Finally, GFP and RFP fusion experiments demonstrated that both CHRK1 and NtPUB4 are localized at the plasma membrane in vivo. These results strongly indicate that NtPUB4 is an interacting partner of CHRK1 receptor-like kinase, and is likely involved in modulating the plant developmental signaling pathway mediated by CHRK1.

© 2003 Elsevier B.V. All rights reserved.

Keywords: Arm repeat; In vitro binding assay; In vivo localization; U-box; Yeast two-hybrid

1. Introduction

Armadillo (arm) motif is a 38–45-amino-acid hydrophobic sequence originally identified in the *Drosophila* segment polarity protein armadillo [1]. The tandem arm repeats were also found in the junctional plaque protein plakoglobin, β -catenin, the tumor suppressor adenomatous polyposis coli (APC), and nuclear transport factor α -importin [2]. The arm repeat domains in these proteins consist of 8–12 tandem repeats of the armadillo motif [3]. In plants, arm repeat containing 1 (ARC1) with five arm repeats and U-box specifically interact with S-locus receptor-like kinase (SRK) that is involved in self-incompatibility response in *Brassica* [4]. The kinase domain of SRK binds to and phosphorylates ARC1 in vitro, and the phosphorylation is essential for the interaction between two proteins. Gene silencing of ARC1 results in loss of self-incompatibility, indicating that ARC1 is an essential downstream component

of SRK signaling pathway [5]. Recently, it has been found that ARC1 is an E3 ubiquitin ligase and promotes the ubiquitination of proteins during self-incompatibility reaction [6]. PHOR1, a photoperiod-responsive protein containing seven arm repeats, is a component of gibberellin signaling pathway [7]. Application of gibberellin induces rapid migration of PHOR1–GFP protein to the nucleus, resembling controlled nuclear localization of the armadillo/ β -catenin. Arm repeats have been found to be involved in protein–protein interaction. The arm repeats of β -catenin bind cadherins, APC, and EGF receptor kinase domain [8]. The plant ARC1 interacts with the SRK kinase domain through its arm repeats [4]. The binding of α -importin by β -importin [9], Ran^{GTP} by transportin [10], and nuclear localization signal peptides by α -importin [11] all involve the arm repeats.

Tobacco CHRK1 is a unique receptor-like kinase containing an extracellular domain that is closely related to the class V chitinase of tobacco and microbial chitinases [12]. In the plant and animal database including more than 600 receptor-like kinases in the *Arabidopsis* genome, no other receptor-like kinase contains the chitinase-like sequence. CHRK1 has been shown to play an important role in growth and development of tobacco plants (manuscript submitted). Expression of the CHRK1 promoter–GUS fusion gene was

[☆] EMBL accession number: AY219234.

^{*} Corresponding author. Tel.: +82-42-860-4195; fax: +82-42-860-4608.

E-mail address: hyunsook@kribb.re.kr (H.-S. Pai).

63 mainly detected in the apical domain of embryos, leaf
64 primordia, young leaves and floral organs. Furthermore,
65 transgenic tobacco plants in which the *CHRK1* expression
66 was suppressed exhibited pleiotrophic developmental ab-
67 normality, including formation of proliferating shooty calli
68 from seeds and severely altered seedling development. At
69 the cellular level, ectopic cell proliferation and aberrant
70 chloroplast development were observed. The transgenic
71 lines contain threefold higher level of cytokinin than the
72 wild-type tobacco, and the transgenic seedlings exhibited a
73 typical cytokinin response in the absence of hormone. These
74 results indicate that *CHRK1* is involved in a signal trans-
75 duction regulating plant development and cytokinin homeo-
76 stasis in tobacco (manuscript submitted).

77 In this study, we attempted to address the related signaling
78 pathway of *CHRK1* by identifying interactive proteins using
79 yeast two-hybrid system, and identified NtPUB4 as a putative
80 downstream element of *CHRK1*. Deletion analysis revealed
81 that five arm repeats are essential for the interaction between
82 two proteins. The recombinant proteins of *CHRK1* and
83 NtPUB4 interacted in vitro. Spatial and temporal expression
84 of NtPUB4 was very similar to that of *CHRK1*. Furthermore,
85 both *CHRK1* and NtPUB4 were localized in the plasma
86 membrane in vivo. These results strongly indicate that
87 NtPUB4 interacts with *CHRK1* receptor-like kinase as a
88 downstream element of the related signaling pathway.

89 2. Materials and methods

90 91 2.1. Yeast two-hybrid assay

92 The MATCHMAKER LexA two-hybrid system (Clon-
93 tech, USA) was used to screen a tobacco flower cDNA library
94 (complexity of 5×10^5 total recombinants) constructed in
95 pB42AD plasmid. The bait plasmid was constructed in
96 pLexA using a partial cDNA corresponding to the *CHRK1*
97 kinase domain or chitinase-like domain. After screening of
98 total 5×10^6 yeast cotransformants, a total of 92 positive
99 colonies that activated transcription of *LEU2* and *lacZ* gene
100 only in the presence of LexA-*CHRK1* kinase domain were
101 obtained. Among them, 25 colonies were randomly chosen,
102 and their cDNA inserts in pB42AD plasmid were PCR-
103 amplified and sequenced. Ten out of twenty five represented
104 a cDNA encoding a protein homologous to AtPUB4 in
105 *Arabidopsis* and *ARC1* in *Brassica*.

106 To test the interaction of different regions of NtPUB4
107 with the kinase domain of *CHRK1*, N-terminal and C-
108 terminal deletion constructs of the NtPUB4 cDNA in
109 pB42AD vector were generated as follows. A partial cDNA
110 sequence of NtPUB4 was PCR-amplified with *EcoRI* and
111 *SallI* at the ends, digested with *EcoRI/SallI*, and cloned into
112 *EcoRI/XhoI*-digested pB42AD. For the construct of the
113 *ARC1* cDNA in pB42AD vector as a control, the entire
114 *ARC1* coding region was PCR-amplified with a *EcoRI* and
115 *XhoI* site in their 5' and 3' ends, then cloned into *EcoRI/XhoI*-

digested pB42AD plasmid. The EGY48[p8op-lacZ] strain
containing pLexA-*CHRK1* kinase domain was transformed
with the pB42AD plasmid containing partial sequences of
NtPUB4 or the whole ORF of *ARC1*. The transformants
were grown on selection plates and assayed for β -galacto-
sidase activity. β -galactosidase activity levels were deter-
mined according to the manual of the MATCHMAKER
LexA two-hybrid system. Three separate colonies were
assayed for each construct. β -galactosidase activity was
determined as the OD₄₂₀ per hour.

2.2. Purification of recombinant proteins and in vitro protein binding assay

For cloning of the MBP-NtPUB4 fusion gene, the entire
NtPUB4 coding region was cloned into pMAL™ c2 vector
(New England Biolabs) using *EcoRI/XbaI* sites. For MBP-
ARC1 cloning, the entire *ARC1* coding region was cloned
into pMAL™ c2 vector (New England Biolabs) using
EcoRI/SallI sites. The maltose binding protein (MBP) or
MBP fusion proteins were purified using amylose resin
(New England Biolabs) following the manufacturer's
instructions. Recombinant polypeptides of the *CHRK1*
kinase domain (*CHRK1*-KD) were produced by in vitro
translation using the TNT-Coupled Wheat Germ Extract
Systems (Promega). The MBP, MBP-NtPUB4, and
MBP-ARC1 were immobilized on amylose resin and
incubated with the in vitro translated ³⁵S-methionine-labeled
CHRK1-KD for 2 h at 4 °C in binding buffer (150 mM
NaCl, 10 mM Tris (pH 8.0), 0.3% Nonident P-40, 1 mM
dithiothreitol (DTT), 0.5 mM phenylmethylsulfonyl fluo-
ride, and 0.25% bovine serum albumin (BSA)), followed by
three washes with binding buffer and a final wash with the
same buffer lacking BSA. The resin-bound fractions were
analyzed by 10% SDS-PAGE. The gel was blotted to PVDF
membranes and exposed to X-ray film.

2.3. DNA gel blot analysis

For DNA gel blot analysis, 10 μ g of the genomic DNA
isolated from *Nicotiana tabacum* leaves was digested with
EcoRI and *HindIII*, electrophoresed on a 0.8% agarose gel,
and blotted onto Hybond-N Nylon membrane (Amersham
Pharmacia Biotech) as described previously [13]. The probe
was the 0.4-kb PCR fragment corresponding to the N-
terminal region of NtPUB4. Prehybridization and hybridiza-
tion were carried out in $5 \times$ SSC, $5 \times$ Denhardt's solution,
and 0.5% SDS at 60 °C overnight. The membranes were
washed twice in $2 \times$ SSC and 1% SDS at room temperature,
then washed in $0.1 \times$ SSC and 0.1% SDS at 60 °C for 30 min.

2.4. RNA gel blot analysis

For RNA gel blot analysis using plant tissues, total RNA
was prepared by using TRIzol™ Reagent (GIBCO-BRL)
following manufacturer's instructions. Approximately 50 μ g

169 of total RNA was electrophoresed on an agarose gel contain-
170 ing 5.1% (v/v) formaldehyde and blotted onto Hybond-N
171 Nylon membrane. Prehybridization, hybridization, and wash-
172 ing conditions were as described in DNA gel blot analysis.
173

174 2.5. Semiquantitative RT-PCR

175 Semiquantitative RT-PCR was carried out as described
176 previously [14]. Twenty micrograms of total RNA isolated
177 from plant tissues was treated with 1 unit of RNase-free
178 DNase (Promega) and 1 unit of RNase inhibitor (Promega)
179 for 15 min at 37 °C, then purified by phenol/chloroform
180 extraction. The first-strand cDNA was synthesized by using
181 5 µg of DNase-treated RNA primed by oligo-dT (50 µM),
182 using 200 U of Superscript II RNase H⁻ Reverse Transcrip-
183 tase (GIBCO-BRL), 20 units of RNase inhibitor, 500 µM
184 each of dNTP and 10 mM DTT. One-fifth, one-twenty fifth,
185 and one-hundredth of 1/20 of the reaction mixture were used
186 for PCR amplification with 1 unit of Taq DNA polymerase
187 (Promega), 100 µM each of dNTP, and 100 pmol each of
188 forward and reverse primer.
189

190 2.6. *In vivo* localization of the *CHRK1*–*GFP* and 191 *RFP*–*NtPUB4* fusion proteins

192 The full-length *CHRK1* cDNA was PCR-amplified and
193 cloned into the 326-GFP vector [15] using *Bam*HI site to
194 generate *CHRK1*:GFP in-frame fusion under the control of
195 the CaMV35S promoter. Similarly, a partial *CHRK1* cDNA
196 was PCR-amplified and cloned into the same vector using
197 *Bam*HI sites to generate the *CHRK1*-KD:GFP, in which the
198 *CHRK1* kinase domain (containing a new ATG codon) was
199 fused to GFP. The full-length *NtPUB4* cDNA was cloned
200 into the 326-GFP vector using *Bam*HI site to generate the
201 *NtPUB4*:GFP fusion gene. The same cDNA was also
202 cloned into the 326-RFP plasmid [15] using *Cl*aI and *Sal*I
203 sites for RFP:*NtPUB4* in which *NtPUB4* was fused to the C
204 terminus of RFP. The fusion constructs and vector controls
205 were either introduced into onion epidermal cells by particle
206 bombardment, or introduced into tobacco protoplasts as
207 described in Ref. [15]. Expression of the fusion constructs
208 and vector controls was monitored at 24 h after transfor-
209 mation using a confocal microscope (Carl Zeiss LSM 510)
210 with two different sets of optical filters (488-nm excitation
211 and LP 505-nm emission to visualize the green fluores-
212 cence; 543-nm excitation and LP 585-nm emission to
213 visualize the red fluorescence).

214 3. Results

215

216 3.1. *CHRK1* receptor-like kinase interacts with an arm 217 repeat protein

218 To isolate proteins that interact with *CHRK1* (Fig. 1A),
219 the yeast two-hybrid assay using LexA system was ap-

220 plied. Using the *CHRK1* kinase domain as bait, a tobacco
221 flower bud cDNA library was screened. Among many
222 positive clones sequenced, a large proportion represented
223 a cDNA encoding an arm repeat-containing protein. The
224 cDNA clone was designated *NtPUB4*. The *NtPUB4* cDNA
225 derived from the pB42AD two-hybrid plasmid was 1314
226 bp in length and encoded the C-terminal region of
227 *NtPUB4*. The full-length cDNA was subsequently obtained
228 by PCR with a flower cDNA library as templates. It was
229 2880 bp in length with the ATG codon at position 220 and
230 stop codon at position 2592, followed by the 288-bp 3'
231 untranslated region with a poly(A) tail. It encoded a protein
232 of 790 amino acids with an estimated molecular mass of
233 86,136 Da.

234 The deduced amino acid sequences of *NtPUB4* indi-
235 cated that the protein contained the U-box (residue 239 to
236 302) and five arm repeats (residue 505 to 711) (Fig. 1A).
237 The U-box (UED2-homology domain) is structurally re-
238 lated to the RING FINGER domain [16], and U-box
239 proteins have been shown to act as a ubiquitin-protein
240 ligase [6,17,18]. The C-terminal region of *NtPUB4*, which
241 was present in the two hybrid clone, contained five
242 arm repeats of 40–41 residues. Arm repeats were first found in
243 armadillo protein in *Drosophila* and its vertebrate homolog
244 β-catenin [1]. Previous studies strongly indicate arm
245 repeats being involved in protein–protein interaction,
246 including SRK–ARC1 interaction during self-incompati-
247 bility reaction in *Brassica* [4,5]. *NtPUB4* is related with
248 arm repeat-containing proteins of plants in amino acid
249 sequences and overall protein structure, such as *AtPUB4*
250 of *Arabidopsis* [16], *ARC1* of *Brassica* [4], and *PHOR1*
251 of *Solanum* [7] (Fig. 1A). However, the sequence similar-
252 ity between these proteins is mostly restricted to the U-
253 box and arm repeats (Fig. 1B and C). *NtPUB4* shows
254 80%, 34%, and 15% sequence identity in the arm repeat
255 domain, and 87%, 46%, and 42% sequence identity in the
256 U-box region, to *AtPUB4*, *ARC1*, and *PHOR1*, respec-
257 tively. Thus, *NtPUB4* is most highly related with *AtPUB4*
258 of *Arabidopsis* with 56% overall sequence identity, indi-
259 cating a possibility that *AtPUB4* is the functional ortholog
260 of *NtPUB4*. Fig. 1D presents the sequence alignment of
261 five arm repeats of *NtPUB4* (R1 to R5). The arm repeats
262 of *NtPUB4* are quite degenerate exhibiting 16–48%
263 sequence identity between each other. Four conserved
264 residues of the arm repeat motif found in animal arm
265 repeat proteins [19] and their positions on the three helices
266 that constitute the arm repeat structural unit [3,11] are
267 indicated.
268

269 3.2. Arm repeats are required for *CHRK1*–*NtPUB4* 270 interaction

271 To verify the interaction between the *CHRK1* kinase
272 domain (*CHRK1*-KD) and *NtPUB4*, the pB42AD plasmid
273 containing *NtPUB4* was reintroduced into yeast cells either
274 alone or with the pLexA/*CHRK1*-KD plasmid, in which the

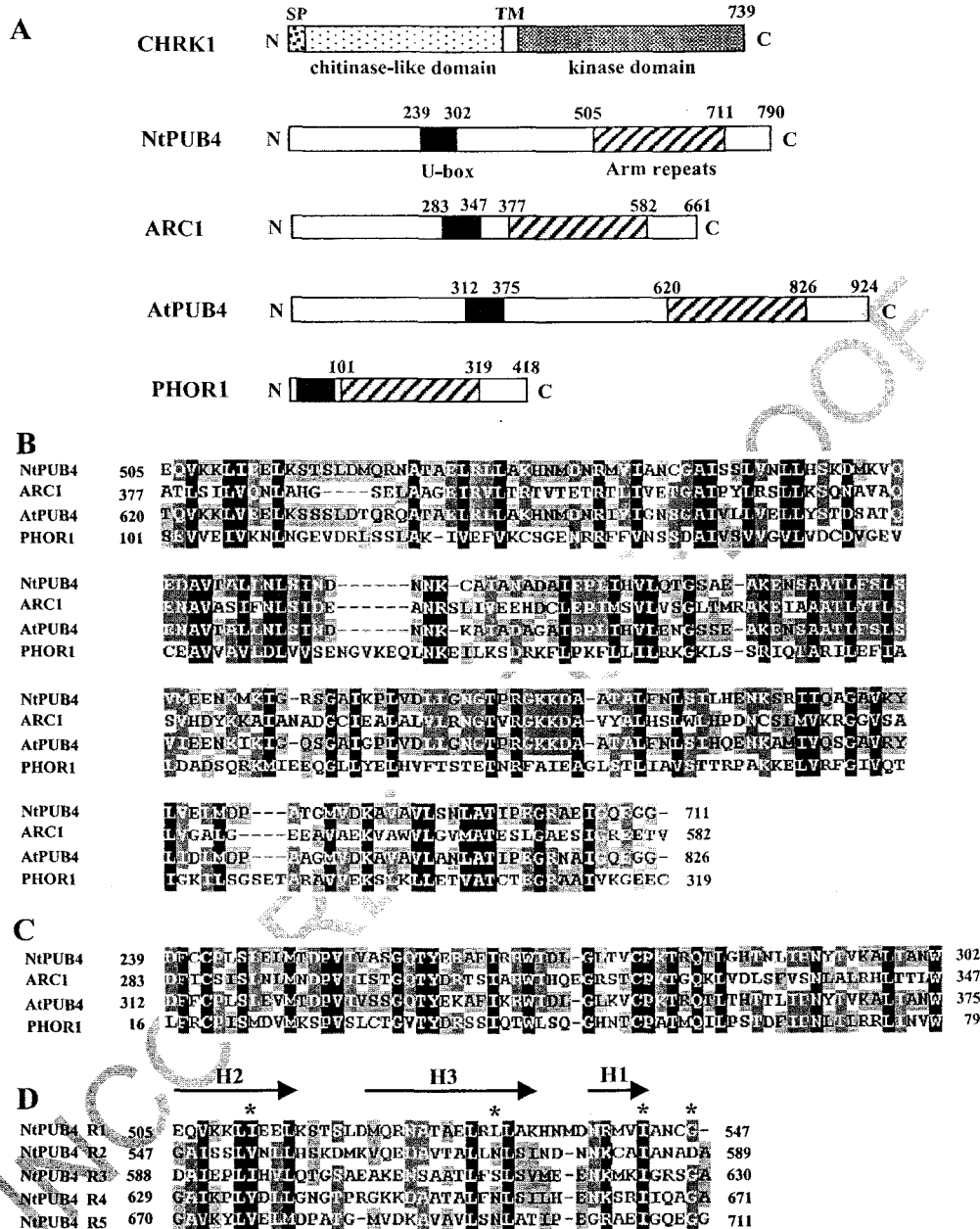


Fig. 1. Sequence alignment of NtPUB4 with other arm repeat-containing proteins of plants. (A) Schematic representation of CHRK1 and arm repeat proteins of plants. The U-box and arm repeat domain are indicated. SP, signal peptide; TM, transmembrane region. (B) Sequence alignment of highly conserved arm repeat domain of NtPUB4 with those of ARC1 from *B. napus*, AtPUB4 from *A. thaliana* and PHOR1 from *S. tuberosum*. The numbers on the left or right indicate the amino acid residues. Gaps, which were introduced to maximize alignment, are indicated by dashes. The residues conserved among the compared sequences are boxed in black or light gray based on the degree of conservation. (C) Sequence alignment of U-box (UFD2-homology domain) of NtPUB4 with related sequences in other plant species. (D) Sequence alignment of five arm repeats of NtPUB4. The four conserved residues identified in the arm repeat domains of animal proteins [19] were marked with asterisks above the alignment. The arrows above the alignment indicate the predicted three α -helices based on the arm repeat domain structure of α -importin [11]. H1, helix 1 (two turns); H2, helix 2 (two to three turns); H3, helix 3 (three to four turns).

275 CHRK1 kinase domain was fused with the LexA DNA
 276 binding domain, and the transformants were tested for β -
 277 galactosidase activity. They showed β -galactosidase activ-
 278 ity only in the presence of both pB42AD/NtPUB4 and

pLexA/CHRK1-KD plasmids. Yeast cells expressing
 CHRK1-KD, but not CHRK1-CD (the chitinase-like do-
 main), together with NtPUB4 grew on the selective media
 (Leu⁻, Trp⁻, Ura⁻, His⁻) and showed the strong expres-

283 sion of the *LacZ* reporter gene (Fig. 2A). To test the
284 specificity of the interaction between CHRK1 and NtPUB4,
285 PRK1 encoding a pollen-expressed receptor-like kinase in
286 petunia [20] and PKC, PP2A, Myb and ENV4 from human
287 yeast two-hybrid assay. PRK1 and other signaling proteins
288 tested did not interact with NtPUB4, as shown by the
289 inability to grow on Leu⁻ and the lack of β -galactosidase
290 activity (Fig. 2A).

292 To map the NtPUB4 region responsible for the inter-
293 action with the CHRK1 kinase domain, the full-length
294 *NtPUB4* and four deletion constructs of *NtPUB4* (three N-
295 terminal deletions or one C-terminal deletion) were cloned
296 separately into pB42AD, and introduced into yeast cells
297 together with the pLexA/CHRK1-KD plasmid (Fig. 2B).
298 As a control, the pLexA construct containing the full-
299 length *ARC1* of *Brassica* was tested for the interaction. As
300 shown in Fig. 2B, the full-length NtPUB4, but not the
301 full-length *ARC1*, exhibited strong interaction with
302 CHRK1, indicating the specificity of NtPUB4 binding to
303 CHRK1. Interaction patterns of the C-terminal deletion
304 mutant (NtPUB4 Δ C) and three N-terminal deletion

305 mutants (NtPUB4 Δ N-1, -2, and -3) demonstrate that the
306 five arm repeats (residue 505 to 711) are important for the
307 interaction. However, for stronger interaction, the region
308 (residue 353 to 504) between the U-box and arm repeats
309 was required in addition to the arm repeats, while the
310 region alone could not support the interaction as shown in
311 NtPUB4 Δ 1C. The region might be necessary for right
312 structural conformation of the arm repeat domain, required
313 for strong interaction with CHRK1. The arm repeats
314 contain highly conserved hydrophobic residues involved
315 in packing interaction of α -helix 2 and 3, in addition to a
316 short α -helix 1 that lies perpendicular to the parallel stack
317 of α -helix 2 and 3 [19]. The parallel stacking of the
318 arm repeat units forms a special groove, which has been shown
319 to be involved in protein–protein interaction between α -
320 and β -importin, and between nuclear localization signal
321 peptides and α -importin [19]. The arm repeats also
322 appeared to be important for interaction between SRK
323 and *ARC1* since the original two-hybrid clone contains
324 only the C-terminal half of *ARC1* encompassing the arm
325 repeats [4]. Interestingly, CHRK1 interaction with
326 NtPUB4 Δ N-1 was stronger than with the full-length

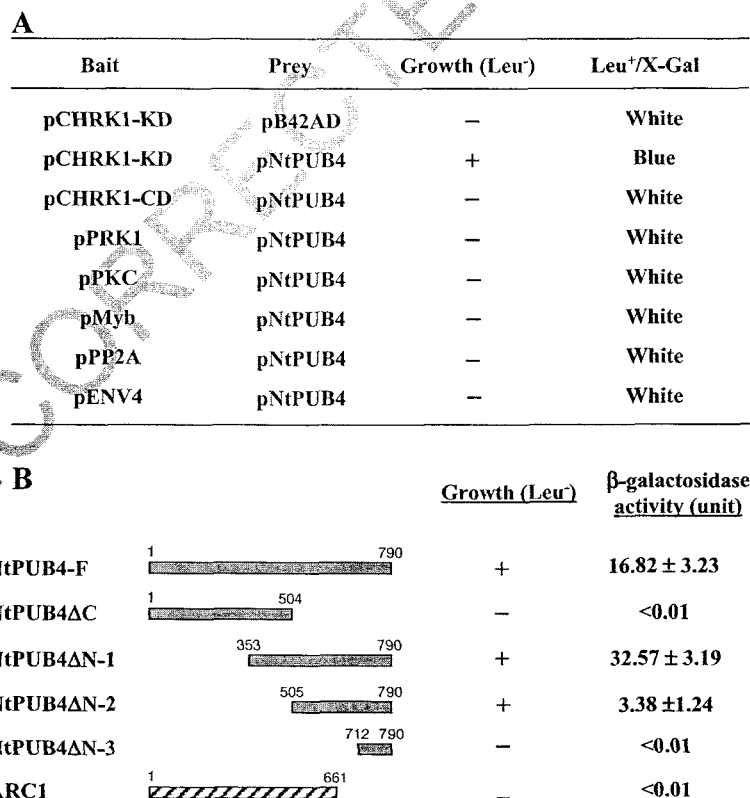


Fig. 2. Specificity of NtPUB4–CHRK1 interaction and mapping of interacting regions. (A) Yeast two-hybrid assay of interactions between NtPUB4 and various signaling components. Yeast growth on the selection medium and β -galactosidase activity was monitored as indicators of the protein interaction. KD, the kinase domain; CD, chitinase-like domain. (B) Mapping of NtPUB4 domains involved in the interaction with CHRK1. The LexA DB-CHRK1 kinase domain was combined with B42AD fusions with NtPUB4 polypeptides carrying various N-terminal or C-terminal deletions, and *Brassica* *ARC1* as a control. Three separate colonies per construct were picked up to examine β -galactosidase activity.

327 NtPUB4. Taken together, these deletion analyses demon-
328 strate that the C-terminal region of NtPUB4 (residue 353
329 to 790) containing the arm repeats is involved in the
330 interaction with the kinase domain of CHRK1.

331 3.3. *In vitro* interaction between CHRK1 and NtPUB4

333 To confirm that NtPUB4 could bind to the kinase
334 domain of CHRK1 *in vitro*, we carried out *in vitro* binding
335 assay using MBP and MBP-NtPUB4 or MBP-ARC1
336 fusion proteins, all of which were bound to the amylose
337 resin (Fig. 3). The ³⁵S-methionine-labeled CHRK1-KD
338 polypeptide was synthesized using *in vitro* translation.
339 The labeled CHRK1-KD was incubated with resin-bound
340 MBP-NtPUB4, MBP-ARC1, or MBP. After washing, the
341 matrix-bound fractions were eluted, separated by SDS-
342 PAGE, then stained with Coomassie, which shows the
343 relative levels of the MBP-NtPUB4, MBP-ARC1 and
344 MBP in the binding reactions (left panel). Separately, the
345 resin-bound fractions were analyzed by SDS-PAGE. To
346 examine the binding efficiency, 10% of the input of the
347 labeled CHRK1 kinase domain used in the assay was also
348 loaded in the gel. The gel was then blotted to membranes
349 and exposed to X-ray film (right panel). The labeled
350 CHRK1 kinase domain was pulled down by resin-bound
351 MBP-NtPUB4, but not by MBP, MBP-ARC1, or resin
352 alone (Fig. 3). The intensity of the pulled-down CHRK1-
353 KD band is similar to that of one-tenth of the CHRK1-KD
354 input, indicating that approximately 10% of the CHRK1-
355 KD input was pulled down by MBP-NtPUB4. These
356 results demonstrate that the NtPUB4 protein specifically
357 interacts with the kinase domain of CHRK1 *in vitro*,
358 consistent with the results in the yeast two-hybrid system
359 (Fig. 2A).

3.4. Genomic organization of NtPUB4

DNA gel blot analysis was performed with *N. tabacum*
genomic DNA digested with restriction enzymes under
high-stringency conditions (Fig. 4A). The specific probe
was the 460-bp PCR fragment corresponding to the central
region of the *NtPUB4* cDNA. *EcoRI* and *HindIII* digestion
both resulted in two hybridizing bands. Considering that
N. tabacum is amphidiploid between *N. tomentosiformis* and
N. sylvestris, these results indicate that *NtPUB4* is a single
gene in the tobacco genome (Fig. 4A).

3.5. Expression of NtPUB4

Using RNA gel blot analysis, we examined expression
of the *NtPUB4* mRNA in various plant tissues (Fig. 4B).
The 2.9-kb *NtPUB4* transcripts (consistent with the size of
the isolated cDNA) were detected at the high level in open
flowers, however, in seedlings, roots, stems, leaves, and
young flower buds, the *NtPUB4* mRNA level was low. It
has been shown that the *CHRK1* mRNA is predominantly
expressed in open flowers with much lower level of
expression in other plant tissues [12]. In the transgenic
plants carrying the *CHRK1* promoter-*GUS* fusion gene,
GUS staining was particularly high in the anthers and
receptacles of mature flowers (Lee and Pai, unpublished
results).

The expression of the *NtPUB4* mRNA in different
developmental stages was examined using semiquantitative
RT-PCR. Without reverse transcription, no amplified PCR
products were generated (results not shown). During seed
germination, the *NtPUB4* mRNA was abundantly detected
at 2 days after sowing (DAS) on MS medium after 3 days of
cold treatment, and the level decreased at 3-5 DAS, then

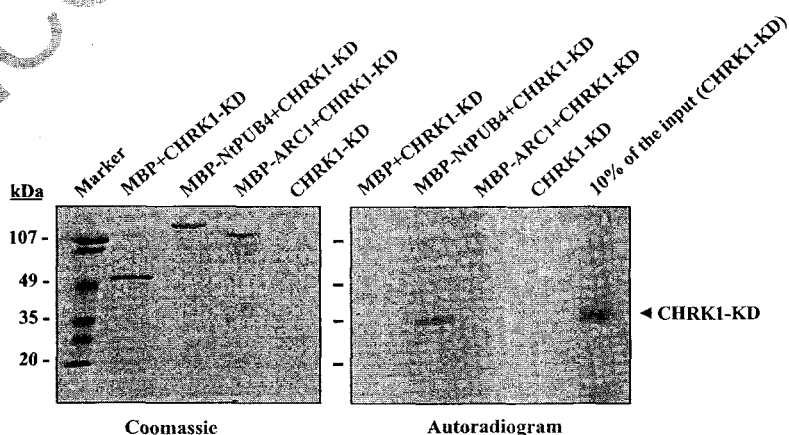


Fig. 3. *In vitro* interaction of CHRK1 kinase domain with NtPUB4. The ³⁵S-methionine-labeled CHRK1-KD polypeptide was incubated with resin-bound MBP-NtPUB4, MBP-ARC1 or MBP. After washing, the amylose resin-bound fractions were separated by SDS-PAGE. The separated proteins were visualized by Coomassie staining (left panel) or transferred to the membrane to autoradiograph (right panel). To examine the efficiency of interaction between CHRK1 and NtPUB4, 10% of the input of ³⁵S-methionine-labeled CHRK1-KD was loaded in the gel (right panel).

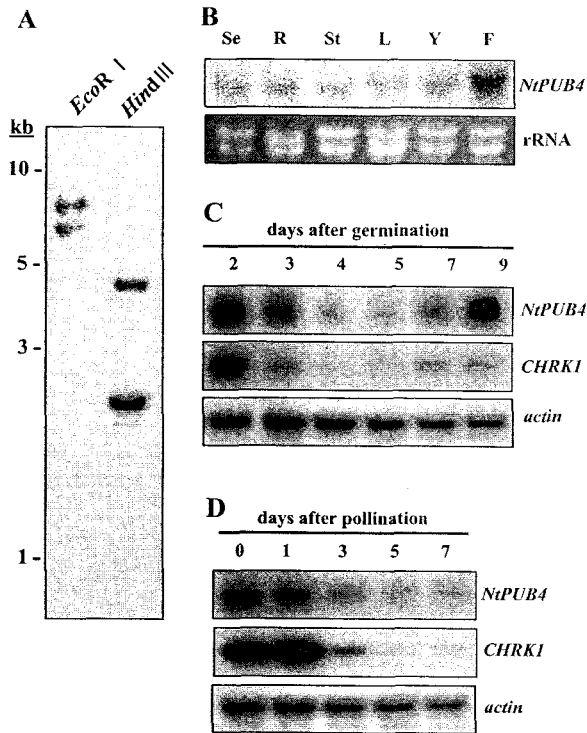


Fig. 4. Genomic organization and expression of the *NtPUB4* gene. (A) Genomic DNA gel blot analysis. The membrane containing 10 μ g of tobacco genomic DNA digested with *EcoRI* and *HindIII* was hybridized and washed, as described previously [13]. The probe was the 460-bp PCR fragment corresponding to the central region of *NtPUB4* cDNA. The DNA size markers are indicated in kilobases. (B) RNA gel blot analysis of the *NtPUB4* mRNA in tobacco. Each lane represents 50 μ g of total RNA from seedlings (Se), roots (R), stems (St), leaves (L), young flower-buds (Y), and open flowers (F). The amount of EtBr-stained rRNA was shown to verify equal loading of RNA in each lane. (C) *NtPUB4* expression during seed germination. The *NtPUB4* and *CHRK1* mRNA levels in water-imbibed seeds for the indicated time (2–9 days) after 3-day cold treatment were measured by semiquantitative RT-PCR using the *NtPUB4*- and *CHRK1*-specific primers. As a control, the transcript level of actin was examined. (D) *NtPUB4* expression during early seed development. The *NtPUB4* and *CHRK1* mRNA levels in ovaries before anthesis (0), and at 1, 3, 5, and 7 DAP were estimated by semiquantitative RT-PCR. As a control, the transcript level of actin was examined.

393 increased at 7–9 DAS (Fig. 4C). *CHRK1* showed a similar
 394 pattern of expression, although its mRNA level was some-
 395 what lower than *NtPUB4*. During seed germination of
 396 tobacco, the radicle comes out from seeds at 2–3 days after
 397 sowing (DAS) after vigorous cell division and expansion,
 398 and after cotyledon opening and greening, rapid hypocotyl
 399 elongation and leaf formation start at 7–9 DAS. Expression
 400 of *CHRK1* and *NtPUB4* might be correlated with rate of cell
 401 division/expansion and metabolic activity required for the
 402 process.

403 During pollination, unpollinated ovaries just before an-
 404 thesis contained high levels of the *NtPUB4* mRNA, and the
 405 level was maintained until 1 day after pollination (DAP).
 406 However, from 3 DAP to 7 DAP, the lower level of the

mRNA was detected in the ovaries (Fig. 4D). Similarly,
 407 *CHRK1* was abundantly expressed in unpollinated or polli-
 408 nated ovaries at 1 DAP, but the mRNA level significantly
 409 decreased from 3 DAP to 7 DAP. These results demonstrate
 410 that expression of *CHRK1* and *NtPUB4* is regulated spa-
 411 tially and temporally in a similar manner.

3.6. *NtPUB4* and *CHRK1* are colocalized in vivo

412
 413
 414
 415 By PSORT program (<http://psort.nibb.ac.jp>), it was pre-
 416 dicted that NtPUB4 is targeted to the nucleus (with high
 417 probability) and to the cytosol and mitochondria (with low
 418 probability). Previously, CHRK1–GFP fusion protein was
 419 localized in the plasma membrane when expressed in
 420 animal cells [12]. Subcellular distribution of the CHRK1
 421 and NtPUB4 proteins in plant cells was examined by
 422 expressing fusion proteins with GFP (green fluorescent
 423 protein) and RFP (red fluorescent protein). DNA constructs
 424 encoding CHRK1:GFP or RFP:NtPUB4, in which NtPUB4
 425 was fused to the C terminus of RFP, under the control of
 426 the cauliflower mosaic virus 35S promoter, were simulta-
 427 neously introduced into onion epidermal cells by particle
 428 bombardment (Fig. 5A). After incubation at 25 $^{\circ}$ C, ex-
 429 pression of the introduced genes was examined under a
 430 fluorescent microscope with two different filters to capture
 431 the image of GFP and RFP. After 24-h incubation, the
 432 green fluorescent signal completely overlapped with the red
 433 fluorescent signal in the vicinity of the plasma membrane,
 434 showing preferential localization of CHRK1 and NtPUB4
 435 in the plasma membrane in vivo (Fig. 5A). Yet unlike
 436 CHRK1, NtPUB4 lacks membrane-targeting signals or
 437 membrane-spanning regions. Thus, these results indicate
 438 that NtPUB4 is likely enriched at the inner surface of the
 439 plasma membrane by interacting with other proteins in-
 440 cluding CHRK1. The plasma membrane-associated pattern
 441 of the fluorescent proteins was reproducibly shown by
 442 separate expression of NtPUB4:GFP, in which NtPUB4
 443 was fused to N terminus of GFP, and CHRK1:GFP in
 444 onion cells (Fig. 5B). GFP or RFP alone was localized in
 445 the cytosol.

446 To provide further evidence for in vivo interaction of
 447 CHRK1 and NtPUB4, the RFP:NtPUB4 and CHRK1-
 448 KD:GFP (a fusion protein between the CHRK1 kinase
 449 domain and GFP) were coexpressed in protoplasts isolated
 450 from tobacco seedlings (Fig. 5C). At 24 h after transforma-
 451 tion of the fusion constructs, the green fluorescent signal
 452 mostly overlapped with the red fluorescent signal in the
 453 cytosolic compartment. Thus the transiently expressed
 454 CHRK1 kinase domain was mostly localized in the cytosol.
 455 Furthermore, the plasma membrane-associated localization
 456 of NtPUB4 was altered to the cytosolic localization, which
 457 is likely due to the interaction with the CHRK1 kinase
 458 domain. These data support CHRK1–NtPUB4 interaction
 459 in vivo. Recently, similar results have been obtained by
 460 Stone et al. [6], in which the SRK kinase domain was
 461 localized in the cytosol when expressed in tobacco BY2

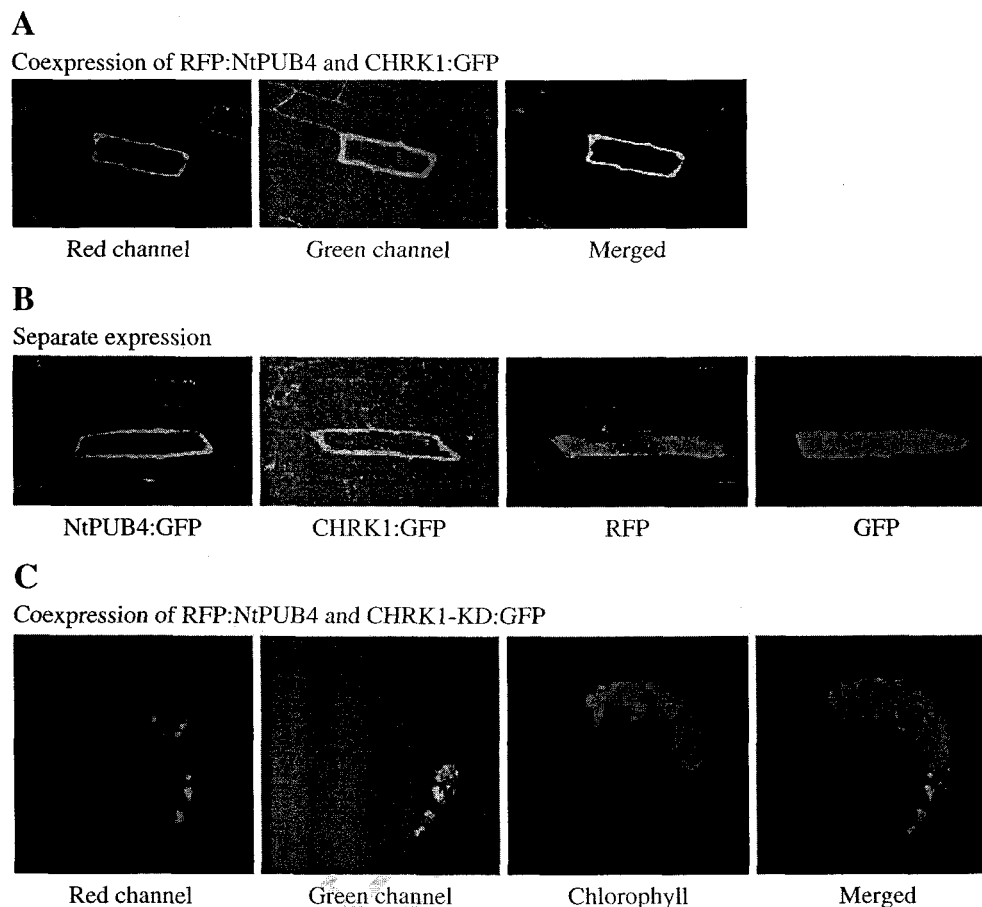


Fig. 5. Localization of CHRK1 and NtPUB4 in vivo. (A) In vivo localization of CHRK1:GFP and RFP:NtPUB4. Onion epidermal cell layers were cotransformed by particle-bombardment with the CHRK1:GFP and RFP:NtPUB4 fusion constructs, and localization of fluorescent signal was examined at 24 h after bombardment. Green and red fluorescent signals indicate GFP and RFP, respectively. From left, GFP, RFP, and the merged image are shown. (B) In vivo localization of CHRK1:GFP and NtPUB4:GFP fusion proteins. As controls, expression of GFP and RFP alone was analyzed. (C) In vivo colocalization of CHRK1-KD:GFP and RFP:NtPUB4. The CHRK1-KD:GFP and RFP:NtPUB4 plasmids were introduced into tobacco protoplasts by polyethylene glycol treatment as described [13].

462 cells. Furthermore, the subcellular localization of ARC1 was
463 changed dramatically when the SRK kinase domain was
464 coexpressed in the same cell [6].

465 4. Discussion

466 In this study, we have investigated the downstream
467 signaling pathway of CHRK1 using yeast two-hybrid sys-
468 tem, and identified an arm repeat-containing protein, desig-
469 nated NtPUB4, as a CHRK1-interacting protein. CHRK1 is
470 unique in the plant and animal kingdom as being an only
471 receptor-like kinase containing a chitinase-related extracel-
472 lular domain [12]. CHRK1 has been found to be involved in
473 a signal transduction regulating plant development and
474 cytokinin homeostasis in tobacco (manuscript submitted).
475 Interestingly, based on the sequence of the CHRK1 kinase
476 domain, CHRK1 was grouped together with the SRK family

among over 600 receptor-like kinases in *Arabidopsis* [21],
indicating a possibility that CHRK1 is evolutionally related
with the SRK family of receptor-like kinases. Thus it is
intriguing that CHRK1 kinase domain interacts with
NtPUB4, a homolog of ARC1 in *Brassica*. ARC1 was
isolated as an interactor of the kinase domain of SRK in
yeast two-hybrid screening [4], and later found to be an
essential component of downstream signaling of SRK
during self-incompatibility response in *Brassica napus* and
to have an E3 ubiquitin ligase activity [5,6]. NtPUB4 is
structurally similar to ARC1, containing the U-box and five
arm repeats (Fig. 1A). The arm repeats of NtPUB4 are
critical for the interaction with CHRK1 (Fig. 2B), similar to
the results from SRK-ARC1 interaction [4]. These results
indicate that arm repeat proteins might be a common
signaling component employed by the SRK group of
receptor-like kinase to relay the signals downstream to
signal transduction pathway.

495 The 42-amino-acid arm repeat was first identified in the
 496 *Drosophila* segment polarity gene product armadillo (β -
 497 catenin), which performs pleiotrophic roles in vivo [8]. β -
 498 Catenin controls cell adhesion by binding to cadherin-based
 499 cell adhesion junctions, and interacts with Wnt/Wingless
 500 growth factor signaling pathway [22]. These functions are
 501 mediated by the 12 tandem arm repeats, which interact with
 502 diverse proteins such as cadherins, TCF family transcription
 503 factors, and the tumour suppressor gene product APC [23].
 504 In addition to β -catenin, a number of proteins with diverse
 505 roles contain arm repeats, including α -importin, guanine
 506 nucleotide exchange factor, and APC in animals [8]. In
 507 plants, ARC1 and PHOR1 are the only arm repeat-contain-
 508 ing proteins whose function has been identified; ARC1 in
 509 self-incompatibility reaction [5] and PHOR1 in gibberellin
 510 signaling pathway [7]. GA-dependent nuclear import of
 511 PHOR1 resembles regulated nuclear localization of β -
 512 catenin [7]. Protein targeting studies with deletion mutants
 513 of PHOR1 fused to GFP demonstrated that the arm repeats
 514 mediate nuclear targeting of the PHOR1 protein. β -Catenin
 515 does not have nuclear localization sequences (NLS), but its
 516 nuclear import occurs by direct docking of the protein at the
 517 nuclear envelope [24]. Thus the arm repeat domain of these
 518 proteins may be involved in docking at the nuclear enve-
 519 lope and in nuclear import of proteins through NLS-
 520 independent mechanism. Recently, it has been found that
 521 ARC1 has an E3 ubiquitin ligase activity and it stimulates
 522 ubiquitination of multiple proteins during self-incompati-
 523 bility response in *Brassica* [6]. ARC1 can shuttle between
 524 the nucleus, cytosol, and proteasome/COP9 signalosome
 525 (CSN) when expressed in tobacco cells. Upon binding to
 526 the activated SRK through its C-terminal arm repeats,
 527 ARC1 may bind and carry ubiquitinated substrates to the
 528 proteasome/CSN for their subsequent degradation during
 529 the self-incompatibility reaction. NtPUB4 may play an
 530 analogous role to that of ARC1 in SRK signal transduction
 531 pathway, although detailed action mechanisms of NtPUB4
 532 remain to be uncovered. CHRK1 activation might lead to
 533 NtARC1 binding to CHRK1 through the arm repeats,
 534 which in turn may recruit the next component involved in
 535 CHRK1-mediated developmental signaling. In addition to
 536 the arm repeats, NtPUB4 contains the U-box. Since U-box
 537 proteins act as a single peptide E3 ligase [6,16] and might
 538 determine the specificity of substrates to be degraded,
 539 binding of NtPUB4 to CHRK1 might render the receptor-
 540 like kinase as the target for ubiquitination. Thus ubiquitin/
 541 proteasome-mediated proteolysis may be involved in
 542 CHRK1 downstream signaling pathways. To provide evi-
 543 dence for this possibility, it would be critical to examine an
 544 E3 ligase activity of NtPUB4 and its possible interaction
 545 with proteasome/CSN.

546 The arm repeat structural unit, revealed by the crystal
 547 structures of β -catenin [3] and α -importin [11], is composed
 548 of three α helices: a short helix of two turns (H1), followed
 549 by two longer helices, H2 (two to three turns) and H3 (three
 550 to four turns). The H2 and H3 helices pack against each

551 other in an antiparallel fashion and are roughly perpendic-
 552 ular to the shorter H1 helix, with a sharp bend between
 553 helices H1 and H2 mediated by a conserved Gly residue
 554 [19]. Continuous arm repeats organize to generate a right-
 555 handed superhelix of α -helices. The conformation of arm
 556 repeats is very similar to one another despite the high
 557 variability of their amino acid sequences. The uniformity
 558 of the inter-repeat packing produces a regular, linear con-
 559 formation of α -importin [11]. The assembly of tandem
 560 repeats of α -helical structural unit produces the extended
 561 superhelical structure with a long groove, which creates a
 562 protein recognition interface. The high degree of conserva-
 563 tion is found in the residue at positions 4 (Val/Ile/Leu),
 564 8 (Gly), 16 (hydrophobic residues), and 34 (hydrophilic
 565 residues) in the arm repeats [19]. Among these residues, the
 566 Gly residue at position 8 is located at the C terminus of helix
 567 H1 and permits the sharp bend between H1 and H2. Residue
 568 34 is a strongly conserved hydrophilic residue, most fre-
 569 quently Asn, and is exposed on the external face of the helix
 570 H3. In α -importin, Asn³⁴ residues are involved in substrate
 571 recognition, forming hydrogen bonds with the main-chain
 572 amide groups of the NLS peptide [11,25]. The arm repeats
 573 of NtPUB4 have those four conserved residues, but they
 574 additionally possess other conserved residues (Fig. 1D).

575 This study demonstrates the involvement of NtPUB4 in
 576 CHRK1 signaling pathway as a putative downstream com-
 577 ponent. Further studies are required to understand functional
 578 roles of NtPUB4 in the CHRK1-mediated developmental
 579 signaling pathway. These efforts may reveal conserved
 580 mechanisms of signal transduction through arm repeat-
 581 containing proteins employed by SRK family of receptor-
 582 like kinases in plant cells. Identifying the ligand and other
 583 downstream targets would give insight into the action
 584 mechanism of the CHRK1 signal transduction and possible
 585 relationship with cytokinin homeostasis. It would also be
 586 very important to investigate how the CHRK1-mediated
 587 signal integrates with the controlling mechanism of growth
 588 and development in plants.

Acknowledgements 589

590 The authors wish to thank Dr. Daphne R. Goring
 591 (University of Toronto) for providing the *ARC1* cDNA,
 592 and Dr. Ji-Won Lee (KBSI) for technical assistance for
 593 confocal microscopy. This research was supported by a
 594 grant (PF003105-02) from Plant Diversity Research Center
 595 of 21st Century Frontier Research Program funded by
 596 Ministry of Science and Technology of Korean government.
 597

References 597

- 598 [1] M. Peifer, E. Wieschaus, The segment polarity gene *armadillo* en-
 599 codes a functionally modular protein that is the *Drosophila* homolog
 600 of human plakoglobin, *Cell* 63 (1990) 1167-1176.

- 601 [2] M. Peifer, S. Berg, A.B. Reynolds, A repeating amino acid motif
602 shared by proteins with diverse cellular roles, *Cell* 76 (1994) 789–791.
- 603 [3] A. Huber, J. Nelson, W. Weiss, Three-dimensional structure of the
604 armadillo repeat region of beta-catenin, *Cell* 90 (1997) 871–882.
- 605 [4] T. Gu, M. Mazzurco, W. Sulaman, D.D. Matias, D.R. Goring. Binding
606 of an arm repeat protein to the kinase domain of the S-locus receptor
607 kinase, *Proc. Natl. Acad. Sci. U. S. A.* 95 (1998) 382–387.
- 608 [5] S.L. Stone, M. Arnoldo, D.R. Goring, A breakdown of *Brassica* self-
609 incompatibility in ARC1 antisense transgenic plants, *Science* 286
610 (1999) 1729–1731.
- 611 [6] S.L. Stone, E.M. Anderson, R.T. Mullen, D.R. Goring, ARC1 is an
612 E3 ubiquitin ligase and promotes the ubiquitination of proteins during
613 the rejection of self-incompatible *Brassica* pollen, *Plant Cell* 15
614 (2003) 885–898.
- 615 [7] V. Amador, E. Monte, J.-L. Garcia-Martinez, S. Prat, Gibberellins signal
616 nuclear import of PHOR1, a photoperiod-responsive protein with
617 homology to *Drosophila* armadillo, *Cell* 106 (2001) 343–354.
- 618 [8] A.I. Barth, I.S. Näthke, W.J. Nelson, Cadherins, catenins and APC
619 protein: interplay between cytoskeletal complexes and signaling path-
620 ways, *Curr. Opin. Cell Biol.* 9 (1997) 683–690.
- 621 [9] G. Cingonali, C. Petosa, K. Weis, C.W. Müller, Structure of importin- β
622 bound to the IBB domain of importin- α , *Nature* 399 (1999) 221–229.
- 623 [10] Y.M. Chook, Y. Blobel, Structure of the nuclear transport complex
624 karyopherin- β 2-Ran-GppNHp, *Nature* 399 (1999) 230–237.
- 625 [11] E. Conti, M. Uy, L. Leighton, G. Blobel, J. Kuriyan, Crystallographic
626 analysis of the recognition of a nuclear localization signal by the
627 nuclear import factor karyopherin α , *Cell* 94 (1998) 193–204.
- 628 [12] Y.S. Kim, J.H. Lee, G.M. Yoon, H.S. Cho, S.-W. Park, M.C. Suh,
629 D. Choi, H.J. Ha, J.R. Liu, H.-S. Pai, CHRK1, a chitinase-related
630 receptor-like kinase in tobacco, *Plant Physiol.* 123 (2000) 905–915.
- 631 [13] M. Kim, S.W. Park, S.H. Yu, H.S. Cho, H.J. Ha, I. Hwang, H.-S.
632 Pai, Molecular characterization of the Nelf2B β gene encoding a
633 putative eIF2B beta-subunit in *Nicotiana tabacum*, *Mol. Cell* 11
634 (2001) 104–108.
- [14] S.S. Lee, H.S. Cho, G.M. Yoon, J.W. Ahn, H.-H. Kim, H.-S. Pai,
Interaction of NtCDPK1 calcium-dependent protein kinase with
NtRpn3 regulatory subunit of the 26S proteasome in *Nicotiana taba-*
cum, *Plant J.* 33 (2003) 1–16.
- [15] Y.J. Lee, D.H. Kim, Y.-W. Kim, I. Hwang, Identification of a
signal that distinguishes between the chloroplast outer envelope
membrane and the endomembrane system in vivo, *Plant Cell* 13
(2001) 2175–2190.
- [16] C. Azevedo, M.J. Santos-Rosa, K. Shirasu, The U-box protein family
in plants, *Trends Plant Sci.* 6 (2001) 354–358.
- [17] S. Hatakeyama, M. Yada, M. Matsumoto, N. Ishida, K.-I. Nakayama,
U box proteins as a new family of ubiquitin-protein ligases, *J. Biol.*
Chem. 276 (2001) 33111–33120.
- [18] D.M. Cyr, J. Höhfeld, C. Patterson, Protein quality control: U-box-
containing E3 ubiquitin ligases join the fold, *Trends Biochem. Sci.* 27
(2002) 368–375.
- [19] M.A. Andrade, C. Petosa, S. O'Donoghue, C.W. Müller, P. Bork,
Comparison of ARM and HEAT protein repeats, *J. Mol. Biol.* 309
(2001) 1–18.
- [20] S.-W. Park, S.H. Yu, M. Kim, S.C. Oh, T.-H. Kao, H.-S. Pai, Inter-
action of PRK1 receptor-like kinase with a putative eIF2B β -subunit in
tobacco, *Mol. Cell* 10 (2000) 626–632.
- [21] S.H. Shiu, A.B. Bleecker, Plant receptor-like kinase gene family: di-
versity, function, and signaling, *Science's STKE* 113 (2001) RE22.
- [22] M.R. Groves, D. Barford, Topological characteristics of helical repeat
proteins, *Curr. Opin. Struct. Biol.* 9 (1999) 383–389.
- [23] B. Rubinfeld, B. Souza, I. Albert, O. Muller, S.H. Chamberlain, F.R.
Masiarz, S. Munemitsu, P. Polakis, Association of the APC gene
product with β -catenin, *Science* 262 (1993) 1731–1734.
- [24] F. Fagotto, U. Glück, B.M. Gumbiner, Nuclear localization signal-
independent and importin/karyopherin-independent nuclear import of
 β -catenin, *Curr. Biol.* 8 (1998) 181–190.
- [25] E.A. Nigg, Nucleocytoplasmic transport: signals, mechanisms and
regulation, *Nature* 386 (1997) 779–787.

Activation of the Programmed Cell Death Pathway by Inhibition of Proteasome Function in Plants*[§]

Received for publication, October 15, 2002, and in revised form, March 13, 2003
Published, JBC Papers in Press, March 13, 2003, DOI 10.1074/jbc.M210539200

Moonil Kim[‡]§, Joon-Woo Ahn[‡], Un-Ho Jin[‡], Doil Choi[‡], Kyung-Hee Paek[§], and Hyun-Sook Pai[‡]¶

From the [‡]Laboratory of Plant Genomics, Korea Research Institute of Bioscience and Biotechnology, P. O. Box 115, Yusong, Taejeon 305-600, and the [§]Graduate School of Biotechnology, Korea University, Seoul 136-701, Korea

Proteasomes constitute the major machinery to degrade or process proteins by ATP/ubiquitin-mediated proteolysis. Recent findings suggest a pivotal role of the ubiquitin/proteasome pathway in the regulation of apoptosis in animal cells. Here we show that virus-induced gene silencing of two different subunits of the 26 S proteasome, the $\alpha 6$ subunit of the 20 S proteasome and RPN9 subunit of 19 S regulatory complex, both activated the programmed cell death (PCD) program, accompanied by reduced proteasome activity and accumulation of polyubiquitinated proteins. These results demonstrate that disruption of proteasome function leads to PCD in plant cells. The affected cells showed morphological markers of PCD, including nuclear condensation and DNA fragmentation, accompanied by the 10-fold higher production of reactive oxygen species and increased ion leakage for 3-fold. Similar to apoptosis in animal system, mitochondrial membrane potential was decreased, cytochrome *c* released from mitochondria to cytosol, and caspase 9- and caspase 3-like proteolytic activities detected in the cells. Interestingly, this proteasome-mediated PCD stimulated the expression of only a subset of transcripts that are highly induced during pathogen-mediated hypersensitive response cell death, indicating that the two PCD pathways are differentially regulated. Taken together, these results provide the first direct evidence that proteasomes play a role in the regulatory program of PCD in plants. Controlled inhibition of proteasome activities may be involved in developmentally or environmentally activated plant cell death programs.

Programmed cell death (PCD)¹ is a genetically defined process associated with distinctive morphological and biochemical

* This work was supported by grants from the National Research Laboratory Program and Plant Diversity Research Center of 21st Century Frontier Research Program, funded by the Korean Ministry of Science and Technology. The costs of publication of this article were defrayed in part by the payment of page charges. This article must therefore be hereby marked "advertisement" in accordance with 18 U.S.C. Section 1734 solely to indicate this fact.

[§] The on-line version of this article (available at <http://www.jbc.org>) contains Supplemental Fig. 1 and legend.

The nucleotide sequence(s) reported in this paper has been submitted to the GenBank™/EBI Data Bank with accession number(s) AY135174

¶ To whom correspondence should be addressed. Tel.: 82-42-860-4195; Fax: 82-42-860-4608; E-mail: hyunsook@kribb.re.kr.

¹ The abbreviations used are: PCD, programmed cell death; HR, hypersensitive response; ROS, reactive oxygen species; Tricine, *N*-[2-hydroxy-1,1-bis(hydroxymethyl)ethyl]glycine; RT, reverse transcription; VIGS, virus-induced gene silencing; H₂DCFDA, 2',7'-dichlorodihydrofluorescein diacetate; POD, peroxidase; APX, ascorbate peroxidase; AFC, 7-amino-4-trifluoromethylcoumarin; AMC, 7-amino-4-methylcoumarin; β NA, β -naphthylamide; TMRM, tetramethylrhodamine methyl ester; VDAC, voltage-dependent anion channel; TRV, tobacco rattle virus.

characteristics (1), and it involves signaling pathways controlling the demolition of cells with the minimum damage to surrounding cells. PCD is an integral part of the life cycle in multicellular organisms including animals and plants (2) and can be induced by various stimuli, such as developmental and environmental cues (3, 4). PCD occurs in plants during developmental processes, such as senescence, embryogenesis, development of vascular tissues, and sex determination in unisexual plants, as well as during interactions with pathogens (5).

As a result of the extensive studies in the past decade, the basic blue print of the molecular control of apoptosis, the most widely studied PCD, has emerged in the animal system (1, 3, 6, 7). The key participants of the apoptotic cell death are the caspases, a family of cysteine proteases, which exist as dormant proenzymes in most cells. During apoptosis, a battery of caspases becomes activated through proteolytic processing at internal aspartic acid residues. The action of the active caspases on their substrates causes apoptotic morphological changes and leads to cell death. Two major pathways to caspase activation have been defined in mammals: the extrinsic death receptor pathway and the intrinsic or mitochondrial pathway (3). The intrinsic pathway is initiated through release of mitochondrial cytochrome *c* into the cytosol in response to cellular stresses. Cytochrome *c* release is a major checkpoint in the initiation of apoptosis, because this protein can induce assembly of the caspase-9 activating complex in the cytosol, termed apoptosome. Upon activation within the apoptosome, caspase-9 can propagate a cascade of further caspase activation events by direct processing of effector caspases.

Evidence is accumulating that the ubiquitin/proteasome pathway plays an important role in apoptosis (8, 9). The 26 S proteasome, consisting of two large subcomplexes, the 20 S proteasome and the 19 S regulatory complex, is a major cytoplasmic proteolytic enzyme complex, responsible for degradation of the vast majority of intracellular proteins in eukaryotes (10). In this pathway, ubiquitin becomes covalently attached to cellular proteins by an ATP-dependent reaction cascade, and then the ubiquitinated proteins are targeted for degradation by the proteasome (11). Proteasomal substrates include metabolic key enzymes, transcription factors, cyclins, inhibitors of cyclin-dependent kinases, and apoptotic regulators (11). In plants, the ubiquitin/proteasome pathway has been linked to cell cycle and to various signal transduction pathways including auxin signaling, photomorphogenesis, and jasmonic acid signaling (11). During apoptosis in animal cells, changes in the expression and activity of different components of the ubiquitin-proteasome system occur (9). Furthermore, proteasome inhibitors have been shown to induce apoptosis in most cell types, whereas in some cells, such as thymocytes and neural cells, these compounds were able to block apoptosis, revealing a complex mechanism of proteasome function in apoptosis (12). Proteasome-mediated steps in apoptosis in animal cells is located upstream

of mitochondrial changes and caspase activation, and could be related with Bcl-2, Jun N-terminal kinase, heat shock protein, Myc, p53, and polyamines (8).

Studies of the involvement of proteasome in plant PCD lag behind those in animal systems. Among a few examples, application of proteasome inhibitor at the initiation of zinnia mesophyll cell culture completely prevented differentiation of the tracheary element, whereas inhibition of proteasome activity following commitment to differentiation did not prevent formation of the organ but delayed the process (13). Additionally, overexpression of a mutant form of ubiquitin unable to form polyubiquitin chains induced formation of local lesion in response to mild stress, indicating that disruption of the ubiquitin pathway induces a HR-like cell death under certain conditions (14). However, no direct evidence of proteasome involvement in plant cell death has been provided. In this study, we demonstrate that disruption of proteasome function by gene silencing of the proteasome subunits activates programmed cell death in plant cells, revealing that proteasome is critically involved in cell death program in plants. The proteasome-mediated PCD exhibited features of apoptotic cell death, such as involvement of reactive oxygen species (ROS), cytochrome *c* release from mitochondria, and activation of caspase-like protease activities. Interestingly, the gene expression profile during the PCD in this study was different from that of the HR cell death in response to pathogen infection, indicating that different pathways for PCD regulation might have evolved in plants. Signaling pathways of some plant PCD programs may include modulation of proteasome activities in response to the death signals.

EXPERIMENTAL PROCEDURES

Virus-induced Gene Silencing—The 0.3-kb N-terminal and 0.3-kb C-terminal fragments, and the full-length *NbPAF* cDNA were PCR-amplified and cloned into the pTV00 vector containing a part of the TRV genome (15) using *Bam*HI and *Apa*I sites. The 0.5-kb *NbRpn9* cDNA was also cloned into the pTV00 vector using the same sites. The recombinant pTV00 plasmids and the pBINTRA6 vector containing RNA1 required for virus replication were separately transformed into *Agrobacterium tumefaciens* GV3101 strain. *Agrobacterium* culture for infiltration was prepared as described (15). The third leaf of *Nicotiana benthamiana* (3 weeks old) was pressure-infiltrated with the *Agrobacterium* suspension. For RT-PCR, the fourth leaf above the infiltrated leaf was used.

Evans Blue Staining—Detached leaves, completely submerged in a 0.1% (w/v) aqueous solution of Evans blue (Sigma), were subjected to two 5-min cycles of vacuum followed by a 20-min maintenance under vacuum. The leaves were then washed by vacuum infiltration of phosphate-buffered saline plus 0.05% (v/v) Tween 20 three times for 15 min each time.

RT-PCR—Twenty micrograms of total RNA isolated from plant tissues were treated with 1 unit of RNase-free DNase (Promega) and 1 unit of RNase inhibitor (Promega) for 15 min at 37 °C, then purified by phenol/chloroform extraction. The first-strand cDNA was synthesized by using 5 µg of DNase-treated RNA primed by oligo(dT) (50 µM) using 200 units of Superscript II RNase H⁻ reverse transcriptase (Invitrogen), 20 units of RNase inhibitor, 500 µM amounts of each dNTP, and 10 mM dithiothreitol. One-fifth, one-twenty-fifth, and one-hundredth of 1/20 of the reaction mixture were used for PCR amplification with 1 unit of *Taq* DNA polymerase (Promega), 100 µM amounts of each dNTP, and 100 pmol each of forward and reverse primer. Primers for RT-PCR were made according to the published cDNA sequences (for *PR1a*, 5'-AATA-TCCCACTCTTGCCG-3' and 5'-CTGGAGGATCATAGTTG-3'; for *PR1b*, 5'-ATCTCACTCTTCTCATGC-3' and 5'-TACCTGGAGGATCAT-AGT-3'; for *PR1c*, 5'-CTTGCTCTACGCTTCT-3' and 5'-AACACGA-ACCGAGTTACG-3'; for *PR2*, 5'-ACCATCAGACCAAGATGT-3' and 5'-TGGCTAAGAGTGGAAGGT-3'; for *PR4*, 5'-ATGGTTGGAACCTCCGG-A-3' and 5'-TCCTGATCTCTCTGCTAC-3'; for *PR5*, 5'-ATGAGAAAG-ACCCACGTC-3' and 5'-ATGCCTTCTTTGCAGCAG-3'; for *S25-PR6*, 5'-ATGCCACAATCTCAACCA-3' and 5'-ACCTAATGCAGCCCGAAT-3'; for *HSR203J*, 5'-TAGCCACGCACATGCAAACC-3' and 5'-GTGAC-AATCAAGACGGTAC-3'; for *630*, 5'-CAAGAAATCCGTCCAGGT-3' and 5'-CTTCTGTATCTGAGGCCT-3'; for *SAR8.2a*, 5'-CTTTGCTTT-

CTTTGGCT-3' and 5'-GACATTTAGGACATTTGCTGC-3'; for *HIN1*, 5'-GAGCCATGCCGGAATCCAAT-3' and 5'-GCTACCAATCAAGATG-CATCTGG-3'; for *NTCP-23*, 5'-ATGAGAATCCGATCAGAC-3' and 5'-ACATAAGCCATTTCTTGCC-3'; for *p69d*, 5'-ACTTCTCACTGCAATTG-G-3' and 5'-TCAGACATGATCAACTCC-3'; for *ClpP*, 5'-AACCAGGAC-ACAGATCGT-3' and 5'-AGGTACAATGCTCCTGG-3'; for *actin*, 5'-T-GGACTCTGGTGATGGTGTGTC-3' and 5'-CCTCCAATCCAAACACTGT-A-3'; for *NbPBC*, 5'-GCAACATCGTTTTGTTCT-3' and 5'-TCAGGCTT-CATTTCCCTC-3'; for *NbPAF-N*, 5'-TCAGCGCAATAGGTTTG-3' and 5'-AAGGTGAGCACCAGACTC-3'; for *NbPAF-C*, 5'-TGCCCTAGTGGT-AACTAC-3' and 5'-TTCATCACTACCAGCTTC-3'; and for *NbRpn9*, 5'-AGCTCTGGCATCAAC-3' and 5'-ACTGAGAAGACACCCAAT-3').

Nuclear Fragmentation Analysis—Genomic DNA was isolated from the fourth leaf above the infiltrated leaf in the virus-induced gene silencing (VIGS) lines using the Genome Isolation Kit (Qiagen) according to the instructions from the manufacturer. Five µg of genomic DNA was separated on a 1.2% agarose gel and transferred to Hybond N⁺ membrane (Amersham Biosciences). As probes, 100 ng each of the total genomic DNA and chloroplast DNA of *N. benthamiana* were labeled with a random labeling kit (Bio-Rad). After hybridization, the membranes were washed with 0.2× SSC, 0.1% SDS at 60 °C for 1 h.

In Vivo H₂O₂ Measurement—Protoplasts isolated from leaves of the VIGS lines were incubated in 2 µM 2',7'-dichlorodihydrofluorescein diacetate (H₂DCFDA, Molecular Probes) for 30, 60, 90, 120, and 150 s. Protoplasts were transferred to wells on microscope slides and illuminated using a confocal microscope (Carl Zeiss LSM 510) with optical filters (488-nm excitation, LP 505-nm emission) to visualize the oxidized green fluorescent probe. Quantitative images were captured and data were analyzed using the LSM 510 program (version 2.8).

Measurement of Peroxidase (POD) and Ascorbate Peroxidase (APX) Activity—For POD activity, 0.2 g of leaves from TRV control and TRV:PAF lines were ground in liquid nitrogen, and suspended in 10 mM potassium phosphate buffer, pH 6.0. After centrifugation at 4 °C, supernatants were taken, and measured for POD activity with 0.5 mM pyrogallol (Sigma) and 0.1 mM H₂O₂ using a spectrophotometer with 420-nm wavelength. For APX activity, the leaves were homogenized in the homogenization buffer (50 mM HEPES, pH 7.0, 0.1 mM EDTA). After centrifugation at 4 °C, supernatants were measured for the APX activity with 0.03 mM ascorbate and 0.1 mM H₂O₂ using a spectrophotometer with 290-nm wavelength.

Ion Leakage—After *Agrobacterium* infiltration, the fourth leaf above the infiltrated leaf from the TRV control and TRV:PAF lines was collected and analyzed. Fifteen leaf discs (7 mm in diameter) were floated on the 0.4 M sorbitol. The leaf discs were incubated in the darkness for 12 h, and this solution was measured for sample conductivity. Then the leaves were boiled in the same solution for 5 min, and the solution was measured for the subtotal conductivity. Membrane leakage is represented by the relative conductivity, which was calculated as sample conductivity divided by total conductivity (the sum of sample conductivity and subtotal conductivity). Conductivity was measured with a conductivity meter (model 162, Thermo Orion, Beverly, MA).

Callose Staining and Autofluorescence Detection—For callose staining, leaves from TRV control and VIGS-NbPAF lines were fixed in 3:1 ethanol:acetic acid for 1 h, washed in distilled water for 15 min, and softened in 8 M sodium hydroxide at room temperature overnight. The leaves were then washed twice in distilled water and incubated in 0.1% aniline blue (Sigma) in 0.1 M potassium phosphate buffer, pH 7.0, for 2 h in the darkness. The stained leaves were observed under a fluorescence microscope (Zeiss Axioskop). For autofluorescence detection, intact leaves were observed under a fluorescence microscope (Zeiss Axioskop).

Measurement of Mitochondrial Membrane Potential—Tetramethylrhodamine methyl ester (TMRM; Molecular Probes) was added into protoplasts isolated from leaves of the VIGS lines at the final concentration of 200 nM. After incubation for 10–15 min at 25 °C, protoplasts were transferred to wells on microscope slides and illuminated using a confocal microscope (Carl Zeiss LSM 510) with optical filters (543-nm excitation, LP 585-nm emission) to visualize the oxidized red fluorescent probe. Quantitative images were captured and data were analyzed using the LSM 510 program (version 2.8).

Measurement of Caspase-like Activity—Leaves were ground and homogenized in caspase extraction buffer (50 mM HEPES, pH 7.5, 1 mM EDTA, 1 mM dithiothreitol, 1% bovine serum albumin, 1 mM phenylmethylsulfonyl fluoride, 20% glycerol). Samples were incubated with shaking on ice for 15 min, centrifuged, and supernatants collected. Samples (50 µl) were mixed with 50 µl of caspase assay buffer (caspase extraction buffer with 150 µM LEHD-AFC (R&D Systems) for caspase 9-like activity and DEVD-AFC (R&D Systems) for caspase 3-like activity, as peptide substrates). After incubation at 37 °C for 1 h, the fluo-

resence of AFC hydrolyzed from the peptide substrates was quantified in a spectrofluorophotometer (Shimadzu, RF-5000) using 400-nm excitation and 505-nm emission wavelengths. Enzymatic activity was normalized for protein concentration and expressed as percentage of activity present in control extracts. Each measurement was carried out with three independent VIGS plants.

Cellular Fractionation and Detection of Cytochrome *c* Release—Two grams of leaves from the TRV control and TRV-PAF line were ground in grinding buffer (0.4 M mannitol, 1 mM EGTA, 20 mM 2-mercaptoethanol, 50 mM Tricine, 0.1% bovine serum albumin, pH 7.8) for 1 min at 4 °C. Extracts were filtered through Miracloth, and the filtrates were centrifuged at 15,000 × *g* for 5 min at 4 °C. The supernatant was centrifuged at 16,000 × *g* for 15 min at 4 °C. Following this second centrifugation, the supernatants obtained were taken to represent the cytosol fraction, and the pellets were resuspended in grinding buffer to represent the mitochondria fraction. Fifty μg of proteins were electrophoresed on a 12% SDS-PAGE, transferred onto polyvinylidene difluoride membranes, and probed with the monoclonal antibody against cytochrome *c* (1:1000 dilution; Pharmingen) and the monoclonal antibody (31HL) against human voltage-dependent anion channel (VDAC/porin) (1:1000 dilution; Calbiochem). They were then reacted with secondary antibodies conjugated with horseradish peroxidase and ECL reagent (Amersham Biosciences) for detection.

Measurement of Proteasome Activity—Proteasome activity was assessed in cell extracts using synthetic peptide substrates (Sigma) linked to the fluorescent reporters, 7-amino-4-methylcoumarin (AMC) or β-naphthylamide (βNA) in the absence or presence of proteasome inhibitor MG132 (Calbiochem). Homogenized leaf extracts were cleared by centrifugation, and the supernatants used for determination of protein concentration and enzymatic activity. Fifty μl of the extracts were assayed by addition of 50 μl of assay mixture (50 mM Tris-HCl, pH 7.5, 40 mM KCl, 5 mM MgCl₂, 1 mM dithiothreitol, 0.5 mM ATP, 2% glycerol), and incubation for 1 h at 37 °C. MG132 was added to the assay mixture at the final concentration of 100 μM. AMC and βNA hydrolyzed from the peptides were quantified in a spectrofluorophotometer (Shimadzu, RF-5000) using 380-nm excitation/460-nm emission wavelengths, and 342-nm excitation/460-nm emission wavelengths, respectively. Enzymatic activity was normalized for protein concentration and expressed as percentage of activity present in control extracts. Each measurement was carried out with three independent VIGS plants.

Western Blot Analysis of the Levels of α Subunits—Western blot analysis was carried out as described (16). Fifty μg of proteins were electrophoresed on a 10% SDS-PAGE, transferred onto polyvinylidene difluoride membranes, and probed with the monoclonal antibody raised against the mixture of six α subunits (α1, α2, α3, α5, α6, and α7) (1:1000 dilution; Affiniti Research Products Ltd). They were then reacted with secondary antibodies conjugated with horseradish peroxidase and ECL reagent (Amersham Biosciences) for detection.

RESULTS

Virus-induced Gene Silencing of the Proteasome Subunits Activated Programmed Cell Death—Phenomic analysis has been carried out to assess functions of signaling genes and hypothetical genes of *N. benthamiana* using TRV-based VIGS. VIGS is based on the phenomenon that gene expression is suppressed in a sequence-specific manner by infection with viral vectors carrying host genes (17). These screening led to the finding that gene silencing of the proteasome subunits, the α6 subunit of the 20 S proteasome and RPN9 subunit of the 19 S regulatory complex of the 26 S proteasome, activated the programmed cell death program. The cDNAs encoding the α6 and RPN9 subunit were designated *NbPAF* and *NbRpn9*, respectively. *NbPAF* and *NbRpn9* show high homology in amino acid sequences with their homologues from *Arabidopsis*, yeast, and human (results not shown). In this study, we investigated the mechanism of the PCD program activated by reduced expression of the proteasome subunit genes.

Suppression of the *NbPAF* and *NbRpn9* Transcripts in the Corresponding VIGS Lines—To confirm gene silencing of *NbPAF*, we cloned three different fragments of the *NbPAF* cDNA into the TRV-based VIGS vector pTV00 (15), and infiltrated *N. benthamiana* plants with *Agrobacterium* containing each plasmid (Fig. 1A). TRV:PAF(N) and TRV:PAF(C) contains the 1.3-kb N- and 0.3-kb C-terminal regions of the cDNA, whereas

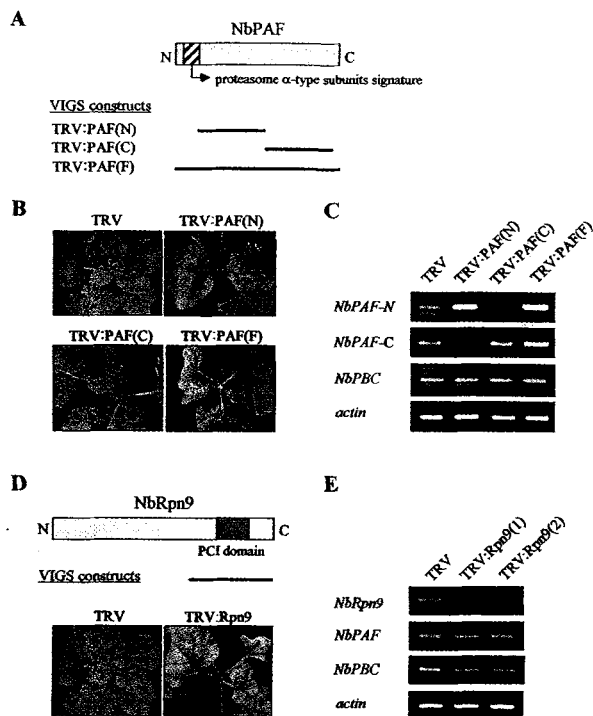


FIG. 1. VIGS phenotypes and suppression of the endogenous transcripts. A, the schematic drawing of the structure of *NbPAF*, and three VIGS constructs containing different regions of the *NbPAF* cDNA (marked by bars). The proteasome α-type subunits signature is indicated. B, VIGS phenotypes of the three *NbPAF* VIGS lines. *N. benthamiana* plants were infected with *Agrobacterium* containing the TRV control and three different forms of TRV-*NbPAF* constructs (TRV:PAF(N), TRV:PAF(C), and TRV:PAF(F)). The photographs of the plants were taken at 20 days after inoculation. C, semiquantitative RT-PCR analysis to examine the transcript levels of *NbPAF*. RNA was extracted from the fourth leaf above the infiltrated leaves from *N. benthamiana* plants infected with TRV, TRV:PAF(N), TRV:PAF(C), and TRV:PAF(F). The *NbPAF*-N and *NbPAF*-C primers were designed to detect the N- and C-terminal regions of the *NbPAF* cDNA, respectively. The *NbPAF*-N and *NbPAF*-C primers do not detect the viral genome transcripts from the TRV:PAF(C) and TRV:PAF(N) lines, respectively, but detect the TRV:PAF(F) viral genomic transcripts. As controls for RNA amount, the mRNA levels of actin and β3 subunit of the 20 S proteasome (*NbPBC*) were examined. D, the schematic drawing of the *NbRpn9* structure and its VIGS phenotypes. *N. benthamiana* plants were infected with TRV control and TRV:Rpn9. The photographs of the plants were taken at 20 days after inoculation, exhibiting the same phenotype as the TRV:PAF VIGS line. The PCI domain (54) is indicated. The bar represents the *NbRpn9* cDNA region used for VIGS. E, silencing of the *NbRpn9* transcripts. Semiquantitative RT-PCR was carried out to examine the endogenous transcript levels of *NbRpn9* using two individual VIGS plants. The primers were designed to exclude the cDNA region used in the VIGS construct. As a control for RNA amount, the mRNA levels of actin, *NbPAF*, and *NbPBC* were examined.

TRV:PAF(F) contains the full-length *NbPAF* cDNA. VIGS with the three constructs all resulted in the same phenotype of severe abnormality in plant development (Fig. 1B). Newly emerged leaves were small, severely curled, and wrinkled, making a cluster near the shoot apex, and the stem growth was completely arrested. Massive cell death soon followed, which resulted in premature death of the whole tissues of newly emerged leaves and flower buds. The effects of gene silencing on the endogenous amounts of the *NbPAF* mRNA were examined using semiquantitative RT-PCR (Fig. 1C), because the level of the transcript was low in the leaves. Primers for RT-PCR were designed to exclude the cDNA regions used in the VIGS constructs, and the transcript levels of the actin and the β3 subunit of the 20 S proteasome (*NbPBC*) were measured as controls. RT-PCR using *NbPAF*-N primers that detect the N-

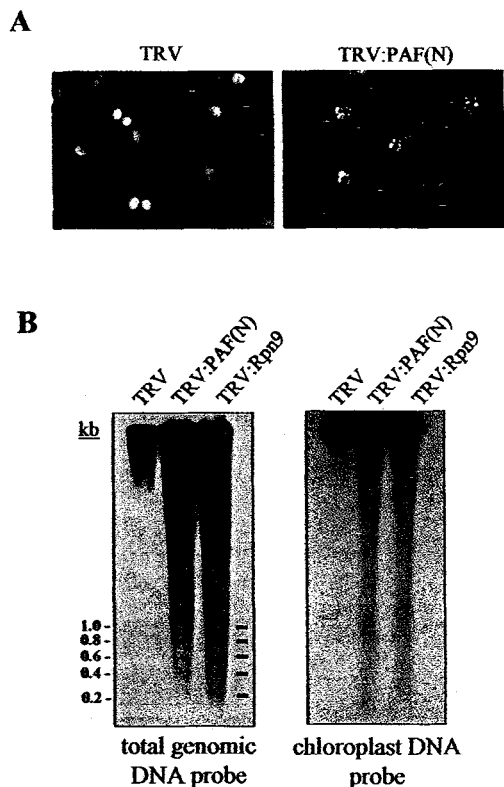


FIG. 2. Phenotypes of programmed cell death. A, nuclear condensation. Fluorescent microscopic picture of the cells from the leaves of the TRV and TRV-PAF(N) VIGS lines after nuclear staining with DAPI (100 $\mu\text{g/ml}$). B, oligonucleosomal DNA fragmentation. Genomic Southern blot was carried out with DNA extracted from the leaves of the VIGS lines using the total genomic and chloroplast DNA of *N. benthamiana* as probes.

terminal region of the *NbPAF* cDNA produced significantly reduced amounts of PCR products in the VIGS lines of TRV:PAF(C) compared with the TRV control, indicating that the endogenous level of the *NbPAF* transcripts is greatly reduced in those plants. The same primers detected high levels of viral genomic transcripts containing the N-terminal region of *NbPAF* in the TRV:PAF(N) and TRV:PAF(F) lines. In contrast, *NbPAF*-C primers that recognize the C-terminal region of the cDNA showed suppression of the endogenous *NbPAF* transcripts in the TRV:PAF(N) lines, whereas they detected the viral genomic transcripts in the TRV:PAF(C) and TRV:PAF(F) lines. The transcript levels of *NbPBC* and actin remained constant. These results demonstrate that expression of *NbPAF* was significantly reduced in the VIGS lines.

The *NbRpn9* VIGS lines showed the same phenotypes as that of the *NbPAF* VIGS lines (Fig. 1D). Silencing of *NbRpn9* was examined via semiquantitative RT-PCR using the primers that detect the cDNA region not covered in the VIGS construct. Compared with TRV control, the endogenous level of *NbRpn9* transcripts was greatly reduced in the TRV:Rpn9 VIGS lines, whereas the transcript levels of *NbPAF*, *NbPBC*, and actin remained constant (Fig. 1E).

Phenotypes of Programmed Cell Death—We examined nuclear morphology of cells in the abaxial epidermal layer from the leaves of the VIGS lines by DAPI staining (Fig. 2A). In the epidermal cells of the TRV:PAF(N) leaves, condensation and margination of nuclear chromatin were evident, whereas chromatin was evenly distributed within the nucleus in the control lines. Furthermore, DNA laddering was observed in the genomic DNA of TRV:PAF(N) and TRV:Rpn9 lines (Fig. 2B).

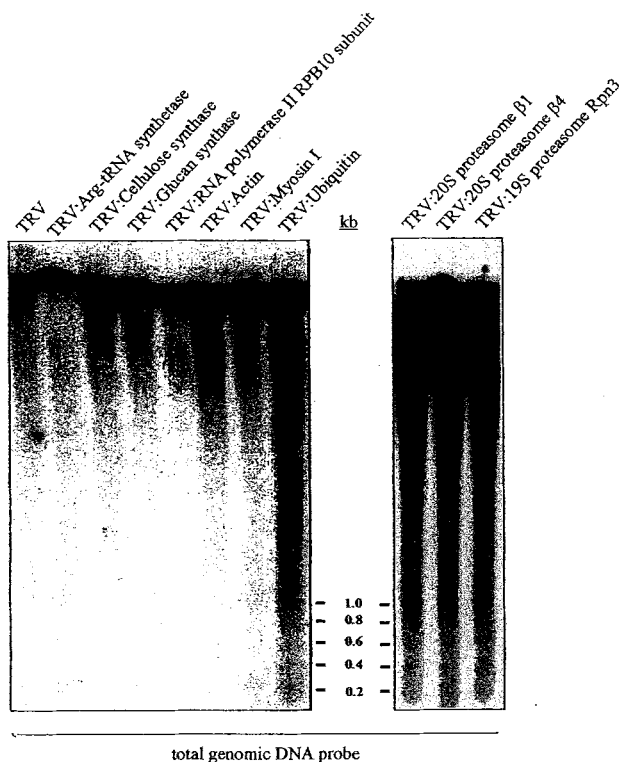
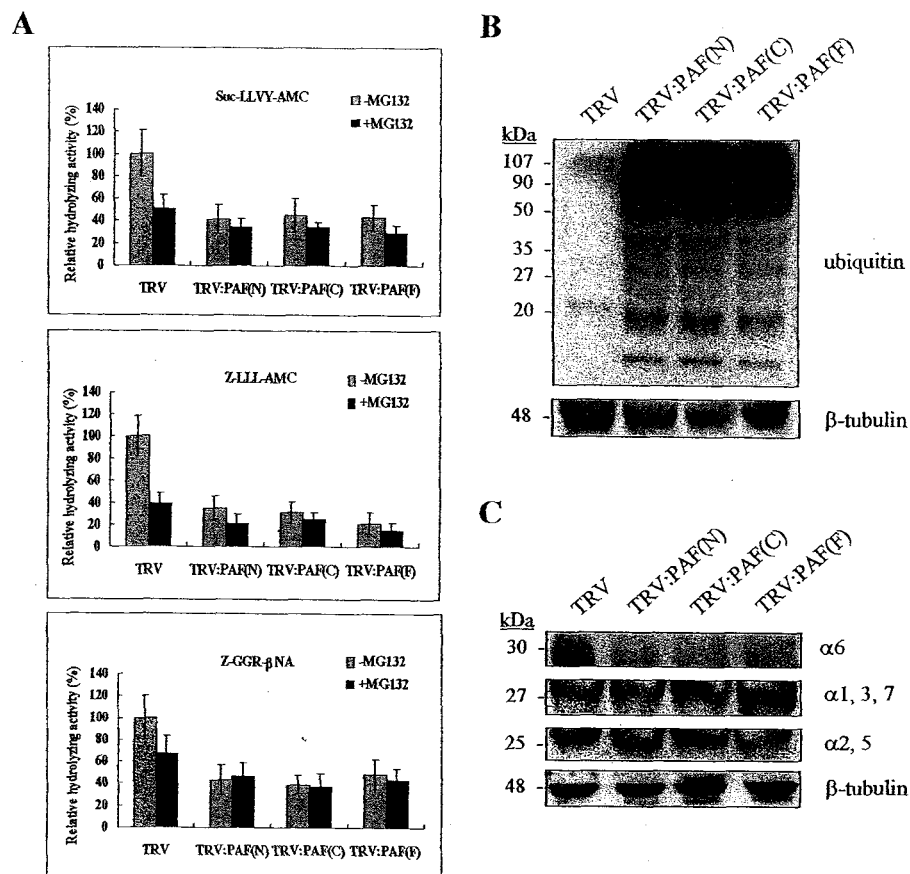


FIG. 3. PCD phenotypes induced by gene silencing of other proteasome subunits. Virus-induced gene silencing was carried out with *N. benthamiana* cDNAs encoding actin, β -tubulin, cellulose synthase, arginyl-tRNA synthetase, glucan synthase, RNA polymerase II subunit RPB10, myosin I, ubiquitin, and three subunits (β 1, β 4, and RPN3) of 26 S proteasome. RPB10 is an essential subunit of RNA polymerase II. To examine DNA laddering, genomic DNA was isolated from the fourth leaf above the infiltrated leaf in each VIGS line, and genomic Southern blot analysis was carried out using the total genomic DNA of *N. benthamiana* as a probe. Five μg of genomic DNA was used per lane.

DNA ladder is formed during PCD because of the activation of cell death-specific endonucleases that cleave the nuclear DNA into oligonucleosomal units. To visualize DNA laddering, the genomic DNA extracts from the VIGS lines were fractionated, transferred to nylon membranes, and hybridized with radiolabeled total genomic DNA and chloroplast DNA of *N. benthamiana*. DNA laddering was observed with the total genomic DNA probe, whereas the chloroplast DNA probe resulted in DNA degradation but without the laddering pattern, because the chloroplast genomic DNA is not packaged into nucleosomes. Because nuclear condensation and DNA laddering are the hallmark features of PCD, these results demonstrate that reduced expression of these proteasome subunits activates programmed cell death in plants. Interestingly, virus-induced gene silencing of other proteasome subunits (β 1, β 4, and Rpn3) also caused DNA laddering, indicating that inhibition of proteasome function by reduced availability of individual subunits is the reason for the PCD activation (Supplementary Fig. 1, available in the on-line edition of this article; Fig. 3). DNA laddering was also observed by gene silencing of ubiquitin, consistent with the previous report (14). In contrast, virus-induced gene silencing of other presumably essential genes of plants, such as cellulose synthase or glucan synthase, did not induce the PCD phenotypes, despite the fact that it resulted in severe morphological phenotypes including growth arrest and premature death of plants (Supplementary Fig. 1; Fig. 3). Thus, PCD appears to be activated by disrupted function of specific sets of genes such as ubiquitin and proteasome subunits.

FIG. 4. Reduced proteasome activity and accumulation of polyubiquitinated proteins. *A*, proteasome activity was measured in cell extracts of TRV, TRV:PAF(N), TRV:PAF(C), and TRV:PAF(F) leaves using three peptide substrates of the 26 S proteasome in the absence (gray) or presence of proteasome inhibitor MG132 (black). Enzymatic activity was normalized for protein concentration and expressed as percentage of activity present in control extracts. Data represent mean values (\pm S.D.) of three independent measurements. *B*, cell extracts (50 μ g of total protein) of TRV, TRV:PAF(N), TRV:PAF(C), and TRV:PAF(F) leaves were subjected to SDS-PAGE and Western blotting with the anti-ubiquitin monoclonal antibody and anti- β -tubulin monoclonal antibody. *C*, cell extracts (50 μ g of total protein) of TRV, TRV:PAF(N), TRV:PAF(C), and TRV:PAF(F) leaves were subjected to SDS-PAGE and Western blotting with the monoclonal antibody raised against the mixture of six α subunits (α 1, α 2, α 3, α 5, α 6, and α 7) and anti- β -tubulin monoclonal antibody.



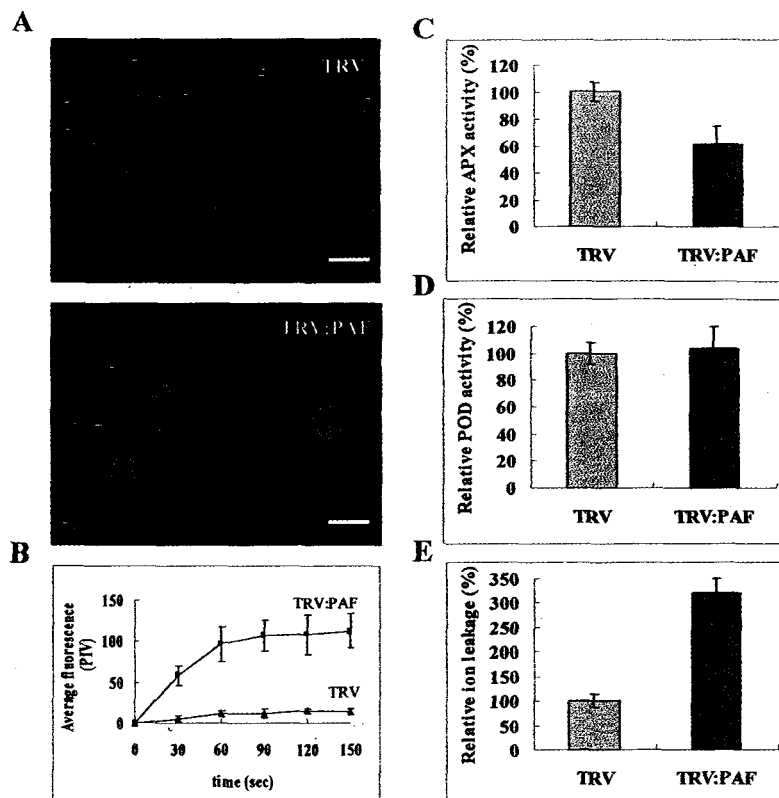
Gene Silencing of the Proteasome Subunits Inhibits Proteasome Activity—To examine functional consequence of gene silencing of the proteasome subunits, we measured proteasome activities in cell extracts from TRV control, TRV:PAF(C), and TRV:PAF(F) lines using peptide substrates in the absence or presence of proteasome inhibitor MG132 (Fig. 4A). Previously, it has been shown that plant proteasomes possess classical chymotrypsin-like, peptidylglutamylpeptide hydrolyzing-like, and trypsin-like activities against fluorescent synthetic peptide substrates (18, 19). Indeed, compared with the control, reduced expression of the α 6 subunit using the three VIGS constructs significantly reduced the hydrolysis of Suc-Leu-Leu-Val-Tyr-AMC, Z-Leu-Leu-Leu-AMC, and Z-Gly-Gly-Arg- β NA, synthetic peptide substrates of the chymotrypsin-like, PGPH-like, and trypsin-like activities of the proteasome, respectively. The degree of reduced activity was comparable with or slightly more than that achieved by lactacystin or RNA interference of the proteasome subunits in animal cells (20, 21). These results demonstrate that VIGS-promoted depletion of the proteasome subunits decreased all three types of proteasome activity. Proteasome inhibitor MG132 significantly reduced all three types of proteasome activity in TRV control, demonstrating that most of the hydrolytic activity indeed comes from proteasome (Fig. 4A). However, the residual peptidase activity, particularly the trypsin-like activity, still remained in the extracts from TRV control as well as from TRV:PAF lines. These inhibitor-resistant residual activities likely represent other proteases besides the 26 S proteasome. The measured peptidase activity of all three types did not differ significantly in the absence or presence of MG132 in the TRV:PAF samples, indicating that VIGS abolished most of active 26 S proteasome complex. The reduced proteasome activity by gene silencing of PAF is likely caused by interference of pro-

teasome assembly resulting from the reduced expression of the subunits. RNA interference of the individual proteasome subunit in *Drosophila* and trypanosome all resulted in disruption of proteasome assembly, and as a consequence, reduction of proteasome activity (20, 21).

Depletion of the Proteasome Subunits Leads to Accumulation of Polyubiquitinated Cellular Proteins—Most physiological substrates of the 26 S proteasome are cellular proteins covalently modified with a polyubiquitin chain. To determine the effect of gene silencing of the proteasome subunits on the degradation of such proteins, we carried out Western blotting with cell extracts of TRV control, TRV:PAF(N), TRV:PAF(C), and TRV:PAF(F) lines with a mouse anti-ubiquitin monoclonal antibody (Fig. 4B). It resulted in a smear of high molecular weight immunoreactive materials displaying many cellular proteins modified by polyubiquitin chains. Compared with the TRV control, gene silencing of the α 6 subunit using the three different VIGS constructs greatly increased the level of polyubiquitinated proteins. Previously, inhibition of proteasome activity by proteasome inhibitors or by RNA interference of the proteasome subunits also increased the intensity of this smear, displaying accumulation of non-degraded cellular proteins in animal cells (20, 21). In plants, mutants of MCB1 (RPN10) and UBP14 (ubiquitin-specific protease) exhibited increased steady state levels of cellular ubiquitinated proteins (22, 23). These results mirrored corresponding effects of gene silencing on proteasome activity against peptide substrates.

Protein Levels of α 6 and Other α Subunits in TRV:PAF Leaves—The protein levels of α 6 and other α subunits in TRV:PAF plants were examined by Western blotting with the monoclonal antibody raised against the mixture of six α subunits (α 1, α 2, α 3, α 5, α 6, and α 7) and β -tubulin antibody as a control (Fig. 4C). In three different TRV:PAF lines, the α 6 subunit

FIG. 5. Involvement of ROS during cell death. *A*, protoplasts isolated from leaves of TRV or the mixture of TRV:PAF VIGS lines were incubated in $2 \mu\text{M}$ H_2DCFDA for the indicated times (30–150 s). H_2DCFDA is a ROS indicator that becomes fluorescent when oxidation occurs within the cell. The bar indicates $100 \mu\text{m}$. *B*, fluorescence of protoplasts from control and the TRV:PAF VIGS lines was quantified as described under “Experimental Procedures.” Data points represent means \pm S.D. of 9–12 individual protoplasts. *PIV*, pixel intensity values. *C*, relative ascorbate peroxidase activity. *D*, relative peroxidase activity. *E*, relative ion leakage.



level significantly decreased because of gene silencing, whereas the combined levels of other five α subunits remained constant.

Involvement of ROS—To test whether ROS are produced in the cells undergoing PCD in the VIGS lines, we prepared protoplasts from leaves from TRV or the mixture of TRV:PAF(N), TRV:PAF(C), and TRV:PAF(F) lines, and incubated the protoplasts with H_2DCFDA to visualize the green fluorescent signal of which activation depends on the presence of H_2O_2 (Fig. 5A). H_2DCFDA is a cell-permeant indicator for ROS that is nonfluorescent until the acetate groups are removed by intracellular esterases and oxidation occurs within the cell (24). The rate of the accumulation of fluorescent H_2DCFDA in protoplasts from the TRV:PAF VIGS lines was significantly higher than that of the TRV control; the mean fluorescence for the protoplasts from the TRV:PAF lines reached ~ 10 -fold higher level than that of the TRV control (Fig. 5B). These results demonstrate that reactive oxygen species are involved in this cell death program. The overall activity of POD and APX, the enzymes hydrolyzing H_2O_2 to water and oxygen, was measured using leaf extracts of the control TRV and the mixture of TRV:PAF VIGS lines. The relative activity of POD was similar in both control and TRV:PAF leaves (Fig. 5C), whereas the APX activity was approximately 1.7-fold lower in the TRV:PAF leaves than control (Fig. 5D). Plant cell death is associated with an increase in cellular membrane leakage (25), which can be measured by ion leakage. The TRV:PAF leaves exhibited 3-fold higher levels of relative ion leakage than leaves from the TRV control (Fig. 5E).

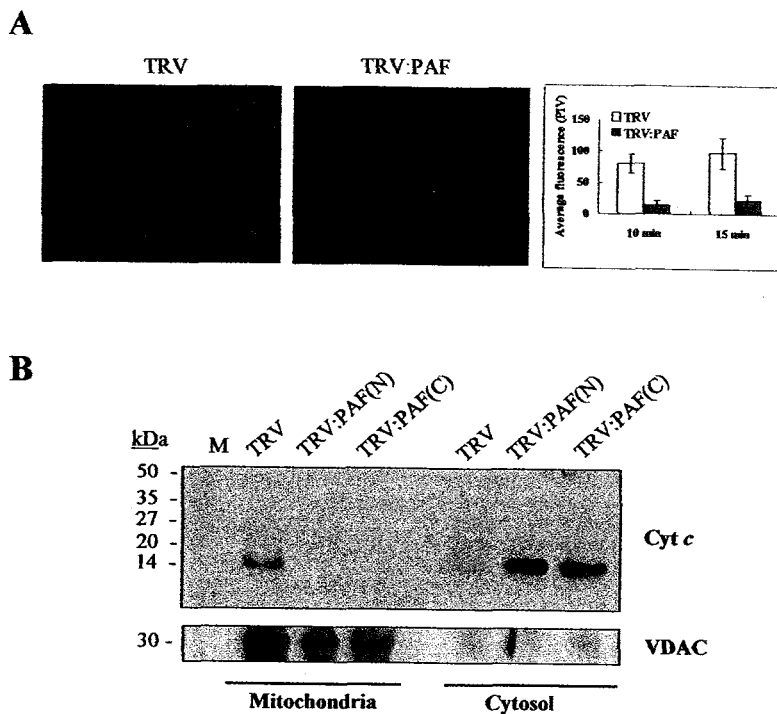
Disrupted Membrane Potential of Mitochondria and Release of Cytochrome *c*—During apoptosis in animal cells, modification of the mitochondrial membrane permeability initiates the death execution pathway. Mitochondrial membrane potential of the protoplasts isolated from leaves of TRV control and the mixture of TRV:PAF VIGS lines was monitored by TMRM fluorescent probes (Fig. 6A). TMRM is a lipophilic cation that is accumulated in mitochondria in proportion to the mitochon-

drial membrane potential (26). A drop in the membrane potential leads to a decrease in fluorescence caused by the diminished capacity of mitochondria to retain the probe. The average fluorescence of protoplasts from TRV:PAF leaves was approximately 4-fold lower than TRV control, indicating disruption of mitochondrial membrane potential. During apoptosis in animal cells, the release of cytochrome *c* occurs before visible morphological changes. We investigated cytochrome *c* relocation during the PCD. Leaves of the VIGS lines were homogenized, and the mitochondria were separated from the cytosol by differential centrifugation. The proteins in each fraction were analyzed by Western blot analysis using a monoclonal cytochrome *c* antibody and a monoclonal antibody against VDAC as a control for fractionation (Fig. 6B). VDAC is localized in the outer membrane of mitochondria and forms a channel through which metabolites pass (27). The Western blot revealed that cytochrome *c* was mainly detected in the mitochondria in the TRV control, whereas it was detected only in the cytosol fraction in the TRV:PAF lines. VDAC was detected only in the mitochondria fraction. This result shows that cytochrome *c* is released from mitochondria to cytosol, an early event of apoptosis in animal cells, during PCD in the VIGS lines.

Activation of Caspase-like Activity—During apoptosis in animal cells, relocated cytochrome *c* induces assembly of the caspase-9 activating complex, which in turn propagates a cascade of further caspase activation, including caspase-3. Using synthetic fluorogenic substrates for animal caspase-9 (LEHD-AFC) and caspase-3 (DEVD-AFC), we found that extracts from TRV:PAF(N), TRV:PAF(C), and TRV:PAF(F) leaves all exhibited both caspases 9-like and caspase 3-like proteolytic activities (Fig. 7). Activation of caspase-like protease activity could not be detected in TRV control leaves compared with the leaves of no treatment.

Markers Associated with HR Cell Death—Plant cells undergoing hypersensitive cell death deposit autofluorescing secondary metabolites and cell wall materials such as callose and

FIG. 6. Disruption of mitochondrial membrane integrity and cytochrome *c* release. *A*, mitochondrial membrane integrity. Protoplasts isolated from leaves of TRV and mixture of TRV:PAF VIGS lines were stained with 200 nM TMRM for 10 and 15 min to visualize mitochondria. The average fluorescence was quantified as described under "Experimental Procedures." Data points represent means \pm S.D. of 10–15 individual protoplasts. *PIV*, pixel intensity values. *B*, immunodetection of cytochrome *c* in mitochondrial and cytosolic fractions of leaves from TRV, TRV:PAF(N), and TRV:PAF(C) VIGS lines. Western blot analysis was performed with the cytochrome *c* monoclonal antibody, which shows cytochrome *c* release into cytosol in the TRV:PAF lines. As a control for cell fractionation, Western blotting was carried out with an anti-VDAC monoclonal antibody. VDAC is localized in the outer membrane of mitochondria (27).



aromatic polymers at infection sites. We examined the presence of the autofluorescent material and callose in the leaves of the TRV:PAF(N) and TRV:Rpn9 VIGS lines that undergo PCD. Fig. 8A demonstrates that leaves of both VIGS lines accumulated substantial amounts of autofluorescent products and callose. TRV control showed only small patches of those materials, primarily along the vein. Both TRV:PAF and TRV:Rpn9 VIGS lines also exhibited intense staining on the leaves with Evans blue indicating localized cell death, whereas TRV control showed no staining (Fig. 8A). These results demonstrate that some features of HR cell death are conserved in the PCD program induced by disruption of proteasome function.

We also examined whether the proteasome-mediated PCD induces expression of defense-related genes using semiquantitative RT-PCR (Fig. 8B). *PR1a*, *PR1b*, *PR1c*, *PR2*, *PR4*, *PR5*, *S25-PR6*, *SAR8.2a*, *HSR203J*, *HIN1*, and *630* genes are all highly induced during HR cell death (28). *NTCP-23* (cysteine protease) and *p69d* (serine protease) have been shown to be involved in pathogen-induced cell death (29), whereas the chloroplastic *ClpP* protease plays a role in chloroplast development but not in senescence or HR cell death (29). Among these genes, only *PR2*, *PR5*, *HIN1*, *ClpP*, and *NTCP-23* genes were transcriptionally induced in both the TRV:PAF(N) and TRV:Rpn9 VIGS lines. Expression of *SGT1*, *RARI*, and *SKPI*, recently identified signaling genes in plant defense (30–32), remained constant. Thus the proteasome-mediated PCD process promotes expression of only a subset of PR genes. Taken together, some features of HR cell death are conserved in the proteasome-mediated PCD program, but its gene expression profile is significantly different from the HR, indicating a possibility of differential regulation of each PCD pathway.

DISCUSSION

In this study, we present direct evidence that interruption of proteasome function activates programmed cell death in plant cells. When expression of proteasome subunits was suppressed by virus-induced gene silencing, the affected cells showed the characteristic features of apoptotic cell death, including nuclear condensation and DNA fragmentation. This proteasome-

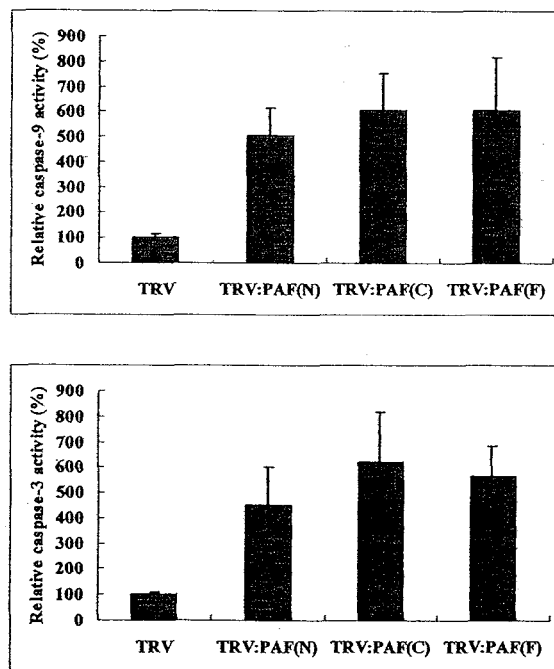


FIG. 7. Activation of caspase 9- and 3-like activity. Extracts from leaves of TRV, TRV:PAF(N), TRV:PAF(C), and TRV:PAF(F) VIGS lines were incubated with peptide substrates of the caspase-9 (LEHD-AFC) and caspase-3 (DEVD-AFC) in the caspase assay buffer, and their relative fluorescence was measured. Enzymatic activity was normalized for protein concentration and expressed as percentage of activity present in control extracts. Data points represent means \pm S.D. of three experiments per line.

mediated cell death pathway involves ROS, cytochrome *c* release from mitochondria, activation of caspase-like activities, and transcriptional induction of a subset of defense-related genes. The role of the proteasome in PCD in animals has been extensively investigated in various cell lines using specific proteasomal inhibitors, such as lactacystin and peptide aldehydes

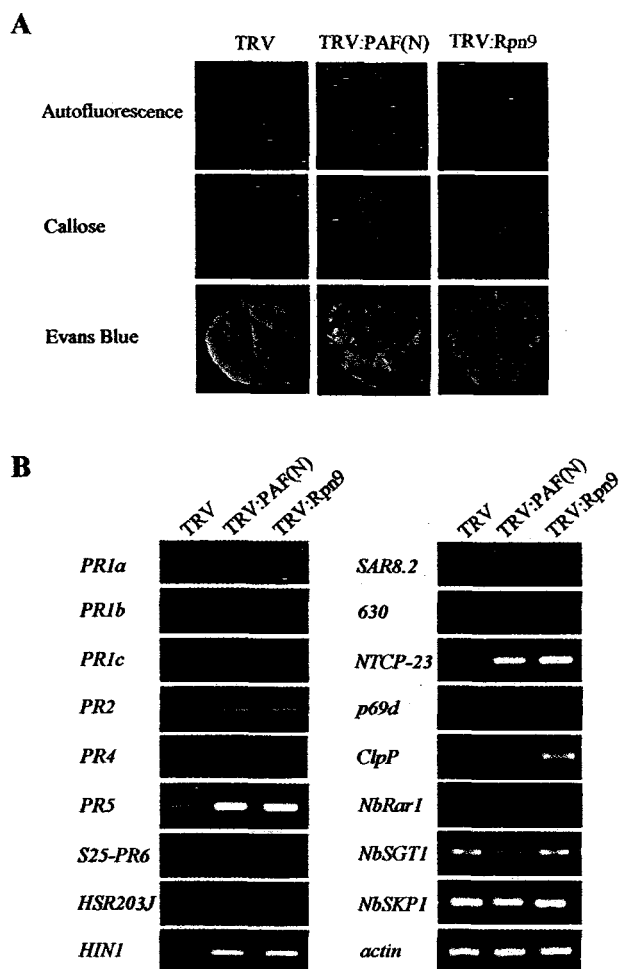


FIG. 8. Accumulation of defense-related markers. A, Autofluorescence, callose staining, and Evans blue staining of detached leaves from TRV control, TRV:PAF(N), and TRV:Rpn9 lines. Evans blue staining indicates dead cells without intact cellular membranes. B, semi-quantitative RT-PCR analysis to examine transcript levels of defense-related genes. RNA was extracted from the fourth leaf above the infiltrated leaves from several independent *N. benthamiana* plants infected with TRV, TRV:PAF(N), or TRV:Rpn9. As a control for RNA amount, actin mRNA levels were examined.

(9). However, the use of proteasome inhibitors has led to some contradictory conclusions, as treatment either promoted or prevented PCD, depending on the cell lines (12). These may be explained by a model summarized by Grimm and Osborne (33), who suggested that proteasome inhibition may have different effects on proliferating versus non-proliferating cells because of cell cycle regulation by the ubiquitin-proteasome pathway. In quiescent cells, the proteasome may be responsible for activating caspase cascade to induce cell death; thus, inhibition of proteasome would prevent PCD. On the other hand, in proliferating cells, accumulation of cell cycle regulators by proteasome inhibition leads to dysregulation of cell cycle, which may drive cells into PCD. This model is consistent with much of the available data in animal system, and our data, because the proteasome-mediated PCD phenotype was evident in newly formed leaves of the VIGS lines.

Recent findings suggest diverse action mechanisms of ubiquitin/proteasome pathway in the regulation of PCD (8). Important regulators of apoptosis, including the Bcl-2 family of proteins and the inhibitor of apoptosis proteins (34), have been newly identified as substrates of the proteasome. Furthermore, the tumor suppressor p53 and other cell cycle proteins that are

already known to be substrates of the proteasome, and inhibitor of apoptosis proteins, which are critically involved in the negative regulation of apoptosis, have been shown to play an active role in the proteolytic inactivation of death executors (8, 9). The evidence of possible involvement of proteasome in PCD in plants has only begun to emerge. Recently, ubiquitin ligase-associated protein SGT1 has been found to be essential for R gene-mediated disease resistance (30, 35) and HR cell death elicited by multiple resistance interactions (35). Furthermore, SGT1 and RAR1 (SGT1-interacting protein) are co-immunoprecipitated with COP9 signalosome, demonstrating a direct interaction between COP9 signalosome and ubiquitin ligases (31). These results suggest that the ubiquitin protein degradation pathway regulate at least a subset of R-mediated defense responses and HR cell death (36).

Compared with animal system, relatively little information is available on the detailed mechanism of PCD in plants. However, some aspects of the molecular machinery of PCD seem to be conserved between plants and animals. Numerous mediators of disease resistance signaling in plants share conserved motifs with proteins that have similar roles in the defense response of animals (7). Furthermore, overexpression of Bax, which encodes a mammalian proapoptotic protein, induces PCD in plants and yeast (37, 38). In animal cells, mitochondria-mediated PCD acts through Bax family of proteins, which associates with the mitochondria membrane and forms an ion-conduction channel through which macromolecules and metabolites can pass (39). Although Bax plays a critical role in mitochondrion-mediated PCD in mammals, plants and yeast lack these proteins and many other regulators of mammalian PCD. Nevertheless, Bax-induced PCD in plant cells indicates common underlying mechanisms between animal and plant cell death programs.

In this study, we have demonstrated that proteasome-mediated cell death in plants involves the common components of apoptosis in animal cells, including decreased mitochondrial membrane integrity, ROS production, cytochrome *c* release, and activation of caspase-like protease activities. Although plant genome lacks direct homologues of caspase genes, caspase-like protease activities have been detected in the HR cell death and in PCD associated with other nonpathogenic responses, such as heat, menadione, and isopentenyladenosine treatment (40–42). Interestingly, HR cell death and the caspase-like activities were specifically inhibited by caspase inhibitors but not by other types of inhibitor including those targeting serine proteases, metalloproteases, calpain, and aspartate proteases (40, 43). The caspase 3-like activity found in barley embryonic cells also could be inhibited by the specific caspase 3 inhibitors, but not by general cysteine protease inhibitors (44). Recently, a family of caspase-related proteases (the metacaspases) has been identified in *Arabidopsis* based on homology searches (45). It remains to be seen whether the metacaspases are functionally equivalent to mammalian caspases in controlling cell-death activation. Several reports point to the importance of the mitochondria in the expression of HR cell death in plants, although it is not clear whether cytochrome *c* leakage occurs during the HR. Cytochrome *c* leakage and activation of caspase-like proteases was detected in our study, and during isopentenyladenosine- and heat-induced PCD, but not during petal senescence-associated PCD (41, 42, 46, 47). It remains to be investigated whether the released cytochrome *c* promotes assembly of the caspase-activating complex in the cytosol, as in the case of animal cells.

Disruption of two different proteasome subunits both induced transcription of defense genes, such as *PR2*, *PR5*, *Hin1*, and *NTCP-23* (cysteine protease), and *ClpP* protease

(Fig. 7B). However, expression of other genes that are also highly induced during the HR cell death, including *PR1*, *PR4*, *HSR203J*, *SAR8.2*, and *p69d* (serine protease), was not stimulated. No induction of *PR1a* and *SAR8.2* indicates that the level of salicylic acid, a positive regulator of the HR cell death, is not elevated during the proteasome-mediated PCD. *Hin1* and *HSR203J*, which showed opposite expression patterns in this study, have been shown to be associated in HR cell death, but not with senescence-related cell death (28). *HSR203J* encoding a serine hydrolase is believed to play a role in the limitation of cell death during HR (48). In addition, the chloroplastic ClpP protease is involved in chloroplast development but not in senescence or HR cell death (29). These different gene expression profiles indicate that PCD pathway activated by the two different means, *i.e.* proteasome inhibition and pathogen, may be differentially regulated, at least partly, with possible involvement of distinct downstream components. A microarray analysis of gene expression of 100 selected genes demonstrated that heat- and senescence-induced PCD each caused stimulated expression of a distinctive set of genes, whereas there is some overlap in the differential gene expression between the two systems (49). Particularly, certain oxidative stress-related genes and cysteine proteases, and several genes involved in the HR cell death, appeared to be commonly involved during PCD induced by the two different means (49). Functions of these genes in programmed cell death remain to be tested.

The 20 S proteasome consists of two copies each of seven distinctive α - and seven distinctive β -type subunits (50). In *Saccharomyces cerevisiae*, gene disruption of the individual genes encoding the 14 subunits of the 20 S proteasome was carried out. The results indicated that 13 of the 14 subunits are essential to the viability of yeast cells; the only subunit that turned out to be nonessential is $\alpha 3$ (51). The deletion mutant of the $\alpha 3$ subunit gene has a longer generation time than the wild-type cells and showed altered chymotryptic activities (51). Finley and co-workers (52) tested the functional effects of mutations in the ATP-binding motif of each of the six *RPT* genes in *S. cerevisiae*; four were lethal, and two conferred a strong growth defect, implying that these ATPases are not functionally redundant. Recently, using RNA interference, effects of reduced expression of individual proteasome subunits of the 19 S regulatory complex were examined in *Drosophila* and trypanosome (20, 21). In both cases, reduced expression of individual proteasome subunits disrupted proteasome complex formation and resulted in increased apoptosis, accumulation of ubiquitinated cellular proteins, and decreased cell proliferation. Among 11 Rpn subunits of the 19 S regulatory complex, Rpn9 and Rpn10 are not essential for the viability of *S. cerevisiae* (50, 53), whereas only Rpn10 is not essential in *Drosophila* (20, 21). In trypanosome, each of the 11 Rpn subunits was found indispensable for the viability (20). Yeast $\Delta rpn9$ cells grow normally at the permissive temperature but displayed strong growth defect at nonpermissive temperature and became arrested at the G₂/M phase of cell cycle (50). These cells contained 26 S proteasome that was shifted to lighter fractions in a glycerol density gradient. However, this incomplete proteasome complex, which also misses Rpn10, is functionally adequate in maintaining cell viability (50). In this study, we found that reduced expression of the $\alpha 6$, $\beta 1$, $\beta 4$, Rpn3, and Rpn9 subunits all activated the PCD pathway; thus, all of these subunits are essential for survival of plant cells.

Our results demonstrated the involvement of the ubiquitin/proteasome pathway in the regulation of PCD in plant cells. The proteasome is expected to play a role in regulation of plant cell death in multilevels, including proteolytic inactivation of

unidentified apoptosis regulators and death executors. Stability of an individual proteasome subunit may be a target of regulation for controlling the PCD program. It will be important to investigate whether various developmentally or environmentally activated cell death programs of plants involve modulation of proteasome function. In this scenario, some PCD pathways of plants may include signaling molecules that modify proteasome activity to activate the cell demolition process when death signals are perceived. To identify the important players in cell death activation in plants, reverse genetic approaches such as virus-induced gene silencing, coupled with bioinformatics approaches, will be useful to screen a large number of candidate regulators. Probing functional roles of the proteasome in PCD activation may give insight into how death signals, including developmental or pathogen-related signals, are perceived and translated into a cascade of changes leading to plant cell death. These efforts may reveal unique mechanisms of PCD program in plant cells, in addition to the conserved mechanisms between animals and plants. Finally, from an applied perspective, the ability to induce cell death by gene silencing of proteasome subunits may have useful applications in agriculture by providing a tool to selectively kill certain cells and tissues.

Acknowledgments—We thank Dr. David C. Baulcombe (John Innes Center, Norwich, United Kingdom) for providing VIGS vectors, Dr. Ki-Sun Kwon (Korea Research Institute of Bioscience and Biotechnology (KRIBB), Taejeon, Korea) for providing the anti-ubiquitin antibody and TMRM, Dr. Hyeon G. Yoo (KRIBB) for anti-VDAC antibody, and Dr. Do Hee Lee (KRIBB) for helpful comments on measuring proteasome activities.

REFERENCES

1. Steller, H. (1995) *Science* **267**, 1445–1449
2. Green, D. R. (1998) *Cell* **94**, 695–698
3. Vaux, D. L., and Korsmeyer S. J. (1999) *Cell* **96**, 245–254
4. Wertz, I. E., and Hanley, M. R. (1996) *Trends Biochem. Sci.* **21**, 359–364
5. Lam, E., Kato, N., and Lawton, M. (2001) *Nature* **411**, 848–853
6. Jacobson, M. D., Weil, M., and Raff, M. C. (1997) *Cell* **88**, 347–354
7. Wilson, I., Vogel, J., and Sommerville, S. (1997) *Curr. Biol.* **7**, R175–R178
8. Jesenberger, V., and Jentsch, S. (2002) *Nat. Rev. Mol. Cell. Biol.* **3**, 112–121
9. Orłowski, R. Z. (1999) *Cell Death Differ.* **6**, 303–313
10. Hershko, A., and Ciechanover, A. (1998) *Annu. Rev. Biochem.* **67**, 425–479
11. Callis, J., and Vierstra, R. D. (2000) *Curr. Opin. Plant Biol.* **3**, 381–386
12. Wojcik, C. (1999) *Cell Mol. Life Sci.* **56**, 908–917
13. Woffenden, B. J., Freeman, T. B., and Beers, E. P. (1998) *Plant Physiol.* **118**, 419–430
14. Becker, F., Buschfeld, E., Schell, J., and Bachmair, A. (1993) *Plant J.* **3**, 875–881
15. Angell, S. M., and Baulcombe, D. C. (1999) *Plant J.* **20**, 357–362
16. Lee, S. S., Cho, H. S., Yoon, G. M., Ahn, J.-W., Kim, H. H., and Pai, H.-S. (2003) *Plant J.* **33**, 825–840
17. Waterhouse, P. M., Wang, M.-B., and Lough, T. (2001) *Nature* **411**, 834–842
18. Ozaki, M., Fujinami, K., Tanaka, K., Amemiya, Y., Sato, T., Ogura, N., and Nakagawa, H. (1992) *J. Biol. Chem.* **267**, 21678–21684
19. Basset, G., Raymond, P., Malek, L., and Brouquisse, R. (2002) *Plant Physiol.* **128**, 1149–1162
20. Li, Z., and Wang, C. C. (2002) *J. Biol. Chem.* **277**, 42686–42693
21. Wojcik, C., and DeMartino, G. N. (2002) *J. Biol. Chem.* **277**, 6188–6197
22. Girod, P.-A., Fu, H., Zryd, J.-P., and Vierstra, R. D. (1999) *Plant Cell* **11**, 1457–1471
23. Doelling, J. H., Yan, N., Kurepa, J., Walker, J., and Vierstra, R. D. (2001) *Plant J.* **27**, 393–405
24. Bethke, P. C., and Jones, R. L. (2001) *Plant J.* **25**, 19–29
25. Pontier, D., Tronchet, M., Rogowsky, P., Lam, E., and Roby, D. (1998) *Mol. Plant-Microbe Interact.* **11**, 544–554
26. Zhang, H., Huang, H. M., Carson, R. C., Mahmood, J., Thomas, H. M., and Gibson, G. E. (2001) *Anal. Biochem.* **298**, 170–180
27. Tsujimoto, Y., and Shimizu, S. (2002) *Biochimie* **84**, 187–193
28. Heath, M. C. (2000) *Plant Mol. Biol.* **44**, 321–324
29. Beers, E. P., Woffenden, B. J., and Zhao, C. (2000) *Plant Mol. Biol.* **44**, 399–415
30. Austin, M. J., Muskett, P., Kahn, K., Feys, B. J., Jones, J. D. G., and Parker, J. (2002) *Science* **295**, 2077–2080
31. Azevedo, C., Sadanandom, A., Kitagawa, K., Freialdenhoven, A., Shirasu, K., and Schultze-Lefert, P. (2002) *Science* **295**, 2073–2076
32. Liu, Y., Schiff, M., Serino, G., Deng, X.-W., and Dinesh-Kumar, S. P. (2002) *Plant Cell* **14**, 1483–1493
33. Grimm, L. M., and Osborne, B. A. (1999) *Res. Probl. Cell Differ.* **23**, 209–228
34. Martin, S. J. (2002) *Cell* **109**, 793–796
35. Peart, J. R., Lu, R., Sadanandom, A., Malcuit, I., Moffett, P., Brice, D. C., Schausser, L., Jaggard, D. A. W., Xiao, S., Coleman, M. J., Dow, M., Jones, J. D. G., Shirasu, K., and Baulcombe, D. C. (2002) *Proc. Natl. Acad. Sci.*

- U. S. A. **99**, 10865–10869
36. Gray, W. M. (2002) *Curr. Biol.* **12**, R352–R354
37. Sato T., Harada, M., Bodrug, S., Irie, S., Iwama, N., Boise, L. H., Thompson, C. B., Golemis, E., Fong, L., Wang, H. G., and Reed, J. C. (1994) *Proc. Natl. Acad. Sci. U. S. A.* **91**, 9238–9242
38. Lacomme, C., and Santa Cruz, S. (1999) *Proc. Natl. Acad. Sci. U. S. A.* **96**, 7956–7961
39. Ferri, K. F., and Kroemer, G. (2001) *Bioessays* **23**, 111–115
40. del Pozo, O., and Lam, E. (1998) *Curr. Biol.* **8**, 1129–1132
41. Mlejnek, P., and Prochazka, S. (2002) *Planta* **215**, 158–166
42. Sun, Y. L., Zhao, Y., Hong, X., and Zhai, Z. H. (1999) *FEBS Lett.* **462**, 317–321
43. D'Silva, I., Poirier, G., and Heath, M. C. (1998) *Exp. Cell Res.* **245**, 389–399
44. Korthout, H. A., Berecki, G., Bruin, W., van Duijn, B., and Wang, M. (2000) *FEBS Lett.* **475**, 139–144
45. Uren, A. G., O'Rourke, K., Aravind, L., Pisabarro, M. T., Seshagiri, S., Koonin, E. V., and Dixit, V. M. (2000) *Mol. Cell* **6**, 961–967
46. Balk, J., Leaver, C. J., and McCabe, P. F. (1999) *FEBS Lett.* **463**, 151–154
47. Xu, Y., and Hanson, M. R. (2000) *Plant Physiol.* **122**, 1323–1333
48. Pontier, D., Gan, S., Amasino, R. M., Roby, D., and Lam, E. (1999) *Plant Mol Biol.* **39**, 1243–1255
49. Swidzinski, J. A., Sweetlove, L. J., and Leaver, C. J. (2002) *Plant J.* **30**, 431–446
50. Voges, D., Zwickl, P., and Baumeister, W. (1999) *Annu. Rev. Biochem.* **68**, 1015–1068
51. Emori, Y., Tsukahara, T., Kawasaki, H., Ishiura, S., Sugita, H., and Suzuki, K. (1991) *Mol. Cell Biol.* **11**, 344–353
52. Rubin, D. M., Glickman, M. H., Larsen, C. N., Dhruvakumar, S., and Finley, D. (1998) *EMBO J.* **17**, 4909–4919
53. Fu, H., Reis, N., Lee, Y., Glickman, M. H., and Vierstra, R. D. (2001) *EMBO J.* **20**, 7096–7107
54. Hofmann, K., and Bucher, P. (1998) *Trends Biochem. Sci.* **23**, 204–205

Interaction of NtCDPK1 calcium-dependent protein kinase with NtRpn3 regulatory subunit of the 26S proteasome in *Nicotiana tabacum*

Sang Sook Lee, Hye Sun Cho, Gyeong Mee Yoon[†], Joon-Woo Ahn, Hyong-Ha Kim[†] and Hyun-Sook Pai^{*}
Laboratory of Plant Genomics, Korea Research Institute of Bioscience and Biotechnology, PO Box 115, Yusong, Taejon 305-600, Korea

Received 19 September 2002; revised 26 November 2002; accepted 3 December 2002.

^{*}For correspondence (fax +82 42 860 4608; e-mail hyunsook@kribb.re.kr).

[†]Present address: Department of Horticulture, Washington State University, Pullman, WA 99164-6414, USA.

[‡]Present address: Division of Chemical Metrology, Korea Research Institute of Standards and Science, PO Box 102, Yusong, Taejon 305-600, Korea.

Summary

Using a yeast two-hybrid system, we identified NtRpn3, a regulatory subunit of 26S proteasome, as an interacting protein of NtCDPK1 calcium-dependent protein kinase in *Nicotiana tabacum*. Rpn3 in yeast is an essential protein involved in proteolysis of cell cycle regulatory proteins, and the carrot homolog of Rpn3 was previously isolated as a nuclear antigen that is mainly expressed in the meristem. NtCDPK1 physically interacts with NtRpn3 *in vitro* in a Ca²⁺-independent manner and phosphorylates NtRpn3 in a Ca²⁺-dependent manner with Mg²⁺ as a cofactor. NtCDPK1 and NtRpn3 are co-localized in the nucleus, nuclear periphery, and around plasma membrane *in vivo*. Both NtCDPK1 and AtRpn3, an NtRpn3 homolog of *Arabidopsis*, are mainly expressed in the rapidly proliferating tissues including shoot and root meristems, and developing floral buds. Virus-induced gene silencing of either NtRpn3 or NtCDPK1 resulted in the phenotypes of abnormal cell morphology and premature cell death in newly emerged leaves. Finally, NtCDPK1 interacts with NtRpn3 *in vivo* as shown by co-immunoprecipitation. Based on these results, we propose that NtCDPK1 and NtRpn3 are interacting in a common signal transduction pathway possibly for regulation of cell division, differentiation, and cell death in tobacco.

Keywords: co-immunoprecipitation, *in vivo* co-localization, meristem, phosphorylation, premature cell death, virus-induced gene silencing.

Introduction

Numerous evidences indicate that degradation of many cytosolic and nuclear proteins is controlled by the ubiquitin/proteasome pathway in eukaryotes (reviewed by Hershko and Ciechanover, 1998). In this pathway, ubiquitin becomes covalently attached to cellular proteins by an ATP-dependent reaction cascade involving E1, E2, and E3 enzymes (reviewed by Callis and Vierstra, 2000). Most of the ubiquitinated proteins are targeted for degradation by the 26S proteasome, a large ATP-dependent, multisubunit protease that is highly conserved in all eukaryotes. Both in animals and in plants, the 26S proteasome consists of two large subcomplexes, the 20S proteasome and the 19S regulatory complex. Proteolysis occurs inside of the 20S proteasome compartment, while the 19S regulatory complex confers the specificity towards ubiquitinated substrates and an ATP dependence on proteolysis. The 26S

proteasome has a general function in the selective removal of various short-lived proteins that are first covalently linked to ubiquitin. Proteasomal substrates include metabolic key enzymes, transcription factors, cyclins, and inhibitors of cyclin-dependent kinases. In plants, the ubiquitin/proteasome pathway has been linked to cell cycle (Criqui *et al.*, 2000) and to various signal transduction pathways including auxin signaling, photomorphogenesis, and jasmonic acid signaling (reviewed by Callis and Vierstra, 2000).

The yeast Rpn3/Sun2, a subunit of the lid complex of the 26S proteasome, is essential in the cell cycle progression (Bailey and Reed, 1999; Kominami *et al.*, 1997). The *rpn3* mutation does not prevent the G₁/S transition but causes a metaphase arrest. Rpn3 function is required for the degradation of the cyclins, such as Cln2, Clb5, and Clb2, and

anaphase inhibitor Pds1; however, degradation of Cdk inhibitor Sic was not affected by the *rpn3* mutation. In contrast, turnover of Sic is severely impaired by a temperature-sensitive mutation of *Rpn12/Nin1*, encoding another essential regulatory subunit of the 26S proteasome, arguing for the requirement of distinct regulatory subunits for efficient proteolysis of specific cell cycle regulators (Bailey and Reed, 1999). The carrot 21D7 protein is a plant homolog of Rpn3, and the lethal phenotype of the yeast *rpn3* mutant is partially complemented by expression of 21D7 (Smith *et al.*, 1997). The 21D7 protein is mainly expressed in plant tissues that contain actively dividing cells, such as shoot and root meristem, developing floral buds, and cell cultures, and is located in the nucleus (Smith *et al.*, 1988, 1993). Later it was found that the 21D7 protein is a component of the 26S proteasome, being co-purified with the 19S regulatory complex (Smith *et al.*, 1997). However, how the 21D7 protein controls protein degradation and whether 21D7 is involved in cell cycle control in plant cells are not known. More recently, multiubiquitin chain binding subunit MCB1 (RPN10) of the 26S proteasome has been found to be essential for developmental progression in moss *Physcomitrella patens* (Girod *et al.*, 1999). Interestingly, auxin and cytokinin partially rescued the $\Delta mcb1$ mutant phenotypes. Furthermore, the RPN12 subunit of *Arabidopsis* has been shown to be involved in cytokinin responses, the mutant of which showed altered growth responses to exogenous cytokinin, reduced leaf formation, and delayed skotomorphogenesis (Smalle *et al.*, 2002), further supporting for a role of the ubiquitin/26S proteasome in plant developmental processes triggered by hormones.

NtCDPK1 belongs to a large group of calcium-dependent protein kinases (Yoon *et al.*, 1999). Calcium-dependent protein kinases (CDPK) function as a potential sensor that recognizes the changes in cytosolic calcium concentration in response to various stimuli, which include light, environmental stress, pathogen attack, and phytohormones, and translates them into activation of downstream signaling pathway (reviewed by Harmon *et al.*, 2001). A large family of CDPK genes has been identified in various plant species including 34 members in *Arabidopsis* (reviewed by Harmon *et al.*, 2001), suggesting that individual CDPK is involved in multiple signaling pathways with differential specificity. Although functions of most CDPKs are still largely unknown, increasing evidence suggests that CDPKs are involved in environmental stress signaling. Previously we have shown that tobacco *NtCDPK1* is transcriptionally induced by various stimuli including phytohormones and abiotic stresses in tobacco BY2 cells and leaves (Yoon *et al.*, 1999). NtCDPK1 was immunodetected and phosphorylated *in vivo* mainly in the membrane fraction of BY2 cells, implicating membrane association of NtCDPK1. We attempted to address biological functions and related sig-

naling pathway of NtCDPK1 by identifying substrates or interactive regulatory proteins. Here we report that NtCDPK1 is interacting with the Rpn3 homolog of tobacco. We present biological, biochemical, and cytological evidence for functional relationship of NtCDPK1 and NtRpn3, and their possible involvement in the control of cell division, differentiation, and cell death in tobacco.

Results

NtCDPK1 interacts with NtRpn3 that is a regulatory subunit of the 26S proteasome

To isolate proteins that interact with NtCDPK1, the yeast two-hybrid assay using LexA system was applied. Using the NtCDPK1 kinase domain as bait, a tobacco flower bud cDNA library was screened. Among many positive clones sequenced, a large proportion represented a cDNA encoding a tobacco homolog of 21D7, whose sequence was previously reported (Ito *et al.*, 1997). The carrot 21D7 protein is the Rpn3 subunit of the 26S proteasome, which could partially complement the yeast *rpn3/sun2* mutant (Smith *et al.*, 1997). The tobacco cDNA was named *NtRpn3*. It encodes a polypeptide of 488 amino acid residues with an estimated molecular mass of 55384 Da. The sequences of NtRpn3 with homologs in other species including carrot, *Arabidopsis*, yeast, and human were aligned (Figure S1). NtRpn3 displays overall 81% identity to 21D7 from carrot (accession number AAF20216), 73–78% identity to two homologs from *Arabidopsis* (accession numbers At1g20200 and At1g75990), 35% identity to Rpn3/Sun2 from yeast (accession number AFO35280), and 46% identity to Rpn3 from human (accession number D67025). Based on the genomic Southern analysis, tobacco genome contains two copies of the *NtRpn3*-related sequences (data not shown).




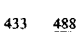

To test the specificity of the interaction between NtCDPK1 and NtRpn3, various plant protein kinases including NtCDPK2 (Romeis *et al.*, 2001), PRK1 (Mu *et al.*, 1994) and WAPK (Lee *et al.*, 1998), and PKC, Myb, and ENV4 from human were examined for their interaction with NtRpn3 using the yeast two-hybrid assay (Figure 1a). NtCDPK2, a tobacco CDPK involved in pathogen response, and other signaling proteins tested were not physically associated with NtRpn3, as shown by the inability to grow on Leu⁻ and by the lack of β -galactosidase activity. In addition, AtRpn10 and AtRpn12, other regulatory subunits of 26S proteasome from *Arabidopsis*, did not show any interaction with NtCDPK1. To map the NtRpn3 region responsible for the interaction with NtCDPK1, the full NtRpn3 and four deletion constructs were fused to B42AD and introduced into yeast cells together with the construct containing the LexA-NtCDPK1 kinase domain. As shown in Figure 1(b), the

Figure 1. Specificity of the NtRpn3–NtCDPK1 interaction and mapping of NtRpn3 domains involved in the interaction with NtCDPK1.

(a) Yeast two-hybrid assay. Yeast growth on the selection medium and β -galactosidase activity were monitored as indicators of the protein interaction.

(b) Yeast two-hybrid assay of interactions between NtCDPK1 and various forms of NtRpn3. The LexA–NtCDPK1 kinase domain was combined with B42AD fusions with NtRpn3 polypeptides carrying various N-terminal or C-terminal deletions. Three separate colonies per construct were picked up to examine β -galactosidase activity.

(a)	Bait	Prey	Growth(Leu-)	Leu+/X-Gal
	NtCDPK1	NtRpn3	+	blue
	NtCDPK2	NtRpn3	-	white
	WAPK	NtRPN3	-	white
	PRK1	NtRpn3	-	white
	PKC	NtRPN3	-	white
	Myb	NtRpn3	-	white
	NtCDPK1	AtRpn10	-	white
	NtCDPK1	AtRpn12	-	white

(b)		Growth	β -Gal activity
NtRpn3		+	3.70 \pm 0.41
NtRpn3- Δ C		+	1.52 \pm 0.38
NtRpn3-P		+	16.02 \pm 0.02
NtRpn3-P Δ N		+	71.92 \pm 5.70
NtRpn3-P Δ C		+/-	0.45 \pm 0.01

full-length NtRpn3, NtRpn3- Δ C, and NtRpn3-P all showed the yeast growth and the β -galactosidase activity, indicating their interaction with NtCDPK1. Interestingly, the strongest interaction came from NtRpn3-P Δ N containing the short C-terminal hydrophilic region of NtRpn3. As shown in NtRpn3- Δ C and NtRpn3-P Δ C, the removal of the C-terminal region reduced the β -galactosidase activity. The C-terminal hydrophilic region is predicted to form a coiled coil, a typical protein–protein interaction module. NtRpn3 contains the PCI domain (residues 346–429), which is present in regulatory subunits of 26S proteasome, COP9 signalosome, and eIF3 (Hofmann and Bucher, 1998; Kim *et al.*, 2001). The PCI domain, an α -helical domain of about 200 amino acid residues, is a protein contact site required for assembly of the multisubunit protein complexes (Fu *et al.*, 2001; Kim *et al.*, 2001). The apparent lack of interaction between NtRpn3-P Δ C and NtCDPK1 indicates that the PCI domain may not be critically involved in the NtCDPK1–NtRpn3 interaction. Together, these analyses demonstrated that multiple regions of NtRpn3, including the C-terminal region, are involved in the interaction with NtCDPK1.

NtCDPK1 interacts with and phosphorylates NtRpn3 in vitro

To further confirm the interaction between NtRpn3 and NtCDPK1 and to determine whether Ca^{2+} regulates the interaction between the two proteins, we carried out the *in vitro* protein binding assay with purified recombinant proteins of NtCDPK1 and NtRpn3. As shown in Figure 2(a), the full-length NtCDPK1 and its kinase domain were

expressed as maltose binding protein (MBP) fusion protein. The full NtRpn3 and two deletion forms were expressed as glutathione S-transferase (GST) fusion proteins.

For the interaction assays, GST, GST–NtRpn3, GST–NtRpn3-P, and GST–NtRpn3- Δ C fusion proteins were incubated with the resin-bound MBP–NtCDPK1 kinase domain, or MBP alone in the presence of Ca^{2+} or EGTA. After washing, the matrix-bound fractions were eluted and separated by SDS–PAGE, then stained with Coomassie, which showed the relative levels of the MBP or MBP–NtCDPK1 in the binding reactions. Separately, the bound fractions were analyzed by Western blotting with the GST antibody to detect the presence of bound GST–NtRpn3 fusion proteins. All three forms of the GST–NtRpn3 proteins were detected in the Western blot showing the interaction, while binding of GST–NtRpn3 protein to MBP was not detected (Figure 2b). The GST protein by itself did not bind to MBP–NtCDPK1 fusion protein. Thus, the NtCDPK1 kinase domain could interact with all three forms of NtRpn3, among which NtRpn3-P showed the strongest binding, consistent with the result from the yeast two-hybrid assay (Figure 1b). The presence of Ca^{2+} in the binding reaction did not significantly affect the binding of all three NtRpn3 forms to the kinase domain of NtCDPK1.

To determine if the interaction between NtCDPK1 and NtRpn3 led to the phosphorylation of NtRpn3, the MBP–NtCDPK1 (full-length) fusion protein was mixed with GST or the GST fusion proteins of the full-length NtRpn3, NtRpn3-P, and NtRpn3- Δ C in a kinase assay with [γ - ^{32}P]ATP and Mg^{2+} as a cofactor in the presence of Ca^{2+} (Figure 2c). The autophosphorylated NtCDPK1 generated multiple

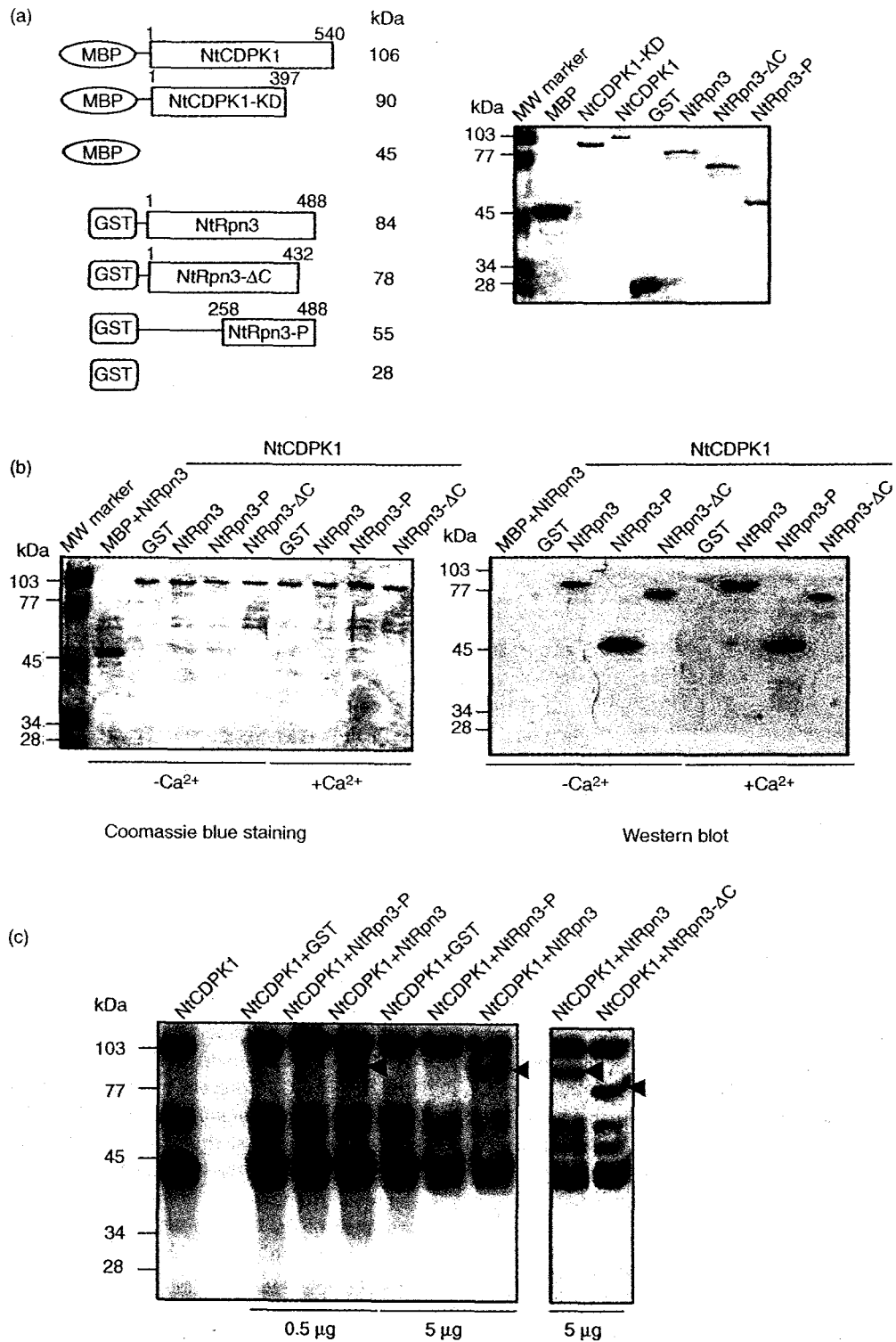


Figure 2. NtCDPK1 interacts with and phosphorylates NtRpn3 *in vitro*.

(a) Purification of the recombinant NtCDPK1 and NtRpn3 proteins (left) visualized with Coomassie staining (right).
 (b) *In vitro* protein binding assay with the NtCDPK1 kinase domain. Various GST-NtRpn3 fusion proteins were incubated with the immobilized MBP-NtCDPK1-KD fusion protein in the presence of either Ca²⁺ (1 mM) or EGTA (2 mM). After washing, the amylose resin-bound fractions were separated by SDS-PAGE. The separated proteins were visualized by Coomassie staining (left), or transferred to the membrane for Western blotting with GST antibody to detect the GST fusion protein (right).
 (c) *In vitro* kinase assay of various forms of NtRpn3 (0.5 or 5 μg) by the full NtCDPK1 in the presence of Mg²⁺ (1 mM) and Ca²⁺ (1 mM).

bands due to protein degradation, and the top band represents the full-length NtCDPK1. GST (28 kDa) was not phosphorylated, demonstrating that the NtRpn3 moiety in the GST-NtRpn3 fusion proteins is phosphorylated by NtCDPK1. The full NtRpn3 and NtRpn3-ΔC were phosphorylated by the full NtCDPK1, while phosphorylation of NtRpn3-P was not visibly detected with repeated experiments. Thus, the interaction between NtCDPK1 and NtRpn3 did lead to phosphorylation of NtRpn3.

NtCDPK1 phosphorylates NtRpn3 in a Ca²⁺-independent manner with Mn²⁺ as a cofactor

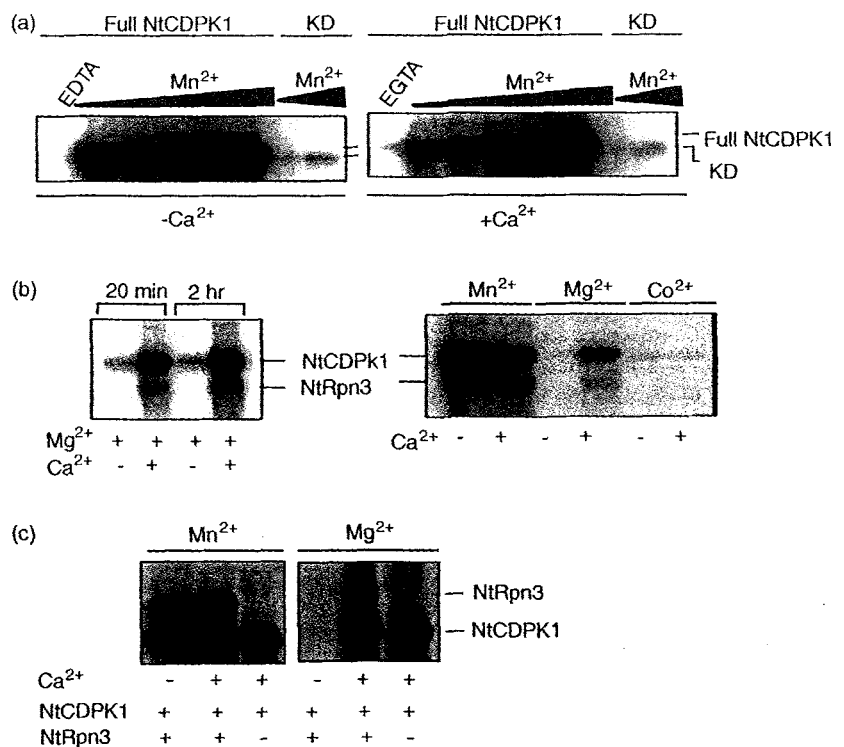
Interestingly, in the presence of Mn²⁺ as a cofactor, NtCDPK1 phosphorylates itself and NtRpn3 in a Ca²⁺-independent manner (Figure 3a,b). The presence or absence of Ca²⁺ did not affect the NtCDPK1 autophosphorylation with different concentrations of Mn²⁺ as a cofactor (Figure 3a). The kinase domain showed only the basal phosphorylating activity. NtCDPK1 also phosphorylates NtRpn3 in a Ca²⁺-independent manner in the presence of Mn²⁺ in contrast to the effect by Mg²⁺ (Figure 3b). Co²⁺ was not used as a cofactor. To further confirm the characteristics of NtCDPK1, the kinase assay was carried out with the cleaved form of NtCDPK1 purified from the MBP-NtCDPK1 fusion protein (Figure 3c). It also exhibited Ca²⁺-dependent autophosphorylation and NtRpn3 phosphorylation in the presence of Mg²⁺, and Ca²⁺-independent phosphorylation in the presence of Mn²⁺. Some plant protein kinases including

NPK5 from tobacco (Muranaka *et al.*, 1994), and CIPK1 (Shi *et al.*, 1999) and RLK5 (Horn and Walker, 1994) from *Arabidopsis* were more active when Mn²⁺ was used as a cofactor. A 67-kDa plasma-membrane-bound CDPK of apple also prefers Mn²⁺ over Mg²⁺ for autophosphorylation (Barker *et al.*, 1998). We found that phosphorylation of NtRpn3 by NtCDPK1 is induced by micromolar amounts of Mn²⁺ (results not shown). As the cellular concentration of Mn²⁺ is in the micromolar range under physiological conditions, this result raises a possibility of a physiological role of Mn²⁺ in NtCDPK1 regulation.

NtRpn3 and NtCDPK1 show a similar expression pattern during cell cycle

The *NtCDPK1* and *NtRpn3* transcript levels were regulated in a similar fashion during cell cycle of tobacco BY2 cells (Figure 4). Suspension-cultured tobacco BY2 cells were synchronized by a 24-h treatment with aphidicolin. After release from the aphidicolin block, mitotic index and the mRNA levels were monitored during cell cycle. As controls, the histone H4 gene and the cyclin B1 gene were used as a marker of S phase and M phase, respectively. The mRNA levels of both *NtCDPK1* and *NtRpn3* were maintained in a similar level through S and G₂ phase until mid-M phase and decreased to an undetectable level during G₁ phase. Both *NtCDPK1* and *NtRpn3* genes were expressed more abundantly in the log phase of BY2 cell growth than in the stationary phase (Figure 4).

Figure 3. Ca²⁺-independent phosphorylation in the presence of Mn²⁺ as a cofactor. (a) Autophosphorylation of the full-length NtCDPK1 or the kinase domain (KD) with increasing concentration of Mn²⁺ in the absence or the presence of Ca²⁺ (1 mM). The concentration of Mn²⁺ is 0.05, 0.2, 1, 5, and 10 mM for the full-length NtCDPK1, and 1 and 5 mM for the KD. EDTA and EGTA were used at 100 μM. (b) Phosphorylation of NtRpn3 by NtCDPK1 with Mn²⁺ (1 mM) or Mg²⁺ (1 mM) as a cofactor. The effects of incubation time in the kinase assay (left) and the presence of various divalent cations at 1 mM concentration (right) on phosphorylation of NtCDPK1 and NtRpn3 are shown. (c) *In vitro* kinase activity of the cleaved NtCDPK1 with Mn²⁺ or Mg²⁺ as a cofactor. The MBP-NtCDPK1 fusion protein was treated with Factor Xa to isolate the NtCDPK1 moiety for the kinase assay.



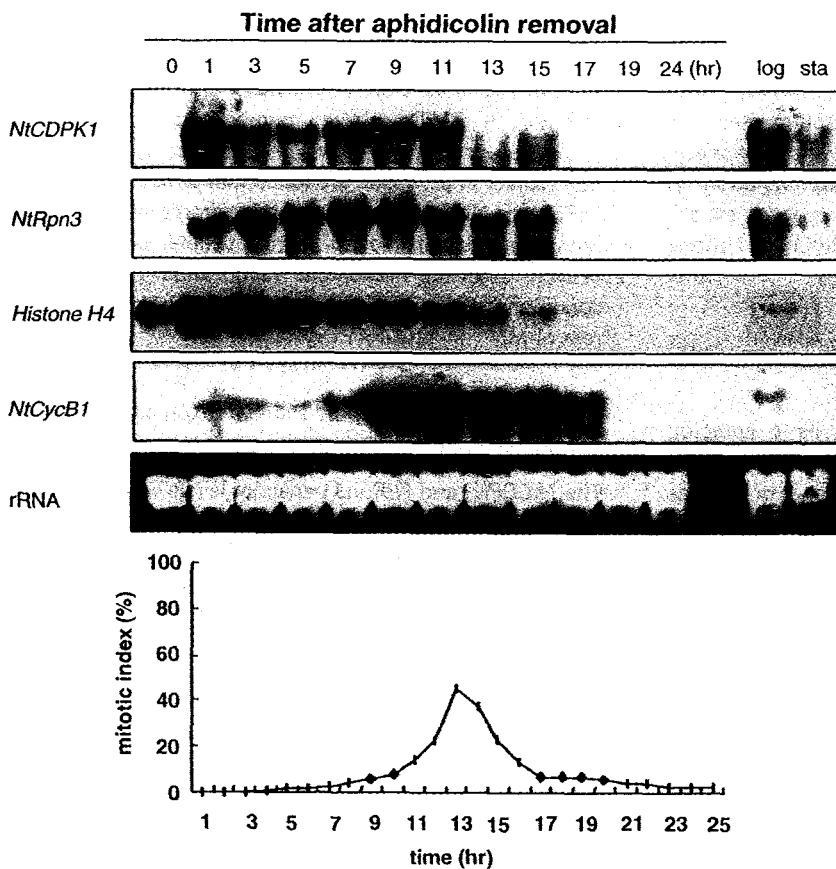


Figure 4. Expression of the *NtCDPK1* and *NtRpn3* mRNAs during cell cycle. Tobacco BY2 cells were synchronized with aphidicolin treatment, and RNA gel blot analysis was carried out with total RNA extracted from cells at different time points after aphidicolin removal. As controls for S and M phase, *histone H4* and *NtCycB1* mRNAs were detected, respectively. Separately, total RNA extracted from BY2 cells in log (log) and stationary phase (sta) of growth was subjected to the same analysis.

NtCDPK1 and *NtRpn3* are co-localized in vivo

Subcellular distribution of the *NtCDPK1* and *NtRpn3* proteins in plant cells was examined by expressing fusion proteins with green fluorescent protein (GFP) and red fluorescent protein (RFP). DNA constructs encoding *NtCDPK1*-GFP or RFP-*NtRpn3*, in which *NtRpn3* was fused to the C-terminus of RFP, under the control of the CaMV35S promoter were simultaneously introduced into protoplasts isolated from *Arabidopsis* seedlings (Figure 5a). After incubation at 25°C, expression of the introduced genes was examined under a fluorescent microscope with three different filters to capture the image of GFP, RFP and autofluorescence of chlorophyll. After 12-h incubation, the green fluorescent signal completely overlapped with the red fluorescent signal in the nucleus, showing the co-localization of *NtCDPK1*-GFP and RFP-*NtRpn3* in the nucleus. After 24-h incubation, the red and green fluorescent signals were associated with the plasma membrane in addition to the nucleus. To confirm that these proteins were indeed targeted to nucleus, RFP-*NtRpn3* was simultaneously expressed with NLS-GFP, a GFP fused with nucleus localization signal (Lee *et al.*, 2001), in the protoplasts (Figure 5b). The red and green fluorescent signals were co-localized in

the nucleus, demonstrating nuclear localization of RFP-*NtRpn3*.

It was noticed that the signals of *NtCDPK1*-GFP or RFP-*NtRpn3* were present not only within the nucleus but also in the nuclear periphery. In yeast, GFP-tagged 20S and 19S proteasome subcomplexes were predominantly accumulated in the nuclear periphery, more precisely in the nuclear envelope (NE)/endoplasmic reticulum (ER) network (Enenckel *et al.*, 1998). Estimation of the GFP signal revealed that approximately 80% of 26S proteasomes are structurally bound to the nuclear periphery, while approximately 20% of these complexes exist in the cyto- and nucleoplasmic compartments. Biochemical fractionation also revealed the presence of about 80% of 26S proteasome in the membrane fraction, and co-enrichment of 26S proteasomes and NE-ER membrane proteins (Enenckel *et al.*, 1998). These results and the previous finding of *NtCDPK1* being detected mainly in the membrane fraction of tobacco BY2 cells (Yoon *et al.*, 1999) indicate a possibility of *NtCDPK1* and *NtRpn3* being associated with NE-ER complexes in plant cells. Interestingly, the GFP fusion protein of the *NtCDPK1* deletion form that lacks the C-terminal calcium-binding domain was mainly associated with the plasma membrane, indicating that the calcium-binding

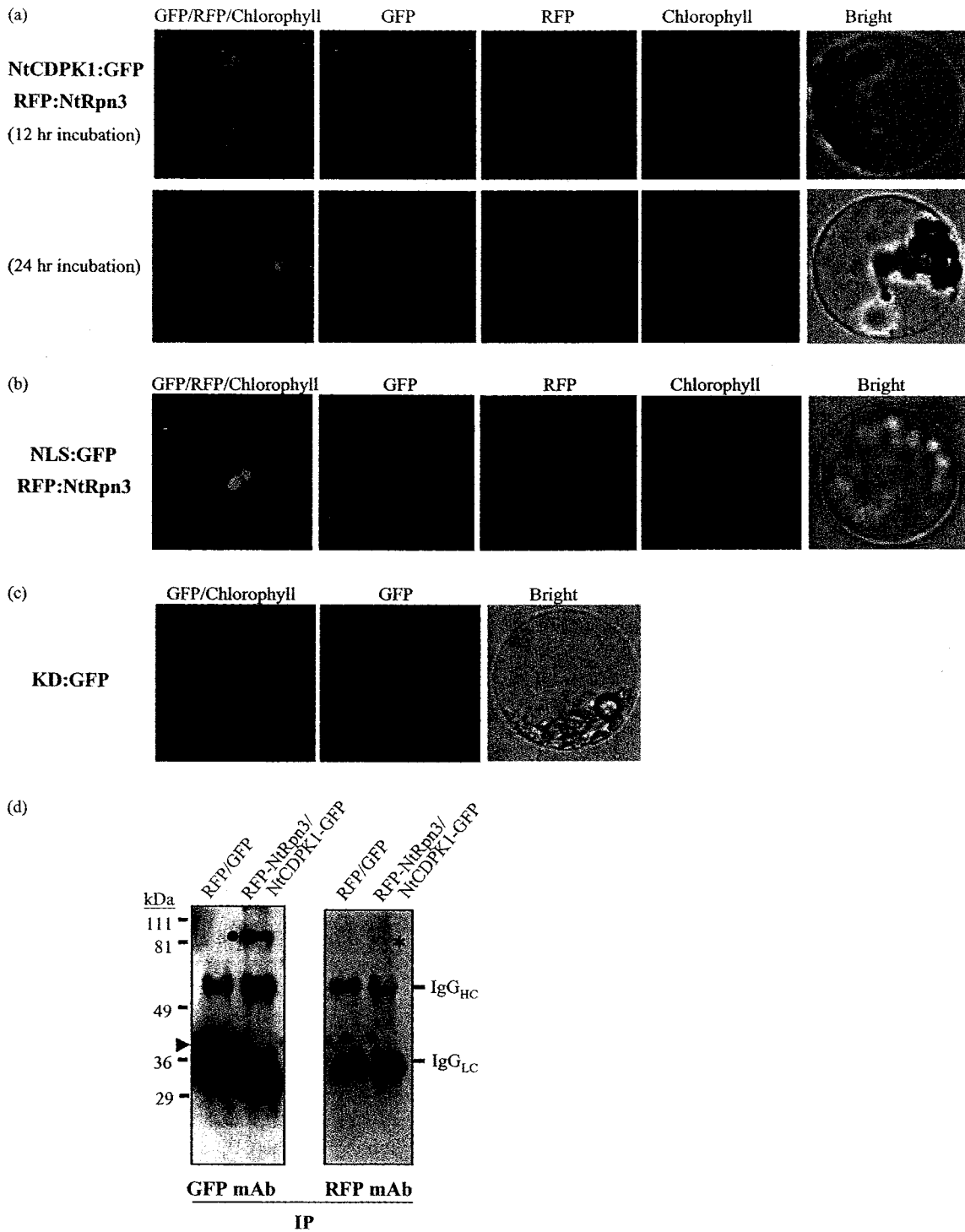


Figure 5. Co-localization of NtCDPK1 and NtRpn3 *in vivo* and co-immunoprecipitation.

(a) *In vivo* targeting of NtCDPK1 and NtRpn3. *Arabidopsis* protoplasts were transformed with both *NtCDPK1:GFP* and *RFP:NtRpn3* fusion constructs, and localization of fluorescent signals was examined at 12 h (top) and 24 h (bottom) after transformation. Green, red, and blue fluorescent signals indicate GFP, RFP, and autofluorescent chlorophyll, respectively. From left, the merged image (GFP, RFP, and chlorophyll), GFP, RFP, chlorophyll, and bright-field images are shown. N represents the nucleus.

(b) Nuclear targeting of NtRpn3. Protoplasts were transformed with both *RFP:NtRpn3* and *NLS:GFP* encoding a GFP containing the nuclear localization signal. After 24-h incubation, fluorescence signals were examined. From left, the merged image (GFP, RFP and chlorophyll), GFP, RFP, chlorophyll, and bright-field images are shown.

domain plays a role in nuclear localization of NtCDPK1 (Figure 5c). GFP or RFP alone was localized in the cytosol (results not shown). When the NtCDPK1-GFP fusion construct was transfected into protoplasts isolated from tobacco seedlings, it also resulted in mainly nuclear and plasma membrane localization of the signal (results not shown). The patterns of protein localization observed here were consistent with the results obtained from particle bombardment of the constructs into onion epidermal cells (results not shown). These data demonstrate co-localization of NtCDPK1 and NtRpn3 *in vivo*.

Interaction between NtCDPK1 and NtRpn3 *in vivo*

Further evidence for the NtCDPK1–NtRpn3 interaction came from observations that NtRpn3 could be co-immunoprecipitated with NtCDPK1 (Figure 5d). The NtCDPK1-GFP and RFP-NtRpn3 constructs, or GFP and RFP vectors as a control, were co-transformed into *Arabidopsis* protoplasts. The expected size of NtCDPK1-GFP and RFP-NtRpn3 is 88 and 83.3 kDa, respectively. After 24-h incubation, total proteins were prepared and reacted with anti-GFP polyclonal antibody to immunoprecipitate GFP or NtCDPK1-GFP fusion proteins. Then, the immunoprecipitated proteins were fractionated on SDS-PAGE, and Western blot analysis was performed using the monoclonal GFP and RFP antibody. The monoclonal GFP and RFP antibodies do not recognize NtCDPK1 or NtRpn3 (results not shown). High levels of GFP and NtCDPK1-GFP proteins were detected with the GFP antibody, showing the efficiency of the immunoprecipitation. The monoclonal RFP antibody visualized the co-precipitated NtRpn3-RFP but not RFP, indicating that NtRpn3 is associated with NtCDPK1 *in vivo* (Figure 5d).

NtCDPK1 and NtRpn3 are mainly expressed in proliferating tissues

To examine the expression pattern of NtCDPK1, we transformed *Arabidopsis* with the NtCDPK1 promoter::GUS fusion construct. The NtCDPK1-GUS fusion construct consists of the 1.1-kb promoter fused in-frame to the GUS gene. Histochemical GUS staining demonstrated that NtCDPK1 expression was strongly detected in the shoot apical meristem and young leaf primordia, while fully expanded leaves displayed very little GUS staining (Figure 6a). The root meristem, elongation zone, and branching points of lateral

roots also showed GUS activity, albeit less strongly. In flowers, NtCDPK1 was strongly expressed throughout the reproductive meristem and in all four whorls of young flower buds. As flowers developed, the expression became more restricted; just before anthesis, GUS staining was detected only in the stigma, pollen, and base of a flower (Figure 6a). In general, NtCDPK1 expression was limited to young tissues where cells were rapidly dividing. As these tissues matured and differentiated, NtCDPK1 expression declined.

The preferential expression of NtCDPK1 in proliferating tissues including meristems prompted us to examine whether cell division-stimulating hormones such as auxin and cytokinin could elevate the expression level. GUS staining was markedly enhanced in the shoot apex and the initiation site of lateral roots upon cytokinin treatment, and in roots, most strongly in the root meristem, upon auxin treatment (Figure 6b,c). Gibberellin treatment markedly reduced the GUS staining in the shoot apex and the initiation site of lateral roots, indicating that gibberellin negatively regulates the NtCDPK1 expression. ABA and brassinosteroid either did not change or slightly weakened the GUS staining (data not shown). These results demonstrate that NtCDPK1 expression is modulated by hormones.

We examined the expression pattern of *AtRpn3*, an *Arabidopsis* homolog of NtRpn3, by transforming *Arabidopsis* with the 0.85-kb *AtRpn3* promoter::GUS fusion gene. Consistent with the previous reports for Rpn3 from carrot and rice (Smith *et al.*, 1988, 1993; Yanagawa *et al.*, 2002), *AtRpn3* expression was mainly detected in the shoot apex (Figure 6d). The root meristem and elongation zone also showed GUS activity. In young flowers, GUS staining was mainly detected in anthers, and after anthesis, in the developing seeds (Figure 6d).

Expression of NtCDPK1 and NtRpn3 in tobacco plants was investigated by using semiquantitative RT-PCR analysis (Figure S2). NtCDPK1 was preferentially expressed in seedlings, shoot apical meristem, and flower organs. In stems, roots, and young and mature leaves, the NtCDPK1 expression was low. NtRpn3 showed a pattern of expression very similar to that of NtCDPK1. These RT-PCR results matched with the GUS staining results in Figure 6(a,d), demonstrating that the GUS staining pattern in the *Arabidopsis* plants correctly depicts the expression profile of NtCDPK1 and NtRpn3 in tobacco. Taken together, these

Figure 5. continued

(c) *In vivo* targeting of the fusion protein between NtCDPK1 kinase domain and GFP (KD:GFP). From left, the merged image (GFP and chlorophyll), GFP, and bright-field images are shown.

(d) Co-immunoprecipitation of NtCDPK1 and NtRpn3. Protein extracts were prepared from *Arabidopsis* protoplasts simultaneously expressing NtCDPK1-GFP and RFP-NtRpn3, or GFP and RFP vectors. Extracts were subjected to immunoprecipitation (IP) with the polyclonal GFP antibody, and then associated proteins were detected by immunoblotting with monoclonal RFP antibody. To check the efficiency of IP, the precipitated fractions were also reacted with the monoclonal GFP antibody. GFP, NtCDPK1-GFP, and co-immunoprecipitated RFP-NtRpn3 are indicated by arrowheads, circles, and asterisks, respectively. The heavy (IgG_{Hc}) and light chains (IgG_{Lc}) of the GFP polyclonal antibody used for IP were marked.

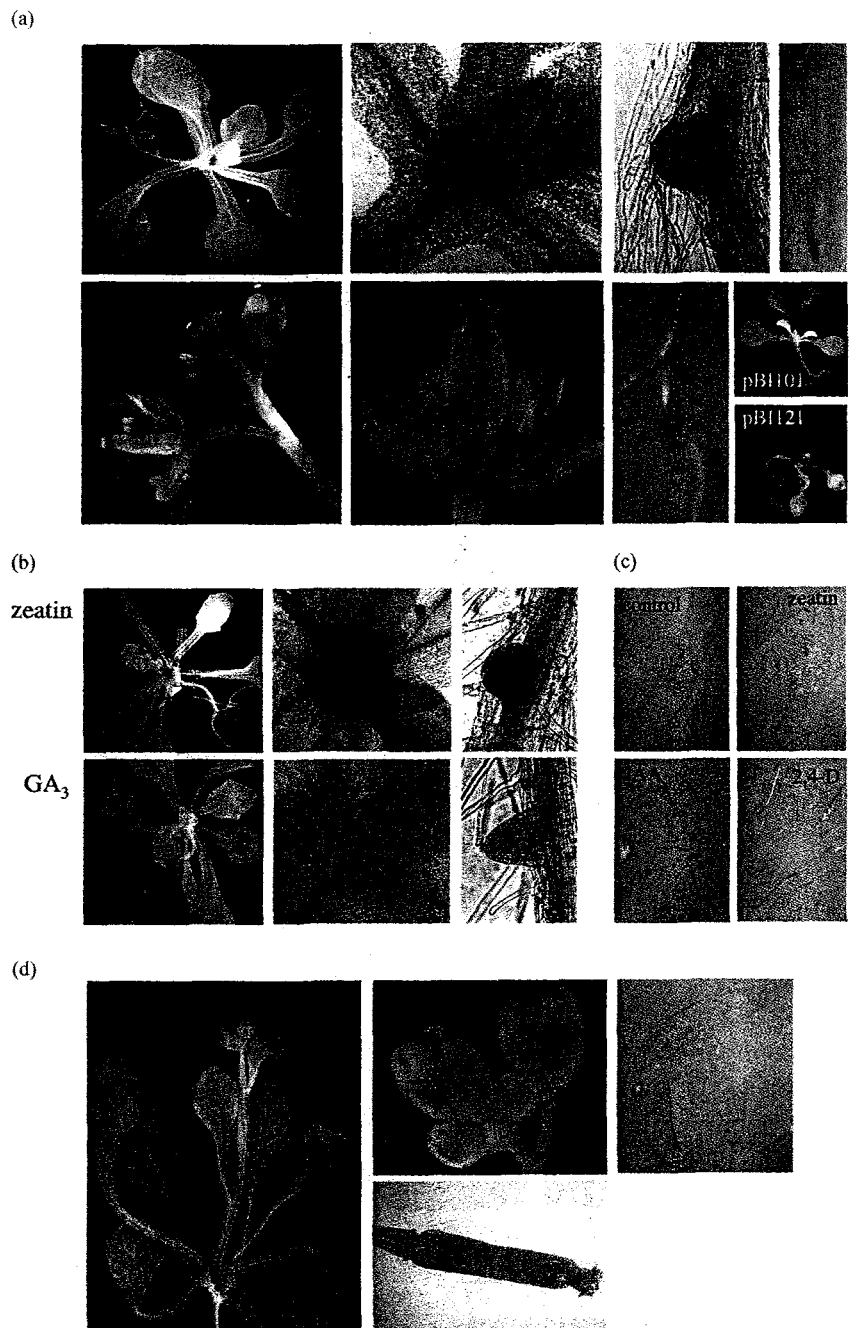
Figure 6. Histochemical staining of the transgenic *Arabidopsis* plants carrying the *NtCDPK1* promoter- or *AtRpn3* promoter-*GUS* fusion construct.

(a) Staining pattern of the *NtCDPK1::GUS* plants. Top: from left, *GUS* staining in shoot apex in seedlings at 14 days after germination (DAG); enlargement of the shoot apex of the seedling at 14 DAG, exhibiting the strong staining in the shoot apical meristem and leaf primordia; *GUS* staining in the initiation site of the lateral root; and *GUS* staining in the root meristem and the elongation zone. Bottom: from left, floral bud clusters showing strong *GUS* staining in young buds; a flower just before anthesis showing *GUS* staining in the stigma, pollen, and base of the flower; *GUS* staining in the branching point of the lateral roots; and seedlings carrying pBI101 (containing the *GUS* gene with no promoter fusion) or pBI121 (CaMV35S promoter:*GUS*) vector as controls.

(b) *GUS* staining pattern of the *NtCDPK1::GUS* plants in response to cytokinin (1 μ M zeatin) and gibberellin (5 μ M GA₃). From left, *GUS* staining patterns in shoot apex in seedlings at 14 DAG, in the enlarged shoot apex, and in the initiation site of the lateral roots are shown. Seedlings were treated with the hormones for 12 h before performing the *GUS* assay.

(c) *GUS* staining pattern in roots of the *NtCDPK1::GUS* plants in response to auxin (10 μ M 2,4-D and 1 μ M IAA) and cytokinin (1 μ M zeatin).

(d) Staining pattern of the *AtRpn3::GUS* plants. From left, *GUS* staining in shoot apex in seedlings at 24 DAG; *GUS* staining in young anthers (top); *GUS* staining in the developing seeds (bottom); and *GUS* staining in the root meristem and the elongation zone.



results demonstrate that *NtCDPK1* and *NtRpn3* are preferentially expressed in plant tissues with high division rates.

Suppression of either *NtCDPK1* or *NtRpn3* mRNA resulted in abnormal cell morphology and premature cell death

To examine the functional relationship between *NtCDPK1* and *NtRpn3*, we employed virus-induced gene silencing (VIGS). VIGS is based on the phenomenon that gene

expression is suppressed in a sequence-specific manner by infection with viral vectors carrying host genes (Waterhouse *et al.*, 2001). As a control, VIGS using PVX vector (pGR106) containing the 0.65-kb fragment of *rbcS* encoding Rubisco small subunit was carried out with *Nicotiana benthamiana*. The symptoms of leaf yellowing and stunted growth appeared in the PVX:*rbcS* VIGS lines in contrast to the PVX vector control (results not shown). The level of the *rbcS* transcripts was severely reduced in the leaves of the PVX:*rbcS* VIGS lines, while PVX control did not show any

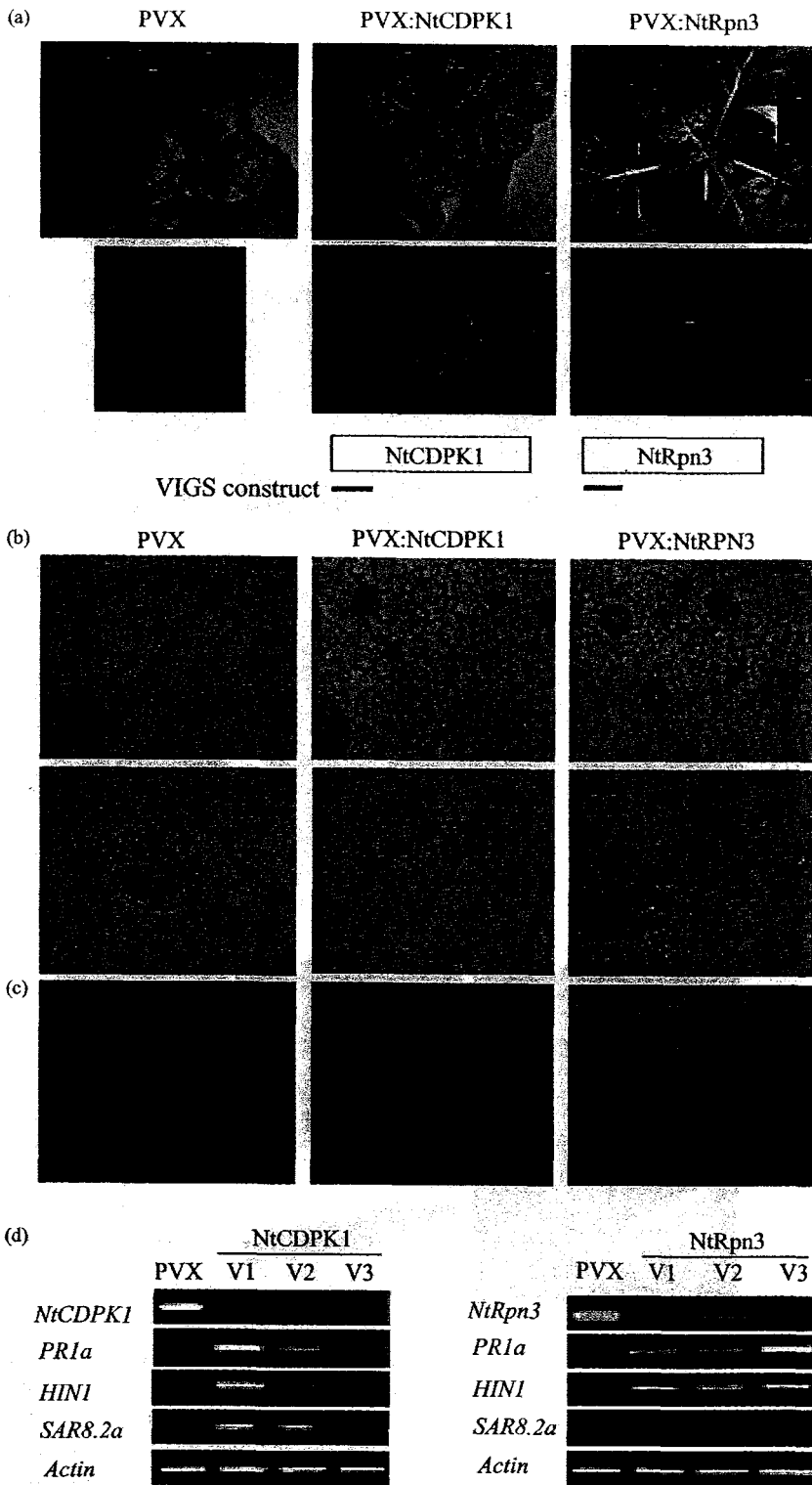


Figure 7. VIGS phenotypes of *NtCDPK1* and *NtRpn3*.

(a) Silencing phenotype of *NtCDPK1* and *NtRpn3*. *Nicotiana benthamiana* plants were infected with PVX, PVX:*NtCDPK1*, or PVX:*NtRpn3*. The photographs of the whole plants and their leaves were taken at 20 days post-inoculation. The cluster of newly emerged leaves in PVX:*NtRpn3* VIGS lines is marked with the red arrowhead. The cDNA regions used for the VIGS constructs are marked.

(b) Light microscopy of the abaxial epidermal cells of the fourth leaf above the infiltrated leaf from the VIGS plants infected with PVX, PVX:*NtCDPK1*, or PVX:*NtRpn3*. Abnormal stomatal development is marked with red arrows. The sample was collected at 20 days post-inoculation. The bars represent 50 μ m.

(c) Evans blue staining of detached leaves from the VIGS lines. Evans blue staining indicates dead cells without intact cellular membranes.

(d) RT-PCR analysis to examine transcript levels of *NtCDPK1*, *NtRpn3*, and HR marker genes. RNA was extracted from the fourth leaf above the infiltrated leaves from several independent *N. benthamiana* plants infected with PVX, PVX:*NtCDPK1*, or PVX:*NtRpn3*. As a marker for HR-related cell death, *PR1a*, *SAR8.2a*, and *HIN1* mRNA levels in the silenced leaves were measured. As a control for RNA amount, *actin* mRNA levels were examined.

change in the *rbcs* mRNA level compared with the uninjected plants (results not shown).

We carried out VIGS of *NtCDPK1* and *NtRpn3* using the PVX vector and *N. benthamiana*. The 0.45-kb *NtCDPK1* cDNA fragment containing the 5' untranslated region and the variable domain, and the 0.40-kb fragment corresponding to the N-terminal region of *NtRpn3* were cloned into PVX vector. VIGS of *NtRpn3* resulted in severe abnormality in plant growth (Figure 7a). Newly emerged leaves were small, severely curled and wrinkled, making a cluster near the shoot apex, and the stem growth was completely arrested. Massive cell death soon followed, which resulted in the whole tissues of newly emerged leaves and flower buds becoming prematurely dead. The plants could not form mature flowers and, as a result, were sterile. The *NtCDPK1* VIGS plants also exhibited shorter stature and smaller leaves than the vector control and their leaves had wrinkled rough surface, although the phenotype appeared less severe than the *NtRpn3* VIGS lines (Figure 7a). Strikingly, the *NtCDPK1* VIGS line exhibited many hypersensitive response (HR)-like necrotic lesions on the surface of the newly emerged leaves. The lesion was initially yellow but soon turned brown in crisp texture, indicating cell death.

We examined cell morphology by peeling off the abaxial epidermal layer of the fourth leaf above the infiltrated leaf of the VIGS lines and examining it under a light microscopy after staining with methylene blue (Figure 7b). The *NtCDPK1* VIGS lines exhibited epidermal cells in irregular sizes depending on the region, containing both larger and smaller cells as compared to the vector control at the corresponding sites. This irregular division and expansion is likely responsible for the irregular texture of the leaves. Development of stomata was also hampered in this line, exhibiting guard cells with abnormal division patterns, prematurely arrested during development. In the *NtRpn3* VIGS lines, expansion of most epidermal cells was severely inhibited, but in some areas, cells were very large. Abnormal stomatal development was also frequently observed. These results demonstrated that suppression of *NtCDPK1* and *NtRpn3* gene expression resulted in aberrant cell division, expansion, and differentiation during leaf development, which apparently resulted in premature onset of the HR-like cell death.

As electrolyte leakage, which indicates damage to cellular membranes, is a common feature of tissues undergoing HR, we stained the detached leaves of the VIGS lines with Evans blue, a dye that is excluded by the membranes of living cells but diffuses into dead cells (Figure 7c). In contrast to the PVX control, both *NtCDPK1* and *NtRpn3* VIGS lines exhibited intense staining on the leaves, especially around the margin of the lesion, indicating localized cell death. We also examined expression of *PR1a*, *SAR8.2a*, and *HIN1* genes that are transcriptionally stimulated during HR

in response to pathogen invasion using semiquantitative RT-PCR (Figure 7d). The *NtCDPK1* VIGS plants accumulated high levels of *PR1a*, *SAR8.2a*, and *HIN1* transcripts, while the *NtRpn3* VIGS plants accumulated high levels of *PR1a* and *HIN1* transcripts. In contrast, none of these transcripts were detected in the PVX control. These results indicate that the cell death phenotype observed in these VIGS lines is related with HR. The effects of VIGS on the endogenous amounts of *NtCDPK1* and *NtRpn3* mRNAs were examined using semiquantitative RT-PCR (Figure 7d) because the levels of both transcripts were very low in the leaves. Primers for RT-PCR were designed to exclude the cDNA regions of *NtCDPK1* and *NtRpn3* used for the VIGS constructs, and the level of *actin* mRNA was measured as a control. A significant reduction of RT-PCR products corresponding to the *NtCDPK1* and *NtRpn3* transcripts was observed in the independent VIGS lines in contrast to PVX control plants, demonstrating that gene expression of *NtCDPK1* and *NtRpn3* was suppressed in the corresponding lines. Interestingly, there was a correlation between the degree of gene silencing and the degree of induction of HR-related genes; the more severely suppressed lines induced higher levels of the HR-related genes. The common features of the VIGS-induced phenotypes of *NtCDPK1* and *NtRpn3*, including abnormal morphology of the leaf epidermal cells, premature cell death, and induction of HR-specific genes, provide biological evidences of interaction of these two gene products in a common pathway regulating cell division and differentiation during leaf development.

Discussion

In this study, we have shown evidence that *NtCDPK1* calcium-dependent protein kinase and *NtRpn3* regulatory subunit of 26S proteasome are interacting in the signaling pathway possibly regulating plant cell division and differentiation, and cell death. We have demonstrated that *NtCDPK1* is physically associated with *NtRpn3* *in vitro* and *in vivo*, and is able to phosphorylate *NtRpn3* *in vitro*. The *NtCDPK1*–*NtRpn3* interaction was further supported by the co-localization and co-expression of the two proteins in the levels of cells and tissues. Recent genetic approaches using yeast mutants defective in cell cycle progression identified several 26S proteasome components, including *Sun2/Rpn3* and *Nin1/Rpn12*. These mutations in genes encoding 26S proteasome subunits cause various cell cycle-related phenotypes in yeast, indicating that different 26S proteasome subunits might specifically target certain cell cycle regulators (Bailey and Reed, 1999; Kaiser *et al.*, 1999). The carrot *Rpn3* could partially rescue the *S. cerevisiae sun2/rpn3* mutant, indicating a possibility that *Rpn3* is involved in degradation of cell cycle regulators in plant cells like *Sun2/Rpn3* in yeast (Smith *et al.*, 1997).

Rpn3 belongs to the regulatory lid of the 19S regulatory complex. The regulatory lid is most exposed to the cytoplasm and, as a result, may interact with other cellular components. The yeast Rpn3 has been shown to interact genetically, physically, and functionally with cyclin-dependent kinase *cdc28* and cyclin-dependent kinase-interacting protein *Cks1/Suc1*, revealing the mechanism of Rpn3 function in cell cycle regulation (Kaiser *et al.*, 1999). The physical interaction between these proteins was shown by co-immunoprecipitation and pull-down assay (Kaiser *et al.*, 1999). In animals and yeast, many subunits of the 19S proteasome complex interact with each other and with other cellular proteins including membrane and nuclear receptors, transcription factors, Ran-binding proteins, and viral proteins (Ferrell *et al.*, 2000). Furthermore, at least five subunits of the 19S complex, in the base as well as the lid, have been shown to be modified by phosphorylation (Ferrell *et al.*, 2000). These interactions are thought to be involved in either the regulation of 26 or 20S proteasome activities or increasing the concentration of proteasomes in discrete cellular subcompartments probably for a large amount of proteolysis in those areas. In *Arabidopsis*, the Rpn3 subunit is found in the lid-like 500-kDa complex, isolated in a free form independently from the 26S proteasome complex (Peng *et al.*, 2001). This raises the possibility that some of the subunits might have roles independent of the proteasome complex. There is a possibility that compartmentalization of Rpn3 is under regulation.

The common phenotypes of the *NtCDPK1* and *NtRpn3* VIGS lines provided more evidence for the interaction between these two gene products. Among many possibilities, *NtCDPK1* may integrate calcium signals with the cell cycle regulating activity of the 26S proteasome through interaction with Rpn3. Upon receiving a calcium-mediated developmental or environmental stimuli, *NtCDPK1* may change the activities of the 26S proteasome, possibly changing the affinity for the target proteins, through interaction and phosphorylation of *NtRpn3* to control degradation of regulatory components required for cell cycle progression. Consistent with the possibility, *NtCDPK1*, as well as *Rpn3*, is preferentially expressed in the log phase of cell culture and in the proliferating tissues. The observation that both *NtCDPK1* and *NtRpn3* VIGS lines exhibited abnormal cell division, differentiation, and premature cell death further supports it. It is important to investigate whether suppression of either *NtCDPK1* or *NtRpn3* block cell cycle progression in plant cells.

In plant cells, cytosolic calcium elevations can be triggered by various signals. It is thought that the different features of calcium signals enable cells to use the same messenger to generate distinct downstream events. There are multiple CDPKs in a given plant species, and this might be related to the specialization of different isoforms with respect to calcium binding and activation (reviewed by

Harmon *et al.*, 2000). Recently, Allen *et al.* (2001) demonstrated that the frequency and duration parameters of the calcium oscillations are crucial for ABA-induced stomatal closure. Different isoforms of CDPKs may decode these parameters of the calcium oscillations to evoke a distinctive downstream physiological response. Which calcium signal *NtCDPK1* mediates is not known. However, it is worth noting that expression of the *NtCDPK1* gene was significantly elevated in the shoot apex and initiation site of lateral roots in response to cytokinin, and in the meristem and elongation zone of roots in response to auxin. Interestingly, the GUS staining pattern of *NtCDPK1* has some similarity to the expression pattern of *ARR5* encoding an *Arabidopsis* response regulator (D'Agostino *et al.*, 2000). Expression of many ARRs is rapidly stimulated by cytokinin, and recently it has been shown that *ARR1* is involved in cytokinin signal transduction pathway (Sakai *et al.*, 2001). Recently, it has been reported that RPN12 from *Arabidopsis* is involved in plants' response to cytokinin (Smalle *et al.*, 2002). In yeast, RPN12 is necessary for the G₁/S and G₂/M transitions of the cell cycle, phases that have been shown to be under cytokinin control in plants (Smalle *et al.*, 2002). It is tempting to speculate that *NtCDPK1* receives hormone signals, possibly cytokinin and auxin, to regulate cell division and differentiation for organ formation through interaction with the 26S proteasome. Interestingly, the *NtCDPK1*-GUS plants showed GUS staining in the entire plant tissues in response to environmental stimuli, such as NaCl, mannitol, hypoxia, and wounding (data not shown). This is consistent with the previous findings that *NtCDPK1* expression was stimulated by abiotic and biotic stimuli by using Northern analysis (Yoon *et al.*, 1999). This raises a possibility that *NtCDPK1* is involved in multiple signaling pathways, executing other functions that are not directly related with developmental control.

Spontaneous formation of HR-like lesions in the absence of pathogen has been reported in a number of transgenic plants that express foreign or modified genes. Expression of antisense constructs for catalase, ascorbate peroxidase, and protoporphyrinogen oxidase, and overexpression of *AmMYB308* transcription factor all resulted in the formation of lesions (Tamagnone *et al.*, 1998; reviewed by Mittler and Rizhasky, 2000). Expression of metabolism-perturbing genes in plants is thought to bring alteration of cellular homeostasis and generation of a signal that activates the programmed cell death pathway. Expression of a modified ubiquitin gene unable to polymerize or suppression of ubiquitin gene expression via the use of a virus-based expression system induced HR-like lesions (Bachmair *et al.*, 1990; Karrer *et al.*, 1998). Both *NtCDPK1* and *NtRpn3* VIGS lines exhibited premature onset of HR-like cell death with induction of PR genes, indicating that the cellular defects caused by abnormal division and differentiation might have induced programmed cell death in the affected tissues.

Among many CDPKs, only a few of CDPK isoforms have clearly assigned functions. These include AtCPK10 of *Arabidopsis* (Sheen, 1996) and OsCDPK7 of rice (Saijo *et al.*, 2000) in osmotic stress signaling, and NtCDPK2 and NtCDPK3 in plant defense response to pathogen (Romeis *et al.*, 2001). Transcription of *AtCPK10* and *OsCDPK7* genes is stimulated by environmental stresses, including salt and drought, and indeed they have been shown to be involved in osmotic stress signal transduction pathway. NtCDPK2 showed response to hypo-osmotic stress and elicitation with reversible interconversion between two enzyme forms (Romeis *et al.*, 2001). AtCPK1, one of the best studied CDPK isoforms, was able to activate tonoplast chloride channel *in vitro* (Pei *et al.*, 1996), and could phosphorylate and inactivate an ER-located calcium pump (Hwang *et al.*, 2000). In addition, other evidence indicates potential CDPK functions in gene expression, metabolism and signaling, traffic of ions and water across membranes, and dynamics of the cytoskeleton (reviewed by Harmon *et al.*, 2000). Major challenges for the future would be to identify functions for individual CDPK isoform and to provide a picture of how CDPK signaling is used in plant development and physiology. In this study, by employing various techniques we have demonstrated that NtCDPK1 interacts with NtRpn3 regulatory subunit of 26S proteasome, possibly controlling cell division, differentiation, and cell death during plant development. Further studies are required to understand the mechanism of NtCDPK1 regulation of NtRpn3 *in vivo*, downstream targets of this signaling pathway, and possible relationship with cell cycle machinery. Furthermore, it is also very important to investigate which calcium signals NtCDPK1 mediates, and how the calcium signal integrates with the controlling mechanism of growth and development in plants.

Experimental procedures

Screening of yeast two-hybrid library

The MATCHMAKER LexA two-hybrid system (Clontech) was used to screen a tobacco flower bud cDNA library (complexity of 5×10^5 total recombinants) constructed in pB42AD plasmid. The bait plasmid was constructed in pLexA using a partial cDNA corresponding to the NtCDPK1 kinase domain. After screening of total 5×10^6 yeast co-transformants, total 107 positive colonies that activated transcription of *LEU2* and *lacZ* gene only in the presence of LexA-NtCDPK1 were obtained. Among them, 42 colonies were randomly chosen, and their cDNA inserts in pB42AD plasmid were PCR-amplified and sequenced. Twenty-five out of 42 represented a cDNA encoding a tobacco homolog of 21D7. To test the interaction of different regions of NtRpn3 with NtCDPK1, a partial cDNA sequence containing the NtCDPK1 kinase domain was PCR-amplified with *Bam*HI and *Sa*II at the ends, digested with *Bam*HI/*Sa*II, and cloned into *Bam*HI/*Sa*II-digested pLexA. For the C-terminal and N-terminal deletion constructs of the *NtRpn3* cDNA in pB42AD vector, the corresponding PCR-amplified DNA fragments contain-

ing *Eco*RI and *Xho*I sites in their 5' and 3' ends were cloned into *Eco*RI/*Xho*I-digested pB42AD plasmid. The EGY48[p8op-lacZ] strain containing pLexA-NtCDPK1 kinase domain was transformed with the pB42AD plasmid containing a partial sequence of *NtRpn3*. The transformants were grown on selection plates and assayed for β -galactosidase activity. β -galactosidase activity levels were determined according to the manual of the MATCHMAKER LexA two-hybrid system. Three separate colonies were assayed for each construct. β -galactosidase activity was determined as the OD₄₂₀ per hour.

Purification of recombinant proteins and *in vitro* protein binding assay

For GST-NtRpn3 cloning, various *NtRpn3* cDNA fragments were cloned into pGEX (Amersham Pharmacia) using *Bam*HI and *Xho*I sites. For cloning of MBP-NtCDPK1, the cDNA fragment was cloned into pMALTMc2 vector (New England Biolabs) using *Bam*HI/*Sa*II sites. The GST fusion proteins were purified using glutathione agarose column (Sigma) and the MBP fusion proteins were purified using amylose resin (New England Biolabs) following the manufacturer's instructions. The binding assay was performed by mixing 2 μ g of MBP or MBP-NtCDPK1 fusion proteins attached to amylose beads with 2 μ g of purified GST or GST-NtRpn3 fusion protein in the presence of 300 μ l binding buffer (20 mM HEPES, pH 7.5, 5 mM MgCl₂, 1 mM DTT, and 0.1% Triton X-100) with 1 mM Ca²⁺ or 2 mM EGTA. Samples were rotated for 2 h at 4°C, pelleted, and washed three times with the binding buffer. The samples were then run on 10% SDS-PAGE. The gel was blotted to PVDF membrane and incubated with the GST monoclonal antibody (1 : 7500 dilution; Clontech).

Kinase assay

To obtain the cleaved NtCDPK1, the purified MBP-NtCDPK1 fusion protein was digested with Factor Xa (New England Biolabs) for 1 h at 37°C and passed through amylose resin (New England Biolabs) to remove the MBP moiety. Unbound eluate containing NtCDPK1 was collected and used for the analysis. For *in vitro* phosphorylation assay, 0.5 μ g of full-length NtCDPK1 was incubated with GST-NtRpn3 fusion proteins (0.5 or 5 μ g) in the phosphorylation buffer (25 mM HEPES, pH 7.5, 1 mM DTT) containing 10 μ Ci of [γ -³²P]ATP (5000 Ci mmol⁻¹) with MgCl₂ (1 mM) or MnCl₂ (1 mM) in the presence of CaCl₂ (1 mM) at 37°C for 1 h, unless indicated otherwise. The reactions were terminated by the addition of 5 \times Laemmli sample buffer and electrophoresed on a 10% SDS-PAGE. The gel was blotted to PVDF membranes and exposed to X-ray film.

Synchronization of tobacco BY2 cells

Synchronization of tobacco BY2 (*Nicotiana tabacum* L. cv. Bright Yellow 2) suspension-cultured cells was achieved by a 24-h subculture of stationary phase cells (7 days old) in a medium containing aphidicolin (5 mg l⁻¹; Sigma) followed by extensive washes, as described (Reichheld *et al.*, 1996). Mitotic index was measured as described (Reichheld *et al.*, 1996). Northern blot analysis was carried out with 50 μ g of total RNA for each lane.

Subcellular localization of NtCDPK1 and NtRpn3

The *NtCDPK1* cDNA corresponding to the entire coding region was cloned into the 326-GFP plasmid (Lee *et al.*, 2001) using *Xba*I sites to generate the NtCDPK1-GFP fusion protein. The *NtRpn3* cDNA corresponding to the entire coding region was cloned into the 326-RFP plasmid (Lee *et al.*, 2001) using *Cl*al and *Sa*II sites for RFP-

NtRpn3. The fusion constructs were introduced into *Arabidopsis* protoplasts prepared from whole seedlings by the polyethylene glycol-mediated transformation (Lee *et al.*, 2001). Expression of the fusion constructs was monitored at various times after transformation by fluorescence microscopy using a Zeiss Axioplan fluorescence microscope (Jena, Germany), and the image was captured with a cooled charge-coupled device camera. The filter sets were used as described (Lee *et al.*, 2001). The data were processed using Adobe Photoshop software (Mountain View, CA) and presented in pseudocolor format.

GUS histochemical assay

The 1.1-kb NtCDPK1 promoter was isolated using GenomeWalker™ kit (Clontech). The 0.85-kb AtRpn3 promoter was isolated by PCR using *Arabidopsis* genomic DNA as a template. The promoters were cloned into the pBI101 vector using *SalI/XbaI* sites to generate in-frame NtCDPK1 promoter- or AtRpn3 promoter-GUS fusion genes. The fixation, staining, and clearing of the transgenic *Arabidopsis* plants (ecotype Columbia) with X-Gluc were performed as described previously (Jefferson *et al.*, 1987). The seedlings were treated with 1 and 10 μM of auxin (2,4-D and IAA), cytokinin (zeatin), brassinosteroid, and ABA, and 5 and 50 μM of gibberellin (GA_3) for 12 h before performing the GUS assay.

Virus-induced gene silencing

The PCR-amplified cDNAs were cloned into the pGR106 vector containing the PVX genome (Angell and Baulcombe, 1999) using *Clal* and *SalI* sites. The recombinant pGR106 plasmids were transformed into *Agrobacterium tumefaciens* GV3101 strain. *Agrobacterium* culture for infiltration was prepared as described (Angell and Baulcombe, 1999). The third leaf of *N. benthamiana* (3-week-old) was pressure-infiltrated with the *Agrobacterium* suspension. For Northern analysis and RT-PCR, the fourth leaf above the infiltrated one of *N. benthamiana* was used. Semiquantitative RT-PCR analysis of the transcript levels of *NtCDPK1*, *NtRpn3*, and HR marker genes in the VIGS lines was carried out as described (Romeis *et al.*, 2001). Oligonucleotide primers for RT-PCR were made according to the published cDNA sequences (for *NtCDPK1*, 5'-GTGCAGTGCTGCCAGA-3' and 5'-GTGTGTGGT-TGTGTTCCAC-3'; for *NtRpn3*, 5'-TCTACTCTACAAATGAG-3' and 5'-CTATGTGCTTAGCAAGCT-3'; for *actin*, 5'-TGGACTCTGGT-ATGGTGC-3' and 5'-CCTCCAATCCAAACTGTA-3'; for *PR1a*, 5'-AATATCCCACCTTGCCG-3' and 5'-CCTGGAGGATCATAGTT-G-3'; for *SAR8.2a*, 5'-CTTTGCCTTTCTTTGGCT-3' and 5'-GACATTAGGACATTTGCTGC-3'; and for *HIN1*, 5'-GAGCCATGCCGGAAT-CCAAT-3' and 5'-GCTACCAATCAAGATGGCATCTGG-3').

Evans blue staining

Detached leaves, completely submerged in a 0.1% (w/v) aqueous solution of Evans blue (Sigma), were subjected to two 5-min cycles of vacuum followed by a 20-min maintenance under vacuum. The leaves were then washed by vacuum infiltration of phosphate buffered saline plus 0.05% (v/v) Tween 20 for 3 \times 15 min.

Co-immunoprecipitation

The *NtCDPK1-GFP* and *RFP-NtRpn3* fusion constructs, and GFP and RFP vectors as a control, were transformed into protoplasts isolated from *Arabidopsis* seedlings as described (Lee *et al.*, 2001). After 24-h incubation at room temperature, protoplasts were collected by centrifugation at 1000 *g* for 5 min, re-suspended in 300 μl immunoprecipitation buffer (25 mM Tris, pH 7.5, 150 mM NaCl,

1 mM DTT, 1 mM PMSF, 25 mM Na_2VO_4 , 5 mM NaF, 25 mM glycerophosphate, protease inhibitor cocktail, 1 mM CaCl_2 , 0.1% Triton X-100, 0.5% NP40), then sonicated briefly. After brief centrifugation to remove debris, protein extracts (600 μg) were incubated with 2.5 μg of the polyclonal GFP antibody (Clontech; IP grade) at 4°C for 4 h. Then, 25 μl packed volume of ProteinG-Agarose resin (Pharmacia) was added to the mixture for further incubation at 4°C for 4 h. After centrifugation at 1000 *g* for 1 min, the resin was washed five times with the immunoprecipitation buffer, and then re-suspended in 2 \times sample buffer. After boiling, the resin was precipitated by brief centrifugation, and the supernatant was run on 10% SDS-PAGE. Western blot analysis was carried out using the monoclonal GFP antibody (Clontech; 1 : 5000) and monoclonal RFP antibody (Clontech; 1 : 1000).

Acknowledgements

This research was supported by the grants from National Research Laboratory Program and Plant Diversity Research Center of 21st Century Frontier Research Program funded by Ministry of Science and Technology of Korean government. The authors wish to thank Dr Doil Choi (KRIBB) for providing HR marker genes and technical advice on VIGS, Dr Inhwan Hwang (POSTECH) for providing facilities and expertise for subcellular localization of proteins, and Dr David C. Baulcombe (John Innes Center) for providing VIGS vectors.

Supplementary Material

The following material is available from <http://www.blackwellpublishing.com/products/journals/suppmat/TPJ/TPJ1672/TPJ1672sm.htm>

Figure S1. Deduced amino acid sequence of NtRpn3 and alignment with other homologous sequences. NtRpn3 is aligned with homologous sequences of carrot (Dc 21D7), *Arabidopsis* (At S3h1 and At S3h2), yeast (Sc Sun2p), and human (Hs p58). The number on the right indicates the amino acid residues. Gaps introduced to maximize alignment are indicated by dashes (-). Residues conserved among at least three of the compared sequences are highlighted by shades. PCI domain that is present in subunits of multisubunit protein complex, such as 26S proteasome, COP9 signalosome and eIF3, is marked with the box above the sequences. The PCI domain is an α -helical domain of about 200 amino acid residues, which could serve as a structural scaffold, possibly by interacting with each other (reviewed by Hofmann and Bucher, 1998; Kim *et al.*, 2001).

Figure S2. RT-PCR analysis of *NtCDPK1* and *NtRpn3* expression in tobacco. Semiquantitative RT-PCR was carried out with total RNA isolated from various tissues from tobacco plants as described in Experimental procedures. DAS, days after sowing; SAM, shoot apical meristem.

References

- Allen, G.J., Chu, S.P., Harrington, C.L., Schumacher, K., Hoffmann, T., Tang, Y.Y., Grill, E. and Schroeder, J.I. (2001) A defined range of guard cell calcium oscillation parameters encodes stomatal movements. *Nature*, **411**, 1053–1057.
- Angell, S.M. and Baulcombe, D.C. (1999) Potato virus X amplicon-mediated silencing of nuclear genes. *Plant J.* **20**, 357–362.
- Bachmair, A., Becker, F., Masterson, R.V. and Schell, J. (1990) Perturbation of the ubiquitin system causes leaf curling, vascular tissue alterations and necrotic lesions in higher plants. *EMBO J.* **9**, 4543–4549.

- Bailey, E. and Reed, S.I. (1999) Functional characterization of Rpn3 uncovers a distinct 19S proteasomal subunit requirement for ubiquitin-dependent proteolysis of cell cycle regulatory proteins in budding yeast. *Mol. Cell Biol.* **19**, 6872–6890.
- Barker, L.D.P., Templeton, M.D. and Ferguson, I.B. (1998) A 67-kDa plasma-membrane-bound Ca^{2+} -stimulated protein kinase active in sink tissue of higher plants. *Planta*, **205**, 197–204.
- Callis, J. and Vierstra, R.D. (2000) Protein degradation in signaling. *Curr. Opin. Plant Biol.* **3**, 381–386.
- Criqui, M.C., Parmentier, Y., Derevier, A., She, W.-H., Dong, A. and Genschik, P. (2000) Cell cycle-dependent proteolysis and ectopic overexpression of cyclin B1 in tobacco BY2 cells. *Plant J.* **24**, 763–773.
- D'Agostino, I.B., Deruere, J. and Kieber, J.J. (2000) Characterization of the response of the *Arabidopsis* response regulator gene family to cytokinin. *Plant Physiol.* **124**, 1706–1717.
- Enenkel, C., Lehmann, A. and Kloetzel, P.-M. (1998) Subcellular distribution of proteasomes implicates a major location of protein degradation in the nuclear envelope-ER network in yeast. *EMBO J.* **17**, 6144–6154.
- Ferrell, K., Wilkinson, C.R.M., Dubiel, W. and Gordon, C. (2000) Regulatory subunit interactions of the 26S proteasome, a complex problem. *Trends Biochem. Sci.* **25**, 83–88.
- Fu, H., Reis, N., Lee, Y., Glickman, M.H. and Vierstra, R.D. (2001) Subunit interaction maps for the regulatory particle of the 26S proteasome and the COP9 signalosome. *EMBO J.* **20**, 7096–7107.
- Girod, P.-A., Fu, H., Zryd, J.-P. and Vierstra, R.D. (1999) Multi-ubiquitin chain binding subunit MCB1 (RPN10) of the 26S proteasome is essential for developmental progression in *Physcomitrella patens*. *Plant Cell*, **11**, 1457–1471.
- Harmon, A.C., Gribskov, M., Gubrium, E. and Harper, J.F. (2001) The CDPK superfamily of protein kinase. *New Phytol.* **151**, 175–183.
- Harmon, A.C., Gribskov, M. and Harper, J.F. (2000) CDPKs – a kinase for every Ca^{2+} signal? *Trends Plant Sci.* **5**, 154–159.
- Hershko, A. and Ciechanover, A. (1998) The ubiquitin system. *Annu. Rev. Biochem.* **67**, 425–479.
- Hofmann, K. and Bucher, P. (1998) The PCI domain: a common theme in three multi-protein complexes. *Trends Biochem. Sci.* **23**, 204–205.
- Horn, M.A. and Walker, J.C. (1994) Biochemical properties of the autophosphorylation of RLK5, a receptor-like protein kinase from *Arabidopsis thaliana*. *Biochim. Biophys. Acta*, **1208**, 65–74.
- Hwang, I., Sze, H. and Harper, J.F. (2000) A calcium-dependent protein kinase can inhibit a calcium-stimulated Ca^{2+} pump (ACA2) located in the endoplasmic reticulum of *Arabidopsis*. *Proc. Natl. Acad. Sci. USA*, **97**, 6224–6229.
- Ito, M., Smith, M.W. and Watanabe, A. (1997) Cloning of a cDNA encoding a tobacco homolog of the carrot 21D7 protein that is a subunit of the 26S proteasome complex. *Plant Physiol.* **114**, 748.
- Jefferson, R.A., Kavanagh, T.A. and Bevan, M.W. (1987) GUS fusion: β -glucuronidase as a sensitive and versatile gene fusion marker in higher plants. *EMBO J.* **6**, 3901–3907.
- Kaiser, P., Moncollin, V., Clarke, D.J., Watson, M.H., Bertolaet, B.L., Reed, S.I. and Bailly, E. (1999) Cyclin-dependent kinase and Cks/Suc1 interact with the proteasome in yeast to control proteolysis of M-phase targets. *Genes Dev.* **13**, 1190–1212.
- Karrer, E.E., Beachy, R.N. and Holt, C.A. (1998) Cloning of tobacco genes that elicit the hypersensitive response. *Plant Mol. Biol.* **36**, 681–690.
- Kim, T.-H., Hofmann, K., von Armin, A.G. and Chamovitz, D.A. (2001) PCI complexes: pretty complex interactions in diverse signaling pathways. *Trends Plant Sci.* **6**, 379–386.
- Kominami, K., Okura, N., Kawamura, M. et al. (1997) Yeast counterparts of subunits S5a and p58 (S3) of the human 26S proteasome are encoded by two multicopy suppressors of *Nin1-1*. *Mol. Biol. Cell*, **8**, 171–187.
- Lee, Y.J., Kim, D.H., Kim, Y.-W. and Hwang, I. (2001) Identification of a signal that distinguishes between the chloroplast outer envelope membrane and the endomembrane system *in vivo*. *Plant Cell*, **13**, 2175–2190.
- Lee, S.H., Lee, M.H., Chung, W.I. and Liu, J.R. (1998) WAPK, a Ser/Thr protein kinase gene of *Nicotiana tabacum*, is uniquely regulated by wounding, abscisic acid and methyl jasmonate. *Mol. Gen. Genet.* **259**, 516–522.
- Mittler, R. and Rizhasky, L. (2000) Transgene-induced lesion mimic. *Plant Mol. Biol.* **44**, 335–344.
- Mu, J.-H., Lee, H.-S. and Kao, T.-H. (1994) Characterization of a pollen-expressed receptor-like kinase gene of *Petunia inflata* and the activity of its encoded kinase. *Plant Cell*, **6**, 709–721.
- Muranaka, T., Banno, H. and Machida, Y. (1994) Characterization of tobacco protein kinase NPK5, a homolog of *Saccharomyces cerevisiae* SNF1 that constitutively activates expression of the glucose-repressible SUC2 gene for a secreted invertase of *S. cerevisiae*. *Mol. Cell Biol.* **14**, 2958–2965.
- Pei, Z.M., Ward, J.M., Harper, J.F. and Schroeder, J.I. (1996) A novel chloride channel *Vicia faba* guard cell vacuoles activated by the serine/threonine kinase, CDPK. *EMBO J.* **15**, 6564–6574.
- Peng, Z., Staub, J.M., Serino, G., Kwok, S.F., Kurepa, J., Bruce, B.D., Vierstra, R.D., Wei, N. and Deng, X.W. (2001) The cellular level of PR500, a protein complex related to the 19S regulatory particle of the proteasome, is regulated in response to stresses in plants. *Mol. Biol. Cell*, **12**, 383–392.
- Reichheld, J.P., Chaubet, N., Shen, W.H., Renaudin, J.P. and Gigot, C. (1996) Multiple A-type cyclins express sequentially during the cycle in *Nicotiana tabacum* BY2 cells. *Proc. Natl. Acad. Sci. USA*, **93**, 13819–13824.
- Romeis, T., Ludwig, A.A., Martin, R. and Jones, J.D.G. (2001) Calcium-dependent protein kinases play an essential role in a plant defence response. *EMBO J.* **20**, 5556–5567.
- Saijo, Y., Hata, S., Kyojuka, J., Shimamoto, K. and Izui, K. (2000) Overexpression of a single Ca^{2+} -dependent protein kinase confers both the cold and salt/drought tolerance on rice plants. *Plant J.* **23**, 319–327.
- Sakai, H., Honma, T., Aoyama, T., Sato, S., Kato, T., Tabata, S. and Oka, A. (2001) ARR1, a transcription factor for genes immediately responsive to cytokinins. *Science*, **294**, 1519–1521.
- Sheen, J. (1996) Ca^{2+} -dependent protein kinases and stress signal transduction in plants. *Science*, **274**, 1900–1902.
- Shi, J., Kim, K.-N., Ritz, O., Albrecht, V., Gupta, R., Harter, K., Luan, S. and Kudla, J. (1999) Novel protein kinases associated with calcineurin B-like calcium sensors in *Arabidopsis*. *Plant Cell*, **11**, 2393–2405.
- Smalle, J., Kurepa, J., Yang, P., Babiychuk, E., Kushnir, S., Durski, A. and Vierstra, R.D. (2002) Cytokinin growth responses in *Arabidopsis* involve the 26S proteasome subunit RPN12. *Plant Cell*, **14**, 17–32.
- Smith, M.W., Ito, M., Miyawaki, M., Sato, S., Yoshikawa, Y., Wada, S., Maki, H., Nakagawa, H. and Komamine, A. (1997) Plant 21D7 protein, a nuclear antigen associated with cell division, is a component of the 26S proteasome. *Plant Physiol.* **113**, 281–291.
- Smith, M.W., Ito, M., Yamada, T., Suzuki, T. and Komamine, A. (1993) Isolation and characterization of a cDNA clone for plant nuclear antigen 21D7 associated with cell division. *Plant Physiol.* **101**, 809–817.

- Smith, J.A., Krauss, M.R., Borkird, C. and Sung, Z.R. (1988) A nuclear protein associated with cell division in plants. *Planta*, **174**, 462–472.
- Tamagnone, L., Marida, A., Stacey, N., Plaskitt, K., Parr, A., Chang, C.-F., Lynn, D., Dow, J.M., Roberts, K. and Martin, C. (1998) Inhibition of phenolic acid metabolism results in precocious cell death and altered cell morphology in leaves of transgenic tobacco plants. *Plant Cell*, **10**, 1801–1816.
- Waterhouse, P.M., Wang, M.-B. and Lough, T. (2001) Gene silencing as an adaptive defence against viruses. *Nature*, **411**, 834–842.
- Yanagawa, Y., Kimura, S., Takase, T., Sakaguchi, K., Umeda, M., Komamine, A., Tanaka, K., Hashimoto, J., Sato, T. and Nakagawa, H. (2002) Spatial distribution of the 26S proteasome in meristematic tissues and primordia of rice (*Oryza sativa* L.). *Planta*, **214**, 703–707.
- Yoon, G.M., Cho, H.S., Ha, H.J., Liu, J.R. and Lee Pai, H.-S. (1999) Characterization of *NtCDPK1*, a calcium-dependent protein kinase gene in *Nicotiana tabacum*, and the activity of its encoded protein. *Plant Mol. Biol.* **39**, 991–1001.

Communication

Molecular Characterization of *NbPAF* Encoding the $\alpha 6$ Subunit of the 20S Proteasome in *Nicotiana benthamiana*

Moonil Kim^{1,2}, Kyoung-Sil Yang¹, Yu-Kyung Kim¹, Kyung-Hee Paek², and Hyun-Sook Pai^{1,*}

¹Laboratory of Plant Genomics, Korea Research Institute of Bioscience and Biotechnology, Daejeon 305-600, Korea;

²Graduate School of Biotechnology, Korea University, Seoul 136-701, Korea.

(Received December 4, 2002; Accepted December 14, 2002)

The 26S proteasome involved in degradation of proteins covalently modified with polyubiquitin consists of the 20S proteasome and 19S regulatory complex. The *NbPAF* gene encoding the $\alpha 6$ subunit of the 20S proteasome was identified from *Nicotiana benthamiana*. *NbPAF* exhibits high sequence homology with the corresponding genes from *Arabidopsis*, human and yeast. The deduced amino acid sequence of *NbPAF* reveals that this protein contains the proteasome α -type subunits signature and nuclear localization signal at the N-terminus. The genomic Southern blot analysis suggests that the *N. benthamiana* genome contains one copy of *NbPAF*. The *NbPAF* mRNA was detected abundantly in flowers and weakly in roots and stems, but it was almost undetectable in mature leaves. In response to stresses, accumulation of the *NbPAF* mRNA was stimulated by methyl jasmonate, NaCl and salicylic acid, but not by abscisic acid and cold treatment in leaves. The *NbPAF*-GFP fusion protein was localized in the cytoplasm and nucleus.

Keywords: Inducible Expression; Plant Defense Response; Single Gene; Subcellular Localization.

Introduction

The 26S proteasome, consisting of two large subcomplexes, the 20S proteasome and the 19S regulatory complex, is a major cytoplasmic proteolytic enzyme complex, responsible for degradation of the vast majority of intracellular proteins in eukaryotes (Hershko and Ciechanover, 1998). In this pathway, ubiquitin becomes covalently attached to cellular proteins by an ATP-dependent reaction

cascade via the action of a ubiquitin activating enzyme (E1), a ubiquitin-conjugating enzyme (E2) and in some cases a ubiquitin-protein ligase (E3), and then the ubiquitinated proteins are targeted for degradation by the proteasome (Hershko and Ciechanover, 1998). In mammals, proteasomes are shown to be involved in not only the degradation of misfolded or truncated proteins, but also the biological processes including cell cycle progression, immune response and programmed cell death (Baumeister *et al.*, 1998; Hilt and Wolf, 1996; Hochstrasser, 1996). Proteasomal substrates include metabolic key enzymes, transcription factors, cyclins, inhibitors of cyclin-dependent kinases, and apoptotic regulators. In plants, the 20S proteasome was shown to be involved in cell cycle progression, and in various signal transduction pathways including auxin signaling, photomorphogenesis and jasmonic acid signaling (Callis and Vierstra, 2000; Genschik *et al.*, 1998; Girod *et al.*, 1999).

The 20S proteasome of eukaryotes consists of two copies each of 7 distinctive α - and 7 distinctive β -type subunits (Voges *et al.*, 1999). The α - and β -type subunits segregate into 7-member heterooligomeric [$(\alpha 1-\alpha 7)(\beta 1-\beta 7)(\beta 1-\beta 7)(\alpha 1-\alpha 7)$] rings. Two juxtaposed rings of β -type subunits flanked on top and bottom by a ring of α -type subunits form the barrel-shaped complex (Voges *et al.*, 1999). In yeast, the 20S proteasome is composed of two copies each of 14 different subunits, 7 distinctive α - and 7 distinctive β -type subunits, of which only three β -type subunits have active sites. Gene disruption of the individual genes encoding the 14 subunits of the 20S proteasome indicated that 13 of the 14 subunits are essential to the viability of yeast cells: the only subunit that turned out to be nonessential is $\alpha 3$ (Voges *et al.*, 1999). The deletion mutant of the $\alpha 3$ subunit gene has a longer generation time than the wild-type cells and showed altered chymotryptic activities (Emori *et al.*, 1991). In mammals, γ -interferon stimulates expression of three additional β -type subunits, each of which replaces a specific, closely related, consti-

* To whom correspondence should be addressed.

Tel: 82-42-860-4195; Fax: 82-42-860-4608

E-mail: hyunsook@mail.kribb.re.kr

tutively-expressed β -type subunits. These immunoproteasomes are implicated in processing of antigens for presentation by MHC class I molecules (Coux *et al.*, 1996).

In *Arabidopsis*, duplicated proteasomal genes were found: 13 α - and 10 β -type genes can be classified into 7 α - and 7 β -type sub-families. Using yeast complementation assay, *Arabidopsis* genes encoding α 3/PAC1, α 5/PAE1, and β 3/PBC2 were able to specifically complement deletions of their counterparts in yeast (Fu *et al.*, 1998), providing the first evidence for cross-species complementation of 20S subunit genes. However, *PBA1* (β 1), *PBB1* (β 2), *PBD1* (β 4), *PBE1* (β 5), *PBF1* (β 6), and *PBG1* (β 7) of *Arabidopsis* could not complement their yeast orthologs. The reason for these duplicated proteasome genes in *Arabidopsis* is not clear. One simple explanation is that the duplications provide backup copies or insure production of sufficient amounts of the corresponding subunits.

Previously we have demonstrated that inhibition of proteasome function by gene silencing of two different subunits of the 26S proteasome, the α 6 subunit of the 20S proteasome and RPN9 subunit of 19S regulatory complex, activated the programmed cell death program in *N. benthamiana* (manuscript submitted). In this study, we report the molecular characterization of *NbPAF* encoding the α 6 subunit, with particular interests in its expression in response to the external stresses that could lead the plant cells to death. The deduced amino acid sequence of *NbPAF* is highly homologous with those of α 6 subunits from *Arabidopsis*, human and yeast. The *NbPAF* transcripts in mature leaves were barely detectable, but significantly increased by external stimuli, including methyl jasmonate, NaCl and salicylic acid. Furthermore, *in vivo* targeting experiment revealed that *NbPAF* is localized in both the cytoplasm and nucleus.

Materials and Methods

Construction of the cDNA library and sequencing analysis

The cDNA library was constructed from a pooled sample of poly(A)⁺ RNA containing equal amounts of RNA extracted from roots, stems, leaves and flowers from *N. benthamiana*. First-strand cDNA synthesis was carried out by oligo(dT) priming, followed by the second-strand synthesis, using a λ ZAPII cDNA Synthesis Kit (Stratagene). Approximately 3000 cDNAs cloned in pBluescript vector were sequenced using T3 and T7 primers. The cDNA encoding the α 6 subunit of the 20S proteasome was identified and characterized.

Plant materials and chemical treatments *N. benthamiana* plants were cultivated in a greenhouse under a regime of 16 h of light and 8 h of dark. Plants grown for 8 weeks were treated with various chemicals for RNA gel blot analysis. For treatment with methyl jasmonate (MeJA), salicylic acid (SA), salts, and

abscisic acid (ABA), detached leaves were placed in Falcon tubes filled with 0.1 mM methyl jasmonate, 2 mM salicylic acid, 200 mM NaCl and 100 μ M abscisic acid. For cold treatment, plants were placed at 4°C for indicated times. Plant materials were frozen in liquid nitrogen and stored at -70°C for RNA or DNA extraction.

DNA gel blot analysis For DNA gel blot analysis, 10 μ g of the genomic DNA isolated from *N. benthamiana* leaves was digested with *EcoRI*, *HindIII* and *EcoRV*, electrophoresed on a 0.8% agarose gel, and blotted onto Hybond-N Nylon membrane (Amersham Pharmacia Biotech) as described by Kim *et al.* (2001). The probe was the 0.4 kb PCR fragment corresponding to the C-terminal region of *NbPAF*. Prehybridization and hybridization were carried out in 5 \times SSC, 5 \times Denhardt's solution, and 0.5% SDS at 60°C overnight. The membranes were washed twice in 2 \times SSC and 1% SDS at room temperature, then washed in 0.1 \times SSC and 0.1% SDS at 60°C for 30 min.

RNA gel blot analysis For RNA gel blot analysis using plant tissues, total RNA was prepared by using TRIzol™ Reagent (Gibco-BRL) following manufacturer's instructions. Approximately 50 μ g of total RNA was electrophoresed on an agarose gel containing 5.1% (v/v) formaldehyde and blotted onto Hybond-N Nylon membrane. Prehybridization, hybridization and washing conditions were as described in DNA gel blot analysis.

Subcellular localization of the *NbPAF*-GFP protein The *NbPAF* cDNA corresponding to amino acid residues 1 to 274 was PCR-amplified and cloned into the 326-GFP vector using *Bam*HI site to generate *NbPAF*-GFP in-frame fusion under the control of the cauliflower mosaic virus 35S promoter. The p*NbPAF*-GFP plasmid or GFP vector as a control was introduced into onion epidermal cells by particle bombardment. Before observation after 12 h incubation, the sample was briefly stained with DAPI (100 μ g/ml) to visualize nuclei. Expression of the fusion protein was monitored by fluorescence microscopy using a Zeiss Axioplan fluorescence microscope (Jena, Germany), and the image was captured with a cooled charge-coupled device camera with the XF116 filter (exciter, 474AF20; dichroic, 500DRLP; emitter, 510AF23) (Omega Inc., Brattleboro, VT).

Results and Discussion

The isolated *NbPAF* cDNA contained an open reading frame with the ATG codon at position 64 and stop codon at position 888, followed by the 209-bp 3' untranslated region with a poly(A) tail, indicating that it is a full-length cDNA. It encoded a protein of 274 amino acids with a molecular mass of approximately 29,876 Da. The deduced amino acid sequence of the *NbPAF* showed high similarity to those of 20S proteasome α 6 subunits from *Arabidopsis* (AtPAF1 and AtPAF2), human (C2) and yeast

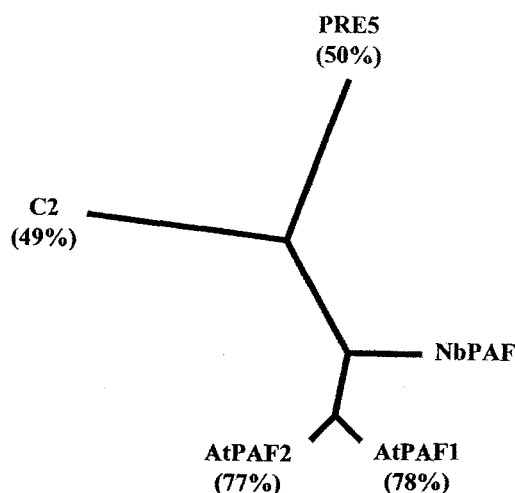


Fig. 1. Phylogenetic tree of the 20S proteasome α_6 subunit from *Nicotiana benthamiana* (NbPAF), *Arabidopsis* (AtPAF1, AtPAF2), human (C2) and yeast (PRE5). The amino acid sequence homology between α_6 subunits from various species is indicated in parentheses.

(PRE5) with 78, 77, 49, and 50% identity, respectively, implying conservation across species (Fig. 1). NbPAF and the α_6 subunits from other species, all contained the proteasome α -type subunits signature and a putative nuclear localization signal at the amino terminus (Fig. 2).

DNA gel blot analysis was performed with *N. benthamiana* genomic DNA digested with restriction enzymes, under high-stringency conditions (Fig. 3). The probe was the 0.4-kb PCR fragment corresponding to the C-terminal end of the *NbPAF* cDNA. *EcoRI* digestion resulted in one hybridizing band, whereas *HindIII* and *EcoRV* digestion showed three hybridizing bands (Fig. 3). Considering that *N. benthamiana* is amphidiploid, these results indicate that the genome contains one copy of *NbPAF*. In *Arabidopsis*, the α_6 subunit is encoded by two genes, *AtPAF1* and *AtPAF2* (Fu et al., 1998).

Using RNA gel blot analysis, we examined the expression of the *NbPAF* mRNA in various plant tissues (Fig. 4). The 1.1 kb *NbPAF* transcripts (consistent with the size of the isolated cDNA) were highly expressed in flowers, but in roots and stems the transcript level was lower than in flowers. The transcripts were almost undetectable in mature leaves (Fig. 4). It has been shown in animal cells that the transcript levels of proteasome subunits vary in different tissues and are under developmental control (Hong et al., 1994; Kawahara et al., 1992). In *Arabidopsis*, transcripts of *PAA1* (α_1), *PAC1* (α_3), *PAG1* (α_7), *PBD1* (β_4), *PBE1* (β_5), and *PBG1* (β_7) were detected in seedlings, stems, roots, cauline leaves, siliques, and flowers (Fu et al., 1998). Their expression was coincident in those tissues, suggesting that these genes are coordinately regulated.

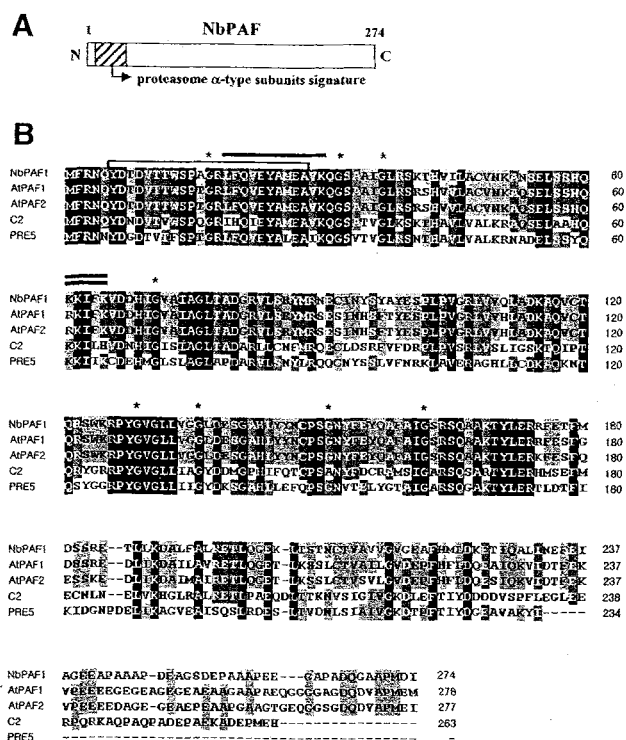


Fig. 2. The schematic diagram of the NbPAF structure and amino acid sequence comparison of NbPAF with related sequences in other species. **A.** The schematic drawing of the structure of NbPAF. The proteasome α -type subunits signature is indicated. Numbers indicate amino acid residues. **B.** Deduced amino acid sequence of NbPAF, and alignment with AtPAF1 and AtPAF2 from *A. thaliana*, C2 from *H. sapiens*, and PRE5 from *S. cerevisiae*. The number on the right indicates the amino acid residues. Gaps, which were introduced to maximize alignment, are indicated by dashes. Identical residues are boxed in black and light gray. The bracket indicates proteasome α -type subunits signature and the line over the alignment indicates the N-terminal α -helical region required for the interaction between the α subunits in yeast. The double line indicates a putative NLS sequence and the asterisks mark the conserved Gly residues present in α -type subunits.

Enhanced expression was observed in flowers and siliques, indicating high demand of proteasome-mediated proteolysis during flower and seed development (Fu et al., 1998). Furthermore, mRNA accumulation of two proteasome subunits (α_4 and β_6) increases during rapid proliferation in suspension cultures of *Arabidopsis* (Genschik et al., 1994). Our previous study also demonstrated that *Rpn3* encoding a regulatory subunit of 26S proteasome is preferentially expressed in the rapidly proliferating tissues including shoot and root meristems, and developing floral buds (Lee et al., 2002). These expression patterns are consistent with the finding that proteasome is involved in proteolysis of short-lived regulatory proteins such as cell

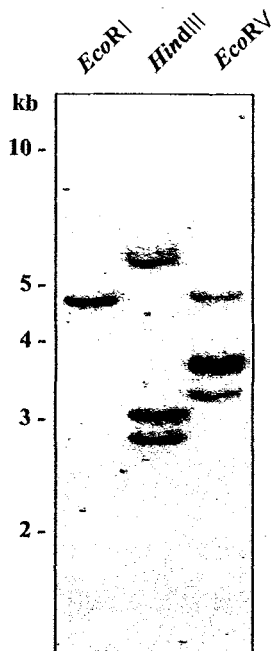


Fig. 3. Genomic DNA gel blot analysis of *NbPAF*. Ten μg of genomic DNA from *Nicotiana benthamiana* was digested with *EcoRI*, *HindIII* and *EcoRV*. DNA gel blots were hybridized with the probes corresponding to the C-terminal region of *NbPAF*. The DNA size markers are indicated in kilobases.

cycle regulators (Hershko and Ciechanover, 1998).

The expression pattern of the *NbPAF* gene was analyzed under various abiotic stress conditions by using a RNA gel blot analysis (Fig. 4). The *NbPAF* gene expression was strongly induced by methyl jasmonate (MeJA), salicylic acid (SA) and NaCl treatment. However, there was no significant change in *NbPAF* mRNA accumulation after ABA and cold treatment. As shown in Fig. 4, the *NbPAF* mRNA was strongly expressed at 6 h after MeJA treatment, but in response to SA, the transcript started to accumulate at 48 h to reach the higher level at 72 h. The *NbPAF* gene expression was also induced by NaCl treatment after 12 h. Up-regulation of the *NbPAF* expression in response to MeJA, SA, and high salt indicates that elevation of proteasome activities may be required for plant cells to cope with the stresses. Previously, it has been shown that ubiquitin-dependent protein degradation pathway plays important roles in senescence, heat stress, and wounding in plants (Belknap and Garbarino, 1996). During senescence, the role of proteasome could be to facilitate bulk protein degradation for nitrogen recycling, while during wounding response, proteasome may have a role in altering the overall protein profile to cope with increase in cellular metabolism required for wound sealing and defense (Belknap and Garbarino, 1996). The tobacco plants perturbed in ubiquitin system by expressing a ubiquitin variant showed altered response to pathogen

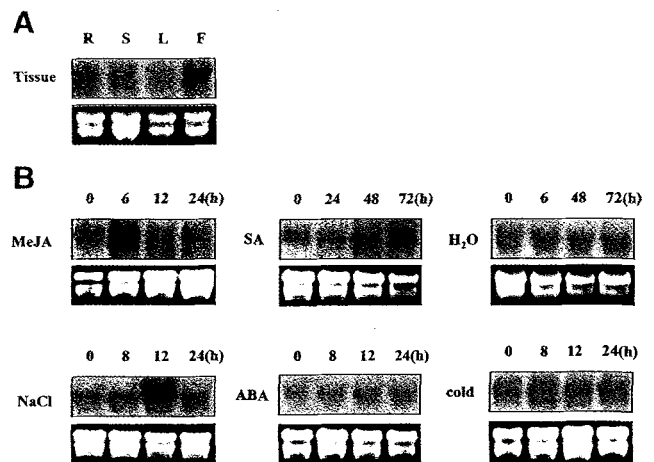


Fig. 4. Expression of *NbPAF*. **A.** RNA gel blot analysis of the *NtFHA1* mRNA in different tissues. Each lane represents 50 μg of total RNA from roots (R), stems (S), leaves (L), and flowers (F). **B.** Expression of the *NbPAF* mRNA in response to methyl jasmonate (MeJA), salicylic acid (SA), NaCl, abscisic acid (ABA) and cold stress. As a control plants were treated with water (H_2O). Each lane represents 50 μg of total RNA from leaves treated with various stimuli for the designated times. The amount of EtBr-stained rRNA was shown to verify equal loading of RNA in each lane. The membranes were hybridized with the probes corresponding to the C-terminal region of *NbPAF*.

infection, demonstrating that ubiquitin-dependent proteolysis plays a role in plant defense (Becker *et al.*, 1993). Additionally, increased transcription of polyubiquitin genes is observed in response to mercuric chloride (Genschik *et al.*, 1992), and of the ubiquitin extension protein in response to dehydration (Kiyosue *et al.*, 1994). Chilling has been shown to activate ubiquitin conjugation in *Clerodendrum speciosum* (Gindin and Borochoy, 1992). These results all indicate that there are increased demands for ubiquitin/proteasome-mediated proteolysis in plant cells to respond to biotic and abiotic stresses. Our results are consistent with these findings.

Subcellular localization of NbPAF was examined by expressing the fusion protein with GFP (green fluorescent protein). DNA constructs encoding NbPAF:GFP or GFP under the control of the CaMV 35S promoter was introduced into onion epidermal cells by particle bombardment (Fig. 5). Simultaneously, the same cell layer was stained with DAPI (100 $\mu\text{g}/\text{mL}$) to localize nuclei. Expression of the introduced genes was examined under a fluorescent microscope with different filters to capture the image of GFP and DAPI staining. The signal of NbPAF:GFP was detected in the cytoplasm and nucleus; while GFP was mainly detected in the cytoplasm (Fig. 5). These results are consistent with previous reports that proteasome particles are found in both the cytoplasm and nucleus in eu-

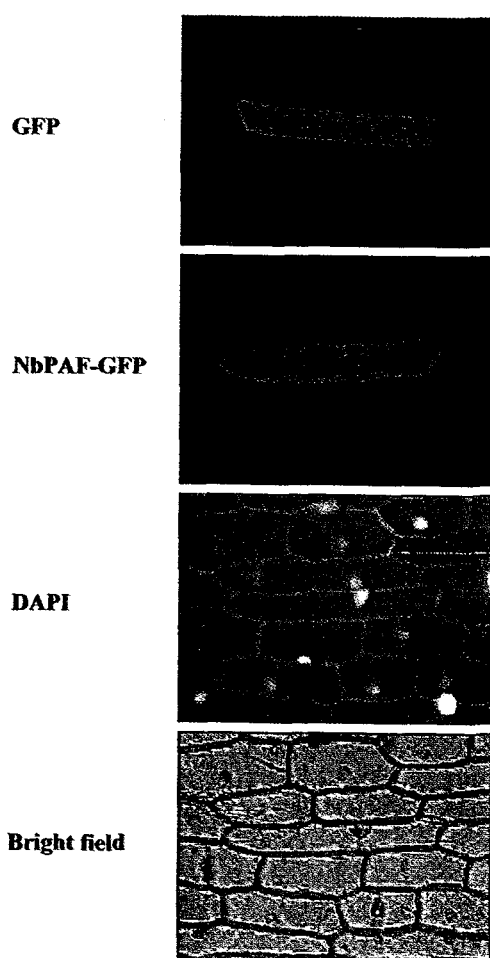


Fig. 5. Subcellular localization of NbPAF. Onion epidermal cell layers were particle-bombarded with the *NbPAF:GFP* fusion construct and *GFP* as a control, and localization of fluorescent signal was examined at 12 h after bombardment. The same cell layer was briefly stained with DAPI (100 µg/ml) to visualize nuclei.

karyotic cells (Enenckel *et al.*, 1998). In plants, the carrot Rpn3 regulatory subunit (21D7) is mainly localized in the nucleus of proliferating cells (Smith *et al.*, 1997). Immunological studies show that distribution of proteasome between these compartments alters during the cell cycle (Palmer *et al.*, 1996) or developmental processes (Machiels *et al.*, 1996). In plant cells, similar to animal cells, nuclear translocation of proteasomes may play an important role in controlling cell division and development (Voges *et al.*, 1999).

Acknowledgments This work was supported by grants from National Research Laboratory Program and Plant Diversity Research Center of 21st Century Frontier Research Program, funded by Ministry of Science and Technology of Korean government.

References

- Baumeister, W., Walz, J., Zühl, F., and Seemüller, E. (1998) The proteasome: paradigm of a self-compartmentalizing protease. *Cell* **92**, 367–380.
- Becker, F., Buschfeld, E., Schell, J., and Bachmair, A. (1993) Altered response to viral infection by tobacco plants perturbed in ubiquitin system. *Plant J.* **3**, 875–881.
- Belknap, W. R. and Garbarino, J. E. (1996) The role of ubiquitin in plant senescence and stress responses. *Trends Plant Sci.* **1**, 331–335.
- Callis, J. and Vierstra, R. D. (2000) Protein degradation in signaling. *Curr. Opin. Plant Biol.* **3**, 381–386.
- Coux, O., Tanaka, K., and Goldberg, A. L. (1996) Structure and functions of the 20S proteasomes. *Annu. Rev. Biochem.* **65**, 801–847.
- Emori, Y., Tsukahara, T., Kawasaki, H., Ishiura, S., Sugita, H., and Suzuki, K. (1991) Molecular cloning and functional analysis of three subunits of the yeast proteasome. *Mol. Cell. Biol.* **11**, 344–353.
- Enenckel, C., Lehmann, A., and Kloetzel, P.-M. (1998) Subcellular distribution of proteasomes implicates a major location of protein degradation in the nuclear envelope-ER network in yeast. *EMBO J.* **17**, 6144–6154.
- Fu, H., Doelling, J. H., Arendt, C. S., Hochstrasser, M., and Vierstra, R. D. (1998) Molecular organization of the 20S proteasome gene family from *Arabidopsis thaliana*. *Genetics* **149**, 677–692.
- Genschik, P., Parmentier, Y., Durr, A., Marbach, J., Criqui, M. C., Jamet, E., and Fleck, J. (1992) Ubiquitin genes are differentially regulated in protoplast-derived cultures of *Nicotiana sylvestris* and in response to various stresses. *Plant Mol. Biol.* **20**, 897–910.
- Genschik, P., Jamet, E., Philipps, G., Parmentier, Y., Gigot, C., and Fleck, J. (1994) Molecular characterization of a beta-type proteasome subunit from *Arabidopsis thaliana* co-expressed at a high level with an alpha-type proteasome subunit early in the cell cycle. *Plant J.* **6**, 537–546.
- Genschik, P., Criqui, M. C., Parmentier, Y., Derevier, A., and Fleck, J. (1998) Cell cycle-dependent proteolysis in plants: identification of the destruction box pathway and metaphase arrest produced by the proteasome inhibitor MG132. *Plant Cell* **10**, 2063–2075.
- Gindin, E. and Borochoy, A. (1992) Ubiquitin conjugation to protein increases following chilling in clerodendrum leaves. *Plant Physiol.* **100**, 1392–1395.
- Girod, P.-A., Fu, H., Zryd, J. P., and Vierstra, R. D. (1999) Multi-ubiquitin chain binding subunit MCB1 (RPN10) of the 26S proteasome is essential for developmental progression in *Physcomitrella patens*. *Plant Cell* **11**, 1457–1471.
- Hershko, A. and Ciechanover, A. (1998) The ubiquitin system. *Annu. Rev. Biochem.* **67**, 425–479.
- Hilt, W. and Wolf, D. H. (1996) Proteasomes: destruction as a programme. *Trends Biochem. Sci.* **21**, 96–102.
- Hochstrasser, M. (1996) Ubiquitin-dependent protein degradation. *Annu. Rev. Genet.* **30**, 405–439.
- Hong, S. H., Ahn, J. Y., Lee, C. S., Kang, M. S., Ha, D. B., Tanaka, K., and Chung, C. H. (1994) Tissue-specific expression of the subunits of chick 20S proteasomes. *Biochem. Mol. Int.* **32**, 723–729.

- Kawahara, H. and Yokosawa, H. (1992) Cell cycle-dependent change of proteasome distribution during embryonic development of the ascidian *Halocynthia roretzi*. *Dev. Biol.* **151**, 27–33.
- Kim, M., Park, S.-W., Yu, S. H., Cho, H. S., Ha, H. J., Hwang, I., and Pai, H.-S. (2001) Molecular characterization of the *NeIF2B β* gene encoding a putative eIF2B β -subunit in *Nicotiana tabacum*. *Mol. Cells* **11**, 110–114
- Kiyosue, T., Yamaguchi-Shinozaki, K., and Shinozaki, K. (1994) Cloning of cDNAs for genes that are early-responsive to dehydration stress (ERDs) in *Arabidopsis thaliana* L: identification of three ERDs as HSP cognate genes. *Plant Mol. Biol.* **25**, 791–798.
- Lee, S. S., Cho, H. S., Yoon, G. M., Ahn, J.-W., Liu, J. R., and Pai, H.-S. (2002) Interaction of NtCDPK1 calcium-dependent protein kinase with NtRpn3 regulatory subunit of the 26S proteasome in *Nicotiana tabacum*. *Plant J.* (in press).
- Machiels, B. M., Henfling, M. E., Schutte, B., van Engelan, M., Broers, J. L., and Ramaekers, F. C. (1996) Subcellular localization of proteasomes in apoptotic lung tumor cells and persistence as compared to intermediate filaments. *Eur. J. Cell Biol.* **70**, 250–259.
- Palmer, A., Rivett, A. J., Thomson, S., Hendil, K. B., Butcher, G. W., Fuertes, G., and Knecht, E. (1996) Subpopulations of proteasomes in rat liver nuclei, microsomes and cytosol. *Biochem. J.* **316**, 401–407.
- Smith, M. W., Ito, M., Miyamaki, M., Sato, S., Yoshikawa, Y., Wada, S., Maki, H., Nakagawa, H., and Komamine, A. (1997) Plant 21D7 protein, a nuclear antigen associated with cell division, is a component of the 26S proteasome. *Plant Physiol.* **113**, 281–291.
- Voges, D., Zwickl, P., and Baumeister, W. (1999) The 26S proteasome: a molecular machine designed for controlled proteolysis. *Annu. Rev. Biochem.* **68**, 1015–1068.

Forkhead-associated Domains of the Tobacco NtFHA1 Transcription Activator and the Yeast Fhl1 Forkhead Transcription Factor Are Functionally Conserved*

Received for publication, February 15, 2002, and in revised form, July 11, 2002
Published, JBC Papers in Press, July 30, 2002, DOI 10.1074/jbc.M201559200

Moonil Kim^{‡§}, Joon-Woo Ahn[‡], Kiwon Song[¶], Kyung-Hee Paek[§], and Hyun-Sook Pai^{‡¶}

From the [‡]Laboratory of Plant Genomics, Korea Research Institute of Bioscience and Biotechnology, Yusong, Taejeon 305-333, the [¶]Department of Biochemistry, Yonsei University, Seoul 120-749, and the [§]Graduate School of Biotechnology, Korea University, Seoul 136-701, Korea

NtFHA1 encodes a novel protein containing the forkhead-associated (FHA) domain and the acidic domain in *Nicotiana tabacum*. NtFHA1 functions as a transactivator and is targeted to the nucleus. The sequence of the FHA domain of NtFHA1 is significantly homologous to that of the Fhl1 forkhead transcription factor of yeast. FHL1 was previously identified as a suppressor of RNA polymerase III mutations, and the *fhl1* deletion mutant exhibited severe growth defects and impaired rRNA processing. Ectopic expression of the FHA domain of NtFHA1 (but not its mutant form) resulted in severe growth retardation in yeast. Similarly, expression of Fhl1, its FHA domain, or chimeric Fhl1 containing the NtFHA1 FHA domain also inhibited yeast growth. Yeast cells overexpressing the FHA domains of NtFHA1 and Fhl1 contained lower levels of mature rRNAs and exhibited rRNA-processing defects, similar to the *fhl1* null mutant. Chimeric Fhl1 (but not the mutant form with a small deletion in its FHA domain) fully complemented the growth and rRNA-processing defects of the *fhl1* null mutant, demonstrating that the FHA domain of NtFHA1 can functionally substitute for the FHA domain of Fhl1. These results demonstrate that the FHA domains of NtFHA1 and Fhl1 are conserved in their structure and function and that the FHA domain of Fhl1 is critically involved in regulation of rRNA processing in yeast. NtFHA1 function in plants may be analogous to Fhl1 function in yeast.

Eukaryotic transcription factors have been divided into many classes depending on their characteristic DNA-binding domains. The forkhead domain is a highly conserved 110-amino acid DNA-binding region found in a class of transcription factors (1). This domain was named after the *Drosophila* forkhead protein that is required for the proper formation of the terminal structure of the *Drosophila* embryos (2). In *Saccharomyces cerevisiae*, several forkhead transcription factors (Fhl1, Hcm1, Fkh1, and Fkh2) have been identified (3–6). Fhl1

has been implicated in RNA polymerase III function, the mutation of which leads to aberrant rRNA processing (3), whereas the Fkh1 and Fkh2 proteins, which share homology with each other in their forkhead domain and N-terminal region, regulate the cell cycle and pseudohyphal growth (5, 6).

In addition to the forkhead DNA-binding domain, some forkhead transcription factors also possess a forkhead-associated (FHA)¹ domain. FHA domains are highly diverse protein-protein interaction modules characterized by a 55–75-residue motif with only 7 residues that are >65% conserved among 120 family members (7). Not being restricted to a group of forkhead transcription factors, the FHA domain has been found in a wide variety of proteins from both prokaryotes and eukaryotes (8). Rad53, a protein kinase involved in DNA damage response and cell cycle arrest in *Saccharomyces cerevisiae*, contains two FHA domains separated by a central Ser/Thr kinase domain (9). Yeast Yhr5 and FraH of *Anabaena* sp. contain zinc finger motifs beside the FHA domain (7). Another group of the FHA domain-containing proteins are protein kinases such as Dun1, Spk1, and Mek1 of yeast, all of which have been reported to act in the nucleus and to respond to signals related to DNA replication and repair (10). In plants, the FHA domain was identified in *Arabidopsis* kinase-associated protein phosphatase (KAPP) through interaction cloning using an *Arabidopsis* receptor-like kinase as bait (11). Further study of the interaction between the KAPP and receptor-like kinase (RLK) proteins provided the evidence for involvement of FHA domains in phosphorylation-dependent protein-protein interactions (12). KAPP is involved in plant RLK signaling pathways on the inner face of the plasma membrane, unlike other FHA domain-containing proteins that are localized in the nucleus. The tertiary structure of the FHA domain has been solved in FHA2 (13) and FHA1 (14) of Rad53. Although the primary sequences of these two FHA domains are divergent, their tertiary structures are remarkably similar. The tertiary structure consists of a β -sandwich containing two twisted antiparallel β -sheets and a short α -helix at the C terminus.

In this study, we report a novel FHA domain-containing transcription activator in plants, designated NtFHA1. The FHA domains of NtFHA1 and the yeast Fhl1 forkhead transcription factor have conserved functions in regulation of cell growth and rRNA processing in yeast. Furthermore, the NtFHA1 FHA domain is fully functional within Fhl1 to rescue the phenotypes of slow growth and defective rRNA processing in the yeast *fhl1* null mutant. These results indicate that Nt-

* This work was supported by grants from the Plant Diversity Research Center of the 21st Century Frontier Research Program and the National Research Laboratory Program funded by the Ministry of Science and Technology of the Korean Government. The costs of publication of this article were defrayed in part by the payment of page charges. This article must therefore be hereby marked "advertisement" in accordance with 18 U.S.C. Section 1734 solely to indicate this fact.

The nucleotide sequence(s) reported in this paper has been submitted to the GenBank™/EBI Data Bank with accession number(s) AF411856.

¶ To whom correspondence should be addressed: Lab. of Plant Genomics, Korea Research Inst. of Bioscience and Biotechnology, P. O. Box 115, Yusong, Taejeon 305-600, Korea. Tel.: 82-42-860-4195; Fax: 82-42-860-4608; E-mail: hyunsook@mail.kribb.re.kr.

¹ The abbreviations used are: FHA, forkhead-associated; KAPP, *Arabidopsis* kinase-associated protein phosphatase; GFP, green fluorescent protein; RFP, red fluorescent protein; NLS, nuclear localization signal.

FHA1 in plant cells may perform a function analogous to that of Fhl1 in yeast, probably by associating with other transcription factors. This is the first functional analysis of the FHA domain-containing transcription factors in plants.

EXPERIMENTAL PROCEDURES

FHA Domain Constructs—FHA domain constructs and site-directed FHA mutants were generated by PCR and recombinant PCR (15) using synthetic oligonucleotides, and the mutations were confirmed by DNA sequencing. cFhl1Δ33 was generated by digestion of the cFhl1 construct (Fhl1 with its FHA domain replaced with the NtFHA1 FHA domain) with *Ssp*BI and *Bss*HIII and subsequent self-ligation. This leads to internal deletion of 33 amino acids that include 4 conserved residues of the FHA domain without causing reading frame shift.

Yeast Strains and Culture—Experiments were carried out in the EGY48 (*MATα, his3, trp1, ura3, LexA_{op}-LEU2*) and W303-1A (*MATα, ade2-1, can1-100, his3-11,15, leu2-3, trp1-1, ura3-1*) genetic backgrounds as indicated. For complementation assay, the *FHL1* gene was deleted in a haploid with the W303 background (*MATα, ade2-1, ura3-52, trp1-1, lys2-801, his3-11,15*). Start cultures for galactose-inducible experiments were grown on selective medium containing 2% glucose. For induction of protein expression, cells were grown in selective medium containing 2% glucose or 4% galactose and 2% sucrose. For growth rate studies, aliquots were removed from the growing cultures, and absorbances were measured at 600 nm. In synchronization experiments, cells were diluted to 0.2 A units and treated twice for 2 h with 20 μg/ml α-factor. Cells were released from α-factor arrest by three washes with selective medium containing 2% sucrose and 4% galactose and resuspended in fresh medium.

Synchronization of Tobacco BY2 Cells and Analysis of NtFHA1 Gene Expression—Cultured cells were achieved by a 24-h subculture of stationary phase cells (7 days old) in medium containing aphidicolin (5 mg/liter; Sigma), followed by extensive washes as described (16). Mitotic index was measured as described (16). Northern blot analysis was carried out with 50 μg of total RNA for each lane as described under "DNA and RNA Gel Blot Analyses."

Flow Cytometry—For cell cycle analyses, 1-ml aliquots were removed from yeast cultures and fixed in 70% ethanol. 300 μl of cells (2–3 × 10⁶ cells) were washed with 50 mM sodium citrate (pH 7) and incubated for 3 h with 0.1 mg/ml RNase A in 50 mM sodium citrate at 37 °C. Cells were treated with 4 μg/ml propidium iodide, sonicated, and analyzed using a BD Biosciences FACScan and CellQuest software.

Transcription Activation Analysis—For effector constructs, various *NtFHA1* cDNA fragments were cloned into pLexA (CLONTECH) using *Eco*RI and *Xho*I sites, generating in-frame fusions of the LexA DNA-binding domain and the full-length or truncated open reading frames of NtFHA1. As a control, the DNA fragment containing the B42 activation domain was PCR-amplified from the pB42AD plasmid (CLONTECH) and cloned into pLexA using *Eco*RI and *Xho*I sites. To measure the transcription activation, the effector constructs were transformed into the EGY48 (*p8_{op}-LacZ*) strain, and the transformants were tested for growth in Leu⁻ and for β-galactosidase activity. Three separate colonies were assayed for each construct, and β-galactosidase activity was determined as A_{420 nm}/h.

Subcellular Localization of the NtFHA1-GFP Protein—The *NtFHA1* cDNA corresponding to amino acid residues 1–209 was PCR-amplified and cloned into the 326-GFP vector (17) using a *Bam*HI site to generate an *NtFHA1-GFP* in-frame fusion under the control of the cauliflower mosaic virus 35 S promoter. As a control for nuclear localization, the pNLS-RFP construct encoding a red fluorescent protein with a nuclear localization signal (17) under the control of 35 S promoter was also prepared. The pNtFHA1-GFP and pNLS-RFP plasmids were introduced into *Arabidopsis* protoplasts by polyethylene glycol treatment as described (17). Expression of the fusion constructs was monitored at various times after transformation by fluorescence microscopy using a Zeiss Axioplan fluorescence microscope, and the image was captured with a cooled charge-coupled device camera. The filter sets (Omega Optical Inc., Brattleboro, VT) were XF116 (exciter, 474AF20; dichroic, 500DRLP; and emitter, 510AF23) for GFP and XF33/E (exciter, 535DF35; dichroic, 570DRLP; and emitter, 605DF50) for RFP. The data were processed using Adobe Photoshop software and presented in pseudocolor format.

DNA and RNA Gel Blot Analyses—For DNA gel blot analysis, the genomic DNA isolated from tobacco leaves was digested with *Eco*RI and *Hind*III, electrophoresed on a 0.8% agarose gel, and blotted onto Hybond-N nylon membrane (Amersham Biosciences). The probe was the 0.4-kb PCR fragment corresponding to the C-terminal region of

NtFHA1. Prehybridization and hybridization were carried out in 5× SSC, 5× Denhardt's solution, and 0.5% SDS at 60 °C overnight. The membranes were washed twice with 2× SSC and 1% SDS at room temperature and then washed with 0.1× SSC and 0.1% SDS at 60 °C for 30 min.

For RNA gel blot analysis using plant tissues, total RNA was prepared using TRIzol™ reagent (Invitrogen) following the manufacturer's instructions. ~50 μg of total RNA were electrophoresed on an agarose gel containing 5.1% (v/v) formaldehyde and blotted onto Hybond-N nylon membrane. Prehybridization, hybridization, and washing conditions were as described for DNA gel blot analysis. To extract total RNA from yeast, yeast cells were grown to 0.8 A units; pelleted; and resuspended in buffer containing 50 mM NaOAc (pH 5.3), 10 mM EDTA, and 0.1% diethyl pyrocarbonate. Then 0.1 volume of 10% SDS was added to the suspension and vortexed. After addition of an equal volume of phenol and vortexing, the whole mixture was kept at 65 °C for 4 min, rapidly chilled on ice, and centrifuged to collect the supernatant. The supernatant was extracted twice with phenol/chloroform and ethanol-precipitated to obtain total RNA. To detect pre-rRNAs in yeast, hybridization was performed using ³²P-end-labeled oligonucleotide probes ITS1-1 (5'-GAAACGGTTTAAATGTGCTCATAAC-3'), ITS1-2 (5'-TGT-TACCTCTGGGCC-3'), and ITS2 (5'-GGCCAGCAATTTCAAGTTA-3'), which correspond to internal transcribed spacers, at 41 °C for 2 h and washed with 2× SSC and 0.1% SDS at 41 °C for 1 h. Membranes were analyzed using a PhosphorImager (Molecular Dynamics, Inc.).

Reverse Transcription-PCR—20 μg of total RNA isolated from plant tissues were treated with 1 unit of RNase-free DNase (Promega) and 1 unit of RNase inhibitor (Promega) for 15 min at 30 °C and then purified by phenol/chloroform extraction. The first-strand cDNA was synthesized using 5 μg of DNase-treated RNA primed by oligo(dT) (50 μM) using 200 units of Superscript II RNase H⁻ reverse transcriptase (Invitrogen), 20 units of RNase inhibitor, 500 μM each dNTP, and 10 mM dithiothreitol. 0.1, 0.01, and 0.005 volume of 0.05 volume of the reaction mixture were used for PCR amplification with 1 unit of *Taq* DNA polymerase (Promega), 100 μM each dNTP, and 100 pmol each of the forward and reverse primers.

Protein Extracts and Immunoblotting—Protein extracts were prepared by resuspending yeast cells in 10% trichloroacetic acid and vigorous vortexing in the presence of glass beads. Crude extract was pelleted, washed with 1 ml of cold acetone, and pelleted again. After resuspending the pellet in SDS sample buffer, 0.1 volume of 10 M NaOH was added. The supernatant was obtained by centrifugation and boiled for 10 min. Proteins were electrophoresed, transferred onto polyvinylidene difluoride membranes, and probed with the monoclonal antibody against the LexA DNA-binding domain (1:10,000 dilution; CLONTECH). They were then reacted with secondary antibodies conjugated with horseradish peroxidase and ECL reagent (Amersham Bioscience) for detection.

RESULTS

The NtFHA1 Gene Encodes a Putative FHA Domain-containing Transcription Regulator in Tobacco—A cDNA encoding a protein of 209 amino acids with structural features of a transcription factor was identified in *Nicotiana tabacum* (cv. *xanthi*). The cDNA is 819 bp in length, and its predicted molecular mass is 22,601 Da. Based on the predicted sequence, the protein contains ~59 amino acids (residues 30–88) that show conserved structural features of the FHA domain in the N terminus and the acidic region (residues 153–185) as a putative transactivation domain in the C terminus, but lacks any known DNA-binding motifs (Fig. 1A). The cDNA clone was designated *NtFHA1*.

We searched the *Arabidopsis* data base for homologs of *NtFHA1* and found two genomic sequences encoding highly homologous proteins (GenBank™/EBI accession numbers AAF20220.1 and AAF20224.1). The corresponding cDNAs were isolated from the *Arabidopsis* cDNA library by PCR and designated *AtFHA1* and *AtFHA2*. *AtFHA1* and *AtFHA2* encode proteins of 253 and 320 amino acids, respectively. The expected molecular masses of *AtFHA1* and *AtFHA2* are 27,980 and 35,994 Da, respectively. Like *NtFHA1*, they contain the FHA domain in the N terminus and the acidic domain in the C terminus and lack any DNA-binding domain. The amino acid sequence of *NtFHA1* and comparison of the sequence with

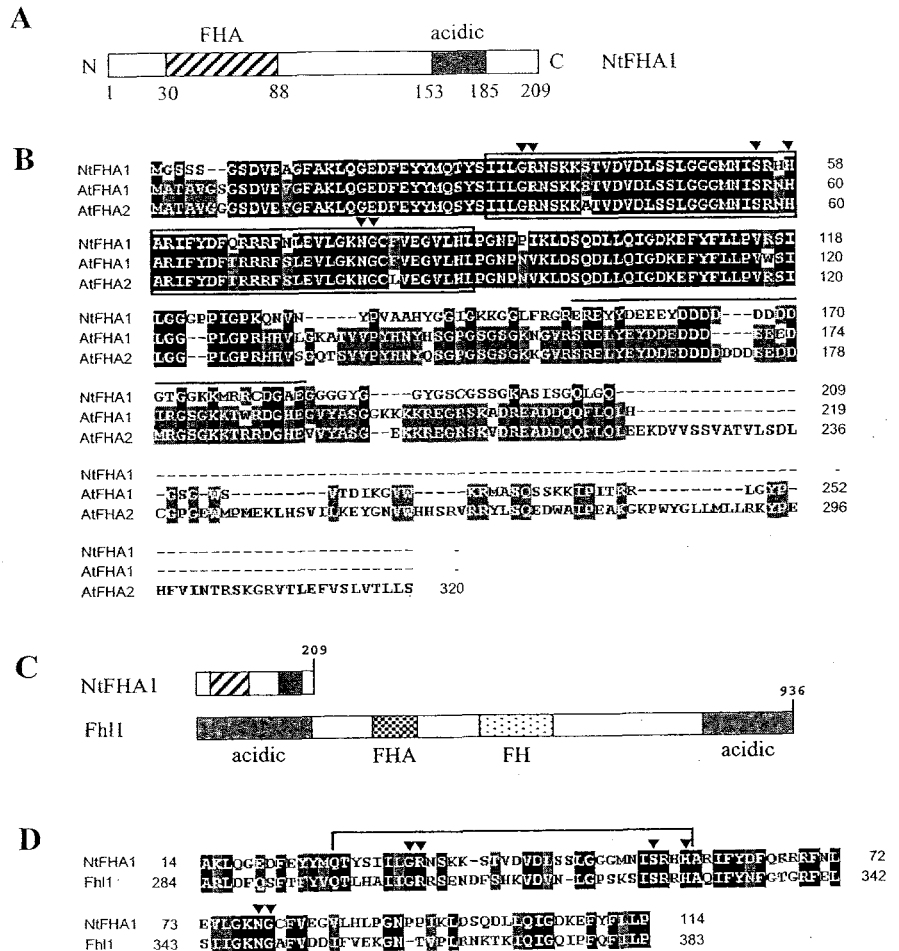


FIG. 1. Structure and amino acid sequence comparison of NtFHA1 with related sequences in other species. *A*, schematic representation of the NtFHA1 protein. The FHA domain, the acidic domain, and the residue numbers are indicated. *B*, deduced amino acid sequence of NtFHA1 and alignment with AtFHA1 and AtFHA2 of *Arabidopsis*. The numbers on the right indicate amino acid positions. Gaps, which were introduced to maximize alignment, are indicated by dashes. The residues conserved among all three of the compared sequences are boxed in black, and the residues conserved among two of the compared sequences are boxed in light gray. The FHA domain and the acidic region are indicated by brackets and overlining, respectively. The conserved residues of the FHA domain are marked with arrowheads above the sequences. *C*, schematic representation of the yeast Fhl1 protein in comparison with NtFHA1. *D*, sequence alignment of the FHA domains of NtFHA1 and Fhl1. Identical residues are boxed in black, and residues belonging to the same group are boxed in light gray. The conserved residues of the FHA domain are marked with arrowheads above the sequences. The 33 residues deleted in cFhl1Δ33 are indicated by the bracket.

those of AtFHA1 and AtFHA2 are shown in Fig. 1*B*. The FHA domain of NtFHA1 exhibits 91–94% sequence identity to those of AtFHA1 and AtFHA2, but the sequences outside the FHA domain are not conserved.

The FHA domain of NtFHA1 also shows significant sequence similarity to the FHA domain of Fhl1, a forkhead transcription factor in yeast. Schematic diagrams of yeast Fhl1 and NtFHA1 and alignment of the FHA domains of the two proteins are shown in Fig. 1 (*C* and *D*, respectively). Yeast Fhl1, consisting of 936 amino acids, contains two large acidic domains at the N and C termini and the FHA domain and a DNA-binding forkhead domain in the center. The amino acid sequence of the FHA domain of NtFHA1 shows 46% identity to that of Fhl1.

Transactivation Activity of NtFHA1—We tested whether NtFHA1 has the ability for transcription activation using the yeast system. Various effector constructs were transformed into the yeast strain that contains two reporter genes (*LEU2* and *LacZ*) under the control of multiple LexA operators (Fig. 2*A*). As effectors, fusion proteins between the LexA DNA-binding domain and full-length NtFHA1 or its deletion mutants were expressed under the control of *ADH1* promoters. Transcription activation was monitored by β -galactosidase activity and yeast growth in medium lacking leucine. The LexA DNA-binding domain alone, used as a negative control, did not exhibit any transactivation activity, whereas the positive control LexA-B42, a fusion protein between the LexA DNA-binding domain and the B42 activation domain, showed strong β -galactosidase activity and growth in Leu⁻. Full-length NtFHA1 was able to transactivate expression of the reporter genes, whereas NtFHA1 deletion mutants such as LexA-Δ1, LexA-Δ2, and

LexA-Δ3 did not show any detectable transactivation activity. These results demonstrate that NtFHA1 is functional as a transcription activator.

Nuclear Localization of NtFHA1—Cellular localization of NtFHA1 was examined by constructing the NtFHA1-GFP fusion protein, the expression of which is controlled by the cauliflower mosaic virus 35 S promoter. As a positive control for nuclear targeting, RFP fused with a nuclear localization signal (NLS) (17) was expressed under the control of the same promoter. DNA constructs encoding NtFHA1-GFP and NLS-RFP were simultaneously introduced into protoplasts isolated from *Arabidopsis* seedlings. After incubation at 25 °C, expression of the introduced genes was examined under a fluorescent microscope with two different filters to capture the image of GFP and RFP. After a 24-h incubation, the green fluorescent signal completely overlapped with the red fluorescent signal in the nucleus, exhibiting colocalization of NtFHA1-GFP and NLS-RFP in the nucleus. This result demonstrates that NtFHA1 is targeted to the nucleus (Fig. 2*B*).

Genomic Organization and Expression of the NtFHA1 Gene—DNA gel blot analysis was performed with tobacco genomic DNA digested with restriction enzymes (Fig. 3*A*). The probe was the 0.4-kb PCR fragment corresponding to the C-terminal region of the *NtFHA1* cDNA. *EcoRI* digestion resulted in three hybridizing bands, whereas *HindIII* digestion showed four hybridizing bands. Considering that *N. tabacum* is amphidiploid between *Nicotiana tomentosiformis* and *Nicotiana sylvestris*, these results indicate that the tobacco genome contains two copies of the *NtFHA1*-related sequences (Fig. 3*A*). We examined expression of the *NtFHA1* mRNA in plant tissues

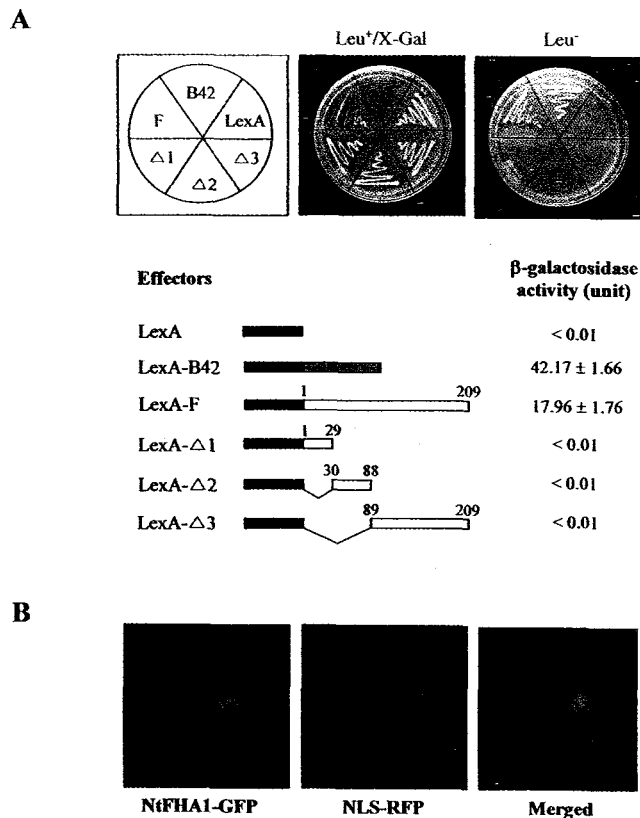


FIG. 2. Transcription activation and nuclear localization of *NtFHA1*. A, structures of six effector constructs and their transactivation activities. Full-length *NtFHA1* (*LexA-F*) and its deletion mutants were fused to the LexA DNA-binding domain. Transcription activation was monitored by β -galactosidase activity and yeast growth in *Leu*⁻ medium. *X-gal*, 5-bromo-4-chloro-3-indolyl- β -D-galactopyranoside. B, *in vivo* targeting of *NtFHA1*. Protoplasts were transformed with both *NtFHA1*-GFP and NLS-RFP fusion constructs, and localization of fluorescent signals was examined 24 h after transformation. Green and red fluorescent signals indicate GFP and RFP, respectively. The GFP (left panel), RFP (middle panel), and merged (GFP and RFP; right panel) images are shown.

at different developmental stages using RNA gel blot analysis and semiquantitative reverse transcription-PCR. In tobacco, the 1.0-kb *NtFHA1* transcript was detected in all of the tissues examined, with the highest level found in open flowers (Fig. 3B). During seed germination, the *NtFHA1* mRNA was detected at 2 days of incubation in MS (Murashige and Skoog) medium after 3 days of cold treatment, and the level decreased at 3–5 days of incubation and then increased at 7–9 days of incubation (Fig. 3C). During pollination, the *NtFHA1* mRNA was detected in unpollinated ovaries just before anthesis at the level that was maintained until 3 days after pollination, and the mRNA level decreased from 5 days after pollination to a barely detectable level at 7 days after pollination (Fig. 3D). The *NtFHA1* mRNA level fluctuated during the cell cycle in tobacco BY2 cells (Fig. 3E). Suspension-cultured tobacco BY2 cells were synchronized by a 24-h treatment with aphidicolin, an inhibitor of DNA polymerases. After release from the aphidicolin block, mitotic index and the *NtFHA1* mRNA levels were monitored during the cell cycle. As controls, the histone H4 gene and the cyclin B1 gene were used as markers of S phase and M phase, respectively. The level of *NtFHA1* mRNA was maintained at a similar level through S phase and G₂ phase until mid-M phase, and then the transcript level decreased to a very low level during G₁ phase.

Overexpression of the *NtFHA1* FHA Domain Causes a Growth Defect in Yeast—To obtain clues to the function of the

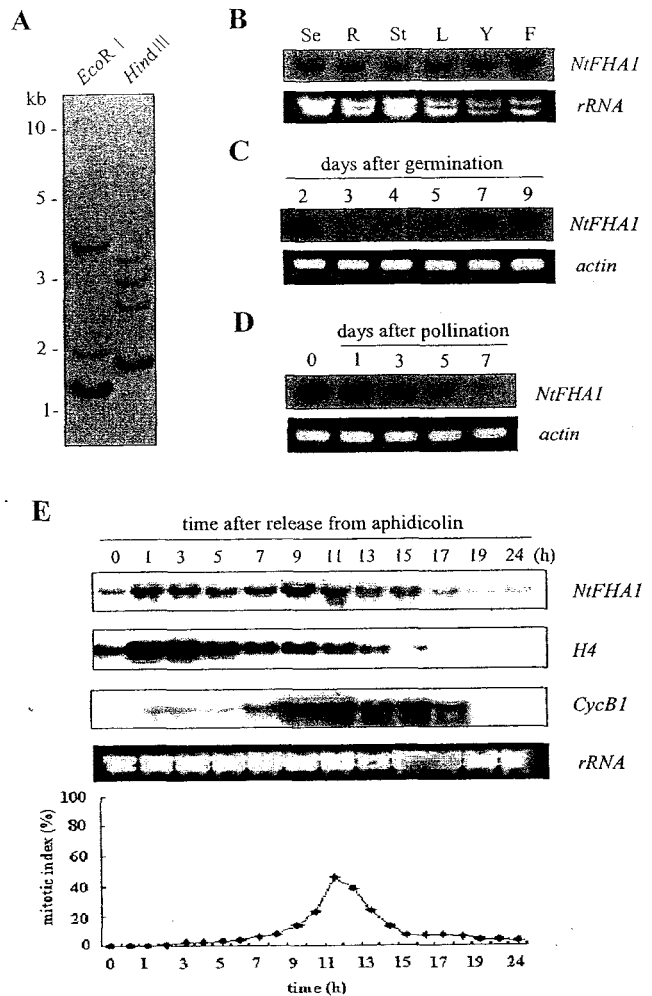


FIG. 3. Genomic organization and expression of the *NtFHA1* gene. A, genomic DNA gel blot analysis. DNA gel blots were hybridized with probes corresponding to the C-terminal region of *NtFHA1*. The DNA size markers are indicated in kilobases. B, RNA gel blot analysis of the *NtFHA1* mRNA in tobacco. Each lane represents 50 μ g of total RNA from seedlings (Se), roots (R), stems (St), leaves (L), young flower buds (Y), and open flowers (F). The amount of EtBr-stained rRNA is shown to verify equal loading of RNA in each lane. C, expression during seed germination. The *NtFHA1* mRNA levels in water-imbibed seeds for the indicated time (2–9 days) after a 3-day cold treatment were measured by semiquantitative reverse transcription-PCR using the *NtFHA1*-specific primers. As a control, the transcript level of actin was examined. D, expression during early seed development. The *NtFHA1* mRNA levels in ovaries before anthesis (0 days) and 1, 3, 5, and 7 days after pollination were estimated by semiquantitative reverse transcription-PCR. E, RNA gel blot analysis of *NtFHA1* mRNA expression during the cell cycle. Tobacco BY2 cells were synchronized with aphidicolin. Each lane contains 50 μ g of total RNA. As controls for S phase and M phase, histone H4 and cyclin B (*CycB1*) mRNAs were detected, respectively.

FHA domain of *NtFHA1*, we overexpressed the domain using a galactose-inducible system in yeast. The DNA construct containing the *NtFHA1* FHA domain fused to the LexA DNA-binding domain for nuclear targeting or the construct containing the LexA DNA-binding domain alone as a vector control was transformed into yeast (Fig. 4A). Additionally, the FHA domain constructs with alanine substitutions of the highly conserved residues of the FHA domain (Mut34 and Mut55) were also overexpressed (Fig. 4A). The transformed yeast strains carrying the FHA domain or the vector showed normal growth in medium containing 2% glucose that repressed expression of the constructs. However, in medium containing 4%

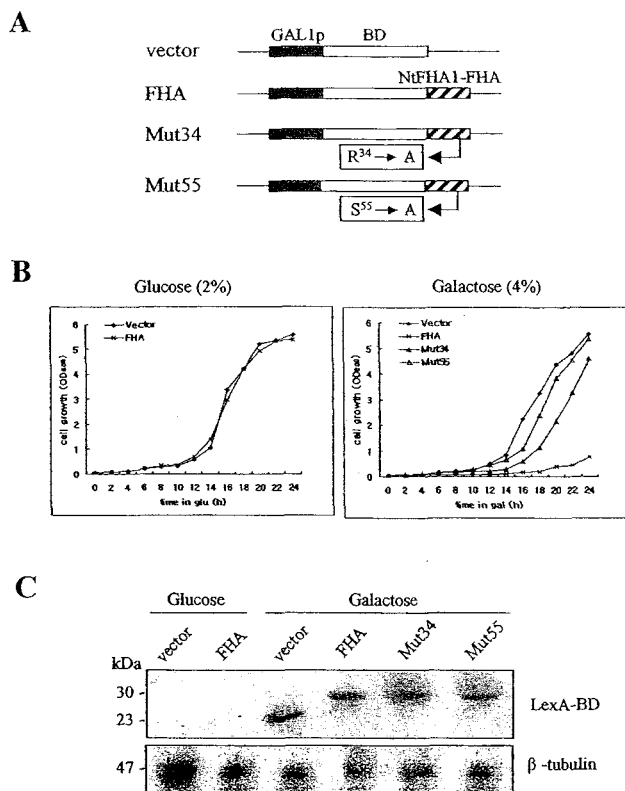


FIG. 4. Yeast growth phenotypes caused by overexpression of the FHA domain of NtFHA1. *A*, schematic diagrams of constructs for overexpression. *GAL1p* and *BD* represent the *GAL1* promoter and the LexA DNA-binding domain, respectively. *B*, yeast cell growth. Yeast strains containing the various constructs were grown for 24 h in 2% glucose or 4% galactose and 2% sucrose. At 2-h intervals, aliquots were removed, and cell growth was monitored by absorbance measurements. *C*, Western blot analysis of FHA domain expression. 30 μ g of total proteins isolated from yeast cells grown to 0.8 A units in glucose or galactose were subjected to immunoblotting with the monoclonal antibody (LexA-BD) against LexA DNA binding domain and the anti-tubulin antibody.

galactose, the strain overexpressing the FHA domain exhibited considerably slower growth kinetics than the vector control (Fig. 4*B*). Overexpression of the FHA domain did not affect cell viability because colony formation per A unit was very similar for FHA domain and vector control cultures when plated on glucose medium (data not shown). As shown in Fig. 4*B*, this growth defect phenotype was dependent on the integrity of the FHA domain, as it was abrogated by alanine substitution of the highly conserved residues Arg-34 and Ser-55 (Fig. 4*B*). The abrogation of the growth defect indicates that these residues may be directly involved in the binding of a target protein that is crucial for the growth defect phenotype in yeast. The corresponding proteins for the FHA domain, Mut34, and Mut55 constructs were expressed at similar levels, as shown by immunoblot analysis using the anti-LexA antibody (Fig. 4*C*).

Slower G_1 -S Transition in NtFHA1 FHA Domain-overexpressing Yeast Cells during the Cell Cycle—To examine whether the NtFHA1 FHA domain reduces cell growth in a specific phase of the cell cycle, aliquots of liquid cultures were analyzed by flow cytometry (Fig. 5). Aliquots were removed from growing cultures expressing the vector control or the NtFHA1 FHA domain before and 6 and 12 h after addition of galactose. Before and 6 h after addition of galactose, when the growth defect was not apparent, both cultures showed essentially identical cell cycle profiles; the majority of cells had a 2n DNA content (corresponding to G_2/M). However, induction of

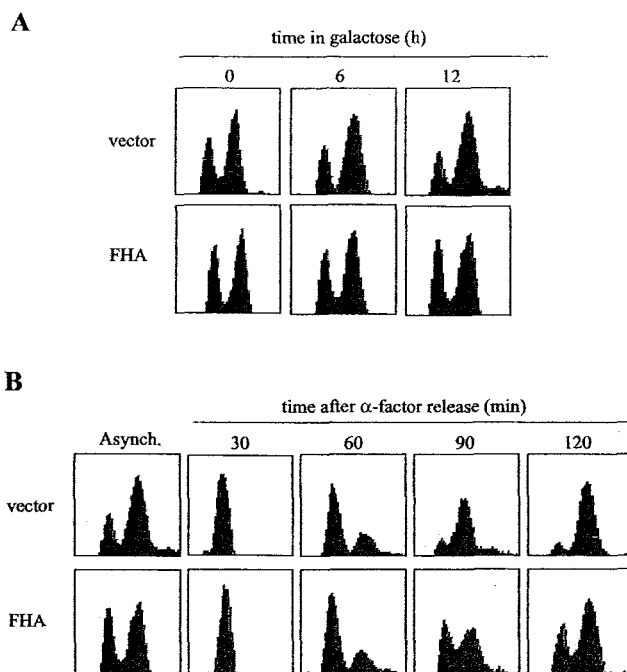


FIG. 5. Cell cycle analysis of growth defects in FHA domain-overexpressing yeast cells. *A*, 1-ml aliquots were removed from growing vector control- and FHA domain-expressing cultures (W303-1A background) in 4% galactose medium at the time points indicated and analyzed by flow cytometry. *B*, vector control and FHA constructs induced for 10 h in 4% galactose were diluted to 0.2 A units, synchronized in G_1 by α -factor, and released into galactose medium. Aliquots removed at the indicated times were analyzed by flow cytometry. *Asynch.*, asynchronized.

the NtFHA1 FHA domains for 12 h resulted in an increase in cells with a 1n DNA content. To determine whether the accumulation of cells in G_1 phase was the result of cell cycle arrest or slower G_1 -S transition, FHA domain-overexpressing and vector control cultures were synchronized in G_1 using α -factor and then released into fresh galactose medium. The majority of control cultures shifted to G_2/M within 120 min after α -factor release. However, yeast cells overexpressing the NtFHA1 FHA domain exhibited slower transition from G_1 to S phase after release from α -factor compared with the control cells. Thus, slow progression in the cell cycle is the reason for the growth retardation phenotype of the FHA domain-expressing yeast cultures. This result indicates that the FHA domain of NtFHA1 interacts with cellular components of yeast that influence progression of cell cycle.

FHA Domains of NtFHA1 and Yeast Fhl1 Are Interchangeable—The high sequence similarity between FHA domains of NtFHA1 and yeast Fhl1 indicates a possibility that the FHA domain of NtFHA1 may be able to interact with components involved in Fhl1 function in yeast cells. Supporting this possibility, overexpression of the constructs encoding either full-length Fhl1 or the FHA domain of Fhl1, both fused to the LexA DNA-binding domain, resulted in severe growth inhibition in yeast in 4% galactose (Fig. 6*A*). We tested whether simultaneous expression of Fhl1 with the FHA domain of NtFHA1 further amplifies the growth defect. In 1% galactose, growth of yeast strains expressing either Fhl1 or the NtFHA1 FHA domain was partially restored, but the growth of the strain expressing both constructs was restored to much lower levels (Fig. 6*A*). Thus, the FHA domain of the yeast Fhl1 transcription factor also influences yeast cell growth when overexpressed. The polypeptides of Fhl1 and the NtFHA1 FHA domain were detected by Western blot analysis using the anti-

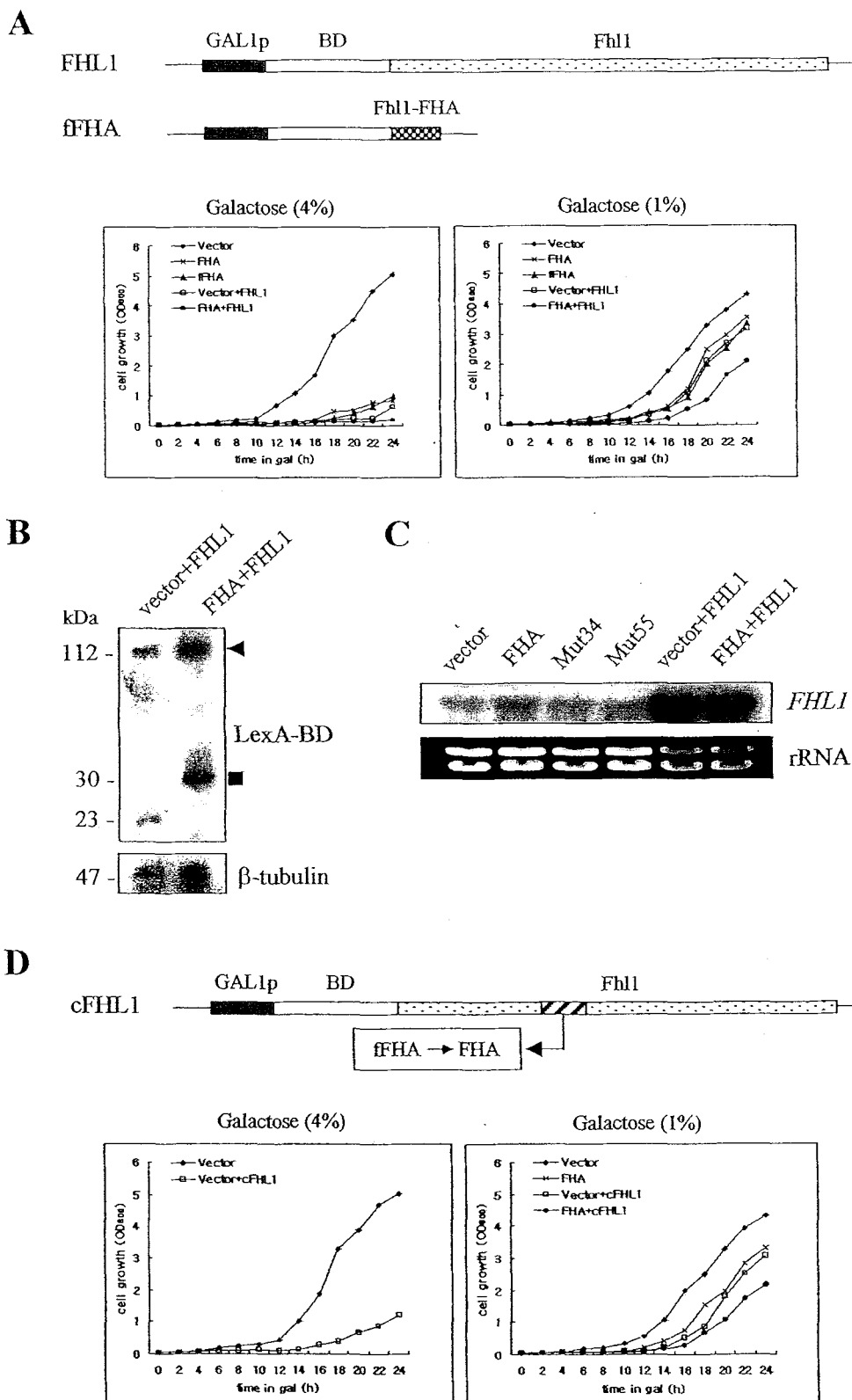


FIG. 6. Interchangeability between FHA domains of NtFHA1 and Fhl1. **A**, schematic diagrams of constructs for overexpression and yeast cell growth. Yeast strains containing various constructs separately or in combination were grown for 24 h in 2% sucrose and 1 or 4% galactose. *GAL1p*, *GAL1* promoter; *BD*, LexA DNA-binding domain. **B**, Western blot analysis of expression of Fhl1 and the FHA domain. 30 μ g of total proteins isolated from yeast cells grown to 0.8 A units in galactose were subjected to immunoblotting with the anti-LexA DNA-binding domain antibody (LexA-BD) and the anti- β -tubulin antibody. The arrowhead and filled square indicate the Fhl1 protein and the FHA domain, respectively. **C**, RNA gel blot analysis of *FHL1* mRNA expression. **D**, schematic diagrams of the chimeric Fhl1 construct (*cFHL1*) for overexpression and resulting yeast cell growth. Yeast strains containing various constructs separately or in combination were grown for 24 h in 2% sucrose and 1 or 4% galactose.

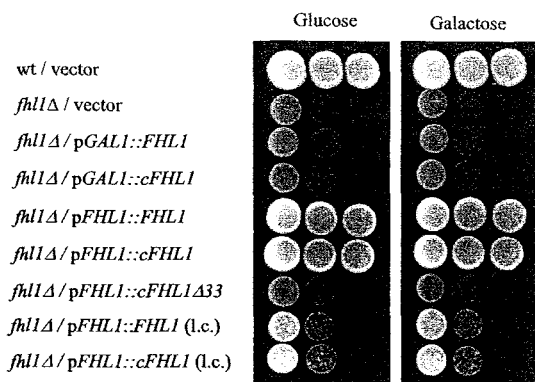


FIG. 7. Complementation of the yeast *fhl1* null mutation by chimeric Fhl1 containing the NtFHA1 FHA domain. The *FHL1* cDNA, chimeric Fhl1 containing the NtFHA1 FHA domain (*cFHL1*), and *cFhl1* with a deletion of 33 amino acids (Fig. 1D) in its NtFHA1 FHA domain (*cFHL1Δ33*) were fused under the control of either the *GAL1* or *FHL1* native promoter on a multicopy plasmid and introduced into the *fhl1* deletion mutant (W303 background). Complementation assay was also carried out with Fhl1 and *cFhl1* under the control of the *FHL1* promoter on a low copy plasmid (*l.c.*), pTS903CL (*CEN*, *LEU*). Cultures were grown to 0.8 A units, and 10 μ l were plated in a series of 10-fold dilutions on 2% glucose (left panel) and on 2% sucrose (right panel). *wt*, wild-type.

LexA antibody, and the results show that the Fhl1 protein was expressed at similar levels in strains expressing either FHL1 and the vector or FHL1 and FHA, standardized by the levels of β -tubulin (Fig. 6B). The *FHL1* mRNA levels were also similar in these strains, being expressed at a higher level compared with the strain that did not contain FHL (Fig. 6C). To test whether the FHA domains of NtFHA1 can replace the corresponding domain of Fhl1, the construct for chimeric Fhl1 in which its FHA domain was replaced with the NtFHA1 FHA domain (*cFhl1*) was introduced into yeast (Fig. 6D). Overexpression of *cFhl1* resulted in growth retardation, similar to Fhl1 expression. Simultaneous expression of chimeric Fhl1 and the NtFHA1 FHA domain additively inhibited yeast growth (Fig. 6D).

Complementation of the *fhl1* Deletion Mutation by Chimeric Fhl1 Containing the NtFHA1 FHA Domain—We further tested the functional similarity between the FHA domains of NtFHA1 and Fhl1 using a complementation assay (Fig. 7). *FHL1* is a nonessential gene in yeast, but its inactivation greatly impairs the growth of the mutant strains (3). The *fhl1* deletion mutant was constructed in the haploid W303 by replacing the open reading frame of the *FHL1* gene with a *HIS3* cassette. The cDNA fragments encoding wild-type Fhl1 and chimeric Fhl1 in which its FHA domain was replaced with the FHA domain of NtFHA1 (*cFhl1*) were fused with either the *GAL1* promoter or the native *FHL1* promoter on a multicopy plasmid. These recombinant plasmids were introduced into the yeast *fhl1Δ* mutant, and were examined whether expression of the chimeric Fhl1 protein could rescue the slow growth phenotype of the *fhl1Δ* mutant. Under the control of the *GAL1* promoter, neither Fhl1 nor *cFhl1* could restore the growth defect of the *fhl1Δ* mutant when their expression was induced by 2% galactose. This is probably due to the galactose-induced overexpression of the Fhl1 protein, which has been shown to inhibit yeast growth (Fig. 6A). However, expression of *cFhl1* by the *FHL1* promoter fully restored the growth of the mutant to a degree similar to expression of wild-type Fhl1 on a multicopy plasmid (Fig. 7). *cFhl1Δ33* (*cFhl1* with an internal deletion of 33 amino acids, residues 26–58 (Fig. 1D), including 4 of 6 conserved residues of the NtFHA1 FHA domain (Fig. 1D)) could not complement the *fhl1Δ* mutant phenotype when expressed under control of the

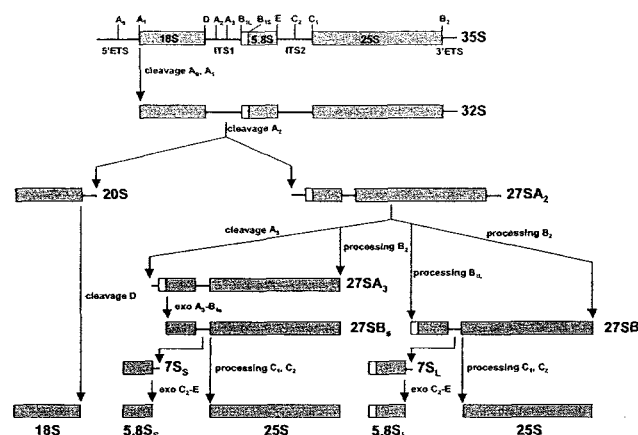


FIG. 8. Pre-rRNA processing in yeast. The structure and major sites of processing of the primary 35 S pre-rRNA are shown. The 5'- and 3'-external transcribed sequences (5'ETS and 3'ETS, respectively) flank the ends of the mature 18 S, 5.8 S, and 25 S rRNA sequences, which are separated by internal transcribed spacers ITS1 and ITS2. The 35 S pre-rRNA is cleaved in succession at sites A_0 and A_1 to generate 32 S pre-rRNA. The cleavage of 32 S pre-rRNA at site A_2 separates the two processing branches that lead to formation of mature rRNAs in the small and large ribosome subunits. The 20 S precursor is cleaved at site D after export to the cytoplasm, generating mature 18 S rRNA. The 27 SA₂ precursor undergoes processing via two alternative pathways to form the long and short forms of 5.8 S rRNA, and 25 S rRNA. The major pathway, which yields the 5.8 S_S form, proceeds through cleavage of 27 SA₂ at site A_3 and B_2 , giving rise to 27 SA₃, followed by exonucleolytic processing from site A_3 to site B_{1S} , which generates 27 SB_S pre-rRNA. In the minor pathway that leads to 5.8 S_L formation, 27 SB_L pre-rRNA is generated by processing at sites B_{1L} and B_2 . The subsequent processing of both 27 SB precursors at sites C_1 and C_2 gives rise to the mature 25 S rRNA and 7 S pre-rRNA. The 7 S pre-rRNA is trimmed by exonucleases from the 3'-end to site E, yielding mature 5.8 S rRNA.

FHL1 promoter, demonstrating that the NtFHA1 FHA domain is critical in *cFhl1* function for complementing the *fhl1Δ* mutant phenotype. Interestingly, both Fhl1 and *cFhl1* could only partially complement the slow growth phenotypes of the *fhl1Δ* mutant to the same degree on a low copy plasmid, indicating that *FHL1* gene expression is regulated by its position in the genome. Taken together, these results further demonstrate that the FHA domains of NtFHA1 and Fhl1 are interchangeable for normal function of Fhl1 in yeast.

Defective rRNA Processing in FHA Domain-overexpressing Yeast Cells—The Fhl1 protein is important for optimal growth and rRNA processing in yeast, leading to a reduced steady-state level of mature 25 S, 18 S, and 5.8 S rRNAs in the *fhl1* deletion mutant strain (3). We investigated whether the growth inhibition by overexpressing FHA domains of NtFHA1 and Fhl1 is related to impaired pre-rRNA processing in yeast by examining the steady-state levels of mature rRNA and pre-rRNA intermediates by Northern blot analysis (Figs. 8 and 9). To assess the levels of mature rRNA, 15 or 1.5 μ g of total RNA were loaded per lane, and the membrane was hybridized with probes corresponding to 25 S and 18 S rRNAs of yeast and, as controls, with tRNA^{Phe} and actin probes (Fig. 9A). Compared with the vector control (*wt* / *vector*), the wild-type yeast cultures overexpressing the NtFHA1 FHA domain (*wt* / *pGAL1::FHA*) or the Fhl1 FHA domain (*wt* / *pGAL1::fFHA*), the *fhl1Δ* mutant complemented with vector (*fhl1Δ* / *vector*), and the *fhl1Δ* mutant complemented with chimeric Fhl1 with deletion of 33 residues in the NtFHA1 FHA domain (*fhl1Δ* / *pFHL1::cFHL1Δ33*) all accumulated less amounts of 25 S and 18 S rRNAs (Fig. 9A), as quantified by the rRNA/tRNA and rRNA/actin mRNA ratios for each rRNA (data not shown). The *fhl1Δ* mutant complemented with *cFhl1* (*fhl1Δ* / *pFHL1::cFHL1*) restored the amounts of 25 S

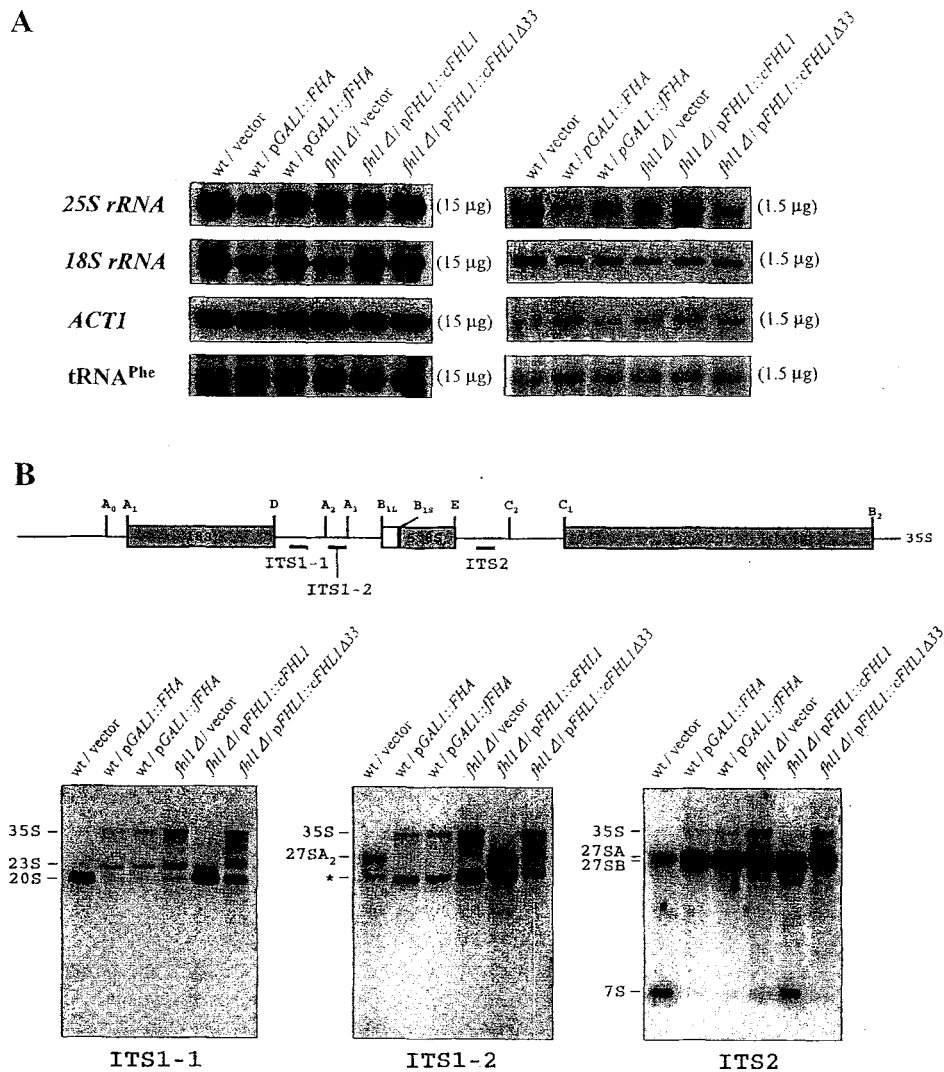


Fig. 9. RNA gel blot analysis of pre-rRNA processing. A, total RNA was extracted from wild-type yeast cells overexpressing the vector (*wt/vector*), the NtFHA1 FHA domain (*wt/pGAL1::FHA*), or the Fhl1 FHA domain (*wt/pGAL1::fFHA*) or from the *fhl1Δ* mutant complemented with vector (*fhl1Δ/vector*), the *fhl1Δ* mutant complemented with cFhl1 (*fhl1Δ/pFHL1::cFHL1*), or the *fhl1Δ* mutant complemented with chimeric Fhl1 with a deletion of 33 residues in the NtFHA1 FHA domain (*fhl1Δ/pFHL1::cFHL1Δ33*), all of which were grown in 2% galactose and 2% sucrose medium to 0.8 A units. The RNA gel blots containing 15 and 1.5 μg of total RNA/lane were hybridized with probes of 25 S rRNA, 18 S rRNA, actin (*ACT1*) mRNA, and tRNA^{Phe}. B, the positions of the ITS1-1 (5'-GAAACGGTTTTAATTGTCCTATAAC-3'), ITS1-2 (5'-TGTTACCTCTGGGCC-3'), and ITS2 (5'-GGCCAGCAATTCAAGTTA-3') oligonucleotide probes in the 35 S rRNA primary transcript are indicated. Northern blot hybridization was carried out using end-labeled ITS1-1, ITS1-2, and ITS2 probes corresponding to part of the ITS1 and ITS2 sequences of 35 S primary pre-rRNA. 15 μg of total RNA were used for each lane. The unidentified pre-rRNA intermediate detected by the ITS1-2 probe is indicated by the asterisk.

and 18 S rRNAs to the wild-type levels.

Three oligonucleotide probes to detect the accumulation of yeast pre-rRNA intermediates were synthesized: ITS1-1 and ITS1-2 (designed to bind to the internal transcribed spacer 1 of yeast pre-rRNA) and ITS2 (designed to bind to the internal transcribed spacer 2) (Fig. 9B) (18, 19). Total RNA was prepared from wild-type cells expressing the vector control, the NtFHA1 FHA domain, or the Fhl1 FHA domain or from the *fhl1Δ* mutant or the *fhl1Δ* mutant complemented with cFhl1 or cFhl1Δ33, all of which were collected from yeast cells grown to 0.8 A units in 2% galactose and 2% sucrose. When total RNA (15 μg) of wild-type control cells was fractionated by agarose gel electrophoresis and probed with ³²P-labeled ITS1-1, a major band of 20 S pre-rRNA was detected (Fig. 9B) (18, 19). However, yeast cells overexpressing the NtFHA1 FHA domain or the Fhl1 FHA domain and the *fhl1Δ* mutant exhibited high accumulation of 35 S pre-rRNA, but with much reduced levels

of 20 S pre-rRNA, indicating that the rRNA-processing steps from 35 S to 20 S pre-rRNA are significantly delayed in these cells. Additionally, they accumulated the 23 S pre-rRNA, which is considered an aberrant product formed by cleavage of 35 S pre-rRNA at site A₃, bypassing processing sites A₀–A₂, often observed when pre-rRNA processing is perturbed (18). The *fhl1Δ* mutant expressing cFhl1 restored the accumulation of 20 S pre-rRNA to the wild-type levels, whereas cFhl1Δ33 expression in the mutant resulted in accumulation of 35 S, 23 S, and 20 S pre-rRNAs, a mixture of the wild-type and *fhl1Δ* phenotypes.

With ³²P-labeled ITS1-2, two major bands were detected corresponding to 27 SA₂ pre-rRNA and an unidentified pre-rRNA, the size of which is slightly larger than the 20 S RNA (Fig. 9B) (18, 19). Overexpression of the FHA domains of NtFHA1 and Fhl1 resulted in high accumulation of 35 S and unidentified pre-rRNAs, with no visible accumulation of

the 27 SA₂ RNA, indicating that rRNA processing is significantly delayed (Fig. 9B). This pattern of pre-rRNA accumulation was very similar to that of the *fhl1Δ* mutant. Expression of cFhl1 under the control of the native *FHL1* promoter in the *fhl1Δ* mutant restored the pre-rRNA accumulation pattern to the pattern of wild-type, whereas expression of cFhl1Δ33 under the control of the *FHL1* promoter exhibited the same pattern of pre-rRNA processing as the *fhl1Δ* mutant.

When the ³²P-labeled ITS2 probe was used, the wild-type control showed bands corresponding to 27 SA/27 SB and 7 S pre-rRNAs, with no visible detection of 35 S RNA (Fig. 9, A and B) (18, 19). However, yeast cells overexpressing the FHA domains of NtFHA1 and Fhl1 exhibited increased levels of 35 S and 27 SA/27 SB pre-rRNAs and significantly decreased levels of 7 S pre-rRNA, similar to the pattern of the *fhl1Δ* mutation. Expression of cFhl1 in the *fhl1Δ* mutant restored the rRNA-processing pattern to that of wild-type, whereas the *fhl1Δ* mutant complemented with cFhl1Δ33 still showed the same pattern of pre-rRNA accumulation as the *fhl1Δ* mutant. Taken together, these results demonstrate that overexpression of the FHA domains of NtFHA1 and Fhl1 results in the same rRNA-processing defects as deletion of the *FHL1* gene. In these cells, RNA processing is defective in multiple steps, indicating that *FHL1* is involved in the general regulation of rRNA processing rather than being involved in a specific step of processing. Complementation of the *fhl1Δ* mutant by cFhl1 (but not by cFhl1Δ33) demonstrated that the intact FHA domain is critical for cFhl1 in controlling rRNA processing in yeast and that the FHA domain of NtFHA1 functionally substitutes for the corresponding domain of Fhl1 in yeast. These results also show that the cellular levels of Fhl1 are critical for normal function. The slow growth phenotypes of the FHA domain- or Fhl1-overexpressing cells and the *fhl1* deletion mutant are likely caused by defective rRNA processing and reduced accumulation of mature rRNAs.

DISCUSSION

NtFHA1 encodes a novel transcription activator in tobacco that contains the FHA domain, a highly diverse protein-protein interaction domain. There are two homologs of *NtFHA1* in *Arabidopsis*, the FHA domains of which show 91–94% sequence identity to the FHA domain of NtFHA1. In this study, we have shown that the FHA domain of NtFHA1 shares the conserved structure and function with the FHA domain of yeast Fhl1, regulating rRNA processing and cell growth in yeast, implying that its function in plant cells is similar to the function of the FHA domain of Fhl1 in yeast. The FHA domain was first identified in a group of forkhead transcription factors and has since been identified in many signaling proteins, including proteins kinases, protein phosphatases, proteases, kinesins, and zinc finger proteins in yeast and animals. This existence of FHA domains in a wide variety of proteins suggests that they are involved in many different cellular processes, although a specific cellular target of these FHA domain-containing proteins is largely unknown. In the plant kingdom, *Arabidopsis* contains 15 FHA domain-containing open reading frames, of which the biological function of only KAPP (7, 11) and zeaxanthin epoxidase (20, 21) has been characterized. Thus, the role of the FHA domain in those open reading frames is entirely unknown, except that the FHA domain of KAPP is involved in phosphorylation-dependent binding to multiple plant receptor-like kinases (12).

Our results demonstrate that overexpression of the FHA domain of NtFHA1 causes a severe growth defect in yeast by slowing down the G₁-S transition in the cell cycle, similar to the result of overexpression of Fhl1, its FHA domain, or chimeric Fhl1 containing the NtFHA1 FHA domain instead of its own.

The growth defect phenotype is associated with defective rRNA processing and reduced rRNA accumulation, as shown by the RNA gel blot analysis using oligonucleotide probes corresponding to internal transcribed spacers 1 and 2 (Fig. 9). The results demonstrate that multiple steps of rRNA processing are defective in the FHA domain-overexpressing yeast cells, including processing from 35 S to 20 S pre-rRNA, from 35 S to 27 SA₂ pre-rRNA, and from 27 SA₃/27 SB_{1S}/27 SB_{1L} to 7 S pre-rRNA and 25 S mature rRNA, and that these defects exactly match those of the *fhl1Δ* mutant (Fig. 9). Our results are also consistent with the results of Hermann-Le Denmat *et al.* (3), who observed accumulation of 35 S and 27 S pre-rRNAs in the *fhl1Δ* mutant by pulse-chase labeling. Based on our results, Fhl1 seems to be involved in an overall regulation of rRNA processing, controlling multiple steps. In addition, the defects we have seen here do not lead to complete blockage of rRNA processing, unlike many mutants in which accumulation of 35 S pre-rRNA and the aberrant 23 S species is often associated with complete depletion of 18 S and 25 S/5.8 S mature rRNAs (22–24). This delayed as well as defective processing of pre-rRNAs apparently contributes to the reduced accumulation of both 18 S and 25 S mature rRNAs and the slower growth rate of the FHA domain-overexpressing cells and the *fhl1Δ* mutant.

Chimeric Fhl1 driven by the native *FHL1* promoter could rescue the slow growth phenotype and defective rRNA processing of the yeast *fhl1Δ* mutant, whereas deletion of 33 amino acids containing 4 conserved residues of the FHA domain from cFhl1 completely abolished the complementing activity. Thus, the intact NtFHA1 FHA domain in cFhl1 is absolutely required for rescuing the *fhl1Δ* mutant phenotypes. These results also demonstrate that the NtFHA1 FHA domain mimics the function of the FHA domain of Fhl1 in yeast, probably interacting with cellular components involved in regulation of rRNA processing. The *FHL1* gene was originally isolated as a multicopy suppressor of RNA polymerase III mutations and later recloned as a multicopy suppressor of a mutation of RNA polymerase III transcription factor IIIC (3). Thus, the Fhl1 protein plays a role in the control of RNA polymerase III transcription and rRNA maturation, presumably by acting as a transcription regulator of genes specifically involved in these processes.

Fhl1 was found to genetically interact with Ifh1, a 122-kDa protein with no homology to any proteins in the data base (25). Partial deletion of Ifh1 led to a slow growth phenotype with impaired pre-rRNA processing, similar to the *fhl1* mutation. A full deletion of Ifh1 was lethal, but growth was restored in a strain deleted for both Ifh1 and Fhl1. Thus, Ifh1 is essential for growth, but only in the presence of a functional Fhl1 protein. Based on these data, a model was proposed in which Fhl1 is converted from a transcription repressor to an activator upon binding of Ifh1 (25). The phenotypes of yeast cells overexpressing Fhl1 observed in this study are consistent with the model; the growth defect phenotype may be caused by excessive production of Fhl1 repressors when Ifh1 is limited.

We have shown that NtFHA1 is targeted to the nucleus and has a transactivation activity; yet NtFHA1, AtFHA1, and AtFHA2 lack an obvious DNA-binding domain in their sequences, which separates them from other forkhead transcription factors in yeast and mammals. An intriguing possibility is that NtFHA1 interacts with other protein molecules with a DNA-binding domain to make a functional transcription complex. Obvious candidates would be protein factors containing the forkhead DNA-binding domain; however, no protein in the plant data base has been identified to contain the forkhead domain. Fkh2, a yeast forkhead transcription factor, forms a transcription complex with the MADS box protein Mcm1 to control cell cycle periodicity of *SWI5* and *CLB2* gene expression

(26, 27). Identifying interacting partners of NtFHA1 would give an insight into understanding the function of this group of plant transcription regulators.

The slow growth phenotype caused by overexpression of the FHA domain requires an intact FHA domain because mutation of the conserved residues of the FHA domain (Arg-34 and Ser-55) abolishes the phenotype (Fig. 5). Furthermore, deletion of 33 residues containing 4 conserved residues of the FHA domain from cFhl1 diminishes its ability to complement the growth and rRNA-processing defects of the *fhl1Δ* mutant, indicating that the FHA domain plays a critical role in the regulation of rRNA processing. Recently, overexpression of the N-terminal FHA domain (FHA1) of Rad53 resulted in growth retardation of yeast cells due to G₁ arrest of the cell cycle, and the phenotype was abrogated by mutation of the conserved residues (28). These residues were critical for phosphopeptide binding of the Rad53 FHA1 domain, and replacement of the RAD53 gene with alleles containing mutations in the FHA1 domain resulted in an increased DNA damage sensitivity *in vivo* (28). Thus, the FHA1 domain contributes to the checkpoint function of Rad53, possibly by associating with a phosphorylated target protein in response to DNA damage in G₁. In the same way, the conserved residues of the NtFHA1 FHA domain, including Arg-34 and Ser-55, may constitute binding sites for phosphorylated target proteins. The target proteins for the FHA domains of Fhl1 and NtFHA1 are currently unidentified, but components of the transcription machinery involved in RNA polymerase III transcription and rRNA processing are likely candidates, given the function of Fhl1 in those processes.

Reduced accumulation of mature rRNAs in FHA domain- and Fhl1-overexpressing yeast cells is a likely reason for delayed progression from G₁ to S phase during the cell cycle. It will be interesting to probe the molecular mechanism by which the defects in rRNA processing in these cells lead to delayed G₁-S transition. It is known that cells can delay or block cell cycle transitions in response to perturbations in a variety of intracellular processes, including ribosome biogenesis. However, the nature of the connection between the cell cycle and ribosome biogenesis has remained unknown. Recently, overexpression of a dominant-negative form of Bop1 (Bop1Δ), a novel nucleolar protein involved in rRNA processing and 60 S ribosome biogenesis, resulted in cell cycle arrest (29). Subsequently, it was found that the p53-dependent signaling pathway connects Bop1Δ-driven aberrant rRNA processing/ribosome biogenesis to cell cycle arrest (30). These results provide clear evidence that the signal transmitted to the cell cycle machinery is generated by a mechanism that monitors ribosome production in the nucleolus. Plant cells likely possess a similar checkpoint mechanism to respond to nucleolar stress such as perturbations in ribosome biosynthesis. Although the functions of NtFHA1 in plant cells remain to be revealed, the conserved nature of the FHA domains of NtFHA1 and Fhl1 indicates a possibility that NtFHA1 is involved in regulation of RNA polymerase III transcription and rRNA processing in

plant cells, possibly through assembly of a functional transcription complex by interacting with other transcription factors. Molecular analysis of transcription and rRNA processing in transgenic or mutant plant cells in which *NtFHA1* expression is blocked would give a clear idea of NtFHA1 function in plants. In addition, identifying the NtFHA1-interacting proteins may yield a new insight into the action mechanism of NtFHA1.

Acknowledgments—We thank Dr. Jae-Gu Pan and Su-Min Ko (GenoFocus, Inc.) for fluorescence-activated cell sorter analysis, Dr. Inhwan Hwang (POSTECH) for *in vivo* targeting of NtFHA1, and Dr. Soon-Chun Jeong (Korea Research Institute of Bioscience and Biotechnology) for helpful comments on the manuscript.

REFERENCES

- Durocher, D., Henckel, J., Fersht, A. R., and Jackson, S. P. (1999) *Mol. Cell* **4**, 387–394
- Weigel, D., Jurgens, G., Kuttner, F., Seifert, E., and Jackle, H. (1989) *Cell* **57**, 645–658
- Hermann-Le Denmat, S., Werner, M., Sentenac, A., and Thuriaux, P. (1994) *Mol. Cell. Biol.* **14**, 2905–2913
- Zhu, G., Muller, E. G., Amacher, S. L., Northrop, J. L., and Davis, T. N. (1993) *Mol. Cell. Biol.* **13**, 1779–1787
- Zhu, G., Spellman, P. T., Volpe, T., Brown, P. O., Botstein, D., Davis, T. N., and Futcher, B. (2000) *Nature* **406**, 90–94
- Hollenhorst, P. C., Bose, M. E., Mielke, M. R., Muller, U., and Fox, C. A. (2000) *Genetics* **154**, 1533–1548
- Hofmann, K., and Bucher, P. (1995) *Trends Biochem. Sci.* **20**, 347–349
- Li, J., Lee, G.-I., Van Doren, S. R., and Walker, J. C. (2000) *J. Cell Sci.* **113**, 4143–4149
- Zheng, P., Fay, D. S., Burton, J., Xiao, H., Pinkham, J. L., and Stern, D. F. (1993) *Mol. Cell. Biol.* **13**, 5829–5842
- Moras, D. (1993) *Nature* **364**, 572–573
- Stone, J. M., Collinge, M. A., Smith, R. D., Horn, M. A., and Walker, J. C. (1994) *Science* **266**, 793–796
- Li, J., Smith, G. P., and Walker, J. C. (1999) *Proc. Natl. Acad. Sci. U. S. A.* **96**, 7821–7826
- Liao, H., Yuan, C., Su, M.-I., Yongkiettrakul, S., Qin, D., Li, H., Byeon, I.-J. L., Pei, D., and Tsai, M.-D. (2000) *J. Mol. Biol.* **304**, 941–951
- Durocher, D., Taylor, I. A., Sarbassova, D., Haire, L. F., Westcott, S. L., Jackson, S. P., Smerdon, S. J., and Yaffe, M. B. (2000) *Mol. Cell* **6**, 1169–1182
- Higuchi, R. (1990) in *PCR Protocols* (Innis, M. A., Gelfand, D. H., Sninsky, J. J., and White, T. J., eds) pp. 177–183, Academic Press, New York
- Reichheld, J.-P., Chaubet, N., Shen, W. H., Renaudin, J.-P., and Gigot, C. (1996) *Proc. Natl. Acad. Sci. U. S. A.* **93**, 13819–13824
- Lee, Y. J., Kim, D. H., Kim, Y.-W., and Hwang, I. (2001) *Plant Cell* **13**, 2175–2190
- Pestov, D. G., Stockelman, M. G., Strezoska, Z., and Lau, L. F. (2001) *Nucleic Acids Res.* **29**, 3621–3630
- de la Cruz, J., Kressler, D., Tollervey, D., and Linder, P. (1998) *EMBO J.* **17**, 1128–1140
- Venema, J., and Tollervey, D. (1995) *Yeast* **11**, 1629–1650
- Sun, C., and Woolford, J. L., Jr. (1994) *EMBO J.* **13**, 3127–3135
- Weaver, P. L., Sun, C., and Chang, T. H. (1997) *Mol. Cell. Biol.* **17**, 1354–1365
- Audran, C., Borel, C., Frey, A., Sotta, B., Meyer, C., Simonneau, T., and Marion-Poll, A. (1998) *Plant Physiol.* **118**, 1021–1028
- Burbidge, A., Grieve, T., Terry, C., Corlett, J., Thomson, A., and Taylor, I. (1997) *J. Exp. Bot.* **48**, 1749–1750
- Cherel, I., and Thuriaux, P. (1995) *Yeast* **11**, 261–270
- Pic, A., Lim, F.-L., Ross, S. J., Veal, E. A., Johnson, A. L., Sultan, M. R. A., West, A. G., Johnston, L. H., Sharrocks, A. D., and Morgan, B. A. (2000) *EMBO J.* **19**, 3750–3761
- Koranda, M., Schleiffer, A., Endler, L., and Ammerer, G. (2000) *Nature* **406**, 94–98
- Pike, B. L., Hammet, A., and Heierhorst, J. (2001) *J. Biol. Chem.* **276**, 14019–14026
- Strezoska, Z., Pestov, D. G., and Lau, L. F. (2000) *Mol. Cell. Biol.* **20**, 5516–5528
- Pestov, D. G., Strezoska, Z., and Lau, L. F. (2001) *Mol. Cell. Biol.* **21**, 4246–4255

A novel dual-specificity protein kinase targeted to the chloroplast in tobacco¹

Hye Sun Cho^a, Gyeong Mee Yoon^{a,2}, Sang Sook Lee^a, Young A. Kim^b, Inhwan Hwang^b, Doil Choi^a, Hyun-Sook Pai^{a,*}

^aPlant Cell Biotechnology Laboratory, Korea Research Institute of Bioscience and Biotechnology, P.O. Box 115, Yusong, Taejeon 305-600, South Korea

^bDivision of Molecular and Life Sciences, POSTECH, Pohang 790-784, South Korea

Received 26 February 2001; revised 23 April 2001; accepted 23 April 2001

First published online 8 May 2001

Edited by Ulf-Ingo Flügge

Abstract The *NtDSK1* cDNA encoding a novel chloroplast-targeted protein kinase was identified in *Nicotiana tabacum*. It contains the kinase domain at the C-terminus and a putative regulatory domain at the N-terminus. The recombinant NtDSK1 underwent autophosphorylation of serine, threonine, and tyrosine residues, indicating that *NtDSK1* encodes a functional dual-specificity protein kinase. The NtDSK1–green fluorescent protein fusion protein was targeted to chloroplasts. Furthermore, the NtDSK1 protein was immunodetected in chloroplast fractions isolated from tobacco seedlings. The *NtDSK1* mRNA expression was developmentally regulated in different tissues, including anthers and germinating seeds, and strongly stimulated by gibberellin. The mRNA was rapidly light responsive during seedling growth. NtDSK1 may play a role in a light-regulated signaling process in tobacco. © 2001 Published by Elsevier Science B.V. on behalf of the Federation of European Biochemical Societies.

Key words: Chloroplast-targeted; Dual-specificity protein kinase; Light- and gibberellin-stimulated expression; NtDSK1; Tobacco

1. Introduction

Protein kinases comprise the largest known family of proteins. Various cellular processes are controlled by phosphorylation of proteins on tyrosine and serine/threonine residues, carried out by protein tyrosine kinases and protein serine/threonine kinases. Dual-specificity protein kinases are a group of protein kinases which are able to phosphorylate both tyrosine and serine/threonine residues [1]. In plants, characterization of dual-specificity protein kinases that do not belong to the MAP kinase kinase family is restricted to ADK1 from *Arabidopsis* [2], PRK1 from petunia [3], and PK12 from tobacco [4]. PRK1 is a predominantly pollen-expressed receptor-like kinase which autophosphorylates on serine and tyrosine [3]. PRK1 has been shown to play an essential role in pollen and embryo sac development in *Petunia inflata* [5,6].

PK12 is a member of the LAMMER kinases. PK12 activity is rapidly and transiently increased when plants are treated with ethylene [4]. The PK12 kinase phosphorylates serine/arginine-rich (SR) splicing factors in vivo to alter their activity and the splicing of target mRNAs [7]. ADK1 was isolated by screening an *Arabidopsis* expression library with anti-phosphotyrosine antibodies. ADK1 autophosphorylated serine, threonine, and tyrosine residues and was also capable of phosphorylating tyrosine residues on poly(Glu/Tyr) as a substrate. However, the function of ADK1 is unknown [2].

In this study, we attempted to isolate kinase cDNAs that are preferentially expressed in the tobacco anthers. As a result, a cDNA encoding a novel dual-specificity protein kinase targeted to chloroplasts was obtained. The cDNA was designated *NtDSK1* (*Nicotiana tabacum* dual-specificity kinase 1). This is the first dual-specificity protein kinase that is localized in chloroplasts. *NtDSK1* mRNA expression was stimulated by gibberellin (GA), by light, and during various developmental processes including seed germination. The possible function of NtDSK1 is discussed based on these results.

2. Materials and methods

2.1. Plant materials

Tobacco plants (*N. tabacum* cv. Xanthi) were cultivated in a greenhouse under a regime of 16 h light and 8 h dark.

2.2. Autophosphorylation and phosphoamino acid analysis

A PCR product corresponding to the kinase domain (residues 294–610) of NtDSK1 was obtained using Pwo DNA polymerase (Boehringer-Mannheim, Germany). It was subcloned into the pET32a vector (Novagen, USA) using *Bam*HI/*Sal*I sites. The construct was introduced into *Escherichia coli* in order to express the kinase domain fused to the C-terminus of thioredoxin. After purification using nickel resin (New England Biolabs, UK), the fusion protein was digested with thrombin for 12 h at 4°C to remove the thioredoxin moiety. Autophosphorylation assays and phosphoamino acid analyses were carried out according to [8].

2.3. Subcellular localization of the *NtDSK1*–green fluorescent protein (GFP) protein

The *NtDSK1* cDNA corresponding to amino acid residues 1–610 was PCR-amplified using Pwo DNA polymerase to generate *Bam*HI sites at both the 5' and 3' ends. This PCR-amplified DNA was cloned into the CD3-326 plasmid using *Bam*HI sites to generate pNtDSK1-soluble modified (sm) GFP, which contained NtDSK1–smGFP in-frame fusion under the control of the cauliflower mosaic virus 35S promoter. The pNtDSK1–smGFP and control CD3-326 plasmids were introduced into protoplasts prepared from *Arabidopsis* seedlings by polyethylene glycol treatment as described in [9]. After 16 h incubation, the protoplasts were viewed under a fluorescence microscope.

*Corresponding author. Fax: (82)-42-860-4608.
E-mail: hyunsook@mail.kribb.re.kr

¹ EMBL accession number: AF106957.

² Present address: Department of Horticulture, Washington State University, Pullman, WA 99164-6414, USA.

plasts were gently suspended in the same buffer with a fine brush. The volume was increased to 30 ml, the suspension was transferred to sterile Corax tubes, and chloroplasts were pelleted at $3000\times g$ for 5 min. The chloroplast fraction was examined under a light microscope. Protein concentration was measured by the Bradford method [11] using the Bio-Rad protein assay kit and BSA as the standard.

2.5. Immunoblotting

The NtDSK1-specific polyclonal rabbit antibody was prepared using the recombinant regulatory domain of NtDSK1 in Iyhyo Biotech (Kwangju, South Korea). Immunoblotting was carried out as described in [12]. Nitrocellulose membranes containing 10 μ g each of the total proteins from uninduced (UI) and induced (I) *E. coli* cells that carry pMAL plasmid (New England Biolabs, UK) containing NtDSK1 regulatory domain, or 70 μ g each of proteins from chloroplast fractions and the supernatant containing non-chloroplastic materials isolated from tobacco seedlings were prepared. The membranes were blocked with 5% skim milk in Tris-buffered saline and 0.05% Tween 20 (TBST), reacted with anti-NtDSK1 antibody (1:2000 dilution) in TBST, and washed with TBST. They were then reacted with horseradish peroxidase-conjugated goat anti-rabbit IgG secondary antibody (1:5000 dilution; Amersham, USA), and the signal was detected by ECL+Plus (Amersham, USA).

3. Results and discussion

3.1. Isolation of a cDNA clone encoding a protein kinase in *N. tabacum*

Reverse transcription-PCR with degenerate kinase primers [8] and the subsequent screening of a tobacco flower cDNA library with one of the PCR-amplified DNA fragments resulted in isolation of a cDNA clone, designated *NtDSK1*. Among four independent clones obtained, the longest cDNA was 2414 bp in length and encoded a protein of 610 amino acids with the structural features of a protein kinase (Fig. 1A,B). Its predicted molecular weight was 68 870 Da. The N-terminal region of NtDSK1 (residues 1–293) contained a novel sequence that did not show any significant sequence similarity with proteins in the plant database. This region may constitute a regulatory domain that modulates the kinase activity of NtDSK1. The C-terminal region contained 12 conserved subdomains of eukaryotic protein kinases (Fig. 1B). Fifteen invariant amino acid residues for protein kinases were conserved in the kinase domain of NtDSK1, with the exception of one glycine residue that was replaced by alanine in NtDSK1 (Ala299 in subdomain I). The amino acid sequence of this clone was analyzed by SMART comparative sequence analysis (<http://coot.embl-heidelberg.de/smart-103/>), and was predicted to encode a dual-specificity protein kinase.

The amino acid sequence of NtDSK1 and comparison of the sequence with other plant kinases using the CLUSTAL W multiple sequence alignment program (version 1.7: <http://dot.imgen.bcm.tmc.edu:9331/multi-align/>) are shown in Fig. 1B. The kinase domain of NtDSK1 is most closely related to the kinase domains of TMK1 [13] from *Arabidopsis* (44% identity), SRK-910 [14] from *Brassica* (37% identity), and BRII [15] from *Arabidopsis* (36% identity). BRII and TMK1 both belong to the group of LRR receptor-like kinases that contain leucine-rich repeats in their extracellular domain, while SRK-910 belongs to the SRK class of receptor-like kinases that contain SLG-like sequences in the extracellular domain.

3.2. *NtDSK1* encodes a functional dual-specificity protein kinase

In order to determine if NtDSK1 encodes a functional dual-

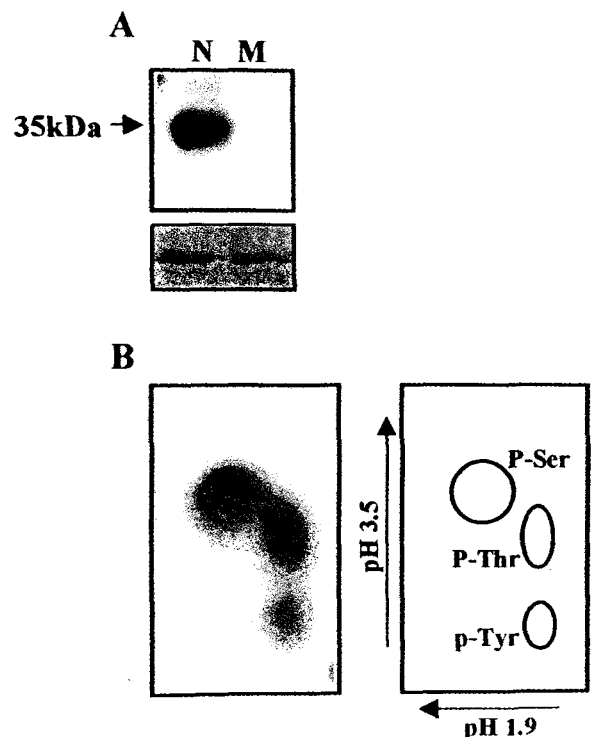


Fig. 2. Phosphorylation of the recombinant kinase domain of NtDSK1. A: Autophosphorylation. Top: autoradiography; bottom: a Coomassie blue-stained gel showing relative amounts of the recombinant proteins. Normal (N) and mutant (M) forms of the kinase domain are indicated. In the mutant kinase the essential ATP binding site Lys320 was mutated to Asn. B: Phosphoamino acid analysis of the autophosphorylated NtDSK1. The 32 P-labeled kinase domain was hydrolyzed with HCl and subjected to two-dimensional thin-layer electrophoresis. The positions of phosphoserine, phosphothreonine, and phosphotyrosine are indicated.

specificity protein kinase, an autophosphorylation assay was performed with the recombinant kinase domain (residues 294–610) of NtDSK1. After removal of the thioredoxin moiety by thrombin, the resulting kinase domain was assayed for autophosphorylation. A single 35-kDa band was detected by autoradiography (Fig. 2A), the position of which matched to that of the kinase domain, as determined by Coomassie blue staining. In order to determine if autophosphorylation requires an active kinase, the mutant form of the kinase domain, which carries a mutation in the essential ATP binding site (Lys320 to Asn), was prepared in the same way and was analyzed for kinase activity. The mutation drastically reduced radiolabeling of the 35-kDa band, indicating that autophosphorylation activity is dependent on a functional kinase (Fig. 2A). To study the specificity of kinase activity, the phosphoamino acid analysis was carried out (Fig. 2B). Major 32 P-labeled spots corresponded to the positions of phosphoserine, phosphothreonine, and phosphotyrosine, indicating that NtDSK1 possesses dual-specificity kinase activity.

3.3. Genomic DNA gel blot of *NtDSK1*

DNA gel blot analysis was performed with tobacco genomic DNA digested with restriction enzymes (Fig. 3). The probe was the 0.4-kb PCR fragment corresponding to the C-terminal region of NtDSK1. With the probe, both *EcoRI* and *HindIII* digestion resulted in two hybridizing bands. Con-

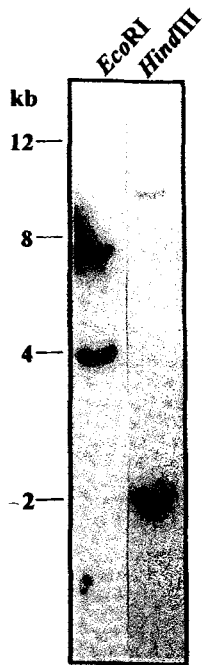


Fig. 3. Genomic DNA gel blot analysis of the *NtDSK1* gene. Each lane contains 10 µg of plant genomic DNA digested with restriction enzymes. DNA preparation, prehybridization, hybridization, and washing were carried out as described in [8]. DNA markers are indicated in kb.

sidering that *N. tabacum* is amphidiploid between *Nicotiana tomentosiformis* and *Nicotiana sylvestris*, these results indicate that the tobacco genome contains a single copy of the *NtDSK1* gene (Fig. 3).

3.4. *NtDSK1* mRNA accumulation is developmentally regulated and strongly stimulated by gibberellin

Using RNA gel blot analysis, a 2.6-kb transcript was detected at a low level in leaves, stems and flowers, but in roots the transcripts were barely detectable (Fig. 4A). The size of the transcript was consistent with the size of the isolated cDNA. During flower development, the *NtDSK1* mRNA

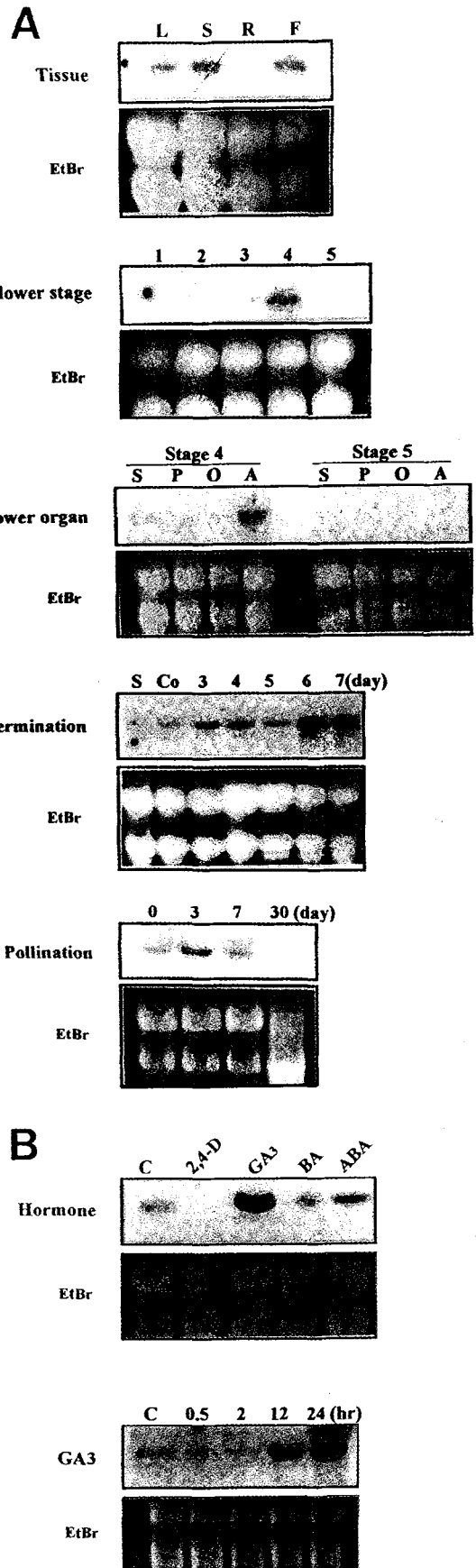


Fig. 4. Expression of the *NtDSK1* mRNA. RNA preparation, prehybridization, hybridization, and washing were carried out as described in [8]. The 0.4-kb PCR fragment corresponding to the C-terminal end of the *NtDSK1* cDNA was used as a probe. Each lane contains 100 µg of total RNA. A: Expression in plant tissues at different developmental stages. (Tissue-specific expression) roots (R), stems (S), leaves (L), and flowers (F); (expression during flower development) stage 1, <1 cm buds; stage 2, 1–2 cm; stage 3, 2–3 cm; stage 4, 3–4 cm; stage 5, open flowers; (expression in floral organs) sepals (S), petals (P), pistils (O), and anthers (A); (expression during germination) mature seeds (S), 3-day cold-treated seeds (Co), and water-imbibed seeds for the indicated time (3–7 days) after 3-day cold treatment; (expression after pollination) ovaries before anthesis (0), and ovaries at 3, 7, and 30 days after pollination are indicated. B: Expression of the *NtDSK1* mRNA in response to GA. Top: young tobacco leaves were cut and their petioles were put into hormone solutions at 100 µM of auxin (2,4-D), abscisic acid (ABA), GA (GA₃), and cytokinin (BA) for 12 h. Control leaves were treated with water in the same manner. Bottom: petioles were put into GA₃ solution (100 µM) for indicated times.

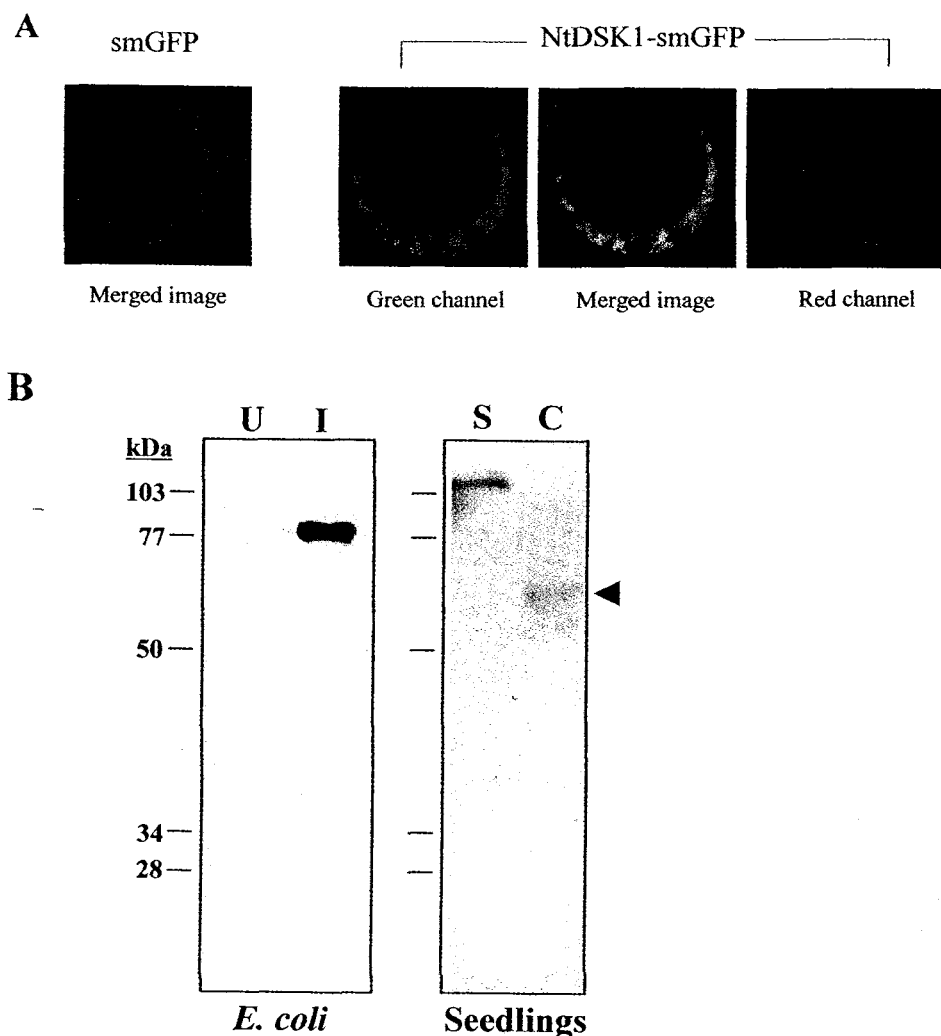


Fig. 5. Subcellular localization of the NtDSK1 protein. A: Localization of the NtDSK1-smGFP fusion protein. B: Immunodetection of the NtDSK1 protein in the chloroplast fractions. Left: protein extracts from uninduced (U) and induced (I) *E. coli* cells that carry the pMAL-NtDSK1 plasmid were subjected to immunoblotting with the NtDSK1 antibody. The fusion protein between maltose binding protein and NtDSK1 regulatory domain was detected only after induction. Right: proteins of chloroplast (C) and supernatant (S) fractions prepared from tobacco seedlings were subjected to immunoblotting with the antibody. The putative NtDSK1 protein is marked with the arrowhead.

was most highly expressed in stage 4 (just prior to anthesis). In stage 4 *NtDSK1* mRNA was predominantly expressed in the anther. Mature seeds contained a barely detectable level of the *NtDSK1* mRNA, but the mRNA levels increased after 3 days of cold treatment and kept increasing up to 7 days of imbibition. Just before anthesis the ovaries contained a low level of *NtDSK1* mRNA, but the level increased at 3 days after pollination, then decreased to a barely detectable level at 30 days (Fig. 4A).

Next we examined changes in the *NtDSK1* mRNA level in response to various stimuli (Fig. 4B). GA (GA_3) treatment resulted in strong induction of *NtDSK1* expression. Abscisic acid and cytokinin did not affect the transcript level significantly, while auxin treatment reduced the mRNA level. GA_3 at the concentration of 10–100 μM was effective in stimulating *NtDSK1* mRNA expression (results not shown). GA_3 (100 μM) treatment caused an increased transcript level at 12 h after treatment, which was maintained until 24 h after treatment (Fig. 4B).

3.5. Localization of the NtDSK1 protein in chloroplasts

Cellular localization of NtDSK1 was examined by constructing a fusion protein between NtDSK1 and a GFP (NtDSK1-smGFP). After transient expression of DNA constructs, encoding NtDSK1-smGFP or smGFP, an individual protoplast was examined under a fluorescence microscope. In contrast to the cytosol-localized staining pattern of smGFP, fluorescence of the NtDSK1-smGFP protein was associated with chloroplasts, indicating that NtDSK1 is primarily targeted to the chloroplast (Fig. 5A).

We further investigated localization of NtDSK1 in the chloroplast using immunoblotting. Polyclonal rabbit antiserum was raised using the recombinant regulatory domain of NtDSK1. After purification, the antiserum specifically recognized the fusion protein between the maltose binding protein and the NtDSK1 regulatory domain from *E. coli* total proteins, only after induction (Fig. 5B, left). Crude chloroplast fractions and the supernatant containing non-chloroplastic materials were prepared from tobacco seedlings. The antise-

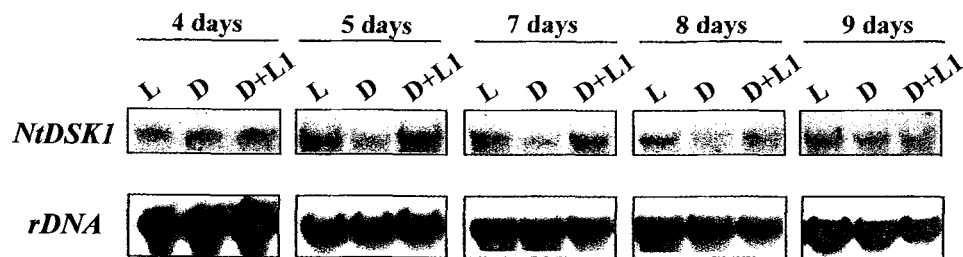


Fig. 6. Light-stimulated expression of *NtDSK1*. RNA gel blot analysis was carried out with RNA from 4–9-day-old tobacco seedlings grown for indicated times after 3-day cold treatment under continuous light (L), under dark (D), or grown under dark and then transferred to the light for 1 h (D+L1). The 0.4-kb *NtDSK1* probe and the ribosomal DNA probe were used.

rum detected a single protein of approximately 65 kDa in the chloroplast fraction (Fig. 5B, right), while a protein of approximately 120 kDa was detected in the supernatant. Pre-immune serum did not detect any signal (results not shown). Based on the expected size of NtDSK1 and localization of the NtDSK1–GFP protein in the chloroplast, the 65-kDa protein in the chloroplast fraction likely represents NtDSK1. The 120-kDa protein detected in the supernatant may be a NtDSK1-unrelated protein containing similar epitopes.

3.6. *NtDSK1* expression is rapidly stimulated by light

Using RNA gel blot analysis, *NtDSK1* mRNA levels were examined in 4–9-day-old tobacco seedlings grown on MS media under continuous light, under dark, or grown under dark and then transferred to the light for 1 h (Fig. 6). In 5–8-day-old seedlings, the *NtDSK1* mRNA level was lower in dark-grown seedlings than light-grown seedlings, but exposure to light for 1 h after the dark-grown period increased the *NtDSK1* mRNA level to the level of light-grown seedlings. Interestingly, there was no visible difference in the mRNA levels between light- and dark-grown seedlings at 4 days of growth when cotyledons were not fully opened, and at 9 days of growth. The results indicate that *NtDSK1* expression is rapidly stimulated by light, but to different degrees depending on the growth stage.

Using NtDSK1–GFP fusion and immunoblotting with the NtDSK1 antibody (Fig. 5A,B), it has been shown that the NtDSK1 protein is targeted to the chloroplast. The number and identity of the protein kinases and phosphatases localized in chloroplasts are still unclear. NtDSK1 is the first dual-specificity protein kinase targeted to chloroplasts. In chloroplasts, light-driven redox reactions provide signals for self-regulation of photosynthetic electron flow, regulating energy transfer via reversible phosphorylation of LHCII antenna [16]. More recent data suggest that redox-controlled protein phosphorylation in chloroplasts has a much wider physiological significance as exemplified by its involvement in the regulation of gene expression and stress-related responses [17]. *NtDSK1* mRNA accumulation is stimulated by light (Fig. 6) and H₂O₂ treatment (Cho and Pai, unpublished) in tobacco seedlings, implicating a role of NtDSK1 in light-induced stress responses.

Alternatively, NtDSK1 may be involved in GA signal transduction. GAs regulate various cellular processes, including seed germination, internode elongation, mobilization of seed reserves in cereals, seed development, and anthocyanin biosynthesis [18,19]. The expression patterns of the *NtDSK1* mRNA during plant development and upon GA treatment

indicate that expression of *NtDSK1* may be regulated by changes of endogenous GA levels in tobacco. The GA content increases during seed germination and the initial stage of seed development [18,20]. GA levels also increase in stamens prior to anthesis in a number of species [21]. NtDSK1 may be an example of a signaling component whose expression is up-regulated by the corresponding signals. GA response of plants is influenced by light [22]. Previous studies have suggested that light enhances both GA biosynthesis and tissue sensitivity to GA in various plant species [22,23]. NtDSK1 may mediate cross-talk between light and GA signal transduction. Interestingly, copalyl diphosphate synthase and *ent*-kaurene synthase, the enzymes catalyzing the first step of GA biosynthesis, are translocated into plastids [24]. It would be interesting to examine if NtDSK1 has the ability to regulate GA biosynthesis and/or signaling in response to light. Despite these possibilities, *in vivo* functions of NtDSK1 remain to be demonstrated. Molecular genetic approaches, such as antisense RNA techniques and dominant negative mutants, would be direct approaches to determine the functions of NtDSK1. In addition, identifying interacting signaling components may also provide insights into cellular functions of NtDSK1.

Acknowledgements: This work was supported by the grant from Plant Diversity Research Center (21C Frontier Program) and Center for Plant Molecular Genetics and Breeding Research.

References

- [1] Lindberg, R.A., Quinn, M.A. and Hunter, T. (1992) Trends Biochem. Sci. 17, 114–119.
- [2] Ali, N., Halfter, U. and Chua, N.-H. (1994) J. Biol. Chem. 269, 31626–31629.
- [3] Mu, J.-H., Lee, H.-S. and Kao, T.-h. (1994) Plant Cell 6, 709–721.
- [4] Sessa, G., Raz, V., Savaldi, S. and Fluhr, R. (1996) Plant Cell 8, 2223–2234.
- [5] Lee, H.-S., Karunanandaa, B., McCubbin, A., Gilroy, S. and Kao, T.-h. (1996) Plant J. 9, 613–624.
- [6] Lee, H.-S., Chung, Y.-Y., Das, C., Karunanandaa, B., van Went, J.L., Mariani, C. and Kao, T.-h. (1997) Sex. Plant Reprod. 10, 341–350.
- [7] Savaldi-Goldstein, S., Sessa, G. and Fluhr, R. (2000) Plant J. 21, 91–96.
- [8] Yoon, G.M., Cho, H.S., Ha, H.J., Liu, J.R. and Lee, H.-s. (1999) Plant Mol. Biol. 39, 991–1001.
- [9] Abel, S. and Theologis, A. (1994) Plant J. 5, 421–427.
- [10] Gualberto, J.M., Handa, H. and Grienenberger, J.M. (1995) Isolation and fractionation of plant mitochondria and chloroplasts: specific examples, in: Methods in Cell Biology (Galbraith, D.W., Bourque, D.P. and Bohnert, H.J., Eds.), Vol. 50, pp. 161–174, Academic Press, NY.

- [11] Bradford, M.M. (1976) *Anal. Biochem.* 72, 248–254.
- [12] Bollag, D.M., Rozycki, M.D. and Edelstein, S.J. (1996) *Protein Methods*, Wiley-Liss, NY.
- [13] Chang, C., Schaller, G.E., Patterson, S.E., Kwok, S.F., Meyerowitz, E.M. and Bleecker, A.B. (1992) *Plant Cell* 4, 1263–1271.
- [14] Goring, D.R. and Rothstein, S.J. (1992) *Plant Cell* 4, 1273–1281.
- [15] Li, J. and Chory, J. (1997) *Cell* 90, 929–938.
- [16] Zito, F., Finazzi, G., Delosme, R., Nitschke, W., Picot, D. and Wollman, F.-A. (1999) *EMBO J.* 18, 2961–2969.
- [17] Vener, A.V., Ohad, I. and Andersson, B. (1998) *Curr. Opin. Plant Biol.* 1, 217–223.
- [18] Bethke, P.C. and Jones, R.L. (1998) *Curr. Opin. Plant Biol.* 1, 440–446.
- [19] Swain, S.M. and Olszewski, N.E. (1996) *Plant Physiol.* 112, 11–17.
- [20] Ait-Ali, T., Swain, S.M., Reid, J.B., Sun, T.-p. and Kamiya, Y. (1997) *Plant J.* 11, 443–454.
- [21] Pharis, R.P. and King, R.W. (1985) *Annu. Rev. Plant Physiol. Plant Mol. Biol.* 36, 517–568.
- [22] Yamaguchi, S., Smith, M.W., Brown, R.G.S., Kamiya, Y. and Sun, T.-p. (1998) *Plant Cell* 10, 2115–2126.
- [23] Kamiya, Y. and Garcia-Martínez, J.L. (1999) *Curr. Opin. Plant Biol.* 2, 398–403.
- [24] Smith, M.W., Yamaguchi, S., Ait-Ali, T. and Kamiya, Y. (1998) *Plant Physiol.* 118, 1411–1419.

여 백

제 4 장 목표달성도 및 관련 분야에의 기여도

*계획대비달성도

구분	연구개발목표	연구개발내용 및 범위	달성도
1차년도 (2003)	-식물발생 조절 신호전달 유전자의 특성 및 생물학 적 기능 분석	- 식물발생 조절 신호전달 유전자와 단백질의 특 성 및 생물학적 기능 분석 o 신호전달 유전자와 단백질의 발현 연구 o 단백질의 생화학적, 세포생물학적 특성 연구 o 모델식물의 형질전환을 통한 기능 연구 o 식물발생의 형태학적, 해부학적 연구 o 식물발생의 분자기작 및 관련 유전자 연구	100%
2차년도 (2004)	-식물발생 조절 신호전달 단백질 의 생체 내 기능 분석	- 식물신호전달 유전자와 단백질의 특성 및 생 물학적 기능 분석 (계속) o 신호전달 유전자와 단백질의 발현 연구 o 단백질의 생화학적, 세포생물학적 특성 연구 o 모델식물의 RNAi, VIGS, overexpression을 통한 기능 연구 o Yeast two hybrid system을 이용한 상호작 용하는 단백질의 탐색 o protein-protein interaction map	100%
3차년도 (2005)	-신호전달 단백질 의 상호작용연구 -신기능성 형질 전환식물체 개발	- 식물 신호전달 단백질의 신호전달체계 내 위치 및 다른 신호전달 단백질과의 상호조절 작용 조사 o yeast two hybrid system o 단백질 상호조절 작용의 생화학적 기작 탐구 o 모델식물의 형질전환을 통한 기능 연구 o 각 구성원의 신호전달 체계 내의 위치 탐구 o 신호전달 체계 간의 상호작용 연구 o 식물발생의 신호전달 네트워크 분석 o 식물신호전달 유전자 발현 및 기능의 database - 신호전달 유전자 조절에 의한 신기능성 형질전 환체의 개발	100%

여 백

제 5 장 연구개발결과의 활용계획

- 식물 신호전달에 관한 연구는 생물학적으로 흥미로울 뿐만 아니라 식물의 응용 측면에서도 중요하기 때문에 추가연구가 필요하다. 또한 여러 연구자 간의 협력연구에 응용 가능.
- 신호전달 유전자 기능연구 방법의 세계적 수준 확보
- 국내의 고유성이 있으며 세계와 경쟁할 수 있는 식물계능 연구의 원천기술 확보
- 다수의 지적재산권을 확보하여 신 종자산업의 기반이 되는 원천기술을 개발
- 타작물로부터의 기능성 유전자의 발굴에 기여
- 타작물의 신품종을 유전공학적으로 개발하는데 기여
- 기능성유전자를 통한 기술료 수익
- 발굴된 유용 유전자의 경제작물로의 형질전환을 통하여 품종개량을 위한 육종소재로 개발
- 새로운 유용 유전자의 특허 획득 및 지적재산권의 산업화
- 주요 농작물에의 확대적용을 통한 고부가가치 신종자 개발 및 산업화
- RNAi와 overexpression 등으로 도출된 유용 유전자는 다양한 작물육종에 쓰일 것이며 우수 품종 개발은 농업생산성의 증가로 연결될 것이다.
- 기능성 유전자들의 licensing과 기업으로의 기술이전을 추진하여 기술료 수익이 예상되고 개발된 기술을 이용하여 벤처기업을 육성하는 등 산업적인 효과가 기대된다.
- 기술적인 측면으로는 식물 기능유전체 연구 관련기술을 개발하여 세계적 수준을 확보하며 기능성유전자 분리 분석기술을 향상시킬 수 있다. 또한 다수의 식물 신호전달 유전자의 기능을 대량으로 분석하므로써 우수논문을 발표하여 기초학문으로서의 가치가 크다.
- 개발된 기술을 활용 희망 연구자에게 이전. 또한 활용 희망자에게 발굴된 유전자들에 관한 정보 및 유전자 제공
- 분리된 기능성 유전자를 고추, 배추등 국내 종묘산업의 관심작물에 도입시켜 품종육성

제 6 장 연구개발과정에서 수집한 해외과학기술정보

- 식물의 다양한 신호전달 체계에 관한 정보
- 식물 기능유전체 연구의 세계적 동향과 정보
- 식물 발달의 분자적 기작에 관한 정보
- 식물 호르몬 작용의 분자적 메카니즘에 관한 정보

여 백

제 7 장 참고문헌

- Bakkers J, Semino CE, Stroband H, Kline JW, Robbins PW (1997) An important developmental role for oligosaccharides during early embryogenesis of cyprinid fish. *Proc Natl Acad Sci USA* **94**, 7982-7986
- Baureithel K, Felix G, Boller T (1994) Specific, high affinity binding of chitin fragments to tomato cells and membranes. Competitive inhibition of binding by derivatives of chito oligosaccharides and a Nod factor of *Rhizobium*. *J Biol Chem* **269(27)**: 17931-17938
- Becraft PW, Stinard PS, McCarty DR (1996) CRINKLY4: a TNFR-like receptor kinase involved in maize epidermal differentiation. *Science* **273**: 1406-1409
- Benhamou N (1996) Elicitor-induced plant defence pathways. *Trends Plant Sci* **1(7)**: 233-240
- Bent AF (1996) Plant disease resistance genes: function meets structure. *Plant Cell* **8**: 1757-1771
- Binns AN, Labliola J, Black RC (1987) Initiation of auxin autonomy in *Nicotiana glutinosa* cells by the cytokinin-biosynthesis gene from *Agrobacterium tumefaciens*. *Planta* **171**: 539-548
- Bollag DM, Rozycki MD, Edelstein SJ (1996) *Protein Methods*. Wiley-Liss Inc, New York
- Bradford MM (1976) A rapid and sensitive method for the quantitation of microgram quantities of protein utilizing the principle of protein-dye binding. *Anal Biochem* **72**: 248-254
- Braun DM, Walker JC (1996) Plant membrane receptors: new pieces in the signaling puzzle. *Trends Biochem Sci* **21(2)**: 70-73
- Brunner F, Stintzi A, Fritig B, Legrand M (1998) Substrate tobacco chitinases. *Plant J* **14(2)**, 225-234.
- Busch SJ, Sassone-Corsi P (1990) Dimers, leucine zippers and DNA-binding domains. *Trends Genet* **6(2)**: 36-40
- Cary AJ, Liu W, Howell SH (1995) Cytokinin action is coupled to ethylene in its effects on the inhibition of root and hypocotyl elongation in *Arabidopsis thaliana* seedlings. *Plant Physiol* **107**, 1075-1082.
- Chaudhury AM, Letham S, Craig S, Dennis ES (1993) *amp1*-a mutation with high cytokinin levels and altered embryonic pattern, faster vegetative growth, constitutive photomorphogenesis, and precocious flowering. *Plant J* **4**, 907-916.
- Chaplin MF (1986) Monosaccharides. In MF Chaplin, JF Kennedy, eds, *Carbohydrate Analysis-Practical Approach*. IRL Press, Oxford, pp 3
- Cheong J-J, Hahn MG (1991) A specific, high-affinity binding site for the

- hepta-beta-glucoside elicitor exists in soybean membranes. *Plant Cell* **3**: 137-147
- Chory J, Reinecke D, Sim S, Washburn T, Brenner M (1994) A role for cytokinins in de-etiolation in *Arabidopsis*. *Plant Physiol.* **104**, 339-347.
- Clark SE (1996) Plant Cell communication: the world outside the plasma membrane. *Trends Plant Sci* **1(12)**: 406-407
- Clark SE, Williams RW, Meyerowitz EM (1997) The *CLAVATA1* gene encodes a putative receptor kinase that controls shoot and floral meristem size in *Arabidopsis*. *Cell* **89**: 575-585
- De Jong AJ, Cordewener J, Lo Schiavo F, Terzi M, Vandekerckhove J, Van Kammen A, De Vries SC (1992) A carrot somatic embryo mutant is rescued by chitinase. *Plant Cell* **4**, 425-433.
- De Jong AJ, Heldstra R, Spaik HP, Hartog MV, Meijer EA, Hendriks T, Lo Schiavo F, Terzi M, Bisseling T, Van Kammen A, De Vries SC (1993) *Rhizobium* lipooligosaccharides rescue a carrot somatic embryo mutant. *Plant Cell* **5**, 615-620
- Dixon RA, Harrison MJ, Lamb CJ (1994) Early events in the activation of plant defense responses. *Annu Rev Phytopathol* **32**: 479-501
- Dwyer KG, Kandasamy MK, Mahosky DI, Acciai J, Kudish BI, Miller JE, Nasrallah ME, Nasrallah JB (1994) A superfamily of S locus-related sequences in *Arabidopsis*: diverse structures and expression patterns. *Plant Cell* **6(12)**: 1829-1843
- Ecker JR (1995) The ethylene signal transduction pathway in plants. *Science* **268**: 667-675
- Feng X-H, Dube SK, Bottino PJ, Kung S-d (1990) Restoration of shooty morphology of a nontunorous mutant of *Nicotiana glauca* x *N. langsdorffii* by cytokinin and the isopentenyltransferase gene. *Plant Mol Biol* **15**: 407-420.
- Fujita T, Kouchi H, Ichikawa T, Syono K (1994) Cloning of cDNAs for genes that are specifically or preferentially expressed during the development of tobacco genetic tumors. *Plant Journal* **5**: 645-654.
- Hakala BE, White C, Recklies AD (1993) Human cartilage gp-39, a major secretory product of articular chondrocytes and synovial cells, is a mammalian member of a chitinase protein family. *J Biol Chem* **268**: 25803-25810
- Harpster MH, Dunsmuir P (1989) Nucleotide sequence of the chitinase B gene of *Serratia marcescens* QMB1466. *Nucl Acid Res* **17**: 5395
- He Z-H, Fujiki M, Kohorn BD (1996) A cell wall-associated receptor-like protein kinase. *J Biol Chem* **271**: 19789-19793
- He ZH, Cheeseman I, He D, Kohorn BD (1999) A cluster of five cell wall-associated receptor kinase genes, *Wak1-5*, are expressed in specific organs of *Arabidopsis*. *Plant Mol Biol* **39(6)**: 1189-1196

- Herve C, Dabos P, Galaud J-P, Rouge P, Lescure B (1996) Characterization of an *Arabidopsis thaliana* gene that defines a new class of putative plant receptor kinases with an extracellular lectin-like domain. *J Mol Biol* **258**: 778-788
- Hewelt A, Prinsen E, Schell J, Van Onckelen HV, Schmulling T (1994) Promoter tagging with a promoterless *ipt* gene leads to cytokinin-induced phenotypic variability in transgenic tobacco plants: implications of gene dosage effects. *Plant J* **6**, 879-891.
- Higuchi R (1990) Recombinant PCR. In MA Innis, DH Gelfand, JJ Sninsky, TJ White, eds, *PCR Protocols*. Academic Press, New York, pp 177-183
- Ichikawa T, Syono K (1991) Tobacco genetic tumors. *Plant Cell Physiol* **32**: 1123-1128.
- Ito Y, Kaku H, Shibuya N (1997) Identification of a high-affinity binding protein for N-acetylchitooligosaccharide elicitor in the plasma membrane of suspension-cultured rice cells by affinity labeling. *Plant J* **12(2)**: 347-356
- Jinn TL, Stone JM, Walker JC (2000) HAESA, an *Arabidopsis* leucine-rich repeat receptor kinase, controls floral organ abscission. *Genes Dev* **14(1)**: 108-117
- Jacobsen JV (1984) The seed: germination. In *Embryology of Angiosperm* (Johri BM, ed). Springer-Verlag, Berlin.
- Jinn TL, Stone JM, Walker JC (2000) HAESA, an *Arabidopsis* leucine-rich repeat receptor kinase, controls floral organ abscission. *Genes Dev* **14(1)**: 108-117
- Kakimoto T (1998) Cytokinin signaling. *Cur Opin Plant Biol* **1**: 399-403
- Kende H (1971) The cytokinins. *Int Rev Cytol* **31**: 301-338
- Kieber JJ, Rothenberg M, Roman G, Feldman KA, Ecker JR (1993) *CTR1*, a negative regulator of the ethylene response pathway in *Arabidopsis*, encodes a member of the Raf family of the protein kinase. *Cell* **72**: 427-441
- Kim YS, Lee JH, Yoon GM, Cho HS, Park S-W, Suh MC, Choi D, Ha HJ, Liu JR, Pai HS (2000) *CHRK1*, a chitinase-related receptor-like kinase in tobacco. *Plant Physiol* **123**: 905-915.
- Kobayashi K, Fukuda M, Igarashi D, Sunaoshi M (2001) Cytokinin-binding proteins from tobacco callus share homology with osmotin-like protein and an endochitinase. *Plant Cell Physiol* **41**: 148-157.
- Kubo M, Kakimoto T (2000) The *CYTOKININ-HYPERSENSITIVE* genes of *Arabidopsis* negatively regulate the cytokinin-signaling pathway for cell division and chloroplast development. *Plant J* **23**, 385-394.
- Kuranda MJ, Robbins PW (1991) Chitinase is required for cell separation during growth of *Saccharomyces cerevisiae*. *J Biol Chem* **266**, 19758-19767
- Lawyton K, Payne G, Moyer M, Ryals J (1992) Acidic and basic class III chitinase mRNA accumulation in response to TMV infection of tobacco. *Plant Mol Biol* **19**:

- Lease K, Ingham E, Walker JC (1998) Challenges in understanding RLK function. *Curr Opin Plant Biol* **1**(5): 388-392
- Lee H-S, Chung Y-Y, Das C, Karunanandaa B, van Went JL, Mariani C, Kao T-h (1997) Embryo sac development is affected in *Petunia inflata* plants transformed with an antisense gene encoding the extracellular domain of receptor kinase PRK1. *Sex Plant Reprod* **10**: 341-350
- Lee H-S, Karunanandaa B, McCubbin A, Gilroy S, Kao T-h (1996) PRK1, a receptor-like kinase of *Petunia inflata*, is essential for postmeiotic development of pollen. *Plant J* **9**(5): 613-624
- Lieberman M (1979) Biosynthesis and action of ethylene. *Annu Rev Plant Physiol* **30**: 533-591
- Li J, Chory J (1997) A putative leucine-rich repeat receptor kinase involved in brassinosteroid signal transduction. *Cell* **90**: 929-938
- Majeran W, Wollman F-A, Vallon O (2000) Evidence for a role of ClpP in the degradation of the chloroplast cytochrome b6/f complex. *Plant Cell* **12**: 137-149.
- Martin GB, Brommonschenkel SH, Chungwongse J, Frary A, Ganai MW, Spivey R, Wu T, Earle ED, Tanksley SD (1993) Map-based cloning of a protein kinase gene conferring disease resistance in tomato. *Science* **262**: 1432-1436
- Martin T, Sotta B, Jullien M, Caboche M, Faure JD (1997) ZEA3: negative modulator of cytokinin responses in plant seedlings. *Plant Physiol* **114**, 1177-1185.
- Melchers LS, Apotheker M, van der Knaap J, Ponstein AS, Sela-Buurlage MB, Bol JF, Cornelissen BJC, van den Elzen PJM, Linthorst HJM (1994) A new class of tobacco chitinases homologous to bacterial exo-chitinases displays antifungal activity. *Plant J* **5**(4): 469-480
- Molano J, Duran A, Cabib E (1977) A rapid and sensitive assay for chitinase using tritiated chitin. *Anal Biochem* **83**: 648-656
- Nandi SK, de Klerk GJM, Parker CW, Palni LMS (1990) Endogenous cytokinin levels and metabolism of zeatin riboside in genetic tumor tissues and non-tumorous tissues of tobacco. *Physiol Plant* **78**: 197-204
- Nasrallah JB, Stein JC, Kandasamy MK, Nasrallah ME (1994) Signaling the arrest of pollen tube development in self-incompatible plants. *Science* **266**: 1505-1508
- Nishimura A, Tamaoki M, Sakamoto T, Matsuoka M (2000) Over-expression of tobacco *knotted1* type class1 homeobox genes alters various leaf morphology. *Plant Cell Physiol* **41**: 583-590.
- Park JM, Kang SG, Pih KT, Jang HJ, Piao HL, Yoon HW, Cho MJ, Hwang I-h (1998) A dynamin-like protein, ADL1, is present in membranes as a high-molecular-mass

- complex in *Arabidopsis thaliana*. *Plant Physiol* **115**: 763-771
- Renkema GH, Boot RG, Au FL, Donker-Koopman WE, Strijland A, Muijsers AO, Hrebicek M, Aerts JM (1998) Chitotriosidase, a chitinase, and the 39-kDa human cartilage glycoprotein, a chitin-binding lectin, are homologues of family 18 glycosyl hydrolases secreted by human macrophages. *Eur J Biochem* **251**: 504-509
- Ryals J, Weymann K, Lawton K, Friedrich L, Ellis D, Steiner HY, Johnson J, Delaney TP, Jesse T, Vos P, Uknes S (1997) The *Arabidopsis NIM1* protein shows homology to the mammalian transcription factor inhibitor I κ B. *Plant Cell* **9**: 425-439
- Semino CE, Specht CA, Raimondi A, Robbins PW (1996) Homologs of the *Xenopus* developmental gene *DG42* are present in zebrafish and mouse and are involved in the synthesis of Nod-like chitin oligosaccharides during early embryogenesis. *Proc Natl Acad Sci USA* **93**, 4548-4553.
- Shikanai T, Shimizu K, Ueda K, Nishimura Y, Kuroiwa T, Hashimoto T (2001) The chloroplast *clpP* gene, encoding a proteolytic subunit of ATP-dependent protease, is indispensable for chloroplast development in tobacco. *Plant Cell Physiol* **42**: 264-273.
- Shibuya N, Kaku H, Kuchitsu K, Maliarik MJ (1993) Identification of a novel high-affinity binding site for N-acetylchitoooligosaccharide elicitor in the membrane fraction from suspension-cultured rice cells. *FEBS Lett* **329**: 75-78
- Song W-Y, Wang G-L, Chen L-L, Kim H-S, Pi L-Y, Holsten T, Gardner J, Wang B, Zhai W-X, Zhu L-H, Fauquet C, Ronald P (1995) A receptor kinase-like protein encoded by the rice disease resistance gene, *Xa21*. *Science* **270**: 1804-1806
- Skoog F, Miller CO (1957) Chemical regulation of growth and organ formation in plant tissues cultured in vitro. *Symp Soc Exp Biol* **11**, 118-131
- Spector DL, Goldman RD, Leinwand LA (1998) *Cells: A Laboratory Manual*. Cold Spring Harbor Laboratory Press, Cold Spring Harbor
- Spena A, Prinsen E, Fladung M, Schulze SC, Van Onckelen H (1991) The indoleacetic acid-lysing synthetase gene of *Pseudomonas syringae* subsp. *savastanoi* induces developmental alterations in transgenic tobacco and potato plants. *Mol Gen Genet* **227**: 205-212
- Stein JC, Howlett B, Boyes DC, Nasrallah ME, Nasrallah JB (1991) Molecular cloning of a putative receptor kinase gene encoded at the self-incompatibility locus of *Brassica oleracea*. *Proc Natl Acad Sci USA* **88**: 8816-8820
- Su W, Howell S (1992) A single genetic locus, *ckr1*, defines *Arabidopsis* mutants in which root growth is resistant to low concentrations of cytokinin. *Plant Physiol* **99**, 1569-1574.
- Suh, M.C., Choi, D., and Liu, J.R (1998). Cadmium resistance in transgenic tobacco plants expressing the *Nicotiana glutinosa* L. Metallothionein-like gene. *Mol.*

- Cells **8(6)**, 678-684
- Suzuki K, Shinshi H** (1995) Transient activation and tyrosine phosphorylation of a protein kinase in tobacco cells treated with a fungal elicitor. *Plant Cell* **7**: 639-647
- Tamaoki M, Kusaba S, Kano-Murakami Y, Matsuoka M** (1997) Ectopic expression of a tobacco homeobox gene, *NTH15*, dramatically alters leaf morphology and hormone levels in transgenic tobacco. *Plant Cell Physiol* **38**: 917-927.
- Thomas JC, Smigocki AC, Bohnert HJ** (1995) Light-induced expression of *ipt* gene from *Agrobacterium tumefaciens* results in cytokinin accumulation and somatic stress symptoms in transgenic tobacco. *Plant Mol Biol* **27**: 225-235.
- Thompson JD, Higgins DJ, Gibson TJ** (1994) CLUSTAL W: improving the sensitivity of progressive multiple sequence alignment through sequence weighting, positions-specific gap penalties and weight matrix choice. *Nucl. Acid Res.* **22**: 4673-4680
- Umemoto N, Kakitani M, Iwamatsu A, Yoshikawa M, Yamaoka N, Ishida I** (1997) The structure and function of a soybean beta-glucan-elicitor-binding protein. *Proc Natl Acad Sci USA* **94**: 1029-1034
- Vogel JP, Woeste KE, Theologis A, Kieber JJ** (1998) Recessive and dominant mutations in the ethylene biosynthetic gene *ACS5* of *Arabidopsis* confer cytokinin insensitivity and ethylene overproduction, respectively. *Proc. Natl. Acad. Sci. USA* **95**, 4766-4771.
- von Heijne G** (1983) Patterns of amino acids near signal-sequence cleavage sites. *Eur J Biochem* **133**: 17-21
- Wang X, Zafian P, Choudhary M, Lawton M** (1996) The PR5K receptor protein kinase from *Arabidopsis thaliana* is structurally related to a family of plant defense proteins. *Proc Natl Acad Sci USA* **93**: 2598-2602
- Watanabe T, Kobori K, Miyashita K, Fujii T, Sakai H, Uchida M, Tanaka H** (1993) Identification of glutamic acid 204 and aspartic acid 200 in chitinase A1 of *Bacillus circulans* WL-12 as essential residues for chitinase activity. *J Biol Chem* **268**: 18567-18572
- Watanabe T, Suzuki K, Oyanagi W, Ohnishi K, Tanaka H** (1990) Gene cloning of chitinase A1 from *Bacillus circulans* WL-12 revealed its evolutionary relationship to *Serratia* chitinase and to the type III homology units of fibronectin. *J Biol Chem* **265**: 15659-15665
- Wilkinson JQ, Lanahan MB, Yen HC, Giovannoni JJ, Klee HJ** (1995) An ethylene-inducible component of signal transduction encoded by never-ripe. *Science* **270**: 1807-1809
- Yamamoto YY, Matsui M, Ang LH, Deng XW** (1998) Role of COP1 interacting protein in mediating light-regulated gene expression. *Plant Cell* **10**: 1083-1094.

특정연구개발사업 연구결과 활용계획서

사업명	중사업명	21C 프론티어연구개발사업			
	세부사업명	자생식물이용기술개발사업			
과제명		신호전달 조절유전자군의 발굴 및 기능네트워크 연구			
연구기관		한국생명공학연구원	연구책임자	배현숙	
총연구기간		2000 년 09 월 16 일 ~ 2003년 06 월 30 일 (28개월)			
총 연구비 (단위 : 천원)		정부출연금	민간부담금	합계	
		750,000	0	750,000	
기술분야		식물분자생물학			
참여기업					
공동연구기관					
위탁연구기관					
연구결과활용 (해당항목에(√) 표시)		1. 기업화 ()	2. 기술이전 ()	3. 후속연구추진(√)	4. 타사업에 활용()
		5. 선행 및 기 초연구()	6. 기타목적활용 (교육연구)()	7. 활용중단(미활용)()	8. 기타()

특정연구개발사업 처리규정 제 31조(연구개발결과의 보고) 제 2항에 의거
연구결과 활용계획서를 제출합니다.

첨부 : 1. 연구결과 활용계획서 1부.
2. 기술요약서 1부

2003년 8월 14일

연구책임자 :

배현숙 (인)

연구기관장 :

양규환 (직인)

과학기술부장관 귀하

여 백

[첨부1]

연구결과 활용계획서

1. 연구목표 및 내용

신호전달 유전자군을 발굴하고 분자생물학적, 세포생물학적, 생화학적인 분석을 통하여 그들 유전자의 생물학적인 기능을 탐색하므로서 신기능성 유전자군을 확보한다. 또한 분석된 신호전달 유전자의 활성조절을 통하여 기능성 식물형질전환체를 개발한다.

2. 연구수행결과 현황(연구종료시점까지)

가. 특허(실용신안) 등 자료목록

국명	특허제목	출원자	출원번호	출원년,월	등록번호	등록년,월
미국	키틴결합능이 있는 새로운 수용체 키나제 및 그 유전자	한국생명공학연구원	09/503,922	2000.2.14	6,410,706	2002.6.25
한국	식물호르몬 지베렐린의 신호전달과정에 관여하는 새로운 키나제 및 그 유전자	한국생명공학연구원	99-906	1999.1.15	305281	2001.7.27
한국	키틴결합능이 있는 새로운 수용체 키나제 및 그 유전자 및 그의 용도	한국생명공학연구원	99-4938	2000.2.14	314907	2001.11.5

나. 프로그램 등록목록

프로그램 명칭	등록번호	등록일자	개발자	비고

다. 노하우 내역

라. 발생품 및 시작품 내역

마. 논문게재 및 발표 실적

○ 논문게재 실적(필요시 별지사용)

1. J.-W. Ahn, M. Kim, J. W. Bang, and H.S. Pai* (2003) Molecular characteristics and differential expression of two nuclear factors containing the FHA domain in *Arabidopsis*. **Plant Science**, In Press.

2. M. Kim, H.S. Cho, J.H. Lee, and H.S. Pai* (2003) CHRK1, a chitinase-related receptor-like kinase, interacts with NtARC1, an armadillo repeat protein, in tobacco. **BBA-Proteins and Proteomics**, In Press.

3. M.C. Suh, S.-K. Oh, Y.-C. Kim, H.-S. Pai, and D. Choi* (2003) Expression of a novel tobacco gene, NgCDM1, is preferentially associated with pathogen-induced cell death. **Physiological and Molecular Plant Pathology**, In Press.

4. M. Kim, J.-W. Ahn, O. Jin, K.-H. Paek, H.S. Pai*. (2003) Activation of the programmed cell death pathway by inhibition of proteasome function in plants. **Journal of Biological Chemistry**, 278, 19406-19415.

5. S.S. Lee, H.S. Cho, G.M. Yoon, J.-W. Ahn, H.H. Kim, H.S. Pai*. (2003) Interaction of NtCDPK1 calcium-dependent protein kinase with NtRpn3 regulatory subunit of the 26S proteasome in *Nicotiana tabacum*. **The Plant Journal**, 33: 825-840

6. M. Kim, K.-S. Yang, Y.-K. Kim, K.-H. Paek, H.S. Pai* (2003) Molecular characterization of *NbPAF* encoding the $\alpha 6$ subunit of the 20S proteasome in *Nicotiana benthamiana*. **Molecules and Cells**, 15; 127-132

7. M. Kim, J.-W. Ahn, K. Song, K.-H. Paek, H.S. Pai*. (2002) FHA domain of tobacco NtFHA1 and yeast FHL1 forkhead transcription factor is functionally conserved. **Journal of Biological Chemistry** 277; 38781-38790.

8. H.S. Cho, G.M. Yoon, I. Hwang, Y.A. Kim, D. Choi, H.S. Pai* (2001) A novel dual-specificity protein kinase targeted to the chloroplast in tobacco. **FEBS Letters** 497: 124-130 (Cover Story)

9. M.C. Suh, S.Y. Yi, S. Lee, W.-S. Sim, H.S. Pai, D. Choi* (2001) Pathogen-induced expression of plant ATP:citrate lyase. **FEBS Letters** 488: 211-212.

○ 학술회의 발표 실적(필요시 별지사용)

학술발표제목	발표자	발표장소 (국명)	일시
Functional genomics using virus-induced gene silencing	M. Kim, S.S. Lee, U.-H. Jin, K.-S. Yang, H.-S. Pai	한국분자세포생물학회 겨울모임 (용평)	2월 12-14일, 2003
NtCDPK1 calcium-dependent protein kinase interacts with NtRpn3 regulatory subunit of the 26S proteasome to control cell division and differentiation in <i>Nicotiana tabacum</i>	S.S. Lee, H.S. Cho, G.M. Yoon, J.-W. Ahn, H.H. Kim, H.-S. Pai	Plant Biology 2002 meeting (Colorado, USA)	8월 3-7일, 2002
CHRK1, a chitinase-related receptor-like kinase regulates cell division and differentiation, and influences cytokinin response in tobacco.	J.H. Lee , H.S. Cho, D.M. Kim, H.-S. Pai	Plant Biology 2002 meeting (Colorado, USA)	8월 3-7일, 2002
FHA domain of tobacco NtFHA1 and yeast FHL1 forkhead transcription factor is functionally conserved.	M. Kim , J.-W. Ahn, K.-H. Paek, H.-S. Pai	The 13th International Conference on Arabidopsis Research, (Sevilla, Spain)	6월 28일-7월 2일, 2002
Function and expression of transcription activators containing the FHA domain in tobacco and Arabidopsis.	M. Kim, J.-W. Ahn , H.-S. Pai	The 4th Japan-Korea Joint Symposium on Plant Biology (Kyoto, Japan)	9월 21일, 2002
NtDRF1 transcription factor is involved in osmotic stress signal transduction in tobacco.	D.M. Kim , J.H. Lee, J. Kim, J.W. Bang, H.-S. Pai	The 4th Japan-Korea Joint Symposium on Plant Biology (Kyoto, Japan)	9월 21일, 2002
Function and expression of transcription activators containing the FHA domain in tobacco and Arabidopsis.	M. Kim , J.-W. Ahn, H.-S. Pai	한국분자세포생물학회 2002 추계대회 (서울교육문화회관)	10월 17-18일, 2002
Silencing of the genes encoding proteasome subunits induces programmed cell death in <i>Nicotiana benthamiana</i> .	M. Kim , U.-H. Jin, J.-W. Ahn, K.-H. Paek, D. Choi, H.-S. Pai	한국분자세포생물학회 2002 추계대회 (서울교육문화회관)	10월 17-18일, 2002
NtDRF1 transcription factor is involved in osmotic stress signal transduction in tobacco.	D.M. Kim , J.H. Lee, J. Kim, J.W. Bang, H.-S. Pai	한국분자세포생물학회 2002 추계대회 (서울교육문화회관)	10월 17-18일, 2002
Interaction of NtCDPK1 Ca ²⁺ -dependent protein kinase with NtRpn3, a regulatory subunit of the 26S proteasome in tobacco	S.S. Lee, H.S. Cho, G.M. Yoon, H.-S. Pai	4th Korea-China joint symposium on bioscience and biotechnology	12월 17일-18일, 2001
CHRK1, a chitinase-related receptor-like kinase, regulates cell division and differentiation, and influences cytokinin response in tobacco	J.H. Lee , H.S. Cho, Y.S. Kim, H.-S. Pai	한국분자세포생물학회 추계학술대회 (서울, 한국)	10월 11일-12일, 2001

학술발표제목	발표자	발표장소 (국명)	일시
Putative functions of FHA transcription factors containing forkhead-associated domain	M. Kim, J.-W. Ahn, K.-H. Paek, H.-S. Pai	한국분자세포생물학회 추계학술대회 (서울, 한국)	10월 11일-12일, 2001
NtCDPK1 calcium-dependent protein kinase phosphorylates Nt21D7, a tobacco homolog of Rpn3 subunit of the 26S proteasome	S.S. Lee, H.S. Cho, G.M. Yoon, H.-S. Pai	한국분자세포생물학회 추계학술대회 (서울, 한국)	10월 11일-12일, 2001
CHRK1, a chitinase-related receptor-like kinase, regulates cell division and differentiation, and influences cytokinin response in tobacco.	J.H. Lee, H.S. Cho, Y.S. Kim, H.-S. Pai	The 2nd Symposium of Plant Molecular Genetics and Breeding (수원, 한국)	8월 31일, 2001
CHRK1, a chitinase-related receptor-like kinase, regulates cell division and differentiation, and influences cytokinin response in tobacco	J.H. Lee, H.S. Cho, Y.S. Kim, H.-S. Pai	The 17th International Conference on Plant Growth Substances. (Brno, Czech Republic)	7월 1-6일, 2001
NtCDPK1 calcium-dependent protein kinase phosphorylates Nt21D7, a tobacco homolog of Rpn3 subunit of the 26S proteasome	S.S. Lee, H.S. Cho, G.M. Yoon, H.-S. Pai	The 2nd Symposium of Plant Molecular Genetics and Breeding (수원, 한국)	8월 31일, 2001
Putative functions of FHA transcription factors containing forkhead-associated domain	M. Kim, J.-W. Ahn, K.-H. Paek, H.-S. Pai	The 2nd Symposium of Plant Molecular Genetics and Breeding (수원, 한국)	8월 31일, 2001

3. 연구성과

기술이전, 기업화 완료 실적 없음

4. 기술이전 및 연구결과 활용계획

가. 당해연도 활용계획

- 새로운 유용 유전자의 특허 획득 및 지적재산권의 산업화
- 기술적인 측면으로는 식물 기능유전체 연구 관련기술을 개발하여 세계적 수준을 확보 하며 기능성유전자 분리 분석기술을 향상시킬 수 있다. 또한 다수의 식물 신호전달 유전자의 기능을 대량으로 분석하므로써 우수논문들을 발표하여 기초학문으로서의 가치가 크다.
- 개발된 기술을 활용 희망 연구자에게 이전. 또한 활용 희망자에게 발굴된 유전자들에 관한 정보 및 유전자 제공
- 분리된 기능성 유전자를 고추, 배추등 국내 종묘산업의 관심작물에 도입시켜 품종육성

나. 활용방법

- 새로운 유용 유전자의 특허 획득
- 우수논문 발표
- 개발된 기술을 활용 희망 연구자에게 이전.
- 발굴된 유전자들에 관한 정보 및 유전자 제공

다. 차년도이후 활용계획

- 다수의 지적재산권을 확보하여 신 종자산업의 기반이 되는 원천기술을 개발
- 타작물로부터의 기능성 유전자의 발굴에 기여
- 타작물의 신품종을 유전공학적으로 개발하는데 기여
- 기능성유전자를 통한 기술료 수익
- 발굴된 유용 유전자의 경제작물로의 형질전환을 통하여 품종개량을 위한 육종소재로 개발
- 새로운 유용 유전자의 특허 획득 및 지적재산권의 산업화
- 주요 농작물への 확대적용을 통한 고부가가치 신종자 개발 및 산업화
- RNAi와 overexpression 등으로 도출된 유용 유전자는 다양한 작물육종에 쓰일 것이며 우수 품종 개발은 농업생산성의 증가로 연결될 것이다.
- 기능성 유전자들의 licensing과 기업으로의 기술이전을 추진하여 기술료 수익이 예상되고 개발된 기술을 이용하여 벤처기업을 육성하는 등 산업적인 효과가 기대된다.
- 개발된 기술을 활용 희망 연구자에게 이전. 또한 활용 희망자에게 발굴된 유전자들에 관한 정보 및 유전자 제공
- 분리된 기능성 유전자를 고추, 배추등 국내 종묘산업의 관심작물에 도입시켜 품종육성

5. 기대효과

- 인력양성 또는 고용창출효과:
매년 12-15명의 연구원을 연구팀에서 고용
석사 및 박사 양성
- 인프라 구축 효과: 이 연구를 통하여 식물신호전달 연구를 위한 기기 및 시설의

인프라가 완성되었고 유전체연구에 필요한 식물대량배양 시설들을 구축하였다.

6. 문제점 및 건의사항(연구성과의 제고를 위한 제도·규정 및 연구관리 등의 개선점을 기재)

해당없음

[첨부2]

기술 요약서

■ 기술의 명칭

식물신호전달체계 조절기술

■ 기술을 도출한 과제현황

과제관리번호	PF003105-02			
과제명	신호전달 조절유전자군의 발굴 및 기능네트워크 연구			
사업명	자생식물이용기술개발사업			
세부사업명	PF3-4			
연구기관	한국생명공학연구원	기관유형	정부출연연구소	
참여기관(기업)				
총연구기간	2000년 09월 16일 ~ 2003년 06월 30일 (28개월)			
총연구비	정부(250,000)천원 민간()천원 합계(250,000)천원			
연구책임자 1	성명	배현숙	주민번호	
	근무기관 부서	한국생명공학연구원 / 식물유전체연구실	E-mail	hyunsook@kribb.re.kr
	직위/직급	책임연구원	전화번호	042-860-4195
연구책임자 2	성명	조혜선	주민번호	
	근무기관 부서	한국생명공학연구원 / 식물유전체연구실	E-mail	hscho@kribb.re.kr
	직위/직급	선임연구원	전화번호	042-860-4465
실무연락책임자	성명	배현숙	소속/부서	식물유전체연구실
	직위/직급	책임연구원	E-mail	hyunsook@kribb.re.kr
	전화번호	042-860-4195	FAX	042-860-4608
	주소	(305-333) 대전시 유성구 어은동 52번지		

과제관리번호			
과제명			
사업명			
세부사업명			
연구기관		기관유형	
참여기관(기업)			
총연구기간			
총연구비	합계 : ()백만원 - 정부 : ()백만원 민간 : ()백만원		
연구책임자	소속		성명
	전화번호		E-mail
연구개발 주요내용			

[기술의 수명주기] (1개씩 선택(√호 표시)하여 주십시오)

	① 기술개념 정립기 : 기술의 잠재적 가능성만 있는 단계
	② 기술실험기 : 기술개발에 성공했으나 아직 실용성, 경제성 등이 확실치 않은 단계
	③ 기술적용 시작기: 최초의 기술개발국에서만 활용되고 있는 단계
√	④ 기술적용 성장기: 기술개발국 및 일부 선진국에서 활용되고 있는단계
	⑤ 기술적용 성숙기: 선진국사이에서 활발한 기술이전이 일어나며, 기술의 표준화가 되어가는 단계
	⑥ 기술적용 쇠퇴기: 선진국에서 개도국으로 기술이전이 활발하게 일어나고, 선진국에서는 기술의 가치가 저하되나, 개도국에서는 아직 시장의 가치가 높은 기술

[기술발전 과정상의 기술수준] (1개씩 선택(√호 표시)하여 주십시오)

	① 외국기술의 모방단계 : 이미 외국에서 개발된 기술의 복제, reverse Eng.
	② 외국기술의 소화·흡수단계 : 국내시장구조나 특성에 적합하게 적용시킴
	③ 외국기술의 개선·개량단계 : 성능이나 기능을 개선시킴
√	④ 신기술의 혁신·발명단계 : 국내 최초로 개발

■ 본 기술과 관련하여 추가로 확보되었거나 개발중인 기술

[기술개요]

기술명	
개발단계	? 연구개발 계획 ? 연구개발 중 ? 연구개발 완료
기술개요	

[기술을 도출한 과제현황]